Investigations into Long-Standing Problems in Radical Polymerization Kinetics: Chain-Length-Dependent Termination Rate Coefficient and Mode of Termination

A thesis submitted in partial fulfilment of the requirement for the

Degree of Doctor of Philosophy in Chemistry

MAJED MOHAMMED ALGHAMDI

University of Canterbury

2014

Abstract

The present thesis investigates some long standing problems in radical polymerization (RP). The major aim is to consider the feasibility of using simple techniques to provide more insight into the kinetics of RP. This can contribute to fundamental knowledge of radical polymerizations, particularly with respect to the mode of termination (λ), average termination rate coefficient ($<k_t>$), chain-length dependence of termination (CLDT) and chain transfer through in-depth investigations of the rate of polymerization (R_p) and molar mass distribution (MMD), the latter especially via mass spectrometric (MS) analysis.

The termination process was first investigated. Observation of changes of $<k_t>$ (or equivalently R_p) and MMD by a variety of factors such as solvent, monomer and initiator concentrations, temperature, pressure and growing radical size were explored. Non-classical kinetics and chain-length dependency of termination were confirmed. Accessibility of CLDT information was clearly evident. Although observed results meet fully with composite-model expectations, issues such as chain transfer were found to have an effect on the CLDT parameters determined from rate measurements. Specifically, dilute-solution polymerization of methyl methacrylate (MMA) in methyl isobutyrate (MIB) showed evidence of such an effect. Scaling of quantities that are experimentally accessible such as $<k_t>$ with DP_n yield CLDT parameters in good agreement with what has been reported from recent PLP experiments. This was confirmed for several monomers. The temperature dependence of termination was also investigated and found to show evidence for CLDT. In contrast, the variation of $<k_t>$ with pressure did not demonstrate similarly strong CLDT effects. Evidence for and determination of chain transfer to MIB was also obtained.

This was followed up by investigations into the important parameter λ using the MS technique. Surprisingly little is known about λ despite its long history and its apparent importance to polymer properties. Firstly, the robustness of using MS was explored, with the method passing numerous consistency checks. Although no large dependence of MS instrument was found, electrospray-ionization mass spectrometry (ESI-MS) provided best resolution. Second, the type of initiator, the initiator concentration and the solvent were found to have no measurable effect on λ, even when chain transfer occurred. In further work, increasing temperature seemed to have an influence on λ, leading to an increase in the proportion of disproportionation. However, pressure was found to have only a small influence on λ. The effect of monomer on λ was also studied.

In the final part of this work, a preliminarily investigation into the viability of using Raman spectroscopic techniques to study auto-acceleration, also called the gel effect, for bulk MMA radical polymerization was presented. The results showed the possibility of using such a technique to follow the reaction to high conversion. The effect of temperature and initiator concentration on auto-acceleration were also presented.

The outstanding results of this thesis are: (1) The application of CLDT theory to better understand rate results from low-conversion polymerizations. (2) In particular, the use of CLDT principles to explain termination activation energies across a range of monomers. (3) The validation of the MS method for quantitative determination of mode of termination by carrying out an array of consistency checks. (4) Showing that MS results are consistent with CLDT theory. (5) Utilization of the MS method for the first ever reliable measurement of the variation of mode of termination with temperature, pressure and monomer.

Acknowledgements

I would like to express my special thanks to my supervisor, Gregory Russell, for his guidance and supervision throughout the duration of this thesis. He has kept me motivated during difficult times, and he has always helped me to be positive by referring to the lighter side of research. I also extend my gratitude to Michael Buback, for his generosity in allowing me to do part of this work in his lab at Göttingen University, Germany, and to Felix Huff for his assistance with some experiments. I would also like to thank Neil Edmonds, from the University of Auckland, for making me a welcome guest for almost two years after I had to leave the University of Canterbury because of the earthquake. I would like to acknowledge the University of Canterbury for giving me the opportunity to complete my thesis comfortably in Auckland University, far from the discomfort of the ongoing aftershocks. Thanks also to graduate research student Omar El-Hadad for his help. Moreover, I want to extend my gratitude to Marie Squire for her help with the University of Canterbury MS experiments. I am also grateful to my family; their patience and support are much appreciated. Also thanks go to my sponsor, King Khalid University, for their financial support, and to all others who have helped me during this time.

Table of Contents

List of Figures

List of Tables

Chapter 1. Introduction

1.1. General introduction

Polymers are defined as large molecules composed of repeating structural units called monomers and typically connected by covalent bonds. Assemblies of less than 100 subunits are often referred to as oligomers. Even though the earliest important work in polymer science started in the early the nineteenth century, when Henri Braconnot did his pioneering work in derivative cellulose compounds, synthetic polymers were only discovered in the mid nineteenth century when the first synthetic polymer, cellulose nitrate, was made in 1846 by Christian Frederick.[1]

More interest in polymers then began when in 1910 Pickles suggested that rubber was made up of long-chain molecules. Twelve years later Staudinger introduced the term ‘macromolecule’.[1] After that there was a slow but gradual acceptance of the idea of macromolecules. For instance, in 1928 Carothers began to study condensation polymerization, which led to two new and important groups of polymers, the polyesters and the polyamides.

Commercial production of synthetic polymers commenced with the manufacture of polystyrene in Germany in 1930; curiously, it was not until nearly a decade after this that the mechanism of radical polymerization was elucidated. Poly(vinyl chloride), PVC was discovered in 1935, while poly(methyl methacrylate) (PMMA) was first produced in 1936, The Second World War then provided further impetus for the take-off in real use of polymers.[2]

Nowadays, polymers receive tremendous interest since they possess many unique and special properties. In fact, polymers are of major economic and social importance, and they play an important role in all activities of our daily lives. Polymers are fundamental to most aspects of modern life: clothing, communication, transportation, packaging, medicine and so on. More than 200 million tons of polymers are produced worldwide annually.[3] Approximately half of this production is by radical polymerization (RP). This is why it is so enormously important to have a detailed knowledge of the kinetics of RP. However, detailed knowledge of this essential method of polymerization remains incomplete and in some aspects elusive. This thesis does its bit to fill in several more of these gaps.

1.2. Polymer production

Classically, the two main processes by which polymers are made are chain-growth polymerization (addition polymerization) and step-growth polymerization (most commonly polycondensation).

Chain polymerization is initiated by a radical followed by the successive addition of individual monomer units to the growing chain via an active site. Some examples of addition polymers are polyethylene, PVC, polystyrene and PMMA. Ionic polymerizations are also chain polymerizations; however; the present research is concerned exclusively with radical polymerization, which is the most widely applied process for the production of polymeric materials.

The major alternative way of making polymer is by step polymerization. It is often characterized by linking two molecules together via the elimination of a small molecule, e.g. water, alcohol, hence the term condensation polymerization. The formation of a condensation

polymer can be best illustrated by the well-known reaction of hexamethylenediamine with adipic acid to form the polyamide known as Nylon 6-6.

1.3. Fundamental reactions of radical polymerization

The process of radical polymerization (RP) can be described by a minimum set of fundamental reactions: initiation, propagation and termination, including chain transfer, as represented in Scheme 1.

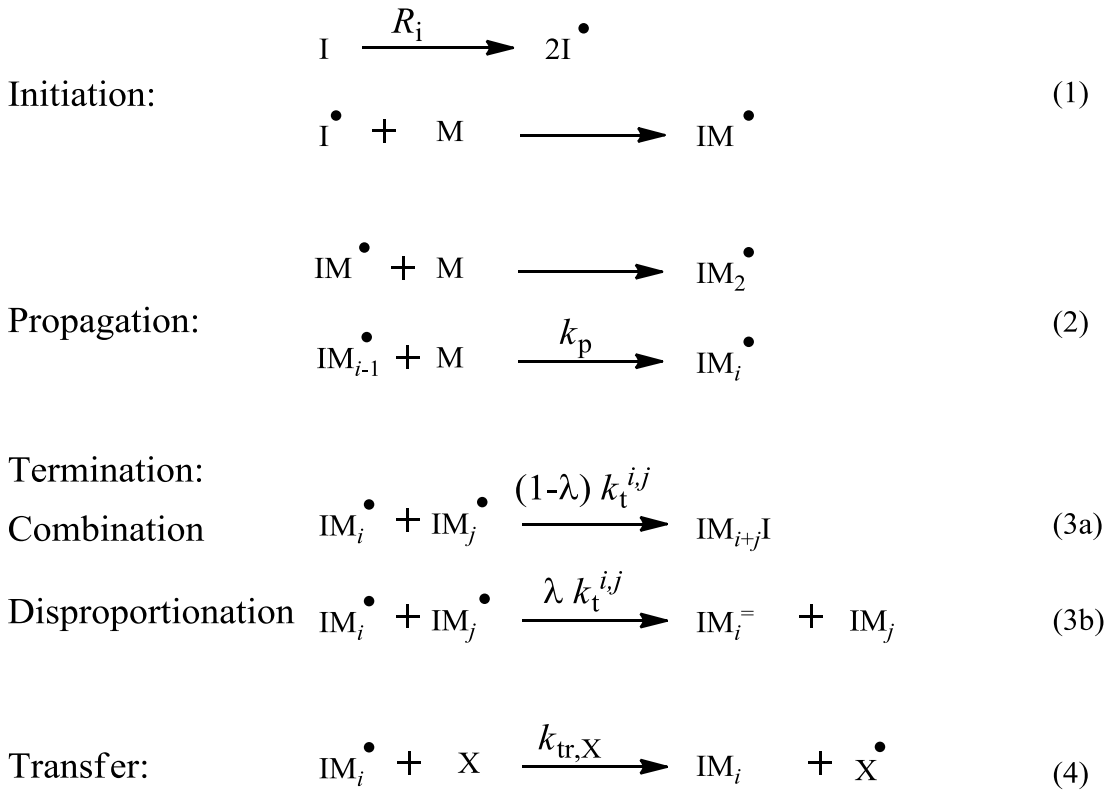

Scheme 1. Fundamental radical-polymerization reactions, where I denotes initiator, M monomer, and subscripts *i* and *j* denote degree of polymerization.

In radical polymerization, the above reactions proceed in parallel. Each of these reactions has distinct parameters. It is the task of all kinetic experiments to determine these parameters via a variety of experimental approaches. The kinetic understanding of these fundamental radical

polymerization processes is of fundamental importance for efficiently generating polymeric products. Therefore, each step of these fundamental reactions is now discussed individually.

1.3.1. Initiation

Initiation generates the free radical active site that is needed for chain growth. Most commonly this is achieved using chemical initiators. Reaction 1 illustrates the initiation steps.

Initiation:

$$I \xrightarrow{R_i} 2I^{\bullet}$$

$$I^{\bullet} + M \longrightarrow IM^{\bullet} \qquad (1)$$

Where chemical initiator is used, $R_i = 2fk_dc_I$, in which R_i is rate of initiation, and f, k_d and c_I denote initiator efficiency, decomposition rate coefficient and concentration, respectively.

1.3.1.1. Initiators

Initiators are usually limited to compounds with a labile bond that can be broken when sufficient energy is supplied to the molecule. There are different types of chemical initiators. Among the most used for radical polymerization are azo compounds (e.g. AIBN) and organic peroxides[4] (e.g. peroxyesters, hydroperoxides, peroxycarbonates, diacyl peroxides and peroxy dicarbonates). The general structures of azo and peroxide initiators are represented by molecules 1 and 2 respectively.

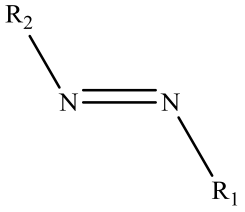

1

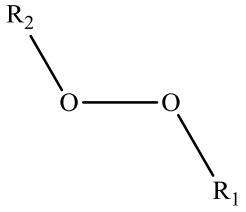

2

The task of chemical initiators in radical polymerization is to generate radicals that may initiate polymerization. A radical is defined as an intermediate compound containing an odd number of electrons that does not carry an electric charge and is not a free ion. Knowledge of the stabilities of the generated radicals is important for understanding how readily radical reaction can occur. This stability can be evaluated by hydrogen bond dissociation energy (BDE), where low BDEs result in increased stability. For example, tertiary and secondary peroxyesters have low BDE and are more stable than primary peroxyesters.[5, 6] Also, any type of substitution at the radical center results in increased stability. In particular, any group that provides an orbital that can mix with the semi-occupied molecular orbital (SOMO) will result in stabilisation.

There are a variety of means to generate radicals. Generally, they can be divided into the broad areas of thermolysis, photolysis and redox methods. The thermal process is a commonly used method. It relies on breaking labile initiator bonds in order to form radicals; bonds of low dissociation energy like peroxide bonds and the bonds in azo compounds are suitable. The photochemical process, on the other hand, relies on the energy of a photon to break weak photoinitiator bonds by production of an excited state that produces radicals. This method is attractive in RP because it is readily controlled and allows the production of radicals at low temperature. However, the use of photoinitiation is in most cases restricted to research. It is commonly used in the laser-induced techniques (e.g. pulsed-laser polymerization, PLP) that have become of pivotal importance for investigations of rate coefficients of radical polymerization.[7-9] On the other hand, its use in industrial process is very limited because of the technical problems associated with the uniform irradiation of large reaction volumes. Other types of initiation include radiation-induced cleavage of bonds and bond cleavage via one-electron transfer reactions. This latter method involves, in many cases, the use of metals and organic substrates.

The other two main essential parameters involved in the initiation process in RP are the decomposition rate coefficient (k_d), and the efficiency of initiation (f).

1.3.1.2. Decomposition rate coefficients, k_d

Although the initiation process involves two steps (viz. the decomposition of initiator and the reaction of primary radical with monomer, see reaction (1)), the decomposition of the initiator is the rate-determining step in the initiation sequence. Continuous initiation employed in this thesis is typically achieved by decomposition of thermally labile compounds such as peroxides and azo-compounds. 2,2'-azobisisobutyronitrile (AIBN) is a commonly used thermal initiator. It decomposes to produce two identical free radicals, reaction (a1), according to a first order kinetic law, so they are especially suited for kinetic investigations. Bis(3,5,5,-trimethanoylhexanoyl peroxide) (BTMHP) also decomposes to produce two identical free radicals, reaction (a2). However, in the decomposition of peroxides, the first step is the formation of an alkoxy radical that then decarboxylates yielding the carbon-centered alkyl.[10]

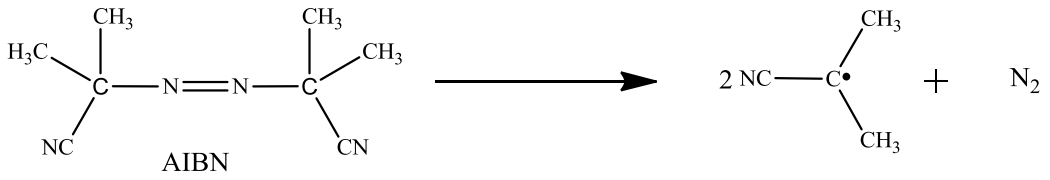

(a1)

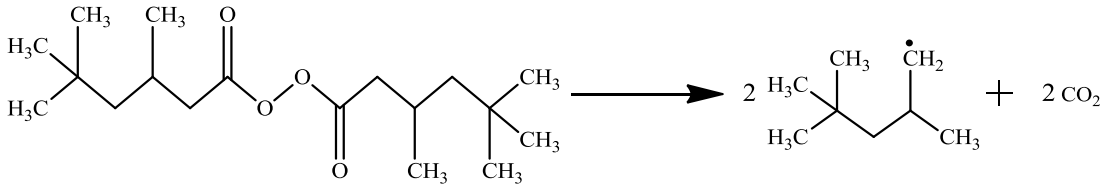

(a2)

The rate of formation of the primary radicals (R_i) is of greater interest in kinetic studies. R_i is described via the following general first order rate law:

$$R_i = -\frac{dc_I}{dt} = 2fk_d c_I \qquad (1)$$

where k_d corresponds to the rate coefficient of initiator decomposition and f is the initiator efficiency. The factor of 2 stems from the use of bifunctional initiators.

The difference in the decomposition rates of various initiators can also be expressed in terms of the initiator half-life. Half-lives of the initiators, which are the time required to reduce the original initiator concentration to half at a certain temperature, are of importance to assure a constant polymerization process. For instance, the half-life of AIBN is one hour at 82 °C and for BTMHP is one hour at 77 °C. On the other hand, the main advantages of choosing to use photo-initiation is that it gives the possibility of defining the exact starting and end times of the initiation, and subsequently those of the polymerization process.

1.3.1.3. Initiator efficiency, *f*

Initiator-derived radicals may have many possible fates. Initially, initiator-derived radicals are very close to each other and recombination can occur, so they have to escape the so-called cage effect in order to initiate the polymerization. Once they have escaped the cage, they can also react in alternative ways before they react with a monomer unit. They may react with solvent, oxygen, impurities, or monomer, thus starting the polymerization. Fragmentation and primary radical termination might also occur. Therefore, initiation is considered incomplete and is not 100% effective. Hence the initiator efficiency factor (*f*) is introduced, which describes the fraction of initiator-derived radicals that escape the initial cage and add to monomer. Thus *f* must have a value between zero and one. Typical values of *f* are between 0.4 and 0.9 depending on the viscosity and temperature of the reaction medium, indicating

that the escaping process is diffusion controlled. The value of *f* varies from initiator to initiator, and with conversion. For example, in passing from primary to tertiary peroxyesters, the initiator efficiency decreases. The in-cage reaction pathways of AIBN derived radicals are depicted in Figure 1-1.

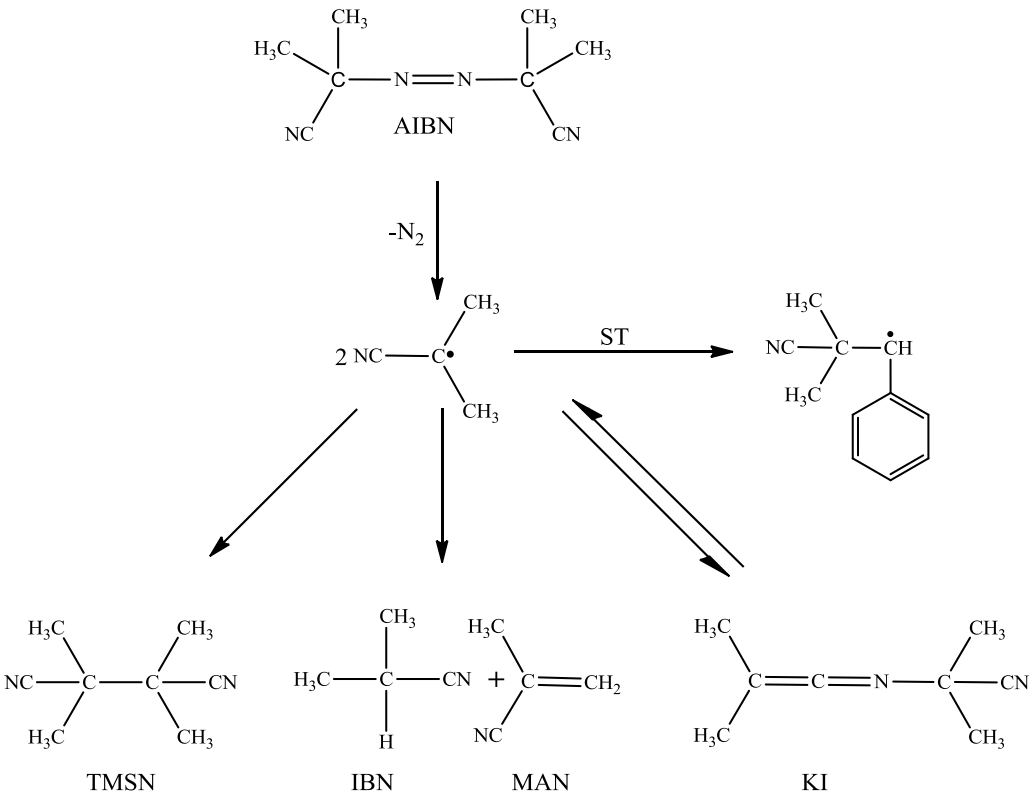

Figure 1-1. AIBN decomposition mechanism and products, where TMSN denotes 2,2,3,3-tetramethylsuccinodinitrile, IBN isobutyronitrile, MAN methacrylonitrile and KI ketenimine.[11]

This process is the first step of the chain reaction, which ultimately involves attack of the radical on the double bond of the monomer regenerating a free radical.

The reaction of the initiator-derived radical with a first monomer is considered as the second step of the initiation process. This step is still subtle and needs to be precisely evaluated. In most polymerizations this step is considered as being much faster than the first step, the decomposition step. The rate of reaction of the radical with the first monomer is chemically controlled and is most affected by substituents either at the site of the attack or at the radical

center. Substituents on the double bond strongly hinder addition at the substituted carbon while leaving the rate of addition at the other end essentially unaffected, making tail addition the predominant pathway. Remote substituents have only a small influence on the tail addition unless these groups are very bulky. Polar effects also have an important influence in determining the rate of addition. The traditional means of assessment of the polar factors is the electrophilicity or nucleophilicity of both radical and addition site. Electron-donating substituents such as alkyl on the double bond will enhance overall reactivity toward the electrophilic radical. Oxygen-centered radicals, for example, have an electrophilic character and enhance overall reactivity toward the nucleophilic attack site. Conversely, carbon-centered radicals have a nucleophilic character, having electron withdrawing substituents; for example, CN, CO_2R and Cl will enhance the overall reactivity toward the electrophilic attack site. The reaction below illustrates the reaction of an electrophilic radical with a nucleophilic monomer (Reaction b) where the overall reactivity of this reaction step is enhanced as a result of the polar effect.

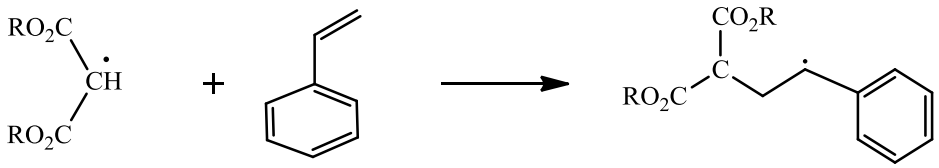

(electrophilic radical) (nucleophilic monomer) (nucleophilic radical)
Malonyl radical Styrene

(b)

Another example is the reaction of methyl radical in solution at room temperature with methyl methacrylate (MMA), which has rate coefficient 4.9×10^5 M^{-1} s^{-1}, while the reaction with styrene (ST) is slower, rate coefficient 2.6×10^5 M^{-1} s^{-1}.[12] The rate coefficient of the reaction of AIBN derived radicals with ST in solution at room temperature is 2 410 M^{-1} s^{-1},

while the reaction with MMA is slower, 1 590 M^{-1} s^{-1}, and the reaction with methyl acrylate (MA) even slower with the value 379 M^{-1} s^{-1}.[12] Conversely, nucleophilic radicals such as 2-hydroxy-2-propyl react very quickly in solution at room temperature with MMA, 1.6×10^7 M^{-1} s^{-1}, compared to 7.3 ×1 0^5 M^{-1} s^{-1} with ST.[13, 14] Furthermore, carbon-centered radicals are very sensitive to oxygen, reacting at greater than 10^9 $M^{-1}s^{-1}$, the diffusion-controlled limit.

Furthermore, this insight is strikingly illustrated by the observation of alternating-like copolymerization of electron-rich and electron-poor alkenes such as ST and MMA. Radical addition to ST will generate a nucleophilic radical that would prefer to react with an electron-poor double bond of alkene, MMA in this case. Therefore, reaction with MMA is faster than reaction with another molecule of ST. This reaction then produces an electrophilic radical that would prefer to react with the electron rich double bond of ST. This process is repeated to produce an alternating-like sequence of monomers.

These observations are simply explained by frontier molecular-orbital theory (FMO). FMO theory may also be applied to provide qualitative understanding of the radical reactions. During the radical addition, the semi-occupied molecular orbital (the SOMO) will interact with both π* antibonding orbital (the LUMO) and π- orbital (the HOMO) of the double bond of the alkene. Nucleophilic radicals with high energy SOMOs will prefer to react with alkenes containing electron-withdrawing substituents, as these have low-energy LUMOs. Conversely, electrophilic radicals with low-energy SOMOs will prefer to react with alkenes containing electron-donating substituents, as these have high energy HOMOs.

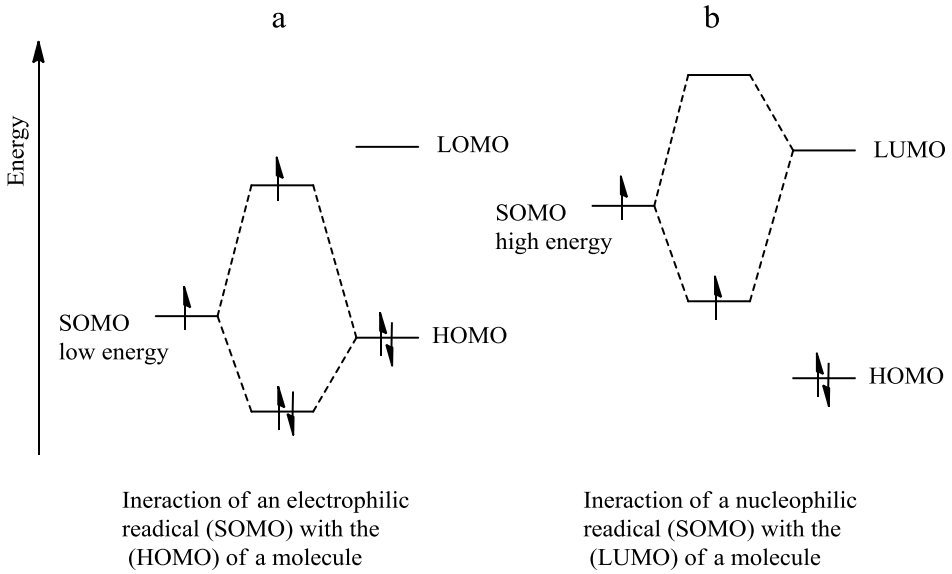

Figure 1-2. Illustration of interaction of an electrophilic radical SOMO orbital with the HOMO and LUMO orbitals of a molecule.

The newly generated radical can then in turn add on extra monomer units. Radical addition to another electron-rich alkene, such as styrene, will generate a nucleophilic radical that would prefer to react with an electron-poor alkene. This explains the alternating sequence of monomers observed in copolymerization of electron-rich (e.g. ST) and electron-poor (e.g. MMA) alkenes. Chain propagation sequences then carry on, starting the propagation stage.

1.3.2. Propagation

Propagation:

$$\begin{aligned} IM^{\bullet} + M &\longrightarrow IM_2^{\bullet} \\ IM_{i\text{-}1}^{\bullet} + M &\xrightarrow{k_p} IM_i^{\bullet} \end{aligned} \qquad (2)$$

The propagation step in radical polymerization, exemplified by Reaction (2), has particularly been a subject of scientific interest since the 1980s. The addition of monomer to a radical

species is considered to be a chemically controlled process, which means it is controlled by electronic, steric and polar effects of both monomers and radicals.

1.3.2.1. Monomers

The monomer is the basic unit in the propagation step that combine together to form repeating structural units that give polymers their unique properties. Polymers can consist of the same or different types of monomer, known as homopolymers or copolymers respectively. A wide variety of monomers are used in RP. Commonly, monomers with carbon-carbon double bonds (C=C) functionality feature are used. The identity of the monomer making up a polymer is the first important factor contributing to the polymer properties. It dictates how the chains interacts through various physical forces. The variety of monomers allows tuning of polymer properties. For example, methyl methacrylate (MMA) enhances the optical properties. The low index of refraction (1.49) and high degree of uniformity make PMMA an excellent lens material for optical applications, in addition to its excellent weatherability and a useful combination of stiffness, density and toughness. Therefore, PMMA is widely used for signs, glazing, lighting, fixtures, sanitary wares, solar panels, and automotive tail and stoplight lenses. Polystyrene, on the other hand, is a major commodity polymer used for other wide variety of commercial applications**.**

1.3.2.2. Propagation rate coefficient, k_p

The propagation rate coefficient (k_p) is found to be chemically controlled and not diffusion controlled, except under glassy conditions, which usually do not occur until very late in the polymerization.

Historically, the method used to measure k_p was by combining a $k_p/\langle k_t \rangle$ measurement from non-steady state polymerization (NSSP) with a $k_p/\langle k_t \rangle^{0.5}$ measurement from steady state

polymerization (SSP). Firstly this method requires accurate measurements without scatter. Secondly, the impossibility of having the same $\langle k_t \rangle$ in different experiments due to chain-length-dependent termination (CLDT) is a problem that cannot be rigorously overcome. Now, however, accurate k_p can be obtained by the IUPAC recommended PLP-SEC method, which was introduced by Olaj et al. in 1987.[8]. This method turned out to be a huge improvement in polymerization kinetic measurements and has resulted in IUPAC benchmark values for the k_p coefficients for many monomers. [9] The advent of this novel method for the accurate determination of k_p has also enabled the reliable measurement of other kinetic parameters such as the rate of termination,[15] which is the main focus of this thesis.

The addition of a macroradical to a monomer unit (Reaction p) leads to the following rate expression:

$$-\frac{\mathrm{d}c_M}{\mathrm{dt}} = k_\mathrm{p} c_\mathrm{R} c_\mathrm{M} \qquad (2)$$

Here k_p is the propagation rate coefficient of the macroradical; c_M is the monomer concentration; and c_R is the radical concentration.

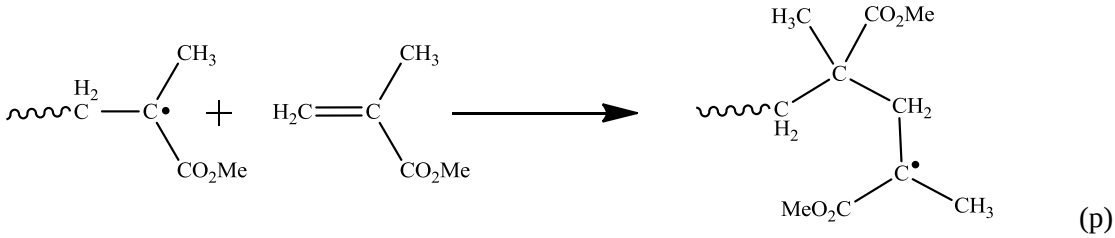

(p)

This rate expression makes the long-chain approximation (LCA), in which the monomer is assumed to be consumed only by propagation and negligibly via initiation and chain transfer.

Because of the chemical control, k_p is considered to be conversion independent except in the glassy region. Furthermore, the absolute propagation rate coefficient is governed by the

nature of the monomer and the reactivity of the propagating radicals. The rate of addition of propagating radicals to monomer is affected by many factors such as polar, resonance, and steric factors resulting from the substituents bound to the reacting carbon-carbon double bond and the radical center. Since propagation is chemically-controlled, solvents usually have no large effect on the propagation rate, except for some specific monomers. Interaction of solvent that can effect internal rotational or hindered vibrational degrees of freedom upon formation of the transition-state structure from radical and monomer molecule can result in a significant lowering of k_p such as in methacylic acid (MAA) polymerization in aqueous solution, where the k_p value is reduced with increasing MAA concentration.[16, 17] Polymer chains surrounding the radical center do not have any significant effect on the stereochemistry of propagation.[18]

The fact that propagation is chemically controlled rather than diffusion controlled does not mean that k_p is exempt from any chain-length dependence (CLD), particularly for oligomeric radicals.[19, 20]. Evidence suggests that the propagation step is chain-length dependent especially for the first few addition steps.[21] These proceed at a markedly increased rate compared to long-chain-propagation, as indicated by pulsed-laser polymerization data.[22] The rate of propagation of MMA for the first propagation steps, for example at 60 °C, is approximately 16 times faster than the long-chain propagation.[23] However, this dependence probably does not extend beyond $i \approx 10$.[24] Although some studies point toward a pronounced propagation effect up to 100 monomer units,[22], CLDP is still a new topic and has not been studied extensively.[21] Due to the lack of CLDP knowledge and not enough information available in literature, CLDP has not been accounted for quantitatively. However, it is important to point out that the key scaling law, $\langle k_t \rangle \sim DP_n^{-e}$, is insensitive to CLDP.[24]

1.3.3. Termination

Radical termination is the main focus of this project. Radical termination is the reaction in which chain radicals are destroyed and dead polymer molecules are formed (Reaction 3):

Termination:

Combination $IM_i^{\bullet} + IM_j^{\bullet} \xrightarrow{(1-\lambda)\, k_t^{i,j}} IM_{i+j}I$ (3a)

Disproportionation $IM_i^{\bullet} + IM_j^{\bullet} \xrightarrow{\lambda\, k_t^{i,j}} IM_i^{=} + IM_j$ (3b)

The termination reaction involves three main aspects: first, the formation of polymer products; second, the rate of termination of the chain radicals; and third, the mode of termination. First, a general overview of polymers is given followed by a discussion of each aspect of the termination process.

1.3.3.1. Polymers

Polymers are the products of the termination reactions. Polymer microstructure is a second major factor contributing to the polymer properties. The arrangement of these monomers along the backbone of the chain and the length of the chain are vital. Polyethylene, which is the most widely used polymer, and polypropene (PP) are good examples. PP is stronger and harder than polyethylene due to the presence of the substituted methyl group, which restricts the rotation of the PP chain and produces a less flexible but stronger polymer. An important microstructural feature of a polymer chain is its architecture. Polymers can be formed with different chain architectures: linear, branched, graft, star or network (see Figure 1-3).

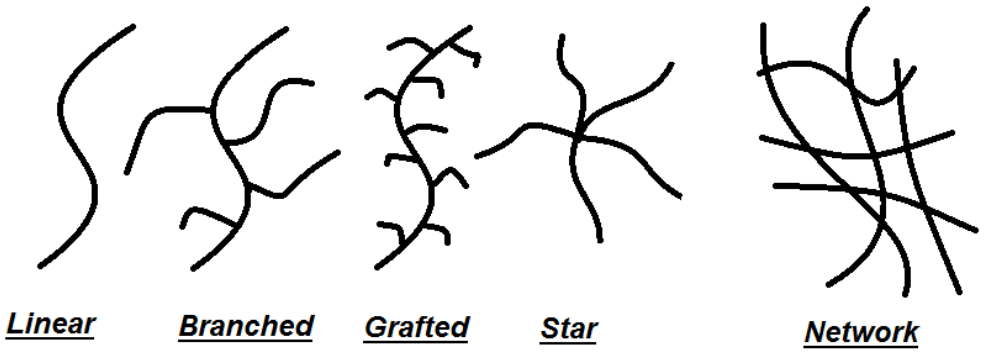

Figure 1-3. Linear and nonlinear chain architectures. The nonlinear polymers can be branched, star-like or a network structure.

Spatial orientation of the side group is also vital and results in different physical properties. They have the same simplified structural polymer formula but the spatial orientation of the side groups allows the different stereoisomeric forms to exist with different physical properties. Atactic polypropene (an amorphous or non-crystalline material) has an irregular structure due to the random arrangement of the methyl groups attached to the main carbon-carbon chain, and tends to be softer and more flexible than the isotactic form, where all the pendant methyl groups have the same regular orientation along the carbon-carbon polymer backbone. The stereoregular structure maximises the molecule-molecule contact, so increasing the intermolecular forces compared to the atactic form. This regular structure is much stronger than the atactic form and is produced efficiently by using Ziegler-Natta catalysts.

1.3.4. Termination rate coefficient, k_t

Radical termination is considered to be the most complex reaction in the radical polymerization process. It involves loss of free radicals, forming dead polymer chains. This complexity can be attributed to it being diffusion controlled rather than chemically controlled.[25] The rate of termination is a second-order reaction and can be expressed as:

$$R_t = -2k_t {c_R}^2 \qquad (3)$$

Here k_t represents the overall rate of termination, the sum of termination rate coefficients of combination ($k_{t,comb}$) and disproportionation ($k_{t,dis}$); and c_R is the total radical concentration. Also, in this termination rate equation, the IUPAC preferred factor 2 is used.[26]

Many parameters influence the value of k_t. The scatter of k_t values for the same monomer at the same temperature, for example tabulated in the *Polymer Handbook*,[27] (presented in Figure 1-4) is a direct demonstration of the influence of many parameters.

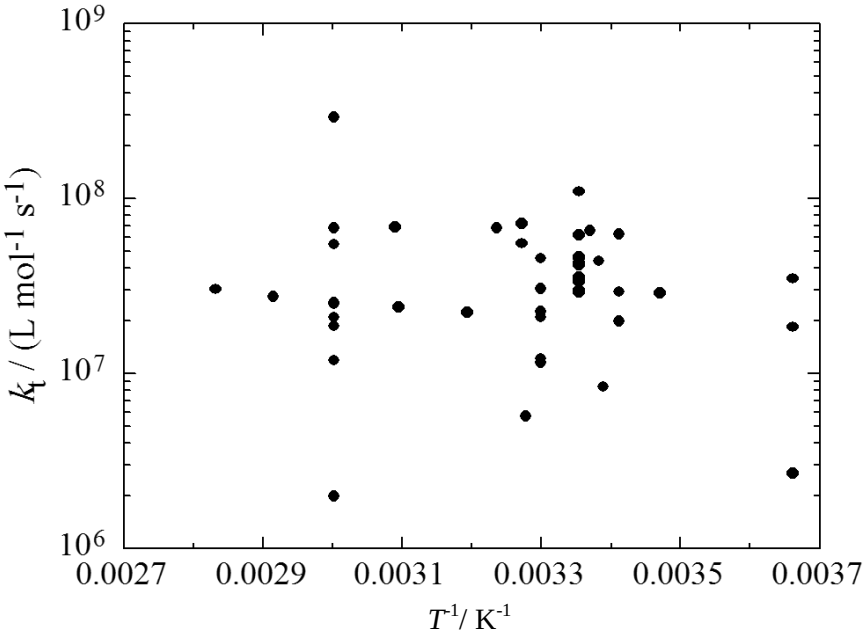

Figure 1-4. Ambient-pressure k_t values versus inverse (absolute) temperature for bulk polymerization of methyl methacrylate (MMA).[28]

k_t is a function of conversion, generally decreasing.[29-31] However, in the initial stage k_t is not very strongly dependent upon conversion of bulk polymerization. Furthermore, this stage is more extensive in solution polymerization. k_t is also affected by the solvent quality, whether good or poor. The value of k_t increases when going from good to poor solvents, as has been observed experimentally[32] and justified theoretically,[33] due to solvent having

an effect on the size of polymer coils.[34-36] Temperature and pressure also are important experimental parameters that affect k_t. In addition, because termination is diffusion controlled, viscosity has a large influence. However, even for low conversion where the impact of viscosity on termination is small, scattering of k_t is still observed.

Furthermore, due to diffusion control of termination, the long radicals must terminate more slowly than small radicals. Therefore, radical termination reactions are complicated further by being chain-length dependent. Consequently, the termination rate is highly system specific resulting in a wide scatter of k_t values in the literature (see above). This is because the radical chain-length distribution will be different from system to system, hence k_t will be different.

Because of the extremely fast reaction of the radical termination reaction, the translational-diffusion or the segmental-diffusion in almost all cases is the rate determining step. For instance, at low conversion the termination is believed to be segmental-diffusion controlled for reasonably large macro-radical chain lengths, and translational diffusion-controlled for short macro-radical chain lengths.[37-39] At intermediate conversion it is thought to be translational diffusion-controlled for all chain lengths.

Various methods are employed in the determination of $<k_t>$, by which chain-length averaged k_t is denoted. Most of these are indirect methods. Steady-state methods and non-steady-state methods based on either kinetics or molar mass measurement are the two main approaches.[7, 39]

1.3.4.1. Steady-state methods

Most radical polymerization is carried out with continuous initiation. This means that to excellent approximation, radical concentration is in a steady state. Thus steady-state polymerization (SSP) is when $dc_R/dt \approx 0$, that is, $R_i \approx R_t$, meaning that

$$c_{\mathrm{R}} = \left(\frac{R_{\mathrm{i}}}{2\langle k_{\mathrm{t}}\rangle}\right)^{0.5} \qquad (4)$$

Two experimental approaches can be thought of as determining the kinetic rate coefficient based on the steady state results: (1) based on the accurate measurement of the overall polymerization rate (R_p), and (2) based on the analysis of the resulting molar mass (molecular weight) distribution (MMD and MWD respectively).

First, substitution of the steady state result for c_R into the rate of propagation (Eq. 2) generates the familiar radical polymerization rate law equation:

$$R_{\mathrm{p}} = -\frac{\mathrm{d}c_{\mathrm{M}}}{\mathrm{d}t} = k_{\mathrm{p}}\left(f\frac{k_{\mathrm{d}}}{\langle k_{\mathrm{t}}\rangle}\right)^{0.5}(c_{\mathrm{M}})^{1}(c_{\mathrm{I}})^{0.5} \qquad (5)$$

Measurement of R_p is the conventional method for measuring average termination rate, $<k_t>$. Using the more recommended index of fractional conversion of monomer into polymer, x, the polymerization rate equation becomes Eq. 6,, which arguably the best suited equation for $<k_t>$ evaluation, for it means the assumption of constant c_M in taking the slope of a plot does not have to be made:

$$\frac{-\mathrm{d}\ \ln(1-x)}{\mathrm{d}t} = k_{\mathrm{p}}\left(\frac{f k_{\mathrm{d}} c_{\mathrm{I}}}{\langle k_{\mathrm{t}}\rangle}\right)^{0.5} \qquad (6)$$

This is called the classical or ideal polymerization rate law and serves as the basis for obtaining $k_p/(k_t)^{0.5}$, using simple techniques such as gravimetry and dilatometry. Of course, if k_p is known, then one can obtain the value of $<k_t>$ easily. Eq. 6 recommends that data be plotted as $-\ln(1-x)$ versus t, where a straight-line fit delivers the coupled parameter $k_p[fk_dc_I/<k_t>]^{0.5}$ as the slope. This equation holds both for CLIT and CLDT. This equation also does not require taking into account the volume contraction, a phenomenon that accompanies the polymerization reaction and contributes to a change in c_M. [40]

The major limitation of the classical kinetics model is that often there are significant variations of k_d, k_p, f and particularly $<k_t>$ with conversion. So it can be inaccurate to assume these parameters are constant. It means that equations must be solved while taking the variations of rate parameters into account, as appropriate, or by limiting the reaction to a small range of conversion. Although classical kinetics has been proven to be valid only for a small range of conversion, it is still incorrect to assume the rates of all reactions are constant, in particular for $<k_t>$, which is now accepted without dispute to be chain-length dependent.[39] In fact, generally, RP termination is diffusion controlled in rate. Consequently, termination rate coefficient is a function of the size of the two terminating chains and it necessarily leads to the reality of chain-length dependent termination (discussed later). Furthermore, Eq. (6) involves the long-chain approximation (LCA), which neglects the consumption of monomer by reactions other than propagation. The additional limitations of this method for $<k_t>$ determination are that it requires prior knowledge of fk_d and k_p, the difficultly of obtaining $<k_t>$ over narrow conversion ranges, and the problem of induction time which may be overcome by rigorous purification. However, many of these limitations are raised in most of the methods for k_t determination.

Measurement of radical concentration by electron paramagnetic resonance (EPR) spectroscopy is another method for k_t determination. It is a direct method in that it probes c_R rather than quantities that are affected by c_R. Then k_t in principle can be obtained from a single value of c_R if the rate has been simultaneously measured (see Eq. (2)). Although this method appears to be a very simple exercise, in reality it requires considerable expertise in order to obtain consistently accurate values. More information on this method can be found in the literature.[41]

Second, I outline the steady-state method based on MWD measurements. This method can employ fitting of molecular weight distribution and/or the use of number-average degree of

polymerization (DP_n) and/or Mayo plots. The fitting of size-exclusion chromatography molecular weight distribution (SEC-MWD), using the two-variable expression (Eq. 7) of the Schulz-Flory expression for MWD yields two parameter values: ν, which corresponds to the position of the MWD, and F_w, which corresponds to the width of the MWD.[42]

$$\frac{w(logi)}{\ln 10} = F_w(\frac{i}{\nu})^2 \exp\left(\frac{-i}{\nu}\right) + 0.5(1 - F_w)(\frac{i}{\nu})^3 \exp\left(\frac{-i}{\nu}\right) \qquad (7)$$

Here ν is the kinetic chain length and F_w is the weight-fraction of dead-chain formation by disproportionation and transfer, these being given by

$$\nu = \frac{k_p c_M}{k_{tr,X} c_X + 2k_t c_R}$$

$$F_w = \frac{k_{tr,X} c_X + 2\lambda k_t c_R}{k_{tr,X} c_X + 2\lambda k_t c_R + 2(1-\lambda) k_t c_R}$$

If all other values are known, then from ν one can obtain k_t and from F_w one can obtain λ. This method considers the body of information that is a MWD, concentrating it into a k_t value. This process obviously gives some feeling for the precision of a k_t value through the quality of the fit. However, the evaluation and analysis of reaction rates and molecular weight distribution resulting from radical polymerization is sometimes difficult, due to the coupled nature of the kinetic coefficients, the different chain lengths, and inaccuracy in experimental MWDs.

Mayo plots can also be used to deliver information about k_t. In principle, if all else is known in the Mayo equation (Eq. 8), then clearly a single measurement of DP_n yields an estimated value of k_t.

$$\frac{1}{DP_n} = \frac{(1+\lambda) k_t R_p}{\left(k_p c_M\right)^2} + C_{tr,X} \frac{c_X}{c_M} \qquad (8)$$

In practice, a series of experiments with constant c_M and varying c_I may be carried out, the results then being plotted as $1/DP_n$ versus R_p. Eq. (8) shows that $C_{tr,X}$, the coefficient of transfer to small-molecule species X, is obtained from the intercept and k_t from the slope, assuming k_p and λ are known. Alternatively, if only k_p is known, then the slope gives the coupled value $(1 + \lambda)k_t$.[43]

1.3.4.2. Non-steady-state methods

The non-steady-state methods are based on the time evolution of radical concentration, c_R, under conditions such that it is not constant. Traditionally, two distinguished periods of the polymerization reaction, known as pre-effect and post effect, were utilized. However, pulsed-laser polymerization (PLP) has revolutionized the study of RP kinetics. This is an example of the post-effect method. It is firstly used in conjunction with SEC to determine propagation rate coefficients, k_p, and then it may additionally be used to determine the coupled parameter k_p/k_t, thus providing access to termination rate coefficients, k_t. PLP offers a unique advantage for the study of k_t over other means of carrying out RP. In particular, it is Buback's SP-PLP method that is uniquely positioned for studying termination.[15] This method involves time-resolved monitoring of the polymerization kinetics on a sub-second timescale following a single laser pulse, where the pulse creates sufficient concentration of radicals, c_R, from photoinitiator that the rate of termination far exceeds the rate of any background initiation processes. Thus the way in which c_R evolves with time, which is the information delivered by a SP-PLP experiment, directly reflects how the rate of termination evolves with time.

The distinct feature of this approach is that radical chain-length distribution (RCLD) is approximately monodisperse at any instant, assuming negligible subsequent reaction of radicals by transfer, and negligible c_R prior to irradiation at t =0. Thus termination rate at any instant reflects the rate coefficient for termination between radicals of the same size at that

instant, making SP-PLP not only suitable for measuring k_t, including its conversion dependence, but also making it ideal for probing CLDT.

The SP-PLP approach has employed different monitoring techniques. Online near infrared (NIR) spectroscopy has been used to monitor the evolution of c_M with time on a microsecond timescale. To obtain the coupled rate k_p/k_t from such measurements, the resulting variation is fitted with Eq. 9 to obtain k_p/k_t, from which k_t can be obtained if k_p is known.

$$\frac{c_M}{c_{M,0}} = \left(2k_t c_{R,0} t + 1\right)^{-k_p/(2k_t)} \qquad (9)$$

This equation assumes k_t is independent of time. Even though SP-PLP-NIR has yielded good quality information on termination kinetics,[44] implementation of this method for measuring $k_t^{i,i}$ across a large range of i has some difficulties, due to the problem of noise in the second-derivative of $c_M(t)$, making it hard to impossible to distinguish between different variations of $k_t^{i,i}$ with i. However, a more direct method has been used where the radical concentration is monitored directly, using EPR spectroscopy, hence the term SP-PLP-EPR. In fact it has rapidly emerged as the most powerful technique for determining $k_t^{i,i}$. This method has greater accuracy as compared with SP-PLP-NIR and in fact it is held by IUPAC task group to be of great potential for investigating termination kinetics.[7] An example of this approach is using Eq. 10, which follows from the power law $k_t^{i,i} = k_t^{1,1}\, i^{-e}$. It suggests plotting data as $\log[(c_{R,0}/c_R)-1]$ versus $\log t$, where a straight line with slope $1-e$ should result.

$$\frac{c_{R,0}}{c_R} - 1 = \frac{2c_{R,0}k_t^{1,1}}{k_p c_M (1-e)}\left[\left(k_p c_M t + 1\right)^{1-e} - 1\right] \qquad (10)$$

Here $c_{R,0}$ is the value of c_R immediately after the laser pulse, k_p is the propagation rate coefficient, c_M is the monomer concentration, $k_t^{1,1}$ denotes the rate coefficient for termination between monomeric free radicals, and e is the chain length dependence.

Although this method is the most powerful tool for detailed investigation into k_t, it involves equipment that is both relatively costly and requiring of a relatively high level of technical expertise.

1.3.5. Chain-length dependent termination, CLDT

Termination has been discussed without much attention to the chain-length dependence of the termination processes. Although by browsing older literature one can encounter a number of suggestions about the nature of non chain-length dependent termination, e.g. [45-49], CLDT has only been recently recognized as an essential factor in RP kinetics.[39] The idea was first suggested in the 1940s as the cause of the autoacceleration of polymerization or the so-called gel effect,[50] in which decreasing k_t was the explanation for the sudden increase in the polymerization rate. Notwithstanding an unverified CLDT suggestion that the reduction in k_t is most reasonably caused by the increase in viscosity that slows the diffusion of terminating polymer radicals, the argument clearly arises that k_t is diffusion controlled, and where CLDT is then an obvious consequence, because diffusion of short polymeric radical chains is self-evidently more rapid than diffusion of long chains. However, a detailed mechanistic account of the diffusion processes that produce the gel effect remains unresolved.

CLDT has been experimentally verified using different approaches, including termination of non-propagating species of different size,[51-54] termination mimic reactions,[55-58] and termination in RP. Early evidence of CLDT can be traced back to various research carried out in the early 1960s,[59] for example in the work of Hughes and North,[60] in which they observed that the $<k_t>$ determined for MMA from relatively small radicals was significantly higher than the one from relatively large radicals. Further, Fischer [61] employed an ESR flow technique to determine the termination rate coefficient of oligomers and found a decrease in the value of $<k_t>$ with increasing size of the radicals.

Schnabel and coworkers found (from a mimic reaction, using quenching techniques) a lower k_t value, by about a factor of two, for the interaction between S-L species compared with S-S interactions,[56, 62], where L and S denote large and small species respectively. They also found that k_t for L-L interactions is much lower than for S-L interactions.[55] Similar results were obtained for S-S and S-L interactions in benzene by Horie, et al., where they used low-PDI polystyrene with functionalized ends.[57, 58, 63] All these results are consistent not just with CLDT, but with it being Smoluchowski-like in nature, as one would expect.

Yasukawa et al.[64, 65] and Ito [32, 66] also found evidence of CLDT based on MWD and polymerization rates of MMA and ST. Yasukawa et al., for instance, calculated the MWD of styrene polymerization with chain-length dependent and chain-length independent termination rate coefficients, where the best agreement between simulation and experimental results was obtained if a chain-length dependence of k_t was used. Furthermore, O'Driscoll and Mahabadi found, using spatially intermittent polymerization, that the termination rate coefficient is a function of chain length for both MMA [67] and ST[68].

As typical free radical termination reactions occur between radicals of different chain length, CLDT means that termination reactions between these radicals should be treated as non-equivalent and should be assigned to a specific microscopic termination rate coefficient, i.e., their chain length should be taken into account; the notation $k_t^{i,j}$ is used, where i and j represent the chain length of the terminating radicals. The termination reaction in typical RP involves many different pairs of i and j, so the k_t values obtained from conventional techniques are macroscopic or average k_t, denoted also as $\langle k_t \rangle$. The observed $\langle k_t \rangle$ at any time in the polymerization is the average of all the $k_t^{i,j}$ weighted by the fraction of chains of each chain length. The relation between the macroscopic and microscopic termination rates, (Eq. 11), was first put forward by Allen and Patrick;[59] it follows simply from equalizing the macroscopic and microscopic rates of the loss of radicals:

$$\langle k_t \rangle = \frac{\sum_i \sum_j k_t^{i,j} [R_i^\bullet][R_j^\bullet]}{\left(\sum_i [R_i^\bullet]\right)^2} \qquad (11)$$

Although there is more direct evidence that the termination process is diffusion controlled[25] and thus chain-length dependent,[39] there is ongoing uncertainty over how this interacts with conversion dependence, which is also a result of diffusion control. For example, bulk polymerization of both *n*-dodecyl methacrylate (DMA) and *n*-dodecyl acrylate (DA) shows a constant k_t over an extended range of conversion,[69], which makes termination processes for DMA and DA difficult to understand.[70] To avoid the dependency of the kinetic parameters upon conversion, experiments have been carried out over conditions such that there were known to be relatively little change in termination rate coefficient with conversion, often at so-called zero conversion. SP-PLP is without peer in this respect, because usually it involves conversion changes that truly are small enough to be neglected. On the other hand, observation of the dual effect has clearly been illustrated using so-called RAFT-CLD-T (Reversible addition-fragmentation chain transfer chain-length-dependent termination), recognizing $k_t^{i,i}$ as a function of i and x.[71] Figure 1-5 exemplifies the use of such a technique to map out the $k_t^{i,i}(i,x)$ of homo-termination of bulk methyl acrylate (MA).

In fact, termination chain-length dependency is considered to be the cause of many mysteries in radical polymerization. It has been pointed out several times that this chain-length dependence of termination kinetics is one of the reasons why such an enormous scatter exists in literature tabulations of kinetic parameters.[72-75]

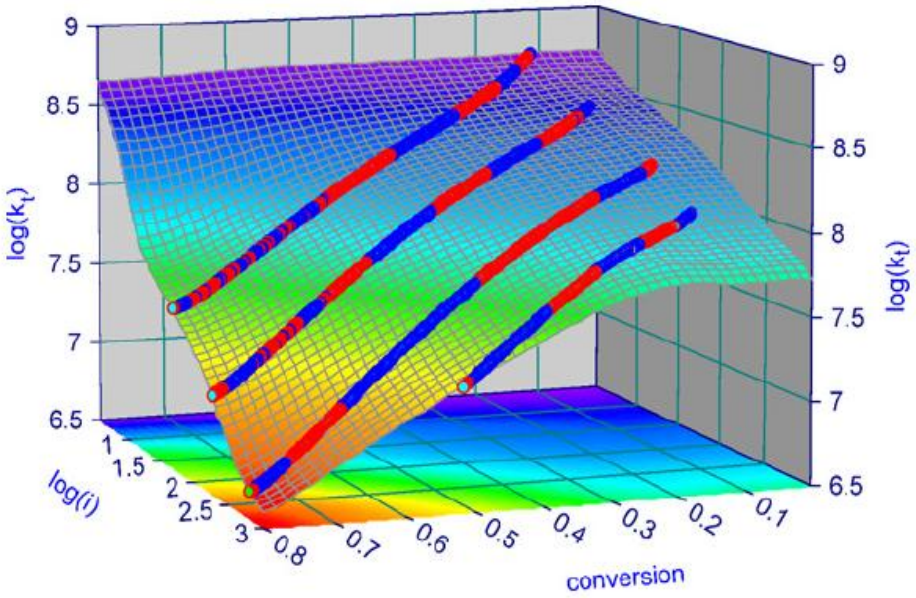

Figure 1-5. 3-Dimensional plot of the homo-termination of rate coefficient $k_t^{i,i}$ (L mol^{-1} s^{-1}) for bulk polymerization of methyl acrylate (MA) at 80 °C as a function of chain length, *i*, and fractional conversion of monomer into polymer. The curves are the results from RAFT-CLD-T experiments; the surface is a contour fit of these results. The red and blue parts of the experimental data indicating very minor under- and overestimates of the fitted surface.[71]

Despite the few directly proposed and tested methods for investigation of CLDT, sufficient evidence of CLDT has been found using different recent techniques such as SP-PLP-EPR, SP-PLP-NIR and RAFT-CLD-T. These methods rely on the control of radical chain length either by using a RAFT agent or by applying SP-PLP techniques. Using a RAFT agent and SP-PLP allowed control of chain length and an establishment of narrow CLD of radicals, which simplified the kinetic treatment by reducing a multitude of $k_t^{i,j}$ values essentially to $k_t^{i,i}$, representing the termination of radicals with identical chain length. The chain length dependence of $k_t^{i,i}$ may be represented by the power law expression,

$$k_t^{i,i} = k_t^{1,1}\, i^{-e} \qquad (12)$$

where $k_t^{1,1}$ denotes the rate coefficient for termination between monomeric free radicals, $k_t^{i,i}$ represents the rate coefficient for termination between identical chain lengths *i*, and *e* is a power-law exponent representing the chain-length-dependence of termination.

Even though PLP is probably the most important advance in experimental methods in the investigation of CLDT, a simple method such as steady-state number average degree of polymerization method (also referred to as SS-DP_n method) can also be used to deliver quantitative information on CLDT, as first published by Mahabadi.[76] He derived an analytical expression relating the macroscopic $\langle k_t \rangle$ to the number-average degree of polymerization, DP_n, expressed via the following power law:

$$\langle k_t \rangle \approx k_t^{1,1} DP_n^{-e} \qquad (13)$$

Thus, remarkably, $\langle k_t \rangle$ closely approximates the homo-termination rate coefficient for mean chain length DP_n. From the above equation the chain-length dependence of $\langle k_t \rangle$ is easily described and quantified. Importantly, of course, the probing of CLDT at small chain lengths brings the issue of CLDP into play. Again, as mentioned earlier, $\langle k_t \rangle \sim DP_n^{-e}$ is relatively insensitive to CLDP.[24]

Mahabadi found the exponent *e* to be approximately 0.24 for ST at 30 °C (where 780 < DP_n < 2 770) and 0.15 for MMA at 25 °C (190 < DP_n < 14 200).[76] Furthermore, this relationship has been found to hold also for PLP experiments, where an approximate value of e = 0.17–0.19 for ST at 25 °C(120 < DP_n < 1 385)[77] and 0.16–0.17 for MMA at 25 °C (270 < DP_n < 1 264) have been obtained.[78] These compare favourably with the ones obtained by Mahabadi.

The value of *e* depends on the size of the terminating macroradicals undergoing termination. Specifically, the value $e \approx 0.5–0.6$ holds, for short chains, where center-of-mass diffusion is held to be the rate determined step, while $e \approx 0.16$ for long chains, where segmental diffusion is the rate determining step. Moreover, CLDT has an effect on MWDs and hence on polymer properties; in fact, it acts to broaden MWDs, as illustrated in Figure 1-6. For equations and theoretical basis one is referred to this recent reference. [79]

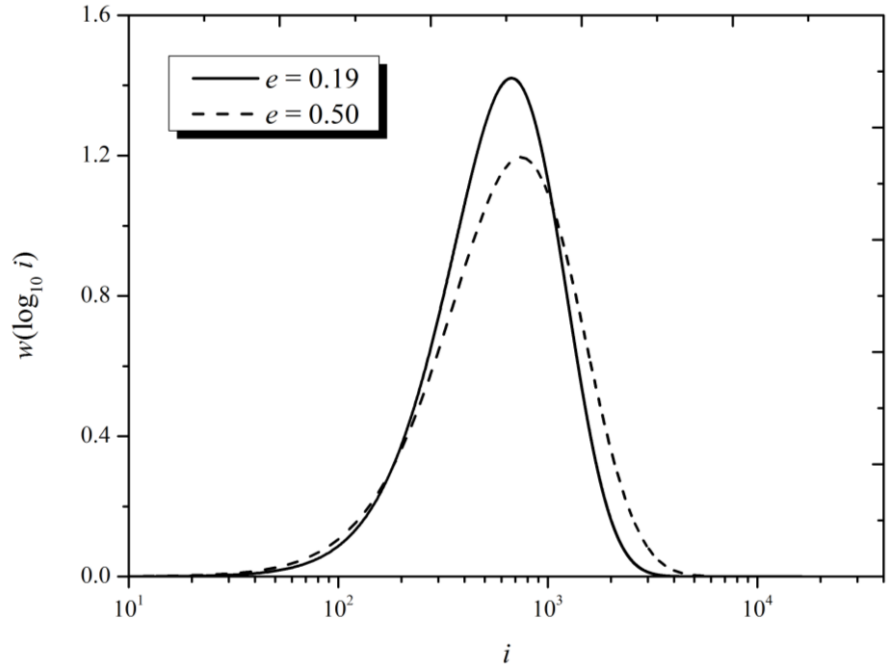

Figure 1-6. Normalized chain-length distributions allowing for CLDT[79] presented as $w(\log_{10} i)$, where w is weight fraction and i is chain length, using $F_w = 0$ and $DP_n = 425$ with $e = 0.19$ ($\nu = 135$) and $e = 0.5$ ($\nu = 65$). These different ν values were chosen so that $DP_n = 425$ in both cases.

1.3.6. Mode of termination, λ

The third element in the termination process, as shown in Reaction 3, is the mode of termination. Termination may take place by one of several processes. One of these is a combination of two growing chains together, reaction (c), while the other is disproportionation through the transfer of a hydrogen atom, reaction (d). The combination reaction leads to the formation of one dead polymer chain, while termination by disproportionation results in the formation of two polymer chains.

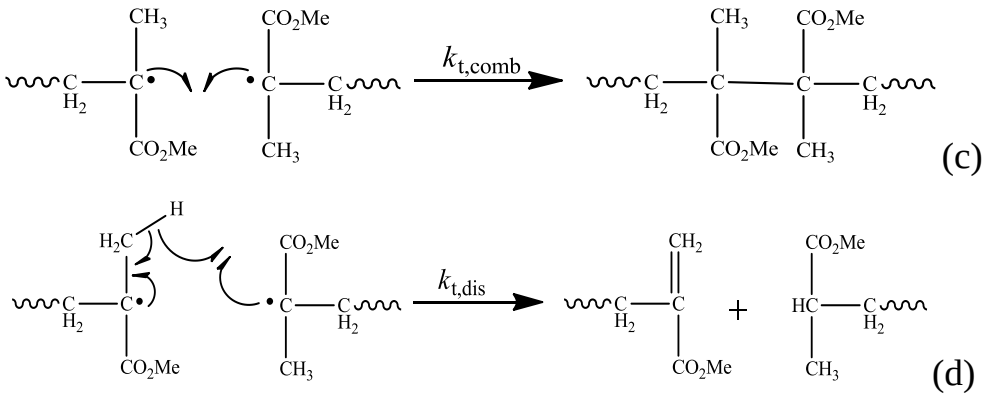

The fraction of termination events that occurs by disproportionation is denoted by λ (Eq. 14) and is referred to as mode of termination:

$$\lambda = \frac{k_{\mathrm{t,dis}}}{k_{\mathrm{t}}} = \frac{k_{\mathrm{t,dis}}}{k_{\mathrm{t,dis}} + k_{\mathrm{t,comb}}} \qquad (14)$$

Here $k_{\mathrm{t,dis}}$ is the rate coefficient for disproportionation, $k_{\mathrm{t,comb}}$ that for combination, and thus $k_{\mathrm{t}} = k_{\mathrm{t,dis}} + k_{\mathrm{t,comb}}$ is the overall rate coefficient for termination

This fact of two distinct pathways of termination in RP immediately raises questions about the relative importance of each of these modes. This fraction of termination events has an influence on the MWD of the dead polymer chain resulting from RP. The mode of termination plays an additional role in terms of polymer modification in that it influences the end groups, which frequently are used for post-modification.

An important feature is that the mode of termination affects the MWD, in particular its broadness. Consequently, information about the mode of termination might also be acquired by analyzing the MWD obtained. The value of λ can be extracted from F_{w} via fitting of Eq. 7 and allowing for CLDT if all else is known. However, one should be careful not to ignore CLDT when using this method, as this would lead to a non-physical value, because CLDT also acts to broaden the MWD (see Figure 1-6).[39] Figure 1-7 illustrates the partial effect of λ, equivalent to F_{w}, on the MWD. However, the accuracy of SEC may still limit the applicability of this method to obtain detailed kinetic information.

Although knowledge of these processes is indispensable, not much data about this parameter can be found in the literature. Figure 1-8, which shows literature values of λ for methyl methacrylate, MMA, using several experimental approaches, clearly presents a displeasing picture.[80]

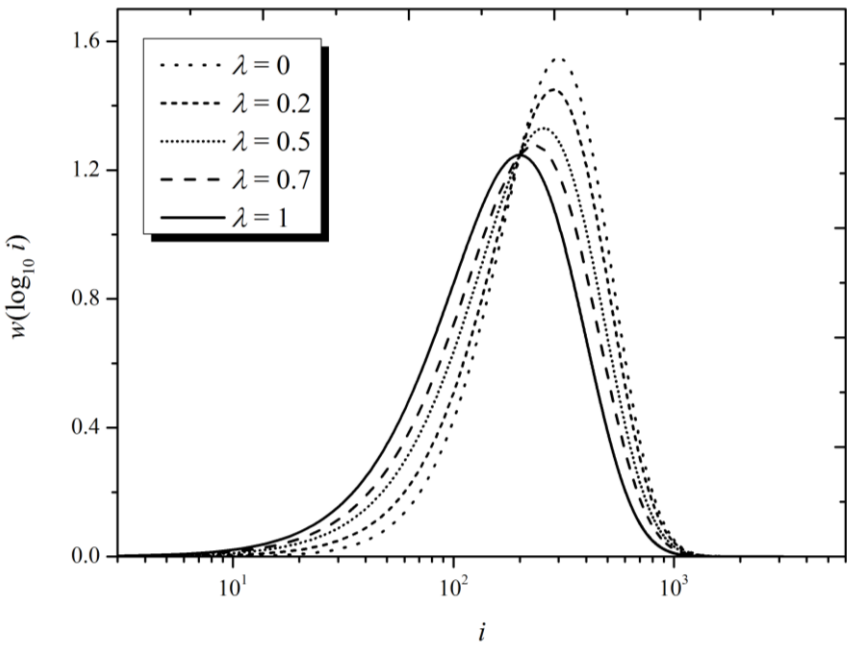

Figure 1-7. Illustration of the effect of λ (equivalent to F_w) on MWD using the Schulz-Flory distribution (which holds for CLIT, i.e., e = 0), calculated using Eq. 9 with v = 100 and different F_w, where F_w = 1 is 100% disproportionation and 0 is 100% combination. The distributions are presented as $w(\log_{10}i)$, where w is weight fraction and i is chain length.

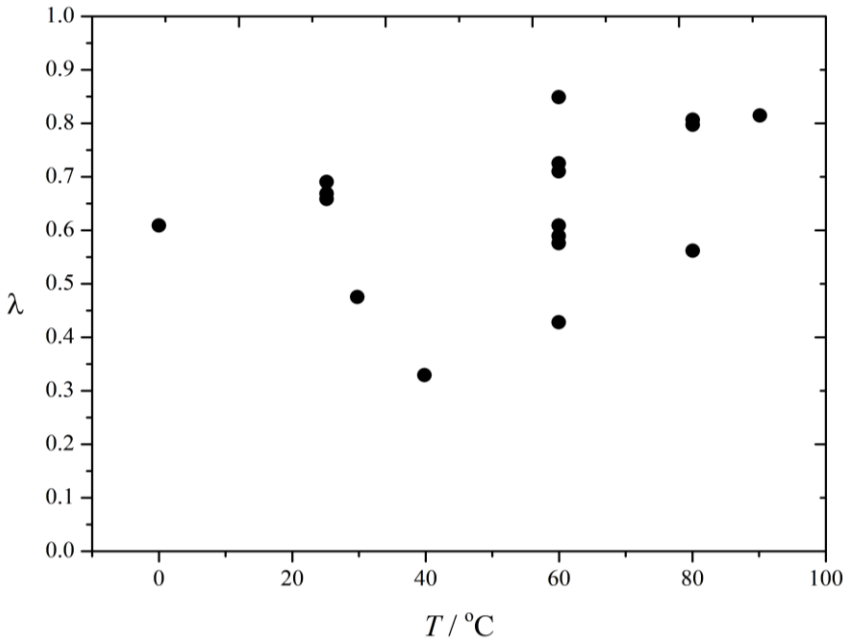

Figure 1-8. Literature measurements of λ for MMA as a function of temperature using several experimental approaches.[80]

How to rectify the situation in Figure 1-8? Fortunately, large-molecule mass spectrometry (MS) seems to provide a more suitable pathway to resolve this problem. Disproportionation and combination give rise to polymer molecules of different molar mass, and thus MS can distinguish species formed by each termination process. Electrospray ionisation mass spectrometry (ESI-MS), in particular, which has been broadly used for polymer characterizations,[10, 81, 82] has been recently used to quantitatively measure this parameter.[83] The idea sketched by Olaj and Schnöll-Bitai, [84] and Sarnecki and Schweer,[85] then developed by Zammit et al. [86], has been improved recently by Buback et al.[83] This technique shows the ability to access qualitative and quantitative information on the termination mode by end-chain analysis, which is the basic idea for determination of λ. This technique, in fact, involves a direct observation of the products of disproportionation and combination. Therefore, quantitative comparison of the signals from disproportionation and combination makes it possible to obtain λ.

Buback et al. determined λ only for MMA and only at a single temperature and ambient pressure.[83] Figure 1-8 shows that nothing is known from the literature about the variation of λ with T and p. Therefore filling this gap is an aim of my project.

1.3.7. Chain Transfer

A further possibility for chain termination is chain transfer (to a small molecule). It is not a complete termination reaction, but it ends the propagation of a growing chain and enables a new one to commence, as represented by Reaction 4:

Transfer: $$IM_i^{\bullet} + X \xrightarrow{k_{tr,X}} IM_i + X^{\bullet} \qquad (4)$$

Chain transfer could occur in the presence or absence of a transfer agent that is deliberately added. An important feature of this reaction is to control the chain length of polymer, allowing for the regulation of the molecular weight of the generated polymers. Indeed, the measured average molecular weights obtained from molecular weight distributions of polymers generated by radical polymerization processes are lower than predicted by accounting for initiation, propagation and termination processes alone. This is attributed to chain transfer reactions. Side benefits of this include reduction of the viscosity of the reaction medium and therefore better heat transfer, making it an important addition for industrial processes.

However, chain transfer often occurs without the specific addition of chain transfer agents. This is because chain transfer may also take place via transfer to monomer, solvent, initiator and polymer. Transfer to monomer is the only one that cannot be avoided. It is usually low, approximately of the order $k_{trX}/k_p \approx 10^{-5}$ at 50 °C.[18, 87]

The transfer is usually reported in a ratio with the propagation rate coefficient, resulting in the so called transfer constant, $C_{tr,X,}$ where X denotes the species to which transfer occurs:

$$C_{\mathrm{tr,X}} = \frac{k_{\mathrm{tr,X}}}{k_{\mathrm{p}}} \qquad (15)$$

Even though most organic solvents exhibit transfer constants similar to those found for common monomers, transfer to solvent can be of considerable importance, because of solvent's high concentration. However, in the event that the transfer constant of the solvent is sufficiently high, it should additionally be thought of as a transfer agent. On the other hand, the transfer to initiator can be minimised via the choice of the initiator employed. For example, azo-compounds are known to have negligible transfer activity.[43]

Intermolecular chain transfer to polymer becomes significant at high monomer conversion. Historically it has been important in ethylene systems where the transfer results in so-called long chain branching. However, over the last decade it has come to be recognized as important in acrylate systems.[88, 89]. Furthermore, intramolecular chain transfer to polymer is an additional important reaction that needs to be considered especially with acrylate as this transfer is also unavoidable. That said, it is not thought to occur to any significant extent in methacrylate and styrene systems, which means that the tremendous kinetic complications introduced by having mid-chain radicals are avoided.[88]

Eq. 16 is the explicit version of the Mayo equation (Eq. 8) which is frequently used to derive the chain transfer constant $C_{tr,X}$ based on the change in the degree of polymerization on addition of a transfer agent:

$$\frac{1}{DP_n} = \frac{(1+\lambda)\langle k_t \rangle R_p}{\left(k_p c_M\right)^2} + C_{tr,M} + C_{tr,I}\frac{c_I}{c_M} + C_{tr,S}\frac{c_S}{c_M} \qquad (16)$$

Here DP_n is again the number-average degree of polymerization, $C_{tr,S}$, $C_{tr,M}$ and $C_{tr,I}$ are the chain transfer constants for solvent, monomer and initiator respectively, c_S solvent concentration, c_M monomer concentration, c_I initiator concentration, R_p rate of polymerization, k_p propagation rate coefficient, $\langle k_t \rangle$ average termination rate constant and λ is mode of termination.

Obtaining a correct $C_{tr,X}$ requires some conditions, all of which basically reduce to CLDT having only a small effect. Of course temperature has an effect on the transfer constant, for example a decrease of the temperature normally lowers the monomer transfer constant, $C_{tr,M}$. The activation energies for $C_{tr,M}$ in MMA and ST are 23.74 kJ mol^{-1} [87] and 23.4 kJ mol^{-1} [90] respectively.

1.3.8. Solvents

Solvent effects are very important when carrying out polymerization in solution. Although solvent effects in radical polymerization are usually much less significant than for ionic reactions, there can still be a medium effect. This is primarily related to solvent viscosity, on account of diffusion playing such a central role in the process. In addition, the solvent effect on polymerization can also be accounted for by reactivity and its ability to dissolve the polymers produced.[91]

With regards to k_p, the solvent effect can be negligible when there are no strong intermolecular interactions. However, strong intermolecular interactions with solvent, such as hydrogen bonding, can affect the k_p. This is exemplified by methacrylic acid polymerization in aqueous solution, as mentioned earlier.[16, 17]

As termination is diffusion-controlled, solvent viscosity and polymer solubility may be major factors relevant to the termination process. For example, the value of k_t of styrene and butyl acrylate increases with $scCO_2$ content. The k_t is significantly higher in $scCO_2$ than in bulk.[92, 93] This has been attributed to the poor solubility of the monomer in this solvent, leading to a reduction in coil size, which, in turn, results in higher rates of segmental diffusion. Importantly, when solvent is the saturated analogue of monomer, for example ethylbenzene and methyl isobutyrate in the cases of ST and MMA respectively, there should be negligible change in the viscosity and solvent power that can influence k_t.

1.4. Aims of this study

Although the technique of RP has been used extensively for over 70 years in the industrial production of polymers, detailed understanding of the termination process in particular still has not been achieved. It is highly advantageous to know the effect of solvent, monomer and

initiator concentration, not to mention pressure and temperature, on this process, not least of all because termination has a large influence on the properties of polymer products, and thus accurate knowledge of the termination kinetics process is essential for improving control of final polymer properties. Particularly when the polymerization process is scaled up to commercial proportions, a detailed understanding of the chemistry behind the kinetic process can make a difference. Moreover, understanding how CLDT and the mode of termination take place are important factors due to their direct influence on polymer properties.

The broad goal of this thesis is to study the effect of different factors on the termination process and, in particular, on the termination rate coefficient and the mode of termination. The major part of this work deals with CLDT, primarily for relatively short polymer chains (i.e. oligomers). In fact, not much radical polymerization investigations have been done on short polymers where a large influence of CLDT is expected. Indeed, this would lead to more understanding of the complete picture of the termination process. Notwithstanding its importance, the synthesis of polymers with relatively low molar masses has recently become of increasing interest. These polymers have been found to be useful in a variety of products such as high solids or solvent-free coatings, in adhesives, as plasticizers in polymeric compositions, and as reactive intermediates for the production of a wide variety of other materials such as surface-active agents;[94] these are all areas where the outcome of this work may have practical importance.

1.5. Thesis outline

The overall work of this thesis can be divided into two main projects. The first part is dedicated to radical termination reactions. Observation of the effects of solvent, monomer,

initiator, temperature, pressure and growing radical size on $\langle k_t \rangle$ (or, equivalently, R_p) is explored in Chapters 3, 4 and 5. The effect of monomers is also considered.

Determination of the mode of termination is the second part of this work, and is discussed in Chapters 6 and 7. The effects of initiator, solvent, instrument, chain length, temperature and pressure on the mode on termination are studied. The effect of monomer on the mode of termination is also considered.

In the final part of this work, Chapter 8, preliminary investigation into the strong auto-acceleration for bulk MMA radical polymerization using Raman spectroscopic techniques is presented. To avoid repetition, common experimental procedures that are employed throughout this thesis are presented next in Chapter 2.

References

[1] C.E.S.R.B. Carraher, Polymer Chemistry, CRC Press, Boca Raton, 2007.
[2] M. Stickler, Die Makromolekulare Chemie, 187 (1986) 1765-1775.
[3] K. Matyjaszewski, N.V. Tsarevsky, Nature Chemistry, 1 (2009) 276-288.
[4] A. Rudin, The elements of polymer science and engineering : an introductory text and reference for engineers and chemists, 2nd ed., Academic Press, San Diego, 1999.
[5] M. Buback, J. Sandmann, Zeitschrift fur Physikalische Chemie, 214 (2000) 583-607.
[6] M. Buback, D. Nelke, H.P. Vögele, Zeitschrift fur Physikalische Chemie, 217 (2003) 1169-1191.
[7] C. Barner-Kowollik, M. Buback, M. Egorov, T. Fukuda, A. Goto, O.F. Olaj, G.T. Russell, P. Vana, B. Yamada, P.B. Zetterlund, Progress in Polymer Science (Oxford), 30 (2005) 605-643.
[8] O.F. Olaj, I. Bitai, F. Hinkelmann, Die Makromolekulare Chemie, 188 (1987) 1689-1702.
[9] M. Buback, R.G. Gilbert, R.A. Hutchinson, B. Klumperman, F.-D. Kuchta, B.G. Manders, K.F. O'Driscoll, G.T. Russell, J. Schweer, Macromolecular Chemistry and Physics, 196 (1995) 3267-3280.
[10] M. Buback, H. Frauendorf, F. Günzler, P. Vana, Polymer, 48 (2007) 5590-5598.
[11] M. Buback, B. Huckestein, F.D. Kuchta, G.T. Russell, E. Schmid, Macromolecular Chemistry and Physics, 195 (1994) 2117-2140.
[12] H. Fischer, L. Radom, Angewandte Chemie - International Edition, 40 (2001) 1340-1371.
[13] H. Fischer, L. Radom, Macromolecular Symposia, 182 (2002) 1-14.
[14] R. Martschke, R.D. Farley, H. Fischer, Helvetica Chimica Acta, 80 (1997) 1363-1374.
[15] M. Buback, H. Hippler, J. Schweer, H.-P. Vögele, Die Makromolekulare Chemie, Rapid Communications, 7 (1986) 261-265.
[16] S. Beuermann, M. Buback, P. Hesse, F.-D. Kuchta, I. Lacík, A.M. Van Herk, Pure and Applied Chemistry, 79 (2007) 1463-1469.
[17] S. Beuermann, M. Buback, P. Hesse, I. Lacík, Macromolecules, 39 (2006) 184-193.
[18] K. Matyjaszewski, T.P. Davis, Handbook of radical polymerization Wiley-Interscience, 2002.
[19] G.B. Smith, J.P.A. Heuts, G.T. Russell, Macromolecular Symposia, 226 (2005) 133-146.
[20] G.B. Smith, G.T. Russell, M. Yin, J.P.A. Heuts, European Polymer Journal, 41 (2005) 225-230.
[21] J. Heuts, G.T. Russell, European Polymer Journal, 42 (2006) 3-20.
[22] O.F. Olaj, P. Vana, M. Zoder, A. Kornherr, G. Zifferer, Macromolecular Rapid Communications, 21 (2000) 913-920.
[23] A.A. Gridnev, S.D. Ittel, Macromolecules, 29 (1996) 5864-5874.
[24] J.P.A. Heuts, G.T. Russell, G.B. Smith, A.M. Van Herk, Macromolecular Symposia, 248 (2007) 12-22.
[25] M. Buback, M. Egorov, R.G. Gilbert, V. Kaminsky, O.F. Olaj, G.T. Russell, P. Vana, G. Zifferer, Macromolecular Chemistry and Physics, 203 (2002) 2570-2582.
[26] M. Buback, R.G. Gilbert, G.T. Russell, D.J.T. Hill, G. Moad, K.F. O'Driscoll, J. Shen, M.A. Winnik, Journal of Polymer Science, Part A: Polymer Chemistry, 30 (1992) 851-863.
[27] J. Brandrup, E.H. Immergut, E.A. Grulke, Polymer Handbook, 4th ed., Wiley, 1999.
[28] D.R. Taylor, K.Y. Van Berkel, M.M. Alghamdi, G.T. Russell, Macromolecular Chemistry and Physics, 211 (2010) 563-579.
[29] S. Beuermann, M. Buback, G.T. Russell, Macromolecular Chemistry and Physics, 196 (1995) 2493-2516.

[30] M. Buback, F.-D. Kuchta, Macromolecular Chemistry and Physics, 198 (1997) 1455-1480.
[31] M. Buback, B. Huckestein, B. Ludwig, Die Makromolekulare Chemie, Rapid Communications, 13 (1992) 1-7.
[32] K. Ito, J Polym Sci Part A-1 Polym Chem, 12 (1974) 2581-2983.
[33] K. Ito, Journal of Polymer Science Part A-1: Polymer Chemistry, 10 (1972) 3159-3164.
[34] G.G. Cameron, J. Cameron, Polymer, 14 (1973) 107-110.
[35] H.K. Mahabadi, A. Rudin, J Polym Sci Polym Chem Ed, 17 (1979) 1801-1810.
[36] H.K. Mahabadi, K.F. O'Driscoll, Macromolecules, 10 (1977) 55-58.
[37] J. Barth, M. Buback, Macromolecular Rapid Communications, 30 (2009) 1805-1811.
[38] J. Barth, M. Buback, P. Hesse, T. Sergeeva, Macromolecules, 42 (2009) 481-488.
[39] C. Barner-Kowollik, G.T. Russell, Progress in Polymer Science (Oxford), 34 (2009) 1211-1259.
[40] G.T. Russell, Macromolecular Theory and Simulations, 4 (1995) 519-548.
[41] B. Yamada, D.G. Westmoreland, S. Kobatake, O. Konosu, Progress in Polymer Science (Oxford), 24 (1999) 565-630.
[42] P.A. Clay, R.G. Gilbert, Macromolecules, 28 (1995) 552-569.
[43] G.G. Odian, Principles of polymerization, in, Wiley, Hoboken, N.J., 2004.
[44] M. Buback, M. Egorov, A. Feldermann, Macromolecules, 37 (2004) 1768-1776.
[45] M.S. Matheson, E.E. Auer, E.B. Bevilacqua, E.J. Hart, Journal of the American Chemical Society, 71 (1949) 497-504.
[46] K. Ito, Journal of Polymer Science Part A-1: Polymer Chemistry, 8 (1970) 1823-1830.
[47] J. Fischer, G. Mücke, G. Schulz, Berichte der Bunsengesellschaft für physikalische Chemie, 73 (1969) 154-163.
[48] V.A. Moroni, G. Schulz, Die Makromolekulare Chemie, 118 (1968) 313-323.
[49] V.G. Schulz, J. Fischer, Die Makromolekulare Chemie, 107 (1967) 253-258.
[50] E. Trommsdorff, H. Kohle, P. Lagally, Makromol. Chem., 1 (1948) 169-198.
[51] H. Fischer, H. Paul, Accounts of Chemical Research, 20 (1987) 200-206.
[52] W. Görlich, W. Schnabel, Die Makromolekulare Chemie, 164 (1973) 225-235.
[53] W. Görlich, W. Schnabel, European Polymer Journal, 9 (1973) 1289-1296.
[54] V.U. Borgwardt, W. Schnabel, A. Henglein, Die Makromolekulare Chemie, 127 (1969) 176-184.
[55] J. Kiwi, W. Schnabel, Macromolecules, 9 (1976) 468-470.
[56] G. Beck, G. Dobrowolski, J. Kiwi, W. Schnabel, Macromolecules, 8 (1975) 9-11.
[57] K. Horie, K. Tomomune, I. Mita, Polymer Journal, 11 (1979) 539-543.
[58] K. Horie, I. Mita, Polymer Journal, 9 (1977) 201-208.
[59] P.E.M. Allen, C.R. Patrick, Die Makromolekulare Chemie, 47 (1961) 154-167.
[60] J. Hughes, A.M. North, Transactions of the Faraday Society, 60 (1964) 960-970.
[61] V.H. Fischer, Die Makromolekulare Chemie, 98 (1966) 179-188.
[62] J. Kiwi, W. Schnabel, Macromolecules, 8 (1975) 430-435.
[63] K. Horie, I. Mita, Macromolecules, 11 (1978) 1175-1179.
[64] T. Yasukawa, T. Takahashi, K. Murakami, The Journal of Chemical Physics, (1973) 3937-3939.
[65] T. Yasukawa, T. Takahashi, K. Murakami, Die Makromolekulare Chemie, 174 (1973) 235-238.
[66] K. Ito, J Polym Sci Part A-1 Polym Chem, 12 (1974) 1991-2004.
[67] K.F. O'Driscoll, H.K. Mahabadi, J Polym Sci Polym Chem Ed, 14 (1976) 869-881.
[68] H.K. Mahabadi, K.F. O'Driscoll, Journal of Macromolecular Science: Part A - Chemistry, 11 (1977) 967-976.
[69] M. Buback, Macromolecular Symposia, 182 (2002) 103-118.

[70] M. Buback, E. Müller, G.T. Russell, Journal of Physical Chemistry A, 110 (2006) 3222-3230.
[71] A. Theis, T.P. Davis, M.H. Stenzel, C. Barner-Kowollik, Macromolecules, 38 (2005) 10323-10327.
[72] H.K. Mahabadi, A review of the kinetics of the low conversion, free-radical termination process, in: Makromolekulare Chemie. Macromolecular Symposia, Wiley Online Library, 1987, pp. 127-150.
[73] K. O'Driscoll, Pure and Applied Chemistry, 53 (1981) 617-626.
[74] T. Yasukawa, K. Murakami, Macromolecules, 14 (1981) 227-228.
[75] O.F. Olaj, G. Zifferer, G. Gleixner, Die Makromolekulare Chemie, 187 (1986) 977-994.
[76] H.K. Mahabadi, Macromolecules®, 18 (1985) 1319-1324.
[77] O.F. Olaj, P. Vana, Macromolecular Rapid Communications, 19 (1998) 433-439.
[78] O.F. Olaj, P. Vana, Macromolecular Rapid Communications, 19 (1998) 533-538.
[79] M. Buback, G.T. Russell, Kinetics of Polymerizations, in: Encyclopedia of Radicals in Chemistry, Biology and Materials, John Wiley & Sons, Ltd, 2012.
[80] G. Moad, D.H. Solomon, The Chemistry of Radical Polymerization, 2nd fully rev. ed. ed., Elsevier, 2006.
[81] Z. Szablan, T.M. Lovestead, T.P. Davis, M.H. Stenzel, C. Barner-Kowollik, Macromolecules, 40 (2007) 26-39.
[82] M.W.F. Nielen, Rapid Communications in Mass Spectrometry, 13 (1999) 826-827.
[83] M. Buback, F. Günzler, G.T. Russell, P. Vana, Macromolecules, 42 (2009) 652-662.
[84] O. Olaj, I. Schnöll-Bitai, European Polymer Journal, 25 (1989) 635-641.
[85] J. Sarnecki, J. Schweer, Macromolecules, 28 (1995) 4080-4088.
[86] M.D. Zammit, T.P. Davie, D.M. Haddleton, K.G. Suddaby, Macromolecules, 30 (1997) 1915-1920.
[87] M. Stickler, G. Meyerhoff, Die Makromolekulare Chemie, 179 (1978) 2729-2745.
[88] J. Barth, M. Buback, P. Hesse, T. Sergeeva, Macromolecules, 43 (2010) 4023-4031.
[89] M. Buback, P. Hesse, I. Lacík, Macromolecular Rapid Communications, 28 (2007) 2049-2054.
[90] A.V. Tobolsky, J. Offenbach, Journal of Polymer Science, 16 (1955) 311-314.
[91] K. Tsutsumi, Y. Tsukahara, Y. Okamoto, Polymer Journal, 26 (1994) 13-20.
[92] S. Beuermann, M. Buback, C. Isemer, A. Wahl, Macromolecular Rapid Communications, 20 (1999) 26-32.
[93] S. Beuermann, M. Buback, C. Schmaltz, Ind. Eng. Chem. Res., 38 (1999) 3338-3344.
[94] D. Colombani, Progress in Polymer Science, 22 (1997) 1649-1720.

Chapter 2. Experimental

In this chapter, common experimental procedures carried out in this work are detailed.

2.1. Monomer purification

This can be achieved by either distillation or column chromatography. Both methods have their own advantages. Distillation removes any polymer dissolved in the monomer, however many inhibitors are volatile, and consequently distillation probably does not completely remove them. As the aim of purification in the work of this Ph.D. thesis is to remove inhibitors, column chromatography was therefore used throughout as the procedure for monomer purification.

2.2. Deoxygenation

Deoxygenation is an important step prior to radical polymerization (in the laboratory). Normal polymerization commences only after complete consumption of the O_2. The molecular O_2 at first inhibits the polymerization, and then there may be a retardation phase prior to the commencement of unrestricted polymerization..

Deoxygenation can be achieved either by freeze-pump-thaw degassing cycles or by purging the solution with an inert gas such as N_2 for a sufficient time. Freeze-pump-thaw is a technique that was sometimes used to remove O_2 from solvent in this work. This technique was carried out as follows. The solvent in the tubes was placed in the vacuum system; the tubes were flushed with nitrogen gas before being frozen using liquid nitrogen while still under a nitrogen atmosphere. When the solvent was frozen, the stopcock was opened to

vacuum, and the atmosphere pumped off for 3 min. Then the tubes were taken off the liquid nitrogen and left at room temperature for 1 min. After this the vacuum stopcocks were closed. The solvent was fully thawed using a tepid water bath. The nitrogen gas then flowed for several minutes. The solvent was replaced in the liquid nitrogen and re-frozen. This process was repeated for three cycles. Finally, while the samples were frozen and under vacuum the tubes were sealed. This was done by closing an attached stopcock. The samples were then left to thaw at room temperature before they were placed in a water bath at a set temperature for polymerization investigations.

2.3. Polymerization

Radical polymerization (RP) was carried out isothermally at temperatures in the range 50–90 °C, and employing different thermal initiators and solvents as indicated. Monomers were purified as above. AIBN was purified by re-crystallization from methanol. Dissolved oxygen was removed mostly by flushing the mixture with nitrogen for about 15 minutes. The freeze-pump-thaw technique was also initially used, especially with bulk MMA polymerization. Flushing the mixture with N_2 was found to be as sufficient as the freeze-pump-thaw.

Polymerization mixtures were prepared at room temperature and it was assumed that the volume fraction remained unchanged in heating to the polymerization temperature. Small scale experiments were used, which made them less dangerous, less expensive, less waste producing and better for fast attainment of uniform, constant temperature. Polymerization mixtures were divided into 5 to 10 small vials after being deoxygenated and before polymerization was carried out in a thermostated water bath.

The monomer conversion data were obtained by means of gravimetric analysis (discussed later), and $<k_t>$ values were calculated using the recommended classical kinetic equation for steady-state polymerization. Molar mass distribution was determined by means of size-exclusion chromatography (SEC) (also discussed later).

It is noteworthy that a reactor vessel may have some influence with kinetic investigations. Rigorous cleaning of the reaction vessel is of great importance, particularly for kinetic investigations, as the surface of a reaction vessel may contribute to the chain initiation or termination processes. Therefore it was ensured that all reaction glassware was cleaned rigorously prior to use.

2.4. Gravimetric analysis

The gravimetric method is the most direct measurement method for obtaining data for conversion of monomer into polymer. The big advantage of this technique is obviously its simplicity: monomer conversion is measured directly and needs no calibration. Although it has been criticized as being too laborious and susceptible to error, it still remains a remarkably widespread technique. In addition, dissolved oxygen is one of the major sources of difficulty in using the gravimetric technique, especially when taking samples for gravimetric analysis: it is very difficult to exclude atmospheric oxygen from coming into contact with the ongoing polymerization system. Therefore, the polymerization reaction mixture was divided into multiple samples prior to polymerization, typically 5-10 samples. Polymerization then was carried out in a controlled-temperature water bath. For each sample, polymerization was stopped at different times by cooling the sample down in ice water. The times were selected so that the rate of polymerization could be determined but the conversion of monomer into polymer remained relatively low. Such a procedure relies on the assumption

of having the same polymerization conditions for each sample; in particular, the presence of oxygen can alter the commencement of polymerization. For this reason there was stringent deoxygenation, so that polymerization would commence immediately in all vials. Conversions were determined gravimetrically after evaporation of the residual monomer and solvent. This drying was performed by heating the material in a conventional or vacuum oven at temperatures slightly above room temperature. Further, it was checked no polymer formation occurred outside the water bath and the polymers were only formed while the tube in the water bath and not during the drying process.

2.5. Size exclusion chromatography, SEC

Size exclusion chromatography (SEC) is also often called gel permeation chromatography (GPC). It is a powerful and popular analytical method that is used to determine the molar mass distribution (MMD) of polymers. SEC separates molecules based on their molecular volume by using a column that is packed with a stationary phase consisting of beads with pores of a defined range of sizes. The separation of materials is based on the amount of time molecules spend percolating through the pores of these beads.

MMDs were determined by SEC using tetrahydrofuran (THF) as eluent and a refractive index (RI) detector. Molar mass calibration was achieved with polystyrene or poly(methyl methacrylate) standards. Two SEC instruments were used. The one at Auckland University had two Polypore 300 × 7.5 mm columns with nominal 5 μm particle size and operating range of 200 – 2 000 000 g mol^{-1}. About 5mg mL^{-1} of polymer were dissolved in THF before being injected into the instrument. A flow rate of 1.0 mL $min^{-1}$of eluent at a temperature of 35 °C was used. Some samples were also measured by means of a regularly calibrated SEC instrument at Göttingen University, Germany, under the same conditions, with SDV columns of nominal 5 μm particle size and with a JASCO AS-2055-plus autosampler. To be precise,

PS standard was used for GPC calibration for PMMA, PBMA, PDMA, PBA and PST at the University of Auckland, while both PS and PMMA standards were used at Göttingen University.

In SEC the elution volume of polymers depends on their hydrodynamic volume; thus universal calibration based on Mark-Houwink parameters was used to determine the molar mass of the polymers produced, employing Eq. 18. Table 2-1 presents the numerical values of Mark-Houwink parameters in THF used. These values have been obtained by Hutchinson et al.[1-3]

$$\ln M_2 = \frac{1}{1+a_2} \ln \frac{K_1}{K_2} + \frac{1+a_1}{1+a_2} \ln M_1 \qquad (18)$$

Table 2-1, Mark-Houwink parameters *K* and α used for universal calibration.

Polymer	K (dL g^{-1})	a	Ref.
PS	11.4×10^{-5}	0.716	[3]
PMMA	9.44×10^{-5}	0.719	[1]
PBMA	14.8×10^{-5}	0.664	[3]
PDMA	5.18×10^{-5}	0.720	[3]
PBA	12.2×10^{-5}	0.700	[2]

Peak molar mass (M_P) of the highest peak in the SEC MMD and number-average molar mass (M_n) is often employed in this thesis. This is explained in detail later in this thesis in its proper section.

References

[1] R.A. Hutchinson, J.H. McMinn, D.A. Paquet, S. Beuermann, C. Jackson, Ind. Eng. Chem. Res., 36 (1997) 1103-1113.
[2] S. Beuermann, D. Paquet, J. McMinn, R. Hutchinson, Macromolecules, 29 (1996) 4206-4215.
[3] R. Hutchinson, S. Beuermann, D. Paquet, J. McMinn, Macromolecules, 30 (1997) 3490-3493.

Chapter 3. The Influence of Monomer and Initiator Concentrations on Termination Rate Coefficients and Average Degrees of Polymerization at Low Conversion via Chain-Length-Dependent Termination

In this chapter the accessibility of fundamental information on chain-length-dependent termination (CLDT) is presented, using a simple technique under different conditions. Correlations for bulk and dilute low conversion rates of polymerization, R_p, (or average termination rate coefficients, $<k_t>$) as a function of initiator concentration and temperature are given. Moreover, the effect of monomer concentration on the rate and degree of polymerization at low conversion using different solvents is examined. In addition, the impact of chain transfer to solvent on polymerization kinetics as a function of temperature is discussed. Information on the transfer constant for methyl isobutyrate (MIB), the solvent used for dilute-solution polymerization, is obtained.

3.1. Introduction

The importance of the termination reactions arises from the profound effect of termination on the overall kinetics of polymerization processes and on the molar mass distribution (MMD, often called molecular weight distribution [MWD]) of the final product and hence on the final product properties. In spite of this importance, there are still ambiguities in understanding the termination process. This process is often considered to be the most complicated step in the set of radical polymerization elementary reactions. The kinetic complexity of termination reactions has been a cause for the slow development of fundamental knowledge of this process. This is due to the termination process being a diffusion-controlled step. In fact, that

termination is diffusion-controlled process has been known for many decades, initially from kinetics studies of bulk polymerization. Although diffusion control was believed to be the case after the onset of the gel-effect, nowadays it has also been confirmed that $<k_t>$ is diffusion-controlled even prior to the onset of the gel-effect, i.e. right from the beginning of a polymerization.

Three mechanistic steps are involved in the termination process: (1) Translational diffusion (center-of-mass diffusion), (2) segmental diffusion and (3) chemical reaction, all depicted in Figure 3-1. This figure shows two macroradicals come into contact first as a result of center-of-mass diffusion. Once this contact has been made, segmental reorientation of the two macroradicals has to occur in order to bring both reactive chain ends into close proximity. Finally, the actual chemical reaction of termination occurs, in which the two radical functionalities are destroyed. Since translational diffusion and segmental diffusion are the rate determining steps in the overall termination process that occur at low conversions, attention will only be given to these two diffusion processes.

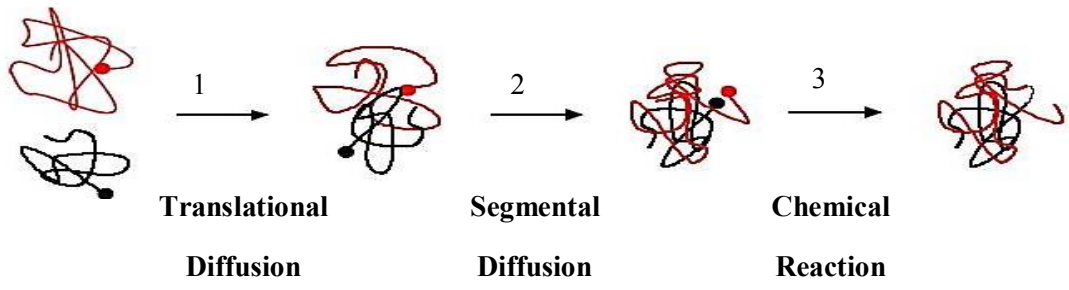

Figure 3-1. Depiction of the three steps involved in the termination process.[1]

The termination reaction being diffusion-controlled results in it being difficult to obtain unique rate coefficient for termination. The termination rate depends upon all parameters that

exert an effect on the diffusional motion of the polymeric radicals undergoing termination. This might include viscosity, solvent interactions, chain flexibility, dynamics of entanglements, polymer weight fraction, temperature and chain lengths of the macro-radicals involved in the termination reaction. Consequently, the termination rate, being highly system specific, results in a wide variation of the values of $<k_t>$ in the literature. This might be interpreted as scatter, but it is also for mechanistic reasons, as just explained.

Fundamental features of termination, such as its chain-length dependence, are of importance. However, they can hardly be derived from the experimental results such as macroscopic $<k_t>$. The measurement of chain-length dependent termination rates necessitates the measurement of microscopic quantities $k_t^{i,j}$ that cannot be accessed directly, as radicals cannot be distinguished on the basis of their chain length during an experiment. Also, extraction of microscopic information from macroscopic quantities is not straightforward. However, the last decade has witnessed significant progress in the study of RP termination kinetics, in particular chain-length dependent termination (CLDT). Notwithstanding this progress, there are several motives for using a simpler experimental method to study termination and to see if it can deliver results that agree with those of more sophisticated methods, as mentioned in Chapter 1. Even though the simple method delivers only overall $<k_t>$ from R_p, such values should vary in well predicted ways that reflect the underlying CLDT. This data can also contribute to the building up of a comprehensive database of $<k_t>$ values.

3.2. Methodology and data analysis

The rate of polymerization (R_p) and the molar mass distribution (MMD) of the polymers formed are the main parameters to be controlled in radical homopolymerization. Most people would still use the steady-state rate equation (Eq. 1) for predicting changes in rate, and the

Mayo equation (Eq. 2) for predicting changes in the average degree of polymerization when changing reaction conditions. In particular, a lot of interest has been generated in the variation of polymerization rate and specifically the termination rate constant as a function of different experimental conditions. Eq. 1 and Eq. 2 clearly show how the classical rate (R_p) and DP_n change with changing reaction conditions.

$$R_p = -\frac{dc_M}{dt} = k_p\left(f\frac{k_d}{\langle k_t\rangle}\right)^{0.5}(c_M)^1(c_I)^{0.5} \sim (c_I)^{0.5}\,(c_M)^{1.0}(\langle k_t\rangle)^{-0.5} \quad (1)$$

$$\frac{1}{DP_n} = \frac{(1+\lambda)(f k_d c_I\langle k_t\rangle)^{0.5}}{k_p c_M} \implies DP_n \sim (c_I)^{-0.5}\,(c_M)^{1.0}(\langle k_t\rangle)^{-0.5} \quad (2)$$

where k_p, k_d and $\langle k_t\rangle$ are the rate coefficients for propagation, initiator decomposition and termination respectively, f is initiator efficiency, c_I and c_M are initiator and monomer concentrations respectively, and λ is the mode of termination. For convenience it has been assumed in Eq. 2 that there is negligible dead-chain formation by transfer.

The rate coefficient of termination, in particular, is diffusion-controlled and hence is chain-length dependent and system dependent. Therefore, it is clear that the termination rate coefficient measured for a given monomer may not be applicable to the same monomer polymerized under different reaction conditions. Furthermore, termination depends on the conversion and viscosity. Nevertheless, by limiting the reaction to low conversion polymerization, the conversion and viscosity dependences can be made inconsequential, while the chain-length dependency will remain.

In order to gain additional insight into chain-length dependence, which becomes an important and fundamental process in free radical polymerization, understanding solvent, initiator and temperature effects on R_p are of importance. Deviation from Eq. 1 is manifest in a change in

the exponents α = 0.5 and β = 1.0 associated with the initiator and monomer concentrations respectively, where Eq. 1 is now recast with terms $(c_I)^{\alpha}$ and $(c_M)^{\beta}$.

The key results of RP for a thermally decomposing initiator is

$$\langle k_t \rangle \sim (c_I)^{a}\,(c_M)^{-2a}\left(k_t^{1,1}\right)^{1+a} \tag{3}$$

$$\text{where } a = \frac{e}{2-e}$$

Eq. 3 is a result deduced from Eq. 3a, which delivers a closed expression for $<k_t>$ and reveals an excellent concurrence with numerical solutions of population balanced equations.[2]

$$< k_t > = k_t^{1,1}\left[\Gamma\left(\frac{2}{2-e}\right)\right]^{-2}\left[\frac{\left(4fk_d c_I k_t^{1,1}\right)^{0.5}}{k_p c_M}\left(\frac{2}{2-e}\right)\right]^{2e/(2-e)} \tag{3a}$$

By substituting Eq. 3 into Eqs. 1 and 2 one obtains

$$R_p \sim (c_I)^{\alpha}\,(c_M)^{\beta}\left(k_t^{1,1}\right)^{\gamma} \tag{4}$$

$$DP_n \sim (c_I)^{-0.5-b}(c_M)^{\beta}\left(k_t^{1,1}\right)^{0.5-b} \tag{4a}$$

$$\text{where } \alpha = 0.5-b, \beta = 1+2b, \gamma = -0.5-b \text{ and } b = \frac{a}{2} = \frac{e}{2(2-e)}$$

These equations illustrate the relation between different scaling factors and *e*, the chain-length dependence. It is clear that classical kinetics results of $<k_t> \sim k_t^{1,1}$ and $R_p \sim (c_I)^{0.5}\,(c_M)^{1.0}\,(k_t^{1,1})^{-0.5}$ (Eq. 1) are obtained for $e = 0$. Any chain-length dependence of termination will induce non-classical polymerization behaviour, where R_p will scale with a weaker than square root dependence on c_I and stronger than linear dependence on c_M. To make this clearer, an example of strong chain-length dependence is $e = 0.65$, which leads to $R_p \sim (c_I)^{0.26}\,(c_M)^{1.49}\,(k_t^{1,1})^{-0.74}$.

The purpose of the following experiments is to determine the chain-length dependence of termination from experimental values of R_p (or $\langle k_t \rangle$) using simple, gravimetric techniques. In particular, Eqs. 3 or 4 suggest determination of e by measuring R_p (or $\langle k_t \rangle$) or DP_n as a function of c_I, c_M or $k_t^{1,1}$. Furthermore, the effect of temperature on α and β will also be examined. In addition, the effects of c_I and c_M on the degree of polymerization (DP) are also measured.

However, one of the critical factors in using this method is the use of the correct values of k_p, k_d and f, which are not always readily available from standard references. In addition, for this procedure to be valid, the value of e may be limited to $e < 0.8$, where the geometric mean result holds; and there should be negligible transfer.

Kinetic Parameters

Kinetic parameters that were used are now presented. Equations 5-10 are IUPAC-recommended propagation rate coefficients, i.e. they are benchmark values.[3] In the absence of more specific information about initiator decomposition rate and efficiency of AIBN, it was assumed that there is no effect of the type of monomer on the k_d and f as this assumption might be fulfilled for the present work since low conversion and dilute solution polymerization were carried out. Hence Eq. 5 [4] and Eq. 5a [5], discussed in Chapter 4, are used for k_d and f respectively. Eqs.6 and 7 are the IUPAC-recommended propagation rate benchmark values.[3]

$$k_d(\text{AIBN}) = 2.89 \times 10^{-15} \text{s}^{-1} \exp\left(\frac{-130.23 \text{ kJ mol}^{-1}}{RT}\right) \qquad (5)$$

$$f(\text{AIBN}) = 5.04 \exp\left(\frac{-5.70 \text{ kJ mol}^{-1}}{RT}\right) \qquad (5a)$$

$$k_{\mathrm{p}}(\mathrm{MMA}) = 2.673 \times 10^{6}\,\mathrm{L\ mol^{-1}s^{-1}} \exp\left(\frac{-22.36\ \mathrm{kJ\ mol^{-1}}}{RT}\right) \qquad (6)$$

$$k_{\mathrm{p}}(\mathrm{ST}) = 4.266 \times 10^{7}\,\mathrm{L\ mol^{-1}s^{-1}} \exp\left(\frac{-32.51\ \mathrm{kJ\ mol^{-1}}}{RT}\right) \qquad (7)$$

The monomers here are methyl methacrylate (MMA) and styrene (ST)

3.3. Initiator concentration effect

3.3.1. Bulk polymerization

First the initiator effect on bulk polymerization is studied. Eq. 8 shows the dependence of the rate of polymerization on the initiator concentration.

$$R_{\mathrm{p}} \sim (c_{\mathrm{I}})^{\alpha} \qquad (8)$$

$$\text{where} \quad \alpha = \frac{1-a}{2} \text{ and } a = \frac{e}{2-e}$$

The qualitative understanding here is that as the initiator concentration increases, the radical concentration increases and hence the rate of termination increases. Thus the distribution of molecular sizes shifts towards smaller chain lengths, which means an increased $\langle k_{\mathrm{t}} \rangle$ on account of CLDT. Thus the order of reaction with respect to c_{I} is weaker than the classical value of 0.5.

The effect of variation of 2,2'-azobisisobutyronitrile (AIBN) concentration on the MMA bulk polymerization at low conversion was investigated. Typical conversion-time data for bulk MMA experiments with 3 different AIBN concentrations are shown in Figure 3-2. The reader is referred to Chapter 2 for information on experimental procedure. The well-known increase

of rate with initiator concentration is immediately evident. The reproducibility of the results is within normal limits. The values of $\langle k_t \rangle$ are obtained using the recommended rate equation (Eq. 9). The values of $\langle k_t \rangle$ obtained from experiments are in agreement with literature values.

$$\frac{-\mathrm{d}\ \ln(1-x)}{\mathrm{d}t} = k_p \left(\frac{f k_\mathrm{d} c_\mathrm{I}}{\langle k_\mathrm{t} \rangle}\right)^{0.5} \tag{9}$$

Here x is the fractional conversion of monomer into polymer, and other parameters are as above.

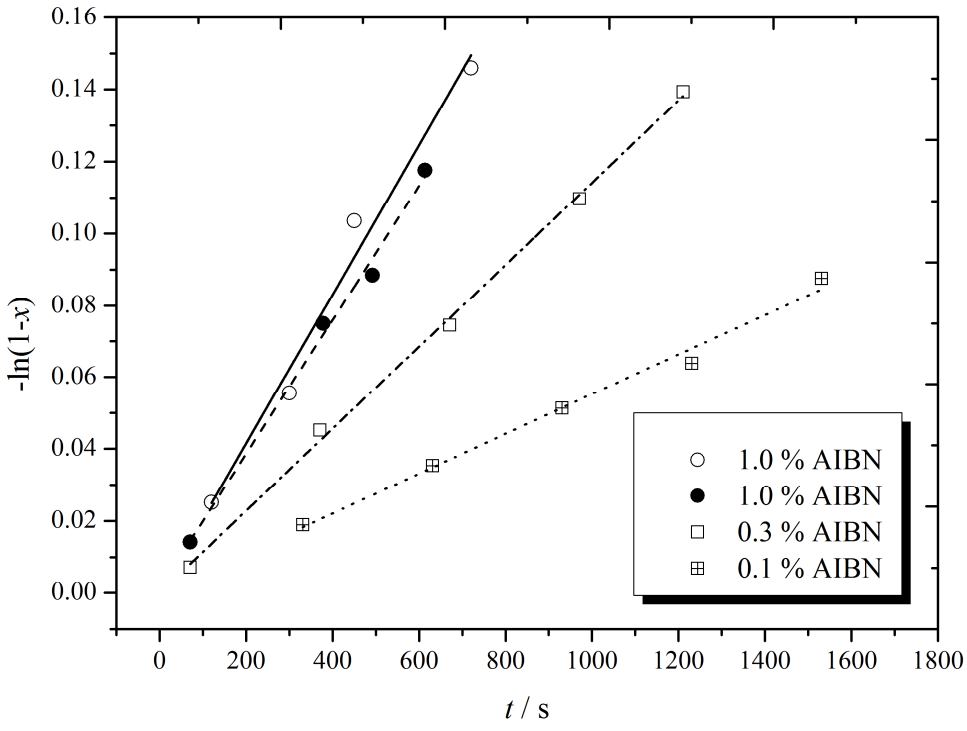

Figure 3-2. Effect of AIBN concentration on bulk MMA polymerization at 70 °C, where x is fractional conversion, t is time, and AIBN amount is as indicated. Points: experimental results; lines: best fits to each set of results. The slope of each line was used to calculate $\langle k_t \rangle$ via well-known Eq. 9.

Plotting the experimental data as suggested by Eq. 8, i.e. as a log-log plot of R_p versus c_I, allows one to obtain α. Deviation from the classical value of 0.5 is not usually observed. One reason for this is that it is not looked for – experiments are habitually plotted as R_p versus

$(c_I)^{0.5}$ – and deviations are small. However, deviation can be observed. Mahabadi and O'Driscoll, for example, report α = 0.42 and 0.46 for bulk polymerization of dodecyl methacrylate at 60 °C and 80 °C respectively.[6] Further, Ito polymerized MMA at 50 °C and found α < 0.5 with a slight effect of solvents.[7] Furthermore, a similar deviation was observed with bulk MMA using different azo compound initiators. For example, a value of 0.44 was obtained by Stickler using the initiator 2,2'-azoisobutyromethylester (AIBME).[8] Styrene bulk radical polymerization showed such a deviation at 50 °C where values of 0.44 [7] and 0.48 at 70 °C [9] were obtained.

My experimental result, for low conversion bulk MMA polymerization, is presented in Figure 3-3. No considerable deviation from 0.5 was observed at 50 °C.

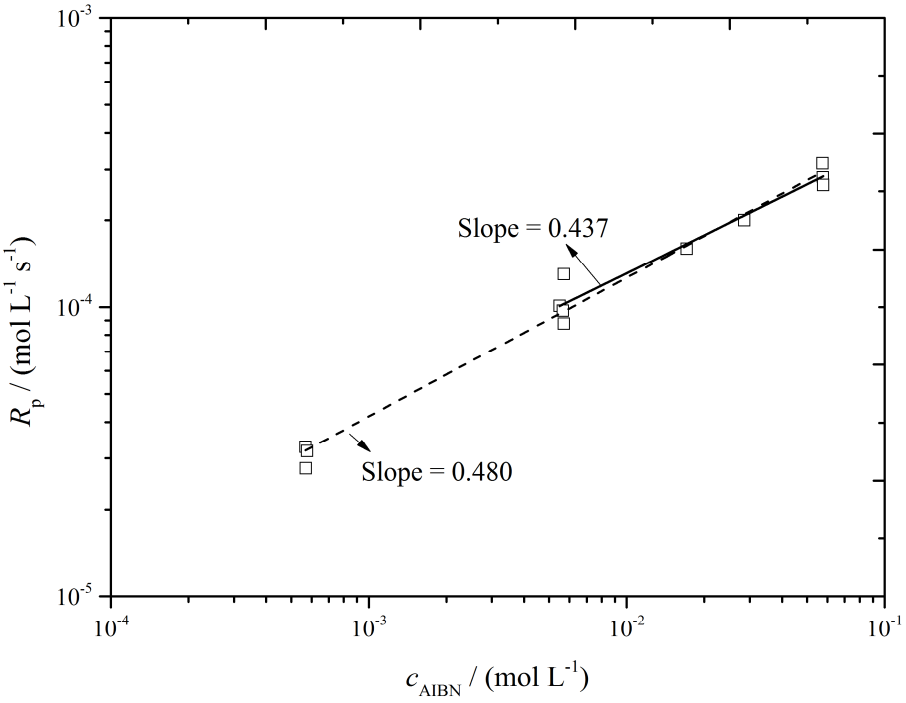

Figure 3-3. Log-log plot of polymerization rate (R_p) versus concentration of AIBN (c_{AIBN}) for bulk polymerization of methyl methacrylate (MMA) at 50 °C. Points: experimental values; lines: linear best fits, having slopes of 0.48 (dashed line) and 0.44 (solid line).

Although the slope is less than the classical value of 0.5, suggesting the fact of CLDT, the deviation is not large: the results of Figure 3-3 have a slope $\alpha = 0.48$. From Eq. 8 this gives $a = 0.04$ and hence $e = 0.08$.

This small deviation can in general be explained in several ways. Firstly, by the termination being only weakly chain-length dependent. Second, the process of transfer, in particular transfer to monomer, acts to move the value of α toward 0.5. Consequently, this suggests α is c_M dependent. In fact, this was found in the literature, where α is c_M dependent [10] and its value decreases slightly with decreasing c_M, demonstrating chain transfer to monomer processes.

It is also important to know that as c_I is lowered, transfer becomes significant and more dominant in determining the living radical distribution. This means using a low concentration of AIBN will lead to α being closer to 0.5. This observation was noticed in this experiment. Therefore, by excluding the data of the very low initiator concentrations of the experiment at 50 °C, the value of α decreases to 0.44 ± 0.04 (Figure 3-3, solid line), the expected value for long-polymer chain length dependency, corresponding to $e = 0.20$. This shows that the value of c_I may have an important bearing on the value of α. Of course the experimental uncertainty associated with this value makes it hard to state this decrease as definite.

Hence, it is suggested that in order to get a true chain-length dependency from the value of α, it is important to take into account the chain transfer reactions, which can be affected by both initiator concentration, and temperature as illustrated in the next subsection.

3.3.2. Temperature effect

The effect of temperature on α was also examined and is illustrated in Figure 3-4. The initiator exponent, α, shows a slight dependency on temperature (Table 3-1). An increase in the temperature leads to α being close to 0.5. In contrast, lowering the temperature leads to α being lower than 0.5, contrary to what is expected. Table 3-1 also shows the corresponding chain-length dependency value, e, obtained from the value of α via Eq. 8.

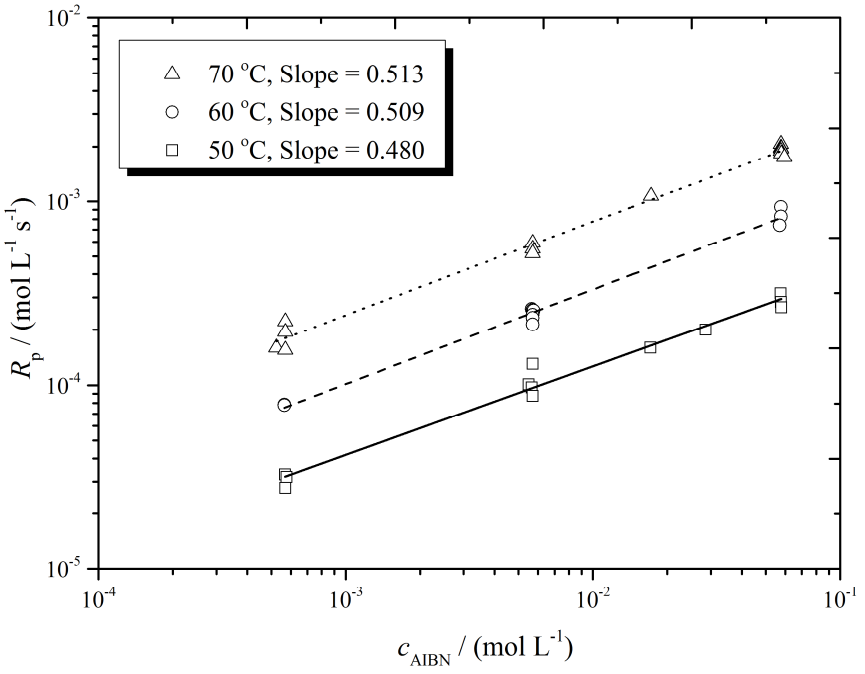

Figure 3-4. Variation of the rate of polymerization, R_p, with initiator concentration, c_{AIBN}, for bulk polymerization of methyl methacrylate (MMA) at different temperatures as indicated, plotted on double logarithmic axes.

Table 3-1. The resulting values obtained for initiator dependency, α, and chain-length dependence, e, as a function of temperature.

Temperature	α	***e* (from α)***
50 °C	0.48 (±0.02)	0.08
60 °C	0.51 (±0.02)	-0.04
70 °C	0.513 (±0.01)	-0.05

*The chain-length dependence is calculated from the value of α via Eq. 8.

This result cannot be related to the chain length of the polymers produced because of the temperature itself. Increasing the temperature should lead to the production of short polymers, which have larger chain-length dependency and so should lower the value of α. Conversely, lowering the temperature leads to the production of larger polymers, which have lower chain-length dependency as it is believed to be due to segmental diffusion control. This should make α closer to 0.5.

In fact, this opposite trend can be explained by chain transfer to monomer, a reaction that cannot be avoided. Lowering the temperature leads to less chain transfer and therefore less classical behaviour, while increasing the temperature leads to more chain transfer reaction to monomer and more classical behaviour, i.e. $\alpha = 0.5$, masking the chain-length dependence from being observed.

Is this true? In order to investigate this suspicion, experiments were carried out under dilute conditions, in the hope of observing larger chain dependence and suppressing chain transfer to monomer.

3.3.3. Dilute-solution polymerization

While the deviation from the classical value, 0.5, is evidence of the chain-length dependency, the initiator effect was also investigated under dilute solution polymerization conditions, where the living radical distribution can be dominated by small chains. High monomer concentration leads to an increase in the frequency of propagation and thus skews the distribution towards long chain. Long chains have a smaller CLDT and thus result in a small deviation from the classical value of 0.5; however, lowering the concentration of the monomer results in shifting the distribution towards small chains, where translational diffusion controls the termination process and should result in a larger deviation from

classical behavior. Short chains are not coiled; hence their rate of termination is determined by translational diffusion rather than chain-end encounter upon coil overlap. Indeed, translational diffusion controlled processes for dilute polymerization and short polymers have been reported by some groups.[11-14] This experiment would suggest, based only on the chain-length dependence assumption, that there is a more observable deviation of the value of α.

MMA and ST were polymerized separately in their analogous saturated compounds, methyl isobutyrate (MIB) and ethyl benzene (EBz), respectively. This ensures similar conditions to the bulk system. Conversion-time results for MMA and ST are presented in Figures 3-5 and Figure 3-6 respectively.

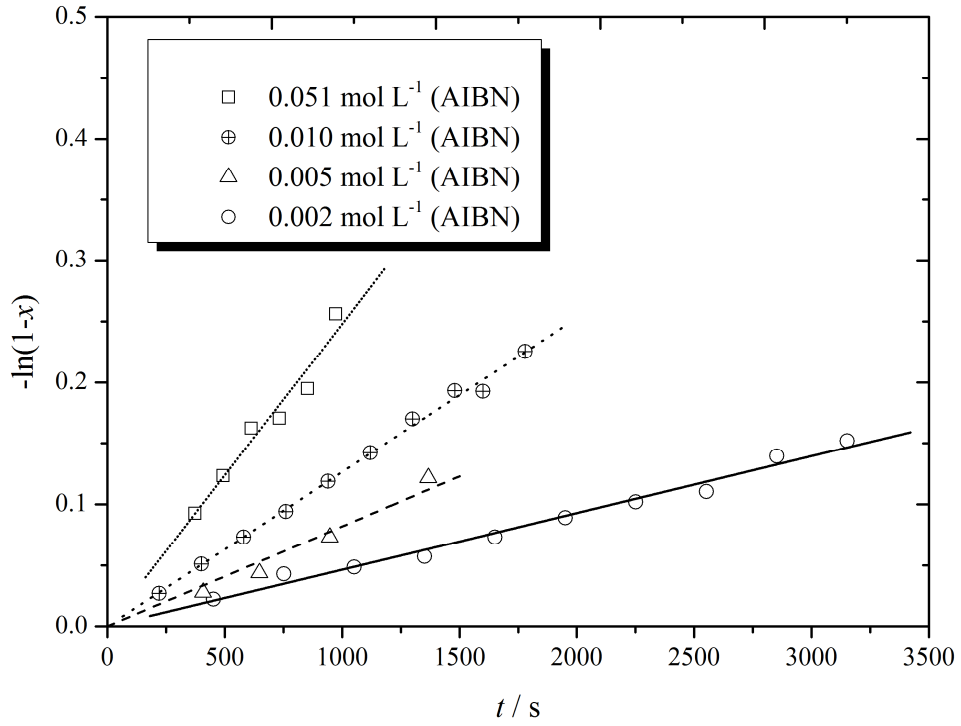

Figure 3-5. Conversion-time data from solution polymerization of 0.67 mol L^{-1} methyl methacrylate (MMA) at 85 °C in MIB, using an amount of AIBN as indicated. Points: experimental results; lines: best fits to each set of results, where x is fractional conversion, t is time.

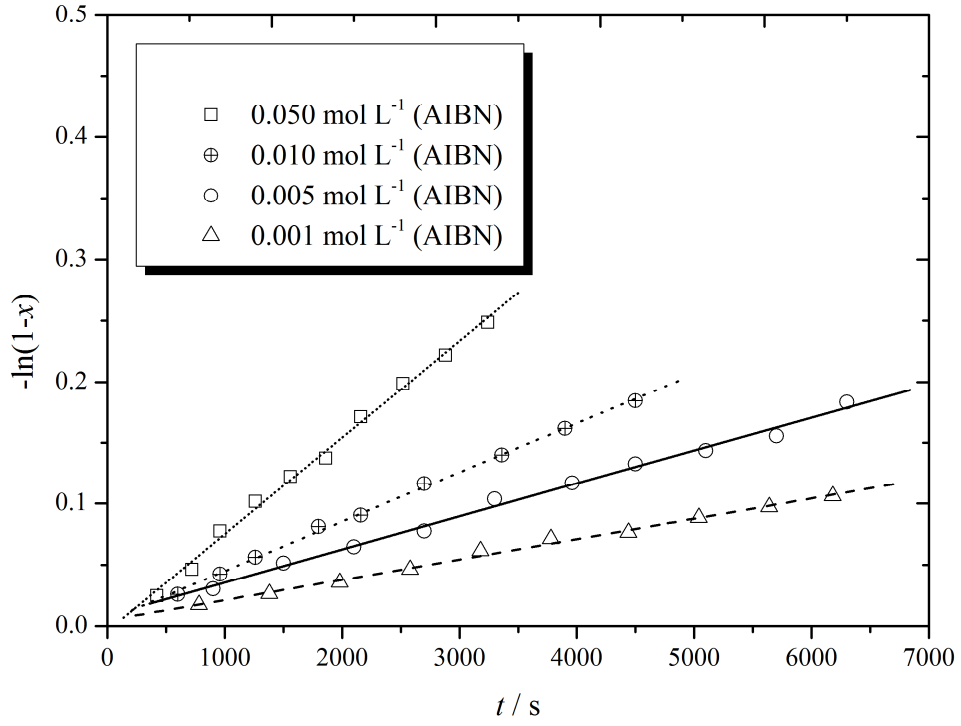

Figure 3-6. Conversion-time data from solution polymerization of 0.67 mol L^{-1} styrene (ST) at 85 °C in ethyl benzene (EBz) using AIBN amount as indicated. Points: experimental results; lines: best fits to each set of results, where x is fractional conversion, t is time.

Direct evidence of the well-known effect of initiator concentration is marked from both Figures 3-5 and 3-6, and is similar to what is observed with bulk polymerization. However, higher termination rates were observed for dilute solution polymerization of both MMA and ST, as compared to polymerization in bulk, as will be shown later in this Chapter (Figures 3-15A and 3-17). This is in accord with the literature where the size of the radical is found to have an effect on the $\langle k_t \rangle$. For instance, Fischer and Paul found, when using ESR, that $\langle k_t \rangle$ for large radicals increased with a decrease in the size and mass of radicals involved.[15] The effect of the initiator concentration on R_p for both MMA and ST low conversion solution polymerization is shown in Figure 3-7.

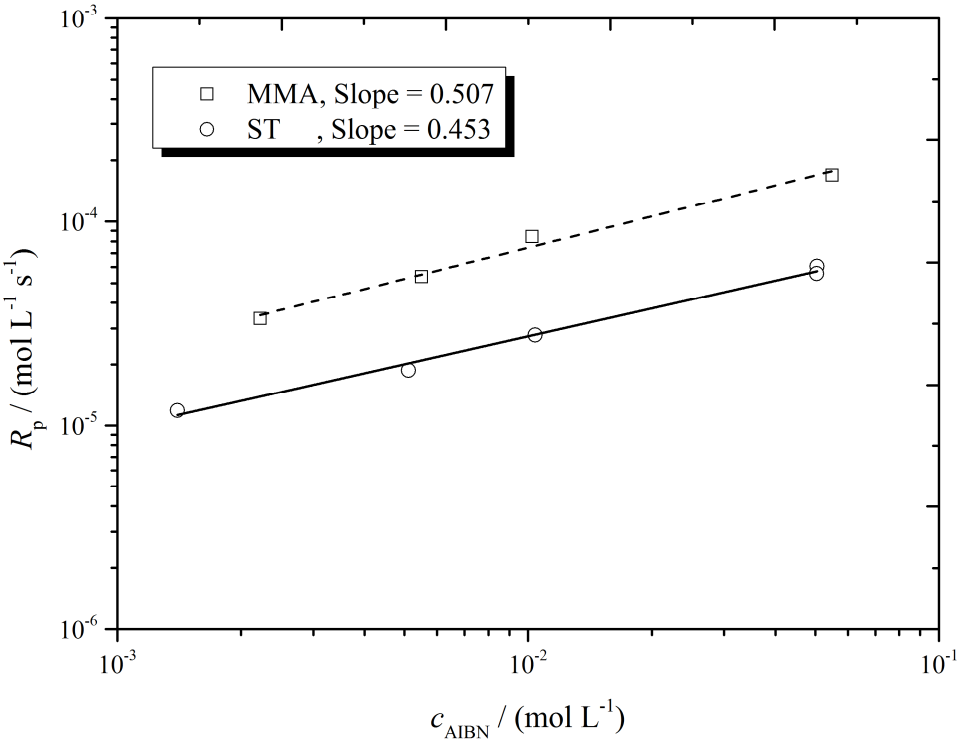

Figure 3-7. Log–log plot of rate of solution polymerization, R_p, of methyl methacrylate (MMA) and styrene (ST) at 85 °C versus initiator concentration of AIBN, c_{AIBN}. Points: experimental results; lines: best fits to each set of results,

Interestingly, polymerization under diluted conditions has no large effect on the value of α, in particular, with MMA. Even though the result for ST shows a small deviation from classical values, the result still is not as one would expect from a transitional diffusion process. The results of Figure 3-7 give chain-length dependence, $e = -0.03$ for MMA, and $e = 0.17$ for ST.

It is evident from these results that the expectation of $R_p \sim (c_I)^{0.26}$ is not nearly met. In fact, the opposite trend could confirm the chain transfer postulate, since the relative frequency of transfer to monomer is independent of monomer concentration, $k_{trX}c_X/k_pc_M$ being the quantity that determines the radical chain-length distribution. In other words, dilution should not influence the transfer to monomer process after all, since $c_X = c_M$ for it. In addition, the high temperature used also should increase the chain transfer reaction to monomer, maintaining

classical behaviour, α = 0.5. Furthermore, transfer to monomer may also be backed up by transfer to solvent, which will also act to bring the value of α towards the classical value. In this respect it is noted that both MIB and EBz possess labile hydrogens, and in fact direct evidence for chain transfer of MMA to MIB will be presented later. All this might suggest the difficulty of obtaining non-classical exponent values from variation of R_p with c_I.

Although this might introduce doubt about the reality of CLDT, a further experiment was performed to probe CLDT. This was done by studying the effect of c_I on the degree of polymerization.

3.3.4. Dependence of DP_n on initiator concentration (c_I)

The equations below (Eqs. 10 and 10a) again illustrate the relation between R_p and c_I. In addition, they also show the relation between DP_n and c_I. Since it was not possible to determine the influence of CLDT on the value α by means of rate measurements as a function of c_I, an investigation into the Number-average molar mass (DP_n) as a function of c_I was undertaken. Number-average molar mass (M_n) is needed to obtain the DP_n by dividing M_n by the monomer molar mass, M_0.

$$R_p \ \alpha \ {c_I}^{0.5} \, {c_M}^{1.0} \quad , \quad DP_n \alpha \ {c_M}^{1.0} \, {c_I}^{-0.5} \qquad (10)$$

$$R_p \ \alpha \ {c_I}^{0.5-b} {c_M}^{1+2b} \quad , \quad DP_n \ \alpha \ {c_I}^{-0.5-b} {c_M}^{1+2b} \qquad (10a)$$

where $b = \dfrac{e}{2(2-e)}$

Notice that Eq. 10a, for CLDT, correctly reduced to Eq. 10, for classical RP, in the event of $e = 0$. As an example of strong chain-length dependence, e = 0.65 leads to $DP_n \sim (c_I)^{-0.74}$ $(c_M)^{1.49}$.

Unfortunately, the University of Auckland's GPC instrument could not provide M_n values directly from its software. This left no choice but to use M_p, the mass of the centre of the chromatogram peak, as an estimate for M_n. No pretence is made that this is rigorous. Nevertheless, there are some advantages to this approach. Most obviously, M_n is well known as being the most difficult average to obtain accurately from GPC data. One reason for this is that M_n is highly susceptible to baseline selection, especially with low molar-mass polymers.[16, 17] By using M_p, some of this error is mitigated. In addition, SEC results also still depend on the correct values of Mark-Houwink parameters [18] and are associated with a certain degree of systematic error in SEC calibration.

Therefore the *DP* reported in this section are actually M_p/M_0. How accurately does this reflect DP_n? It is well known that the peak position of a GPC chromatogram approximates DP_w closely, sometimes exactly. Thus $DP \approx DP_w = DP_n \times PD$. In the event that $DP = DP_w$, one clearly has that $PD = PDI$. More importantly, is it justified to use peak *DP* to obtain information about CLDT? Consider the relationship of Eq.10a, this becomes

$$\left(\frac{DP}{PD}\right) \alpha \ {c_I}^{-0.5-b} {c_M}^{1+2b} \qquad (10b)$$

So the slope of a plot of log(*DP*) versus log(c_I) still equals -0.5-*b*, thus giving *e* from *b*, as long as *PD* is constant from experiment to experiment. This is never perfectly the case with CLDT, however to good approximation it will be accurate. In fact there is reason to think that *PD* dose not vary much and can be approximated as a constant. This is supported by our experimental measurements of *PDI* carried out using the GPC instrument in Gottingen University. *PDI* was found to be nearly constant with temperature variation, see Figure 3-8. Also the effect of polymer chain length on *PDI* is shown in Figure 3-9 for MMA polymerization.

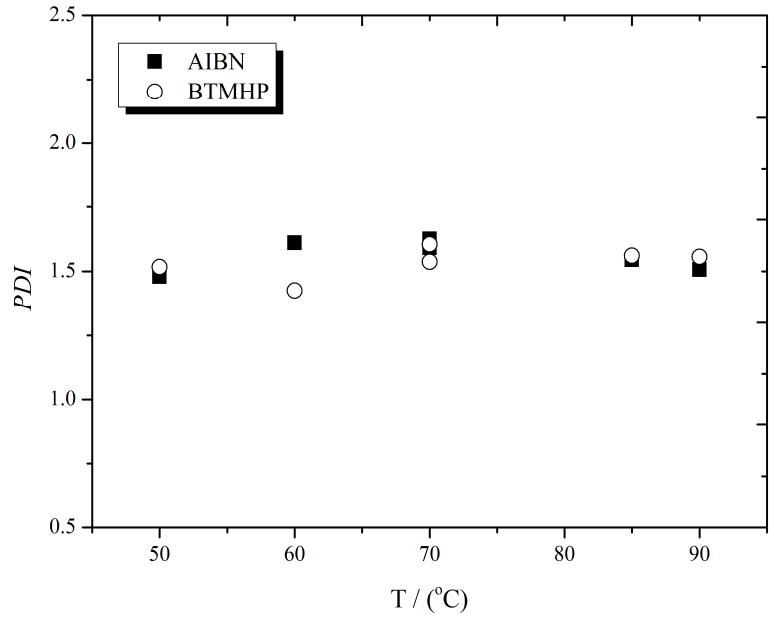

Figure 3-8. Experimental *PDI* (= M_w/M_n) for PMMA as a function of temperature for polymerizations using AIBN of concentration 0.05 mol L^{-1} and MMA of concentration 0.67 mol L^{-1} in TFT.

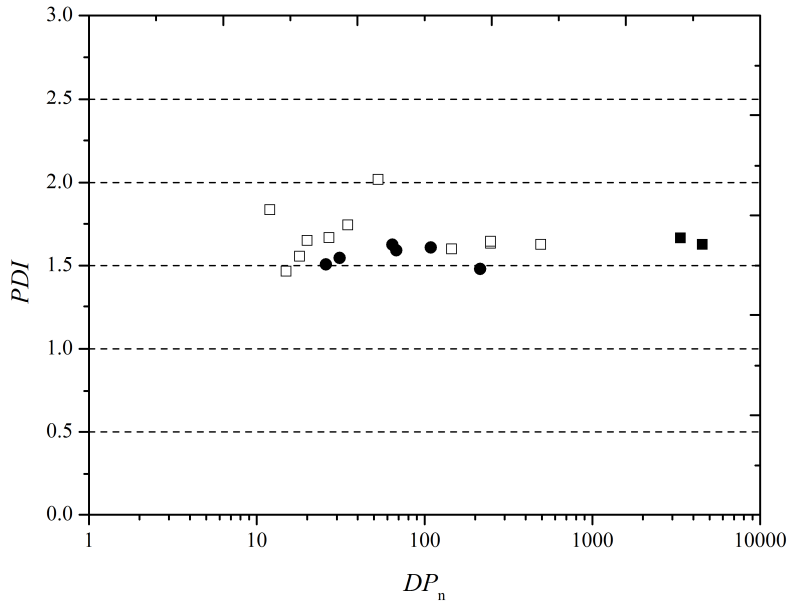

Figure 3-9. Experimental *PDI* (= M_w/M_n) values for PMMA as a function of DP_n for polymerizations under different conditions using AIBN as initiator. Open squares: literature values for PMMA from bulk polymerization in the presence of dodecyl mercaptan.[19] Filled circles: values for PMMA from Figure 3-8. Filled squares: literature values for PMMA from bulk polymerization at 60 °C.[19]

Figure 3-10 shows our experimental result presented as log-log plot of *DP* versus initiator concentration with slope less than the classical value of –0.5 predicted by Eq. 10. A value of –0.74 is obtained which corresponds to chain-length dependence of e = 0.65. This

exemplifies the reality of CLDT and that its effect can be clearly observed. This is very consistent with what one would expect for short chains and with what has been reported in recent literature.[20] On the other hand, one has to admit that this result may be an artefact of using peak *DP* rather than DP_n.

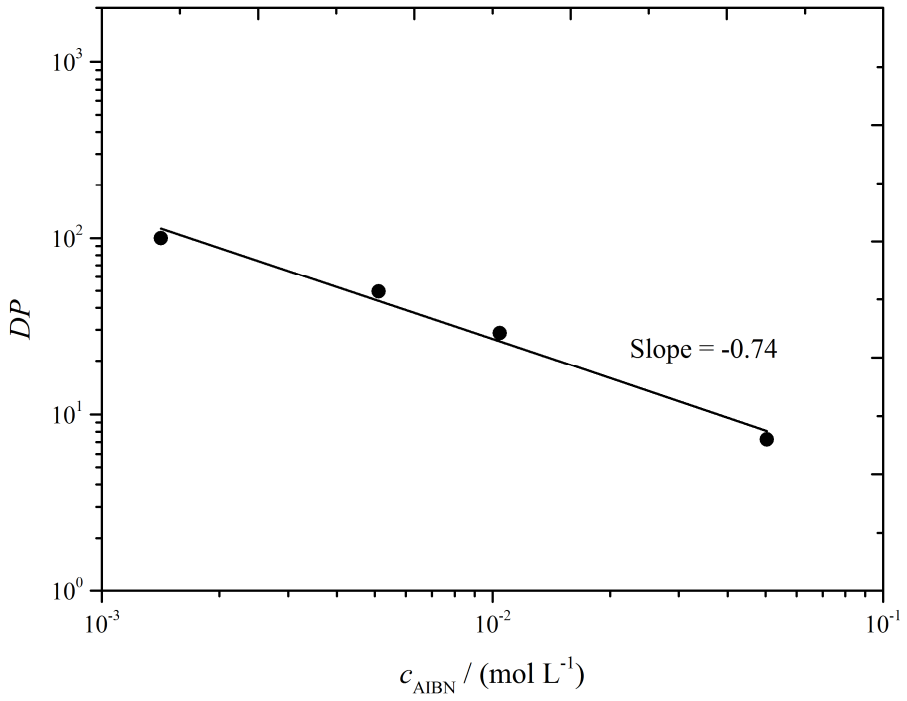

Figure 3-10. Log-log plot of degree of polymerization, *DP*, versus initiator concentration, c_{AIBN}, for styrene polymerization at 85 °C with 0.67 mol L^{-1} of styrene (ST) in ethyl benzene (EBz). Points: experimental results; line: linear best fit with slope as displayed.

Although this is in contrast to what the rate measurement found (e = 0.17), it might support the idea of side reactions affecting the rate of polymerization measurements such as transfer to solvents and reaction with O_2, as found later (Chapter 6), on the ST rate measurements.

Additionally, Eq. 11 gives DP_n for CLDT in the absence of transfer.

$$DP_n = \frac{DP}{PD} = \Gamma\left(\frac{2}{2-e}\right)\left[\frac{\left(4fk_d c_I k_t^{1,1}\right)^{0.5}}{k_p c_M}\left(\frac{2}{2-e}\right)\right]^{-2/(2-e)}\left(\frac{2}{2-e}\frac{2}{1+\lambda}\right) \qquad (11)$$

Therefore, one can get information about chain-length dependence, e, and $k_t^{1,1}$ if all else is known. An evaluation of Eq. 11 in Mayo form as a function of c_I is presented first in Figure 3-11. It is immediately evident that the effect of CLDT is to impart upward curvature.

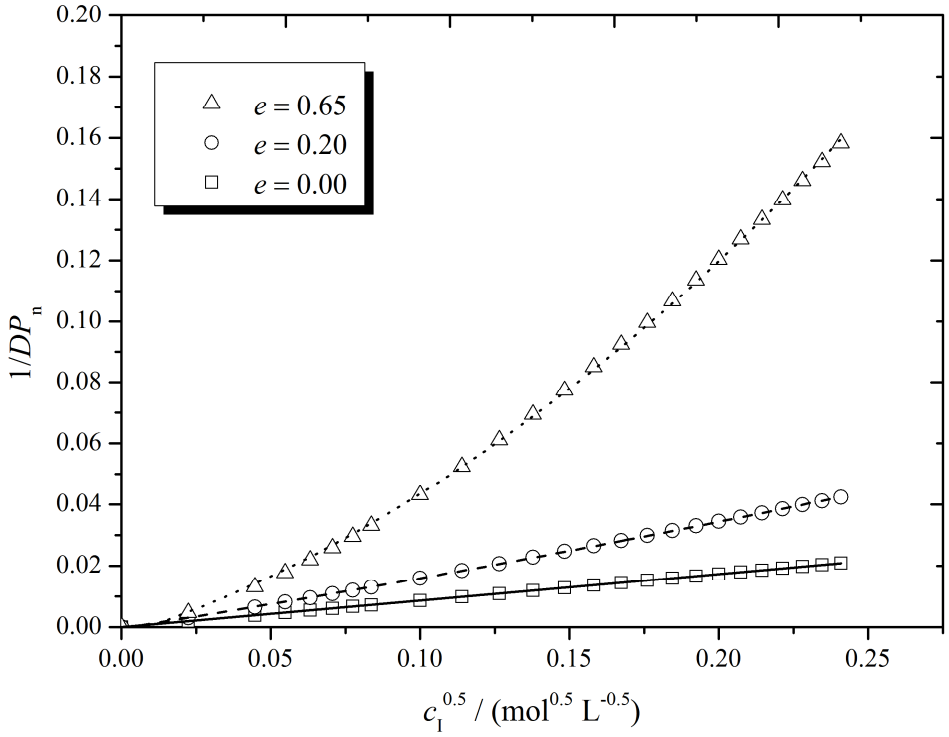

Figure 3-11. Reciprocal number-average degree of polymerization, $1/DP_n$, as a function of square root of initiator concentration, $c_I^{0.5}$, calculated using Eq. 11 with $k_p c_M = 539$ s^{-1}, $\lambda = 0$, $fk_d = 2.17 \times 10^{-4}$ s^{-1} and varying c_I. Points: calculations with $e = 0$ ($k_t^{1,1} = 1{\times}10^7$ L mol^{-1}s^{-1}), $e = 0.20$ ($k_t^{1,1} = 6 \times 10^7$ L mol^{-1} s^{-1}), e =0.65 ($k_t^{1,1} = 8 \times 10^8$ L mol^{-1}s^{-1}) as indicated; curves: quadratic fits. Values of $k_t^{1,1}$ for each e were chosen so that the fits have approximately the same slope as c_I approaches zero.

This is interesting as presenting our experimental data in this form clearly shows non-linear behaviour (Figure 3-12). Indeed, it shows clear upward curvature suggesting CLDT. Fitting of Eq. 11 to our experimental DP as a function of c_I is presented in Figure 3-12. Values of e = 0.65 and $k_t^{1,1} = 6.60 \times 10^8$ L mol^{-1} s^{-1} provided the best fit to the experimental data. This is only an approximate value for $k_t^{1,1}$ because of the approximation $DP = DP_n$ (i.e. PD =1). One could refine this by assuming $PD \approx PDI = 1.5$, which is the case for classical combination, to

yield $k_t^{1,1} = 1.14 \times 10^9$ L mol^{-1} s^{-1}. But even *PDI* = 1.5 is not correct for CLD, which acts to broaden MMDs and thus increase the value of *PDI*. Furthermore, there is also the assumption that $DP = DP_w$, which is not exact. So it is hopeless to try to exact $k_t^{1,1}$ exactly.

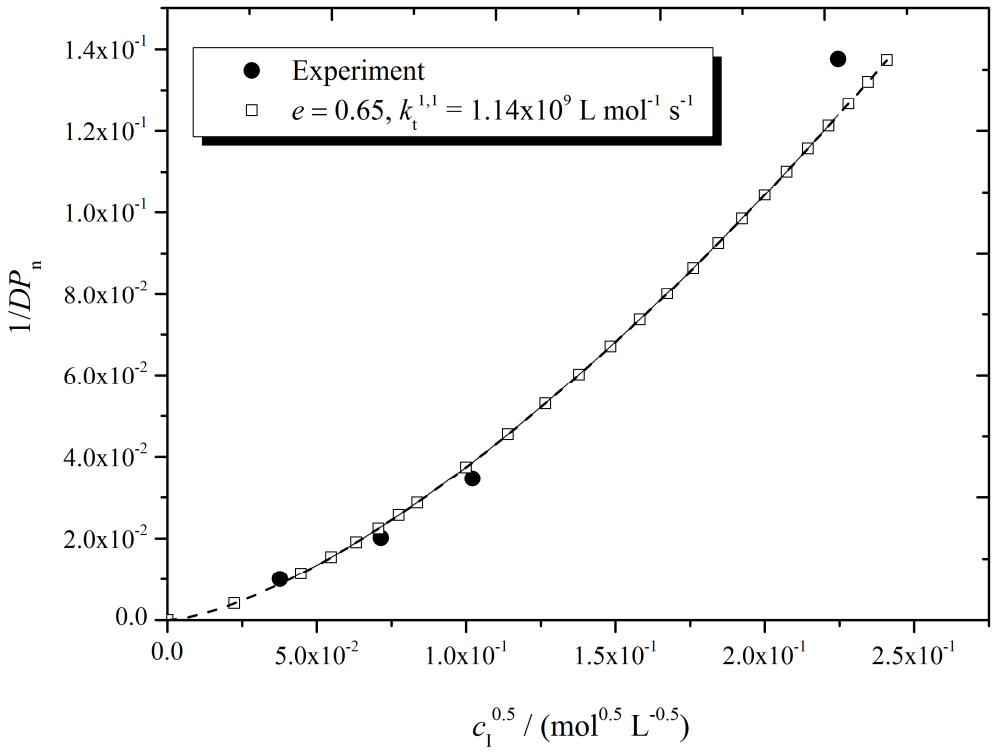

Figure 3-12. Reciprocal number-average degree of polymerization, $1/DP_n$, as a function of square root of AIBN initiator concentration, $c_I^{0.5}$, for styrene polymerization at 85 °C and 0.67 mol L^{-1} styrene in ethyl benzene. Filled circle: experimental results; Empty square: calculated results using Eq. 11 with $k_p c_M = 518$ s^{-1}, $\lambda = 0$, $fk_d = 2.17 \times 10^{-4}$s^{-1}, $DP_n = DP/PD$, $PD = 1.5$, $e = 0.65$ and $k_t^{1,1} = 1.14 \times 10^9$ L mol^{-}1 s^{-1}.

3.4. Monomer concentration effect

Monomer concentration effect on the rate of polymerization was also studied; Eq. 12 shows the dependence of the rate of polymerization on monomer concentration.

$$R_p \sim (c_M)^{\beta} \qquad (12)$$

$$\text{where } \beta = 1 + 2b \text{ and } b = \frac{a}{2} = \frac{e}{2(2-e)}$$

Monomer concentration, c_M, has a larger quantitative effect on the rate of polymerization (R_p) than c_I. Classical kinetics suggests that R_p should be proportional to $(c_M)^{1.0}$. However, deviation of the monomer exponent β from the value 1 is often observed. Mahabadi and O`Driscoll found β = 1.5 and 1.4 in polymerization of dodecyl methacrylate in benzene at 60 °C and 80 °C respectively.[6]

Two important factors should be considered when studying the effect of monomer concentration. First, solvents can have an influence on the kinetics of radical polymerization processes as the solvent affects the system properties such as viscosity and mobility of the radical in the system. The rate of termination relation, $<k_t> \alpha (1/\eta)^1$,[21] has been found for MMA and ST, were η represents solution viscosity. This means that $k_t^{1,1}$ will change, due to viscosity change, providing a second avenue by which R_p (or $<k_t>$) is altered. Furthermore, solvents have been found to have a low influence on the initiation processes,[22-24] and exert only a small effect on k_p.[25-28] However, initiator efficiency will still be affected by any change in viscosity. Also, solvents might contribute as chain transfer molecules.

In this study, it was tried to achieve optimum ideal conditions. Viscosity effects were minimised by using solvent of similar viscosity. In these systems it is assumed that the rate of initiation is not affected. As a solvent may have other effects, two polymerization systems were used in this study, MMA/methyl isobutyrate (MIB) and MMA/trifluorotoluene (TFT).

With these choices, solvents should exert at most a small effect on $k_t^{i,j}$ values, thus allowing the effect of c_M on $\langle k_t \rangle$ to be isolated. This is because both solvents have a very similar viscosity to MMA, especially at high temperatures. Figure 3-13 shows our experimental data for viscosities obtained for similar systems. Literature values of viscosity for MMA, MIB and TFT at 20 °C are presented in Table 3-2.[29, 30] This will ensure that $\langle k_t \rangle$, which is diffusion-controlled, does not change much due to any viscosity changes.

Table 3-2. Literature viscosity values at 20 °C

	Viscosity
MMA	0.6 cp
MIB	0.58 cp
TFT	0.57 cp

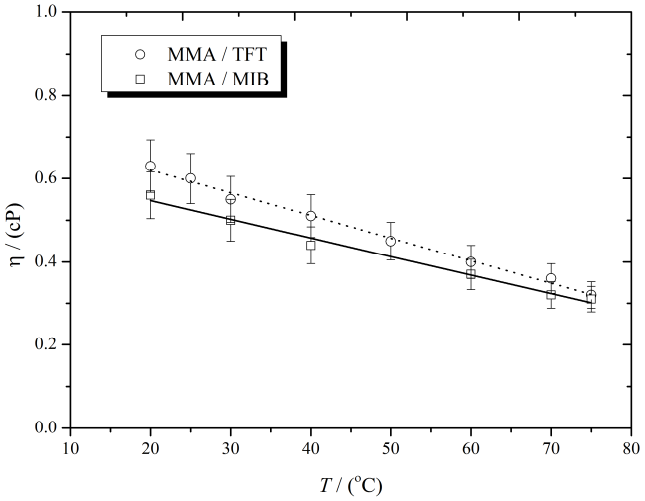

Figure 3-13. Experimental viscosity measurements of 0.67 mol L^{-1} MMA in TFT and MIB as a function of temperature that were obtained using Brookfield DV-II+ Pro viscosity meter.

Dependence of rate of polymerization on monomer concentration is clearly evident from the result in Figure 3-14, where two polymerization systems are presented. First, a polymerization system of MMA/TFT was used to minimize solvent chain transfer reactions. This is because trifluorotoluene does not contain any methyl hydrogens, and thus has no potential sites for transfer to solvent (as opposed to toluene). The results show that with such a system the value of β deviates from the classical value of 1.0, yielding 1.18. This is evidence that chain-length dependency is the cause of this deviation in the value of β.

Second, the system of MMA/MIB was used. This allows chain transfer to solvent to occur exactly as if the solvent were replaced by monomer. In other words, the net rate of transfer (to solvent and monomer) should be the same as in bulk polymerization, meaning that c_M change is the sole variable causing change in $\langle k_t \rangle$ (although the ideal of dead-chain formation being entirely by termination is therefore not met, meaning that Eq. 11 is not strictly valid). This change leads to an obvious increase of the value of β from 1.18 to 1.30, as shown in Figure 3-14 and reported in Table 3-3.

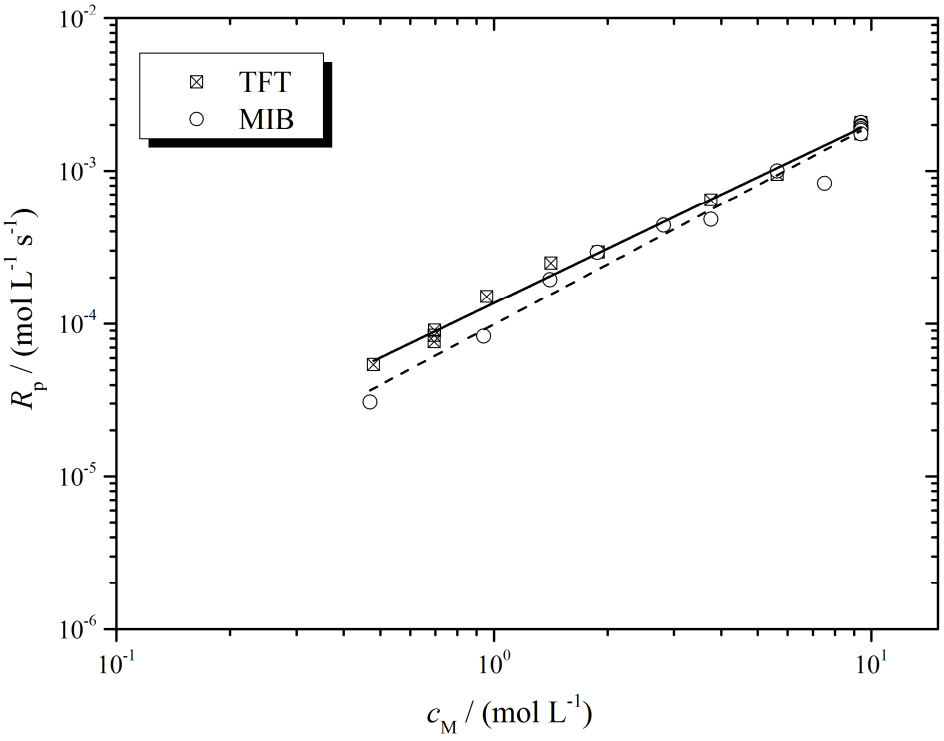

Figure 3-14. Variation of the rate of polymerization, R_p, with monomer concentration, c_M, for solution polymerization of MMA at 70 °C with c_{AIBN} = 0.05 mol L^{-1} in different solvents as indicated, plotted on double logarithmic axes.

Firstly the general effect of solvent on termination will be outlined. Introducing solvent into a polymerization decreases the frequency of propagation, $k_p c_M$. While termination is occurring, assuming no transfer, this leads to the living radical distribution becoming weighted towards

lowers chain lengths, and hence increasing $<k_t>$. Thus R_p is lowered more than expected, and so β is raised above 1.0.

Table 3-3. The values obtained for monomer dependence, β, and from it chain-length depenedence, e, for MMA polymeization at 70 °C in TFT and MIB as indicated.

solvent	β (at 70 °C)	e (from β)*
TFT	1.18 (± 0.02)	0.30
MIB	1.30 (± 0.05)	0.46

*The chain-length dependence is calculated via Eq. 12.

It should be clear from the above discussion why the value of β is different in these cases: while both solvents eliminate any variation of $<k_t>$ on account of viscosity (because there is no viscosity change), in the case of TFT there is change in $<k_t>$ due to both c_M variation and variation in the rate of transfer, while with MIB there is only change due to c_M variation. The question is why the value of β is lower in TFT than in MIB. At first it does not make sense that introducing a solvent that leads to transfer (i.e., MIB) should result in a stronger non-classical effect, whereas above it was argued that transfer to monomer or solvent leads to α being more classical in value. The answer may be attributed to the fact that the former effect relates to transfer to a solvent of fixed concentration, whereas the latter relates to transfer to a solvent of changing concentration. In addition, in the case of MIB, there is further change in $<k_t>$ due to chain transfer to MIB. As the concentration of MIB is increased, more chain transfer occurs, which results in higher $<k_t>$, hence lower R_p, and thus an increased deviation of β from 1 and even from 1.18 obtained for MMA/TFT system. This is exactly as observed in the data. We believe that this difference in the rate of polymerization is due to additional greater chain transfer reaction to the solvent, MIB. In other words, the net rate of transfer (to MIB and monomer) should not be the same as in bulk polymerization as assumed earlier, as will be shown later in this chapter. Therefore, choosing the right solvent becomes crucial.

3.4.1. Composite model

Since, nowadays, it is well established that termination occurs well with the so-called composite model, where two distinguished regimes are observed (Eqs.13). [2, 31, 32]

$$k_{\mathrm{t}}^{i,i} = k_{\mathrm{t}}^{1,1} i^{-e_S}, i \leq i_c \qquad (13)$$

$$k_{\mathrm{t}}^{i,i} = k_{\mathrm{t}}^{1,1} (i_c)^{-e_S+e_L} i^{-e_L}, i > i_c \qquad (13a)$$

Therefore, relating the data analysis to each regime becomes crucial because of different chain-length dependent termination that is correlated with chain length. In view of this, the CLDT is required to be assessed for a definite chain-length regime. To address this appropriately, information about chain lengths is essential. This information, of course, can be obtained experimentally using size exclusion chromatography (SEC) or at least it can be estimated using the Mayo equation (Eq.2). Of course, estimation of DP_{n} using the Mayo equation requires determination of $\langle k_{\mathrm{t}} \rangle$ for the same polymerization alongside an accurate value of other kinetic parameters.

Therefore, it was also interesting to look more specifically into the average termination rate constant ($\langle k_{\mathrm{t}} \rangle$) dependence on the monomer concentration. Surprisingly, in a pleasant way, the results that were obtained show evidence of a strong effect of c_{M} on $\langle k_{\mathrm{t}} \rangle$. This is a surprise, because workers generally have not observed such a strong effect. However it is a pleasant surprise because both theory and experiments by other techniques predict that such an effect should be observed (see Figure 3-15A). Furthermore, as chain-length dependent termination, $\langle k_{\mathrm{t}} \rangle$, is correlated with DP_{n} [1, 33] through the following very important result:[34]

$$\langle k_{\mathrm{t}} \rangle = \mathrm{G}\, k_{\mathrm{t}}^{1,1}\, DP_{\mathrm{n}}{}^{-e} \qquad (14)$$

$$\text{where } G = \left[\Gamma\left(\frac{2}{2-e}\right)\right]^{e-2}\left(\frac{2}{2-e}\frac{2}{1+\lambda}\right)^{e}$$

Because G is close to 1 in value, Eq. 14 gives $\langle k_t \rangle \approx k_t^{1,1} (DP_n)^{-e}$, where the variation of $\langle k_t \rangle$ with DP_n almost exactly mirrors the underlying variation of $k_t^{i,i}$ with i, which is identical in form to the equation $\langle k_t \rangle \approx k_t^{1,1} i^{-e}$. Consequently, the $\langle k_t \rangle$ also was plotted versus the best-estimate DP_n for the experiment carried out, where the slope is e. To be precise, termination behaviour is dictated by the long-chain regime when $DP_n > i_c$ and by the small-chain regime when $DP_n < i_c$, where i_c is a crossover chain length and is 100 for MMA and 50 for ST. Moreover, again termination is related to c_M through the equation $\langle k_t \rangle \sim (c_M)^{-2a}$ where $a = \frac{e}{2-e}$.

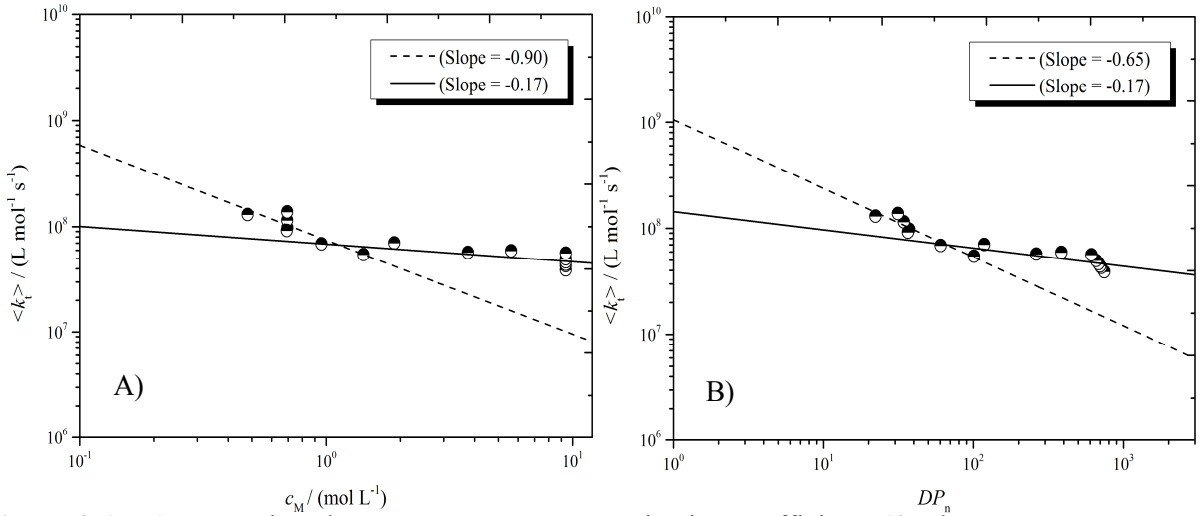

Figure 3-15. A comparison between average rate termination coefficient, A) $\langle k_t \rangle$, versus monomer concentration (c_M). B) $\langle k_t \rangle$ versus calculated number average degree of polymerization (DP_n) for MMA polymerization in TFT solution at 70 °C, plotted on double logarithmic axes.

Interestingly, the result (Figure 3-15) shows an almost identical picture of both $\langle k_t \rangle$ versus c_M and estimated DP_n, where very close chain-length dependence values are obtained from both plots, i.e. $\langle k_t \rangle$ versus c_M yielded values of e_S= 0.62 and e_L= 0.16. The results in Figure 3-15 agree remarkably well with the so-called composite model equations of termination (Eqs.13). [2, 31, 32]

The analyses of MMA/TFT polymerization experiment, taking into account the two different regimes, yields $e_L = 0.16$ for long chains ($DP_n > 100$), in accord with literature [1, 13, 35-38], and $e_S = 0.62$ for small chains ($DP_n < 100$), also in agreement with measurements [13, 20, 39] and with theoretical expectations.[31] For ST, the situation is the same. A result that is consistent with large-chain dependence of termination, $e_L = 0.11$, can be obtained (Figure 3-16).[40-42] In general, the resulting CLDT kinetics of MMA and ST were found to be well described by the composite model.[1]

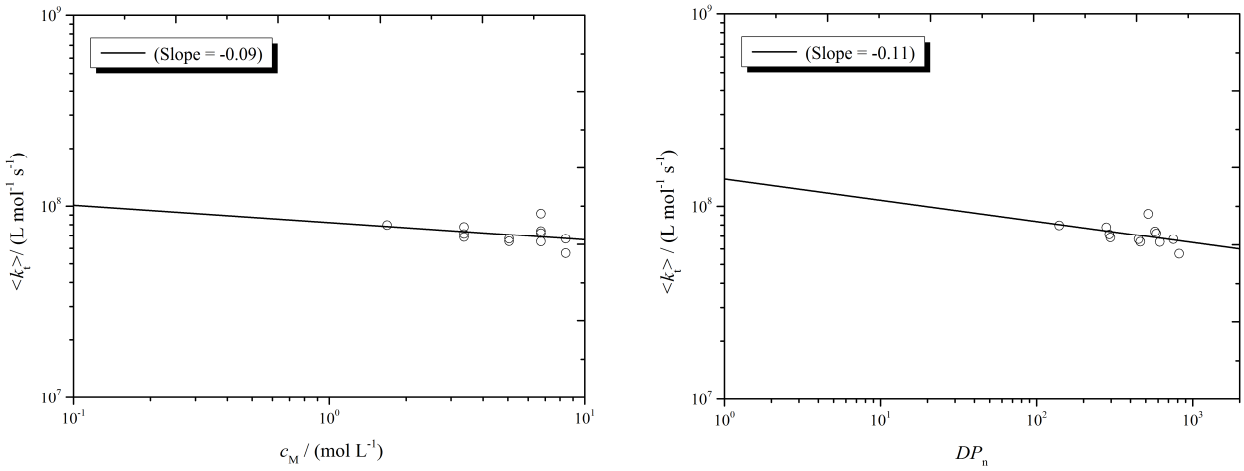

Figure 3-16. Log-log plot of $<k_t>$ versus c_M (left) and $<k_t>$ versus calculated number average degree of polymerization (DP_n) (right) for ST polymerization in ethyl benzene solution at 50 °C and 1.00 wt.% AIBN. Points: experimental values;[9] lines: linear best fits, with slopes as displayed.

The analyses of MMA/MIB polymerization experiment (Figure 3-17) yields $e_L = 0.36$ for long chains ($DP_n > 100$), and $e_S = 0.79$ for small chains ($DP_n < 100$), which are larger than chain-length dependences that are obtained for MMA/TFT, which might be ascribed to the effect of chain transfer to the MIB.

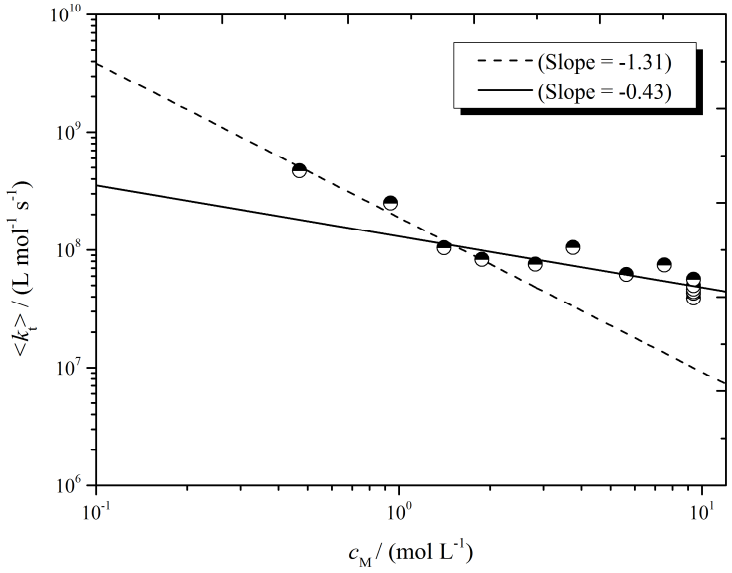

Figure 3-17. $<k_t>$, versus monomer concentration (c_M) for MMA polymerization in MIB solution at 70 °C, plotted on double logarithmic axes.

Table 3-4 summarises the corresponding chain-length dependency value, *e*, obtained from both β and the $<k_t> \sim c_M$ plot for MMA/TFT and MMA/MIB at 70 °C.

Table 3-4. The results for β for MMA solution polymerization in two different solvents as indicated. The corresponding chain-length dependency value, *e*, obtained from β is shown. Also, the *e* values obtained from $<k_t> \sim c_M$ plot taking into account the two different regimes are reported.

solvent	β (at 70 °C)	*e* (from β)	*e* (from $<k_t> \sim c_M$)*
TFT	1.18 (±0.02)	0.30	0.16 (L) 0.62 (S)
MIB	1.30 (±0.05)	0.46	0.36 (L) 0.79 (S)

(S) Denotes short polymers, $DP_n < 100$ (L) Denotes long polymers, $DP_n > 100$ *Using Eq. 3

Furthermore, obtaining identical results from both estimated DP_n and c_M as shown in Figure 3-15 may support the capability of using the calculated DP_n to obtain chain-length dependence of termination under different conditions. The pleasant thing about the above result is that one can use results from experiments in which c_I, c_M and temperature are varied, as long as $k_t^{1,1}$ does not vary much, to obtain information on CLDT. Figure 3-18 shows a plot

of my experimental $<k_t>$ obtained under different reaction conditions and its corresponding estimated DP_n.

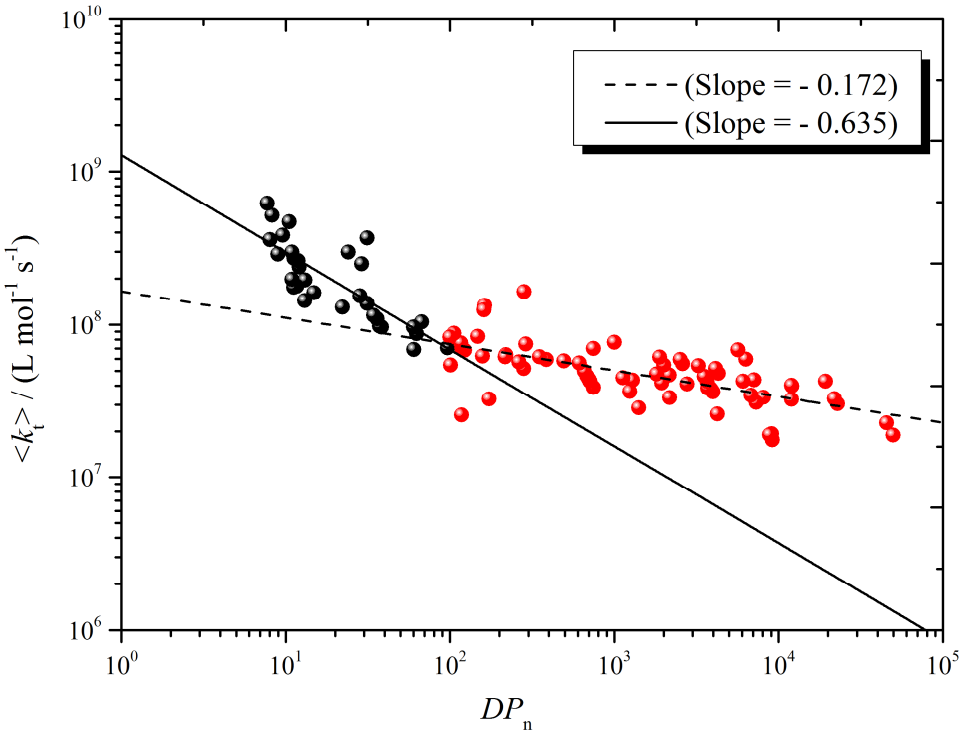

Figure 3-18. Experimental $<k_t>$ vs. calculated number average degree of polymerization (DP_n) for methyl methacrylate (MMA) radical polymerization obtained at ambient pressure and different polymerization conditions, plotted on double logarithmic axes.

The results obtained from Figure 3-18, e_L= 0.17 ± 0.09, e_S = 0.64 ± 0.12 and $k_t^{1,1}$= (1.3 ± 1.1)×10^9 L mol^{-1} s^{-1}, are in excellent agreement with recent studies into CLDT. The change in behaviour at $i = i_c$ is evident. In addition, it is also in agreement with the Smoluchowski equation for small polymers, predicting $k_t^{1,1} \approx 10^9$ L mol^{-1} s^{-1} for dilute-solution radical polymerization.[43] The assumption of temperature-independent e_S, e_L and i_c values has been made in the figure above and supported by recent SP-PLP-EPR studies into chain-length dependent termination, in which the temperature effect on any of the above parameters has not been observed.[12, 14, 20, 44, 45]

3.4.2. Temperature effect

Investigation of the effect of temperature, carried out in this work, shows an influence of the temperature on the value of β. Increasing the temperature increases the value of β while decreasing the temperature decreases the value of β and makes it very close to 1.0. Further, lowering the temperature is found to decrease the effect of the solvents used on the value of β (Figure 3-19).

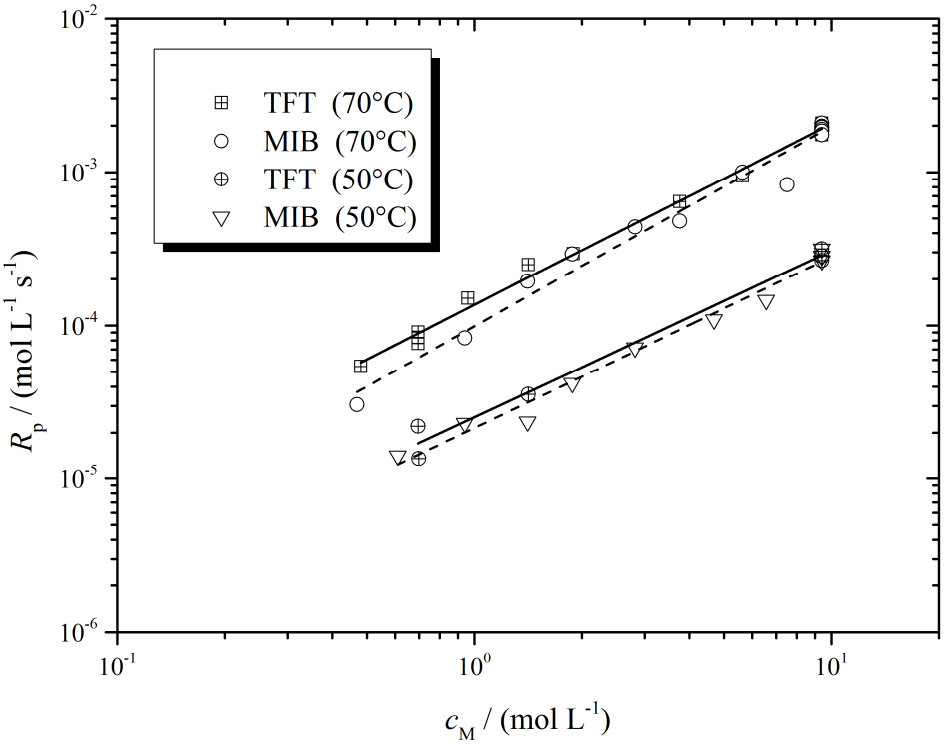

Figure 3-19. Variation of the rate of polymerization, R_p, with monomer concentration, c_M, for solution methyl methacrylate (MMA) polymerization at 50 °C and 70 °C with c_{AIBN} = 0.05 mol L^{-1} in different solvents as indicated, plotted on double logarithmic axes.

Temperature has two effects, firstly on polymer chain length and secondly on the chain transfer rate. First, in the system of MMA/MIB, where chain transfer reactions play an essential role, the following was observed. Increasing the temperature leads to an increase in the process of chain transfer reactions. This is obvious with MIB where chain transfer to MIB

is known and confirmed. Increasing the temperature increases the value of β from 1.11 to 1.30 at 50 °C and 70 °C respectively (Figure 3-19, Table 3-5).

To explain this, the chain transfer reaction should be considered. Indeed, the chain transfer reaction seems to play a major role in this difference with temperature. As the chain transfer to solvent dominates the dead chain formation with increasing temperature, and as c_M is lowered, the frequency of propagation is lowered, and the frequency of chain transfer $k_{tr}\, c_S$ is increased. Both factors act to weight the living radical distribution towards smaller chain lengths and so to increase the $<k_t>$ value. Thus chain transfer to solvent acts to move β further from 1.0 in value. At the same time, it will move α closer to 0.5 in value, because changing initiator concentration does not change the transfer frequency.

Second, in the system of MMA/TFT, where it is believed that there is no chain transfer to solvent happening, the β value increased from 1.08 to 1.18 at 50 °C and 70 °C respectively (Table 3-6). Because of the fact that there is no or negligible chain transfer to the solvent in this system, one rationalization explain this change is chain-length dependency. As the temperature increases the weight of the living radical distribution moves toward smaller chain lengths, leading to a large chain-length dependency that we see as a deviation in the value of β. Lowering the temperature leads to the production of large polymers that have low chain-length dependency that lowers the value of β. Table 3-6 shows the resulting values of β and the corresponding chain-length dependency, e, obtained from both β and the $<k_t> \sim c_M$ plot taking consideration of the two different regimes as suggested by the composite model. The results are very close to the literature and the theoretical values. The chain transfer to initiator can be ignored in the present system, as the initiator is AIBN. Another possible explanation is that there is some variation in the value of e with temperature, although insofar as this has been investigated it has been reported that long-chain e decreases as temperature increases,

contrary to the pattern here. Finally, as c_M increases there will be more transfer to monomer. At higher temperature this will be more important, which could also explain that β increases with temperature.

Table 3-5. The results for β as a function of temperature for MMA/MIB system. The corresponding chain-length dependency value, e, obtained from β is shown. Also, the e values obtained from $\langle k_t \rangle \sim c_M$ plot taking into account the two different regimes are reported.

Temperature	β	e (from β)	e (from $\langle k_t \rangle \sim c_M$)*
50 °C	1.11 (± 0.05)	0.20	0.26 (L)
70 °C	1.30 (± 0.05)	0.46	0.36 (L) 0.79 (S)

(S) Denotes short polymers, $DP_n < 100$ (L) Denotes long polymers, $DP_n > 100$ * Using Eq. 3

Table 3-6. The results for β as a function of temperature for MMA/TFT system, with the corresponding chain-length dependency values, e, as in Table 3-5.

Temperature	β	e (from β)	e (from $\langle k_t \rangle \sim c_M$)
50 °C	1.08 (± 0.06)	0.15	0.11 (L)
70 °C	1.18 (± 0.02)	0.30	0.16 (L) 0.62 (S)

3.4.3. Dependence of DP_n on monomer concentration (c_M)

Classically, the rate of polymerization is dependent on the first power of the monomer concentration, c_M, and the square root of the initiator concentration, c_I, (Eq. 15). Similarly, the degree of polymerization also depends on the monomer concentration and inversely on the square root of the initiator concentration (Eq. 15a). High R_p and high molar mass polymer result from high c_M, whereas high R_p and low molar mass polymer result from high c_I. Thus, either R_p or DP_n can be used to determine the polymerization dependence of monomer and initiator. Again DP is used rather than DP_n for reasons that are explained earlier. Figure 3-20 shows the dependence of DP on the monomer concentration of a wide range of DP.

Deviation from classical kinetics is clearly observed, which is an indication for CLDT. Although a larger dependence is observed with MIB as a result of chain transfer to solvent (Figure 3-14), it was not as large as observed from the rate of polymerization. Constraining the data to only large polymers (DP > 100) gives a slope of 1.083 with the MMA/TFT system (Figure 3-20 right), corresponding to e = 0.15, which is in very good agreement with what has been found experimentally and theoretically in the literature. Although the use of DP still has some accuracy-related issues, such as assuming constant PD for all experiments, it demonstrates an alternative way to using the rate of polymerization.

$$R_\mathrm{p} \; \alpha \; {c_\mathrm{I}}^{0.5} \, {c_\mathrm{M}}^{1.0} \qquad (15)$$

$$DP \; \alpha \; {c_\mathrm{M}}^{1.0} \, {c_\mathrm{I}}^{-0.5} \qquad (15a)$$

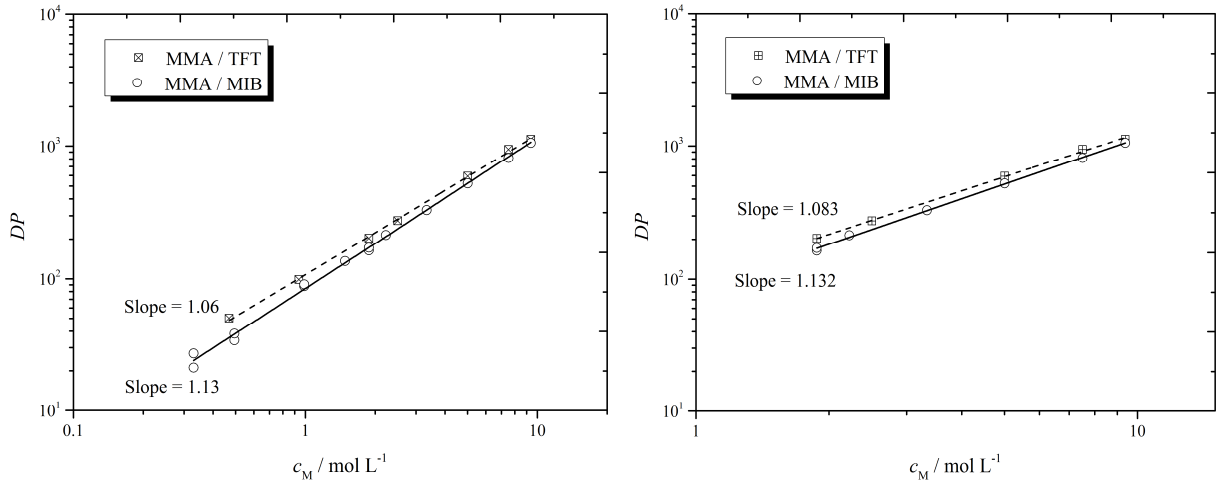

Figure 3-20. Log-log plots of DP versus monomer concentration, c_M for MMA polymerization at 70 °C and 0.05 mol L^{-1} AIBN in solvents as indicated. Points: experimental values, lines: linear best fits, with slopes as displayed. The figure on the right shows data restricted to DP > 100.

3.5. Chain transfer rate to solvents

Chain transfer reactions affect the polymerization process. In particular, they have an effect on the polymer molar mass. This results in a lower molar mass of polymer products than the predicted one of the theoretical kinetic equations by disproportionation and combination. This

effect is due to the earlier termination of growing macroradicals by the transfer reaction, such as transfer of hydrogen or other atom to it from compounds present in the system, such as initiator, solvent, polymer and monomer. In contrast to transfer to initiator, transfer to solvent can be of considerable importance, because solvent is often used in high concentrations in polymerization processes. Chain transfer to solvent results in a lower molar mass polymer product than the one prepared in the absence of solvents and is observed in many polymer reaction systems.[46] Even though the effect of the transfer reactions on the rate of polymerization is not as pronounced as observed in the molar mass, it is dependent on whether the rate of re-initiation is comparable to that of the original propagating radical, it can be especially observed when low molar mass polymers are formed and where termination chain-length dependence is large. The latter is because any reaction that acts to produce small radicals will cause $<k_t>$ to rise on account of CLDT.

3.5.1. Chain transfer rate constant to MIB

Methyl isobutyrate (MIB) is the saturated analogue of methyl methacrylate (MMA). It is used as a replacement of monomer and should result in negligible change of the physical properties of the solution, in particular any that can affect the rate of termination, such as viscosity and solvent power. Although the use of this solvent would be ideal, it shows some chain transfer reactivity.

First, a proof of chain transfer to the solvent MIB was found by ESI-MS (Figure 3-21) (discussed later in Chapter 6). The signals are quite observable and may indicate a large chain transfer rate constant relative to other possible transfer reactions to monomer and initiator.

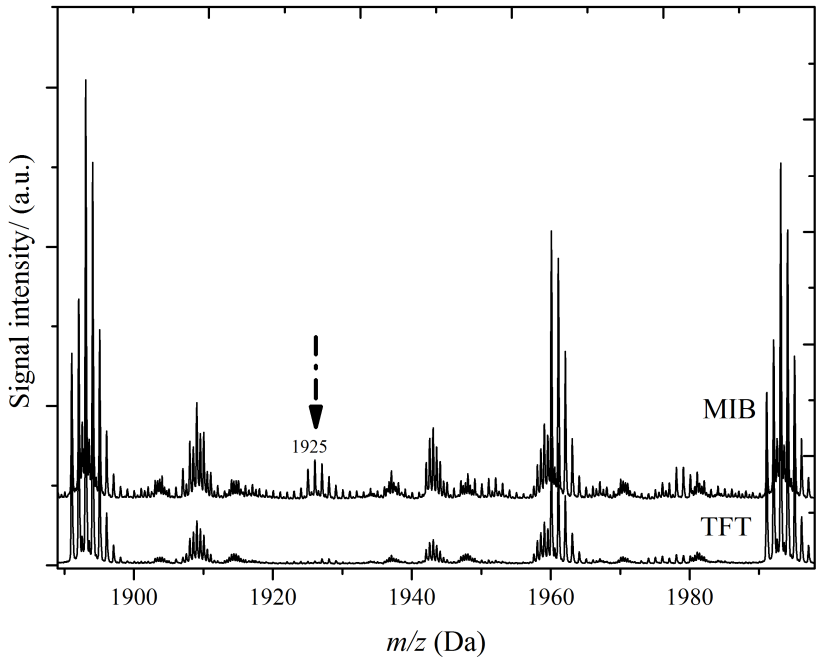

Figure 3-21. Portions of the ESI-MS spectra of poly (methyl methacrylate) obtained from radical polymerization in methyl isobutyrate (MIB; upper spectrum) and trifluorotoluene (TFT; lower). The arrow indicates pure polymer of chain length 19 (together with Na from the ESI process). This species is not observed with TFT and results from chain transfer to MIB, as in Scheme 1.

The chain transfer to MIB might be attributed to the low bond dissociation energy (BDE) of the tertiary C-H bond. The MIB contains an H that is bonded to tertiary C, and thus this H is relatively labile to chain transfer, as illustrated in Scheme 1.

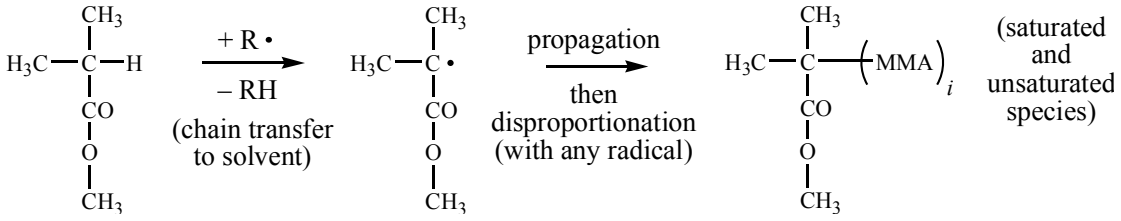

Scheme 1. Showing how chain transfer to methyl isobutyrate (MIB) occurs, and how this leads to dead polymer with MMA as end-groups.

The bond dissociation energy of the labile tertiary C-H in MIB is estimated to be equal 344.55kJ mol^{-1}, using standard enthalpy of formations as illustrated in the reaction below, with $\Delta H^{\circ}_{f}(H^{\bullet})$ = 218.13 kJ mol^{-1}. [47] In general, this bond dissociation energy is in good agreement with literature tertiary C-H bond energies.[48] In addition to the labiality of C-H, the chain transfer reaction is supported by the stabilizing nature of the adjacent carbonyl group in the resulting radical.

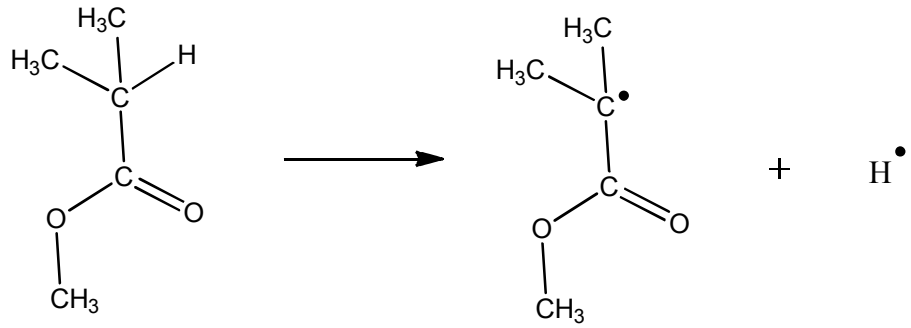

ΔH^{0}_{f} = - 452.99 kJ/mol ΔH^{0}_{f} = -326.57 kJ/mol ΔH^{0}_{f} = 218.13 kJ/mol

Additionally, in fact chain transfer to solvent is probably ascribed to be the cause of obtaining different values of monomer concentration dependence (β) with TFT and MIB solvents. Experimental results shown in Figure 3-14 express the deviation from classical kinetics using TFT and MIB as solvents for MMA polymerization, giving β = 1.18 and β =1.30 respectively, indicating CLDT. This difference in monomer dependence is believed to be due to the occurrence of chain transfer to MIB as the concentration of MIB is increased, which results in higher $<k_t>$, hence lower R_p, and thus increasing deviation of β from what is expected from classical kinetics, resulting in higher monomer dependence. Also, the same is found from *DP* as a function of c_M (Figure 3-20). In view of the above findings, quantitative determination of the chain transfer constant to MIB, $C_{tr,MIB}$ is carried out experimentally.

3.5.2. Determination of chain transfer constant to MIB

The transfer rate constant, $C_{tr,X}$, is defined as the ratio of the chain transfer and propagation rate coefficients $k_{tr,X}/k_p$, where X denotes a compound to which transfer occurs. This ratio is commonly determined using the well-known Mayo procedure (Eq. 16).[46, 49] This equation can be used to predict the DP_n, or alternatively may be used to analyze data to obtain the values of rate parameters, where DP_n is measured.

$$\frac{1}{DP_n} = \frac{PD}{DP} = \frac{(1+\lambda)(0.5R_i\langle k_t\rangle)^{0.5}}{k_p c_M} + C_{tr,M} + C_{tr,I}\frac{c_I}{c_M} + C_{tr,S}\frac{c_S}{c_M} \qquad (16)$$

Here DP_n is number-average degree of polymerization, $C_{tr,S}$, $C_{tr,M}$ and $C_{tr,I}$ chain transfer constants of solvent, monomer and initiator respectively, c_S solvent concentration, c_M monomer concentration, c_I initiator concentration, R_i rate of initiation, k_p propagation rate coefficient, $\langle k_t\rangle$ average termination rate coefficient, λ is mode of termination and DP peak degree of polymerization. The new quantity PD is the ratio of $DP = M_p/M_0$, the degree of polymerization of the centre of the SEC chromatogram peak, and DP_n. In the event that $DP = DP_w$, which is often the case to good approximation, one clearly has that $PD = PDI$. However it is stressed that this only gives a better estimate of DP_n from DP in the absence of any other information, and by no means should $PD = PDI$ be taken as an exact result.

This method requires knowledge of measuring average degree of polymerization for a range of c_X/c_M. By plotting data as $1/DP_n$ versus a varied c_X/c_M, the resulting linear fits are used to obtain the rate coefficient from the slope and the intercept, relying on the assumption of the independent intercept with the variation of c_X/c_M.

Although this procedure is commonly employed with chain transfer agent (CTA), where termination is dominated by transfer, it is also used to determine other transfer constants.

Chain transfer to the solvent, MIB, as in our experiment, can be determined using the Mayo procedure, neglecting chain transfer to monomer, initiator and polymer, an assumption that should be fulfilled in this system. The determination of $C_{tr,S}$ using Eq. 16 requires appropriate choice of polymerization conditions. For instance, the use of Eq. 16 to determine $C_{tr,S}$ by plotting c_S/c_M versus $1/DP_n$ in principle requires keeping the first term on the right side of the equation constant by, for example, adjusting the initiator concentration and neglecting the chain-length dependence of termination. Alternatively, the $C_{tr,S}$ can be determined by Eq. 17, which suggests plotting the terms on the left-hand side versus c_S/c_M.

$$\left(\frac{1}{DP_n} - \frac{(1+\lambda)(0.5R_i\langle k_t\rangle)^{0.5}}{k_p c_M}\right) = C_{tr,S}\frac{c_S}{c_M} \qquad (17)$$

However, such usage of Eq. 17 requires further knowledge of the rate of termination, $\langle k_t \rangle$, which is known to be system dependent and has to be determined experimentally in addition to DP_n.

In this work, a different approach is adopted as an attempt to determine $C_{tr,S}$. This approach builds upon the determination of the relative difference of the average degree of polymerization between two polymerization experiments with the variation of c_X/c_M, one with MIB and another with an inert solvent. In this experiment, again the *DP* value is used, as it can be measured with higher accuracy than DP_n. This leads to Eq. 18, which shows that information is required about *PD*:

$$\frac{1}{DP} = \frac{(1+\lambda)(0.5R_i\langle k_t\rangle)^{0.5}}{(PD)k_p c_M} + \frac{C_{tr,M}}{PD} + \frac{C_{tr,I}}{PD}\frac{c_I}{c_M} + \frac{C_{tr,S}}{PD}\frac{c_S}{c_M} \qquad (18)$$

DP is affected by changing the monomer concentration (c_M) and chain transfer to solvent when it takes place. The c_M is proportionally related to the *DP*, i.e. increasing the c_M results

in an increase in the *DP*. Accordingly, the slope of the plot of 1/*DP* versus c_{MIB}/c_{MMA}, in case of MIB, should be correlated with the change in c_M and the chain transfer to the solvent.

In order to obtain the chain transfer constant to MIB, the same experiment is performed under the same conditions, in a different solvent, trifluorotoluene (TFT), which has a similar viscosity[29] to MMA and negligible chain transfer potential, as indicated by ESI-MS results (see Figure 3-21). Thus one can determine the effect of chain transfer to MIB from the difference between the slopes of the two experiments, where any other effects should largely be cancelled out.

This may be shown by evaluating 1/*DP* as a function of c_S/c_M to determine the effect of chain transfer on the intercept and the slope (Figure 3-22), using constant $\langle k_t \rangle$, i.e., assuming CLIT.

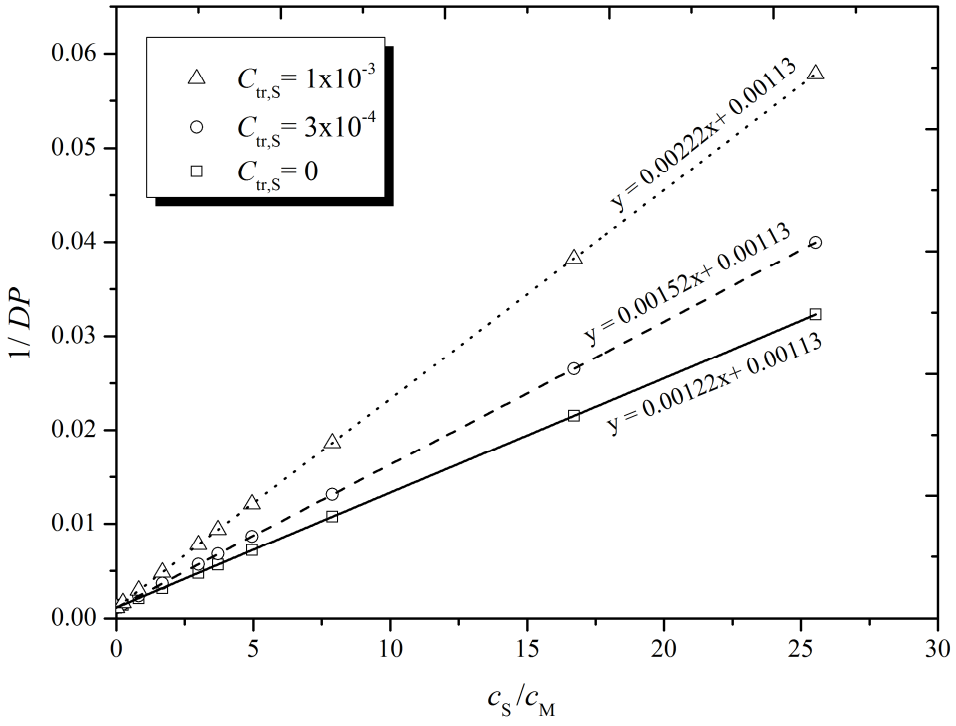

Figure 3-22. 1/*DP* as a function of c_S/c_M calculated using Eq. 18 assuming negligible chain transfer to monomer and initiator and with k_p=1055 L mol^{-1} s^{-1}, R_i = 3.00 × 10^{-6} mol L^{-1} s^{-1}, $\langle k_t \rangle$ = 4.0 × 10^7 L mol^{-1} s^{-1}, λ= 0.45, *PD* =1 and varying $C_{tr,S}$ as indicated. Points: calculated values; lines: linear best fit.

It is clear from Figure 3-22 how the slope varies with $C_{tr,S}$. Also, it is important to be aware that with $C_{tr,S}$ = 0 the slope of the line is not zero and the slope corresponds only to the change in the monomer concentration where there is zero chain transfer to solvent (and monomer). The presented $C_{tr,S}$ values correspond to the difference between the slope of the line with chain transfer and the slope of the one with zero chain transfer, thus enabling determination of $C_{tr,S}/PD$ from the difference of the slopes. Moreover, Figure 3-22 illustrates how the intercept is constant with varying $C_{tr,S}$ and not 0.

Because this method relies on the relative difference in slopes, and as the polymerizations were carried out at very similar conditions, one would assume very similar *PD* in both experiments and even with MIB system where chain transfer occurring. Under this assumption, the difference in the slope will be related only to $C_{tr,S}/PD$.

The experimental results of MMA polymerization in MIB and TFT solvents under the same condition are presented in Figure 3-23, resulting in slopes of 0.0016 and 0.0012 for MIB and TFT respectively. This difference of 4×10^{-4} corresponds to $C_{tr,MIB}/PD$, i.e., it is ascribed to the effect of chain transfer to the MIB that has been observed in ESI-MS spectrum, with a corresponding value of $k_{tr,MIB}$ = 0.844 and 0.633 M^{-1} s^{-1}, employing *PD* = 2 and 1.5 respectively and k_p= 1055 M^{-1} s^{-1}[25], since $(4 \times 10^{-4}) \times PD = C_{tr,MIB} = k_{tr,MIB}/k_p$. This value is about 30 to 40 times larger than the transfer rate coefficient to monomer, MMA, which is $C_{tr,M} = 0.2 \times 10^{-4}$ at 70°C.[50] This difference is because MMA does not possess a tertiary C-H bond, in contrast to MIB. By limiting the data analysis to the linear portion of the data one can obtain $C_{tr,MIB}$= $(3.4 - 2.5) \times 10^{-4}$, employing *PD* = 2 and 1.5 respectively, which still larger than $C_{tr,M.}$ Of course this would be more accurate than the value obtained from the linear fit of the whole points as it results in positive intercept similar to MMA/TFT system.

Of course the value $PD = 2$ is likely to be more accurate for transfer-dominated systems, for which $PDI = 2$.

This result is in good agreement with what is found in literature for solvents with a single tertiary C-H bond with adjacent functionality to stabilize a radical, for example $C_{tr,S} = 2.6 \times 10^{-4}$ at 60 °C is reported for MMA in cumene.[51] However, one still need to know accurately the *PD* value in order to determine exactly $C_{tr,MIB}$. Further, this result is based on an approximation (that of everything else being the same in the two different solvents, see above), therefore error might be still expected in this result.

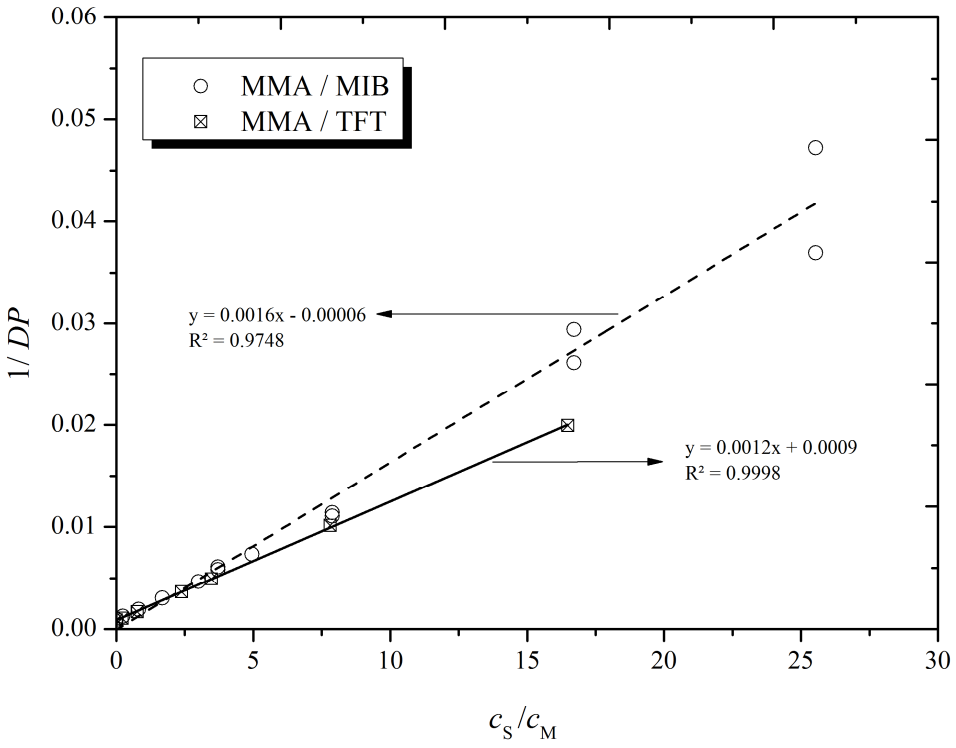

Figure 3-23. 1/*DP* from low conversion solution polymerization of methyl methacrylate (MMA) as a function of concentration of c_S/c_M at 70 °C. Points: experimental values; lines: linear best fit, with slopes and intercepts as displayed.

On the other hand, information can also be potentially obtained from the intercept, which has been found to be equal to

$$\frac{(1+\lambda)(0.5R_{\mathrm{i}}\langle k_{\mathrm{t}}\rangle)^{0.5}}{(PD)k_{\mathrm{p}}c_{\mathrm{M}}}+\frac{C_{\mathrm{tr,M}}}{PD}+\frac{C_{\mathrm{tr,I}}}{PD}\frac{c_{\mathrm{I}}}{c_{\mathrm{M}}} \qquad (19)$$

For instance, from the intercept the average rate of termination $\langle k_t \rangle$ could be estimated when other kinetic parameters are available. So, by employing the appropriate kinetic parameters at 70 °C, $k_d = 4.33 \times 10^{-5}$ s^{-1}, $k_p = 1055$ M^{-1} s^{-1}, $f = 0.68$, $c_M = 9.39$ mol L^{-1}, $c_I = 0.05$ mol L^{-1} and $\lambda = 0.45$, as found in this PhD work, the rate of termination for MMA/TFT system has been evaluated, assuming no chain transfer reactions are occurring ($C_{tr,M} = 0$, $C_{tr,I} = 0$), to yield values of 1.03×10^8 L mol^{-1} s^{-1} and 5.78×10^7 L mol^{-1} s^{-1} employing values of 2 and 1.5 for *PD* respectively. Again, the validity of this value required accurate information about *PD*. In comparison, MMA/MIB results in a negative value. This is attributed to the deviation from linearity as the contribution of transfer to solvent increases the result in small polymers with large termination chain-length dependence, causing the line to deviate more, leading to a negative intercept value when a linear fit is employed. However, consistent $\langle k_t \rangle$ ($\approx 5.7 \times 10^7$ L mol^{-1} s^{-1} employing *PD* =1.5) values are obtained from MMA/MIB and MMA/TFT system using only the linear portions of each data set.

Alternatively, again assuming no chain transfer to monomer and initiator ($C_{tr,M} = 0$, $C_{tr,I} = 0$), Eq. 18 can be rearranged to give Eq. 18a.

$$\frac{c_{\mathrm{M}}}{DP}=\frac{(1+\lambda)(0.5R_{\mathrm{i}}\langle k_{\mathrm{t}}\rangle)^{0.5}}{k_{\mathrm{p}}\,PD}+\frac{C_{\mathrm{tr,S}}\,c_{\mathrm{S}}}{PD} \qquad (18a)$$

One now can plot the data as c_M/DP versus c_S to get slope equal to $C_{tr,s}/PD$ and intercept equal to

$$\frac{(1+\lambda)(0.5R_{\mathrm{i}}\langle k_{\mathrm{t}}\rangle)^{0.5}}{k_{\mathrm{p}}PD}$$

A plot of the experimental data as suggested by Eq. 18a is shown in Figure 3-24. The interesting thing about plotting data this way is that it makes it more explicit. Inspection of Figure 3-24 shows clearly the previously mentioned linear deviation caused by small chains for MMA/MIB results. Again, taking the difference between the slopes of the linear portion of the two experiments results in $C_{tr,s}/PD$ that is consistent with the value obtained previously using Eq. 18 ($C_{tr,MIB}$= (3.4 –2.5) × 10^{-4}, employing PD = 2 and 1.5 respectively). Importantly, taking the difference between slopes ensure that effects other than transfer to solvent would be largely cancel out. Moreover, similarly, $\langle k_t \rangle$ can be estimated from the intercept. Also an evaluation of Eq. 18a with $C_{tr,s}$ = 0 is shown in Figure 3-24, where a flat line is obtained. In spite of the fact that MMA/TFT suppose to results in a flat line, it shows non zero value for $C_{tr,s}$ ($C_{tr,TFT}/PD$ = 1.45×10^{-4}). Nevertheless, this is in fact can be attributed to the CLDT effect, which results in curving the line up as will be discussed in the next subsection.

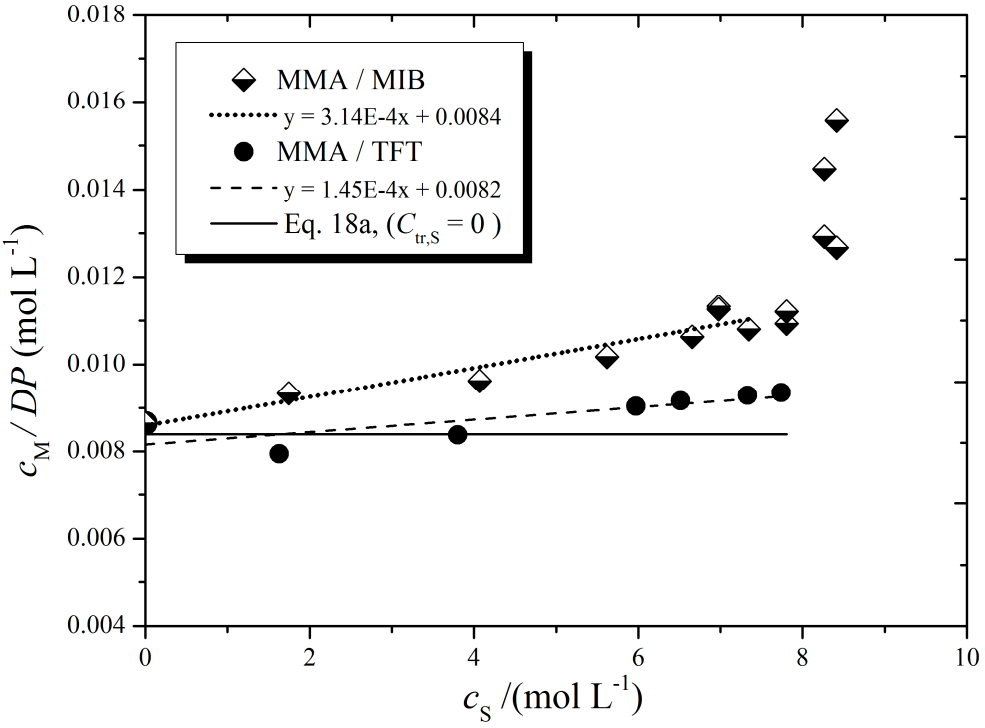

Figure 3-24. c_M/DP as a function of c_S, the concentration of the solvent, for low conversion solution polymerization of MMA at 70 °C. Points: experimental values; lines: solid line is an evaluation of Eq. 18a with $\langle k_t \rangle = 5.70\times10^7$ L mol^{-1} s^{-1}, k_p = 1055 L mol^{-1} s^{-1}, $R_i = 2.49\times10^{-6}$ mol L^{-1} s^{-1}, PD = 1.5, λ= 0.45 and $C_{tr,S}$ = 0. Dashed lines are linear best fits, with slopes and intercepts as displayed.

3.5.3. CLDT effect

So far only the effect of CLIT on DP_n has been considered. However, CLDT also affects molar mass. Figure 3-25 illustrates the effect of CLDT on the Mayo plot using Eq. 16, substituting the CLDT expression for $\langle k_t \rangle$, Eq. 20. Similarly, Figure 3-26 illustrates the effect of CLDT using Eqs. 18a and 20.

$$< k_t > = k_t^{1,1} \left[\Gamma\left(\frac{2}{2-e}\right)\right]^{-2} \left[\frac{\left(2R_i k_t^{1,1}\right)^{0.5}}{k_p c_M}\left(\frac{2}{2-e}\right)\right]^{2e/(2-e)} \qquad (20)$$

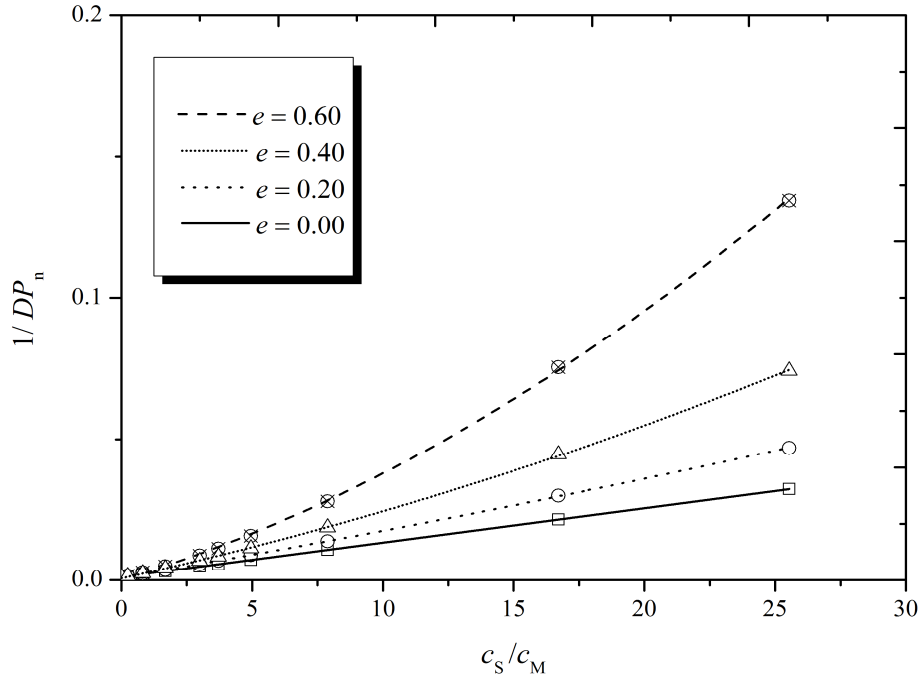

Figure 3-25. Reciprocal number-average degree of polymerization $1/DP_n$ as a function of c_S/c_M calculated using Eqs. 16 and 20 with k_p = 1055 L mol^{-1} s^{-1} and varying c_S/c_M at 70 °C. Points: calculated values; curves: quadratic fits. Values of $k_t^{1,1}$ for each e were chosen so that fits have approximately the same slope as c_S/c_M approaches zero: e = 0, $k_t^{1,1}$ = 4.0 × 10^7 L mol^{-1} s^{-1}; e = 0.2, $k_t^{1,1}$ = 1.3 × 10^8 L mol^{-1} s^{-1} ; e = 0.4, $k_t^{1,1}$ = 4.1 × 10^8 L mol^{-1} s^{-1} ; e = 0.6, $k_t^{1,1}$ = 1.3 × 10^9 L mol^{-1} s^{-1}.

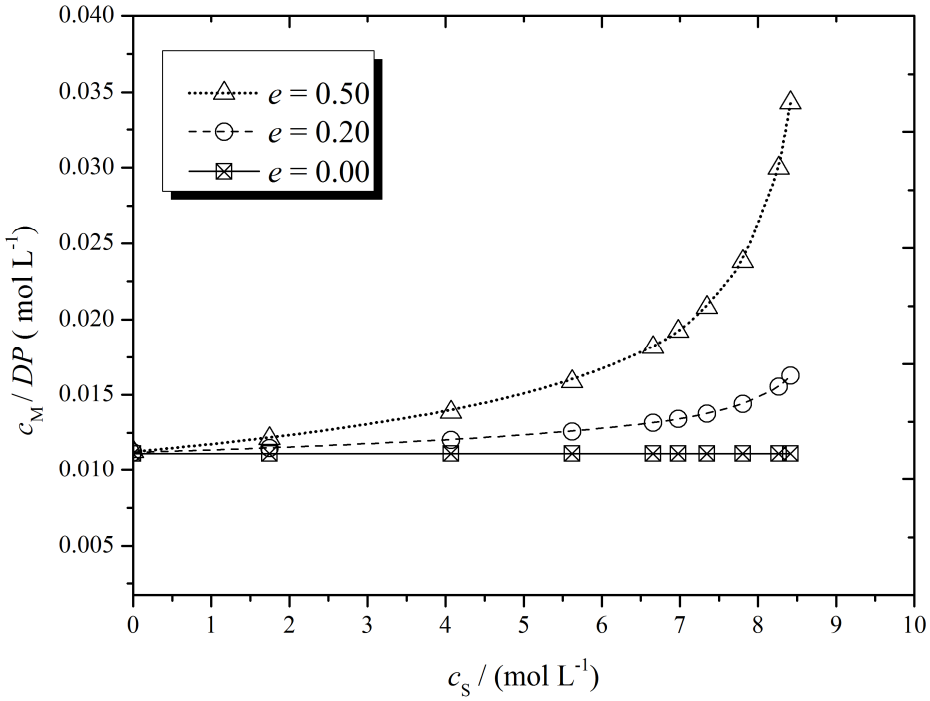

Figure 3-26. c_M/DP as a function of c_S calculated using Eqs. 18a and 20 with k_p = 1055 L mol^{-1} s^{-1} and varying c_S at 70 °C with R_i = 2.49 ×10^{-6} mol L^{-1} s^{-1}, PD =1.5, λ= 0.45 and $C_{tr,S}$ = 0. Points: calculated values. Values of $k_t^{1,1}$ for each e were chosen so that fits have approximately the same value as c_S approaches zero: e = 0, $k_t^{1,1}$ = 1.0 × 10^8 L mol^{-1} s^{-1}; e = 0.20, $k_t^{1,1}$ = 3.0 × 10^8 L mol^{-1} s^{-1} ; e = 0.50, $k_t^{1,1}$ = 1.5 × 10^9 L mol^{-1} s^{-1}.

It is clear from Figure 3-26 that chain-length dependent termination, CLDT, leads to upward curvature. This is interesting as presenting our experimental data in this form clearly shows such behaviour for both systems. (see Figure 3-24). It is recognized that chain transfer to solvent affects the molar mass and results in smaller polymers. So, increasing the solvent will lead to more chain transfer process, producing smaller polymer chains. Currently, it is well established that termination is chain-length dependent and that smaller growing radicals will terminate faster than larger ones.[1] In view of this, one would expect non-linear behaviour with the Mayo plot when it is carried out to a region where small polymers are produced. Therefore, small polymer chains will have large chain-length dependence and deviate from linearity, causing the line to curve upward.

3.6. Conclusion

The results of this chapter show the possible accessibility of CLDT information using a simple technique such as gravimetry to measure the rate of polymerization. Evidence has been put forward in macroscopic rather than in microscopic terms. The rate of polymerization and the reaction orders with respect to monomer and initiator have been determined as a function of temperature. Although the results observed partially meet with expectations from the composite model of termination, issues such as chain transfer have been found to have an effect on the deduced CLDT from rate measurements. Dilute-solution polymerization of MMA in MIB was evidence of such an effect. Conformation of this was derived from temperature dependence. Results suggest that careful steady-state polymerization can be useful for determining $k_t^{1,1}$ and e, although there is no doubt that a technique such as SP-PLP-EPR is more definitive.

References

[1] C. Barner-Kowollik, G.T. Russell, Progress in Polymer Science (Oxford), 34 (2009) 1211-1259.
[2] G.B. Smith, J.P.A. Heuts, G.T. Russell, Macromolecular Symposia, 226 (2005) 133-146.
[3] S. Beuermann, M. Buback, T.P. Davis, R.G. Gilbert, R.A. Hutchinson, A. Kajiwara, B. Klumperman, G.T. Russell, Macromolecular Chemistry and Physics, 201 (2000) 1355-1364.
[4] "Initiators for High Polymers", in, AKZO Nobel Chemicals, 2006.
[5] M. Buback, B. Huckestein, F.D. Kuchta, G.T. Russell, E. Schmid, Macromolecular Chemistry and Physics, 195 (1994) 2117-2140.
[6] H.K. Mahabadi, K.F. O'Driscoll, Die Makromolekulare Chemie, 179 (1978) 1921-1928.
[7] K. Ito, J Polym Sci Part A-1 Polym Chem, 12 (1974) 2581-2983.
[8] M. Stickler, Die Makromolekulare Chemie, 187 (1986) 1765-1775.
[9] D.R. Taylor, K.Y. Van Berkel, M.M. Alghamdi, G.T. Russell, Macromolecular Chemistry and Physics, 211 (2010) 563-579.
[10] G.T. Russell, Macromolecular Theory and Simulations, 4 (1995) 519-548.
[11] M. Strukelj, J.M.G. Martinho, M.A. Winnik, R.P. Quirk, Macromolecules, 24 (1991) 2488-2492.
[12] M. Buback, E. Müller, G.T. Russell, Journal of Physical Chemistry A, 110 (2006) 3222-3230.
[13] G. Johnston-Hall, A. Theis, M.J. Monteiro, T.P. Davis, M.H. Stenzel, C. Barner-Kowollik, Macromolecular Chemistry and Physics, 206 (2005) 2047-2053.
[14] J. Barth, M. Buback, P. Hesse, T. Sergeeva, Macromolecules, 42 (2009) 481-488.
[15] H. Fischer, H. Paul, Accounts of Chemical Research, 20 (1987) 200-206.
[16] J.P.A. Heuts, D. Kukulj, D.J. Forster, T.P. Davis, Macromolecules, 31 (1998) 2894-2905.
[17] G. Moad, C.L. Moad, Macromolecules, 29 (1996) 7727-7733.
[18] K. Matyjaszewski, T.P. Davis, Handbook of radical polymerization Wiley-Interscience, 2002.
[19] G.B. Smith, G.T. Russell, M. Yin, J.P.A. Heuts, European Polymer Journal, 41 (2005) 225-230.
[20] J. Barth, M. Buback, Macromolecular Rapid Communications, 30 (2009) 1805-1811.
[21] J. Fischer, G. Schulz, Berichte der Bunsengesellschaft für physikalische Chemie, 74 (1970) 1077-1082.
[22] C.H. Bamford, S. Brumby, Die Makromolekulare Chemie, 105 (1967) 122-131.
[23] M. Kamachi, J. Satoh, D.J. Liaw, S.-i. Nazakura, Macromolecules, 10 (1977) 501-502.
[24] M. Fernández-Garcia, J.J. Martinez, E.L. Madruga, Polymer, 39 (1998) 991-995.
[25] S. Beuermann, M. Buback, T.P. Davis, R.G. Gilbert, R.A. Hutchinson, O.F. Olaj, G.T. Russell, J. Schweer, A.M.v. Herk, Macromolecular Chemistry and Physics, 198 (1997) 1545-1560.
[26] M. Buback, R.G. Gilbert, R.A. Hutchinson, B. Klumperman, F.-D. Kuchta, B.G. Manders, K.F. O'Driscoll, G.T. Russell, J. Schweer, Macromolecular Chemistry and Physics, 196 (1995) 3267-3280.
[27] S. Beuermann, N. García, Macromolecules, 37 (2004) 3018-3025.
[28] B.R. Morrison, M.C. Piton, M.A. Winnik, R.G. Gilbert, D.H. Napper, Macromolecules, 26 (1993) 4368-4372.
[29] D.S. Viswanath, N.V.K. Dutt, T.K. Ghosh, D.H.L. Prasad, K.Y. Rani, Viscosity of Liquids Theory, Estimation, Experiment, and Data, Springer, Dordrecht, 2007.
[30] M. Stickler, D. Panke, W. Wunderlich, Die Makromolekulare Chemie, 188 (1987) 2651-2664.

[31] G.B. Smith, G.T. Russell, J.P.A. Heuts, Macromolecular Theory and Simulations, 12 (2003) 299-314.
[32] C. Barner-Kowollik, G.T. Russell, Progress in Polymer Science (Oxford), (2009).
[33] J.P.A. Heuts, G.T. Russell, G.B. Smith, A.M. Van Herk, Macromolecular Symposia, 248 (2007) 12-22.
[34] O.F. Olaj, G. Zifferer, G. Gleixner, Macromolecules, 20 (1987) 839-850.
[35] G.B. Smith, G.T. Russell, Macromolecular Symposia, 248 (2007) 1-11.
[36] H.K. Mahabadi, Macromolecules®, 18 (1985) 1319-1324.
[37] M. Buback, M. Egorov, A. Feldermann, Macromolecules, 37 (2004) 1768-1776.
[38] O.F. Olaj, P. Vana, Macromolecular Rapid Communications, 19 (1998) 533-538.
[39] J. Barth, M. Buback, G. Schmidt-Naake, I. Woecht, Polymer, 50 (2009) 5708-5712.
[40] G. Johnston-Hall, M.J. Monteiro, Macromolecules, 41 (2008) 727-736.
[41] G. Johnston-Hall, M.J. Monteiro, Journal of Polymer Science, Part A: Polymer Chemistry, 46 (2008) 3155-3173.
[42] O.F. Olaj, P. Vana, Macromolecular Rapid Communications, 19 (1998) 433-439.
[43] G.T. Russell, Macromolecular Theory and Simulations, 4 (1995) 497-517.
[44] M. Buback, M. Egorov, T. Junkers, E. Panchenko, Macromolecular Rapid Communications, 25 (2004) 1004-1009.
[45] M. Buback, M. Egorov, T. Junkers, E. Panchenko, Macromolecular Chemistry and Physics, 206 (2005) 333-341.
[46] F.R. Mayo, Journal of the American Chemical Society, (1943) 2324-2329.
[47] L. Tang, E.T. Papish, G.P. Abramo, J.R. Norton, M.H. Baik, R.A. Friesner, A. Rappé, Journal of the American Chemical Society, 125 (2003) 10093-10102.
[48] S.J. Blanksby, G.B. Ellison, Accounts of Chemical Research, 36 (2003) 255-263.
[49] G.G. Odian, Principles of polymerization, in, Wiley, Hoboken, N.J., 2004.
[50] M. Stickler, G. Meyerhoff, Die Makromolekulare Chemie, 179 (1978) 2729-2745.
[51] J. Brandrup, E.H. Immergut, E.A. Grulke, Polymer Handbook, 4th ed., Wiley, 1999.

Chapter 4. The Effect of Temperature on Termination Rate Coefficients at Low Conversion

In this chapter the effect of temperature on the average rate coefficient of termination, $\langle k_t \rangle$, of radical polymerization at low conversion will be discussed. Also, the correlation of its activation energy with polymer chain length will be examined.

4.1. Introduction

The effect of temperature on the rate and degree of polymerization is of fundamental importance. Increasing the temperature of thermally induced polymerization usually leads to an increase in the polymerization rate (R_p) and a decrease in the number-average degree of polymerization (DP_n), i.e. polymer molar mass. However, coming to a kinetic understanding of the quantitative effect of temperature is complex, since R_p and DP_n depend on a combination of fk_d, k_p and $\langle k_t \rangle$ (and, in the case of DP_n, λ). Studying the variation of overall termination rate coefficient, $\langle k_t \rangle$, with temperature is particularly of importance. This is because such variations are usually taken as making a direct statement about the actual process of the termination reaction. In other words, the $E_a(\langle k_t \rangle)$ observed is usually correlated with the underlying $k_t^{i,j}$, which in turn reflects the $E_a(k_t^{i,j})$ for the termination process that controls the rate of termination. Therefore, a precise determination of $E_a(\langle k_t \rangle)$ has the potential to yield information about the chain-length dependence. For this reason it is troubling that the variation of termination rate coefficient with temperature is found to scatter in the literature. Figure 4-1 demonstrates the enormous variation of $\langle k_t \rangle$ as a function of temperature for the well-studied monomer methyl methacrylate. This results in great scatter in its value of $E_a(\langle k_t \rangle)$.[1]

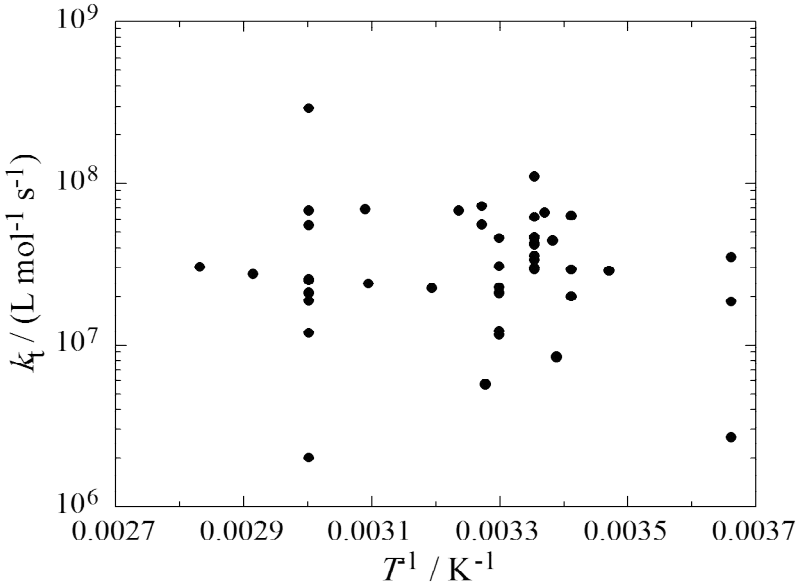

Figure 4-1. Ambient-pressure k_t values versus inverse (absolute) temperature for bulk polymerization of methyl methacrylate (MMA) from the *polymer hand-book*.[2]

In fact the scatter of the $\langle k_t \rangle$ values in Figure 4-1 can be partly attributed to two easily remedied factors. First, inconsistent use of the termination rate law, where some results were reported assuming $-\langle k_t \rangle c_R^2$ as the rate of termination rather than the IUPAC-recommended $-2\langle k_t \rangle c_R^2$. This immediately explains apparent variations by a factor of 2. Second, error associated with the employment of incorrect k_p in many works, especially ones from the early decades of RP research. Although there are some attempts of critical evaluation and refining of the results shown in Figure 4-1 based on the two mentioned factors [1, 2], there is still appreciable scatter in $\langle k_t \rangle$ values. This indicates that there is more complexity to $\langle k_t \rangle$.

Since termination is acknowledged as a diffusion controlled reaction, its $E_a(\langle k_t \rangle)$ is generally assumed to be similar to what is obtained for diffusion processes. However, this is not always the case, especially when thermally induced polymerization is carried out.

It is noteworthy and therefore to be borne in mind that this situation is different for other modes of initiation. For example, in photochemical polymerization, the initiation step is temperature-independent ($E_a(R_i) = 0$) to good approximation. It is found that the overall polymerization rate activation energy for photochemical polymerization is relatively insensitive to temperature. However, the effect of temperature on photochemical polymerization can be complicated when carried out at a relatively high temperature, since many photochemical initiators may undergo appreciable thermal decomposition under such conditions.

Likewise, the effect of temperature on polymer molar mass also depends on the type of initiation. For thermally initiated polymerization, DP_n decreases rapidly with increasing temperature. In contrast, for photochemical initiation, DP_n increases moderately with temperature, resulting in a positive $E_a(DP_n)$. Therefore, the temperature effect on the polymer molar mass, particularly when thermal induced polymerization is carried out, has to be considered.

4.2. Experiments and data analysis

In the investigation of the temperature effect on the termination rate coefficient of radical polymerization (RP) at low conversion, polymerization was carried out isothermally mostly employing the initiator 2,2'-azobisisobutyronitrile (AIBN). To measure the effect of temperature on the termination rate coefficient, polymerization was studied at temperatures between 50 – 90 °C at atmospheric pressure. The conversion-time data was obtained by means of gravimetric analysis, and $<k_t>$ was calculated using the recommended classical kinetic equation of steady state polymerization (see Chapter 3 for more details). Polymer product was analyzed by size exclusion chromatography (SEC).

Typical experimental results for styrene (ST) polymerization are presented in Figure 4-2. Inspection of these results clearly demonstrates the effect of temperature on the polymerization rate: an increase with increasing temperature is observed.

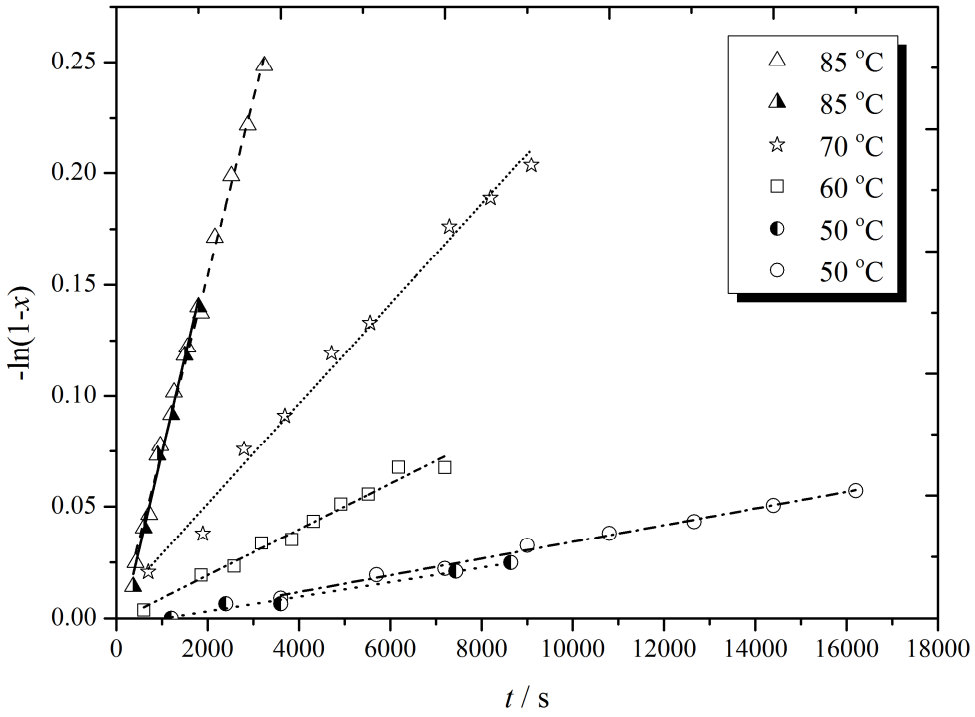

Figure 4-2. Results from radical polymerization of styrene at different temperatures as indicated with c_{AIBN} = 0.05 mol L^{-1} and c_{MMA} = 0.67 mol L^{-1} in ethyl benzene, where x is fractional conversion and t is time. Points: experimental results; line: best fit for determination of $\langle k_t \rangle$.

Results presented in Figure 4-2 clearly demonstrate good reproducibility, which gives confidence in the results deduced from such experiments. The temperature effect was determined using the Arrhenius equation (Eq. 1):

$$\langle k_t \rangle = A \exp\left(\frac{-E_a}{RT}\right) \qquad (1)$$

As usual, A is pre-exponential factor; $\langle k_t \rangle$ is average termination rate constant, E_a activation energy, R the gas constant and T the absolute temperature. Activation energy was obtained from the slope of the linear fitting. Results are presented in Table 4-1 for solution

polymerizations for methyl methacrylate (MMA), *n*-butyl methacrylate (BMA), *n*-dodecyl methacrylate (DMA), *n*-butyl acrylate (BA) and Styrene (ST).

Table 4-1. Results from low-conversion, solutions polymerization of different monomers as indicated, employing 0.67 mol L^{-1} of monomer in TFT, except for EBz being used for ST; 0.05 mol L^{-1} AIBN or 0.02 mol L^{-1} BTMHP as indicated. The experimentally determined quantity $\frac{-\mathrm{dln}(1-x)}{\mathrm{d}t}$, has been used to calculate average termination rate coefficient $<k_t>$, according to Eq. 6.

Monomer(Initiator)	**Temperature /(°C)**	$\frac{-\mathrm{dln}(1-x)}{\mathrm{d}t}$ **/(s^{-1})**	$<k_t>$**/(L mol^{-1} s^{-1})**
MMA(AIBN)	50	1.93×10^{-05}	8.85×10^{7}
	50	1.96×10^{-05}	8.60×10^{7}
	60	5.07×10^{-05}	9.64×10^{7}
	60	5.32×10^{-05}	8.75×10^{7}
	70	9.89×10^{-05}	1.69×10^{8}
	70	1.30×10^{-04}	9.81×10^{7}
	71	1.14×10^{-04}	1.54×10^{8}
	85	3.81×10^{-04}	1.62×10^{8}
	85	2.03×10^{-04}	5.70×10^{8}
	85	3.46×10^{-04}	1.96×10^{8}
	85	2.33×10^{-04}	4.35×10^{8}
	85	3.00×10^{-04}	2.61×10^{8}
	85	2.47×10^{-04}	3.85×10^{8}
	85	2.45×10^{-04}	3.91×10^{8}
	90	5.23×10^{-04}	1.98×10^{8}
	90	3.74×10^{-04}	3.88×10^{8}
MMA (BTMHP)	70	6.86×10^{-05}	1.84×10^{8}
	70	7.93×10^{-05}	1.38×10^{8}
	85	1.63×10^{-04}	4.14×10^{8}
	85	1.58×10^{-04}	4.44×10^{8}
	90	3.99×10^{-04}	3.41×10^{8}
BMA(AIBN)	50	2.96×10^{-05}	5.07×10^{7}
	50	3.57×10^{-05}	3.52×10^{7}
	50	2.80×10^{-05}	5.74×10^{7}
	60	6.51×10^{-05}	8.07×10^{7}
	60	7.97×10^{-05}	5.39×10^{7}
	70	1.77×10^{-04}	7.44×10^{7}
	70	1.65×10^{-04}	8.51×10^{7}
	70	1.70×10^{-04}	8.01×10^{7}
	70	1.44×10^{-04}	1.12×10^{8}
	85	4.67×10^{-04}	1.53×10^{8}
	85	4.20×10^{-04}	1.89×10^{8}
	87	4.74×10^{-04}	2.09×10^{8}
	90	5.74×10^{-04}	2.35×10^{8}
	90	5.59×10^{-04}	2.45×10^{8}

Table 4-1 continued

Monomer(Initiator)	Temperature /(°C)	$\frac{-\mathrm{dln}(1-x)}{\mathrm{d}t}$ /(s^{-1})	$<k_t>$/(L mol^{-1} s^{-1})
DMA(AIBN)	50	5.53×10^{-05}	2.62×10^{7}
	60	1.72×10^{-04}	1.98×10^{7}
	70	3.86×10^{-04}	2.55×10^{7}
	85	9.94×10^{-04}	5.25×10^{7}
	85	1.03×10^{-03}	4.91×10^{7}
	90	1.07×10^{-03}	1.03×10^{8}
BA(AIBN)	60	2.18×10^{-04}	1.38×10^{7}
	70	3.73×10^{-04}	2.50×10^{7}
	70	3.26×10^{-04}	3.28×10^{7}
	70	4.43×10^{-04}	1.77×10^{7}
	85	7.47×10^{-04}	6.59×10^{7}
	85	5.73×10^{-04}	1.09×10^{8}
	90	8.75×10^{-04}	9.91×10^{7}
ST(AIBN)	50	3.26×10^{-06}	4.11×10^{8}
	50	3.74×10^{-06}	3.13×10^{8}
	60	1.02×10^{-05}	3.95×10^{8}
	70	2.24×10^{-05}	6.8×10^{8}
	85	8.66×10^{-05}	8.76×10^{8}
	85	9.34×10^{-05}	7.51×10^{8}

4.3. Discussion

The rate coefficient for termination, $\langle k_t \rangle$, is well described by Eq. 2, which delivers a closed expression and has been found to give excellent concurrence with exact numerical solutions of population-balance equations.[3]

$$\langle k_t \rangle = k_t^{1,1} \left[\Gamma\left(\frac{2}{2-e}\right) \right]^{-2} \left[\frac{\left(4 k_d c_I k_t^{1,1}\right)^{0.5}}{k_p c_M} \left(\frac{2}{2-e}\right) \right]^{2e/(2-e)} \qquad (2)$$

From Eq. 2 one has that

$$E_a(\langle k_t \rangle) = (1+a) E_a\left(k_t^{1,1}\right) + a E_a(f) + a E_a(k_d) - 2a E_a\left(k_p\right) \qquad (3)$$

$$\text{where } a = \frac{e}{2-e}$$

Although unexpectedly complicated, even this makes the assumptions of e and concentrations (c_M and c_I) being independent of temperature. Eq. 3 is a paradigm-shifting result, for it reveals that in fact the activation energy of overall termination rate coefficients are very significantly determined by how the rates of initiation and propagation vary with temperature. All this is because of CLDT, which means that anything affecting the radical chain-length distribution – e.g. initiation and propagation – also affects $\langle k_t \rangle$.

Eq. 3 is plotted in Figure 4-3 by using estimates of all constituent activation energies (see Table 4-2) for both MMA and ST. Figure 4-3 shows that $E_a(\langle k_t \rangle) = E_a(k_t^{1,1})$ for chain-length independent termination, e = 0, as expected, and an increase in the activation energy with increasing chain length dependence of termination.

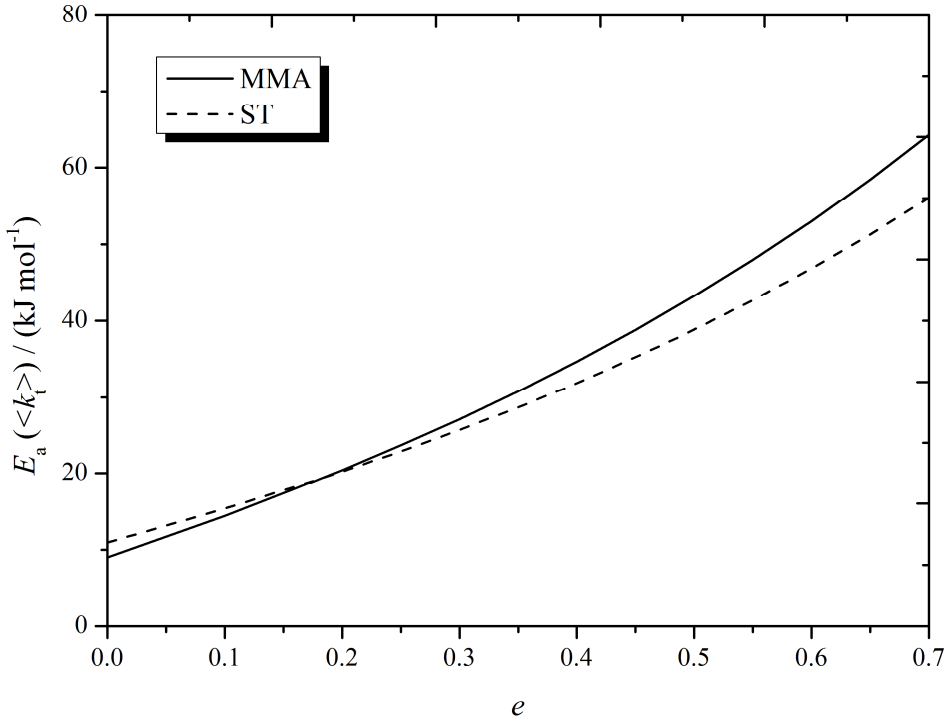

Figure 4-3. Predicted activation energy of the overall termination rate coefficient, $E_a(<k_t>)$ for bulk MMA and ST polymerization as a function of e, the strength of chain-length dependence of termination. Values are calculated with Eq. 3 using the parameter values given in Table 4-2.

Table 4-2. Activation energies used in Eq. 3 to calculate $E_a(<k_t>)$ value of Figure 4-3.

Quantity	E_a in MMA/(kJ mol^{-1})	Ref.	E_a in ST/(kJ mol^{-1})	Ref.
$k_t^{1,1}$	9.0	[4]	10.9	[5]
f	5.70	[6]	5.70	[6]
k_d	130.23	[7]	130.23	[7]
k_p	22.36	[8]	32.51	[9]

4.3.1. Previous results

It is firstly of interest to refer back to the original work for these recent experimental results, where there was an inconsistency of experimental $E_a(<k_t>)$ to what Eq. 3 predicts, in particular with MMA. The values of $E_a(<k_t>)$ = 5.89 kJ mol^{-1} and 14.34 kJ mol^{-1} were found for MMA and ST respectively.[2] The activation energy obtained for MMA was

unexpectedly small, even smaller than $E_a(k_t^{1,1})$, and thus contrary to what one would expect for thermal initiation polymerization, for which $E_a(<k_t>) > E_a(k_t^{1,1})$ (see above). The obtained activation energy of termination for MMA is also inconsistent with other methods, where usually the observed $E_a(<k_t>)$ are as anticipated for the diffusion process. Although there was no direct explanation for such a low activation energy value, there was a suspicion about the uncertainty of the values of kinetic parameters. Since reliable numbers for the propagation rate exist,[10] this puts the initiator decomposition rate coefficient and initiator efficiency under suspicion. As a result, an examination into the $E_a(fk_d)$ of AIBN was undertaken.

The small activation energy found for MMA termination, 5.89 kJ mol^{-1}, was obtained by employing the initiator decomposition activation energy $E_a(fk_d)$ = 123.5 kJ mol^{-1} for AIBN as found by Berger.[11] Berger determined this activation energy for the rate of incorporation of AIBN initiator fragments into polymer chains in bulk polymerization of styrene at low conversion. However, considering the fact that fk_d is expected to be system dependent, i.e. environment polarity and viscosity can have an influence on the k_d and f respectively,[6] awareness of using such a value for MMA is of importance. For instance, Fukuda et al. measured $fk_d = 3.73 \times 10^{-7}$ s^{-1} for AIBN in ST and $fk_d = 2.68 \times 10^{-7}$ s^{-1} in MMA.[12] Therefore, it is important to be aware of this effect and to find reliable values for f and k_d.

4.3.2. Decomposition rate coefficient, k_d, for AIBN

First the activation energy of k_d will be discussed. Initial use of the Berger value for fk_d was chosen as a good option since it takes into account the initiator efficiency that was measured under real polymerization conditions. However, inspection of the literature data with respect to k_d of AIBN indicates some scatter of its value, as measured in a range of solvents.[13-15] Therefore, using a value provided by the world's leading producer of initiators for polymer

production, AkzoNobel,[7] was another option. Notwithstanding the discrepancy between the value of k_d obtained by AkzoNobel and the Berger measurements, a range of studies was found in the literature that consist satisfyingly with the AkzoNobel values of k_d for AIBN. A comparison of a range of studies is presented in Figure 4-4.

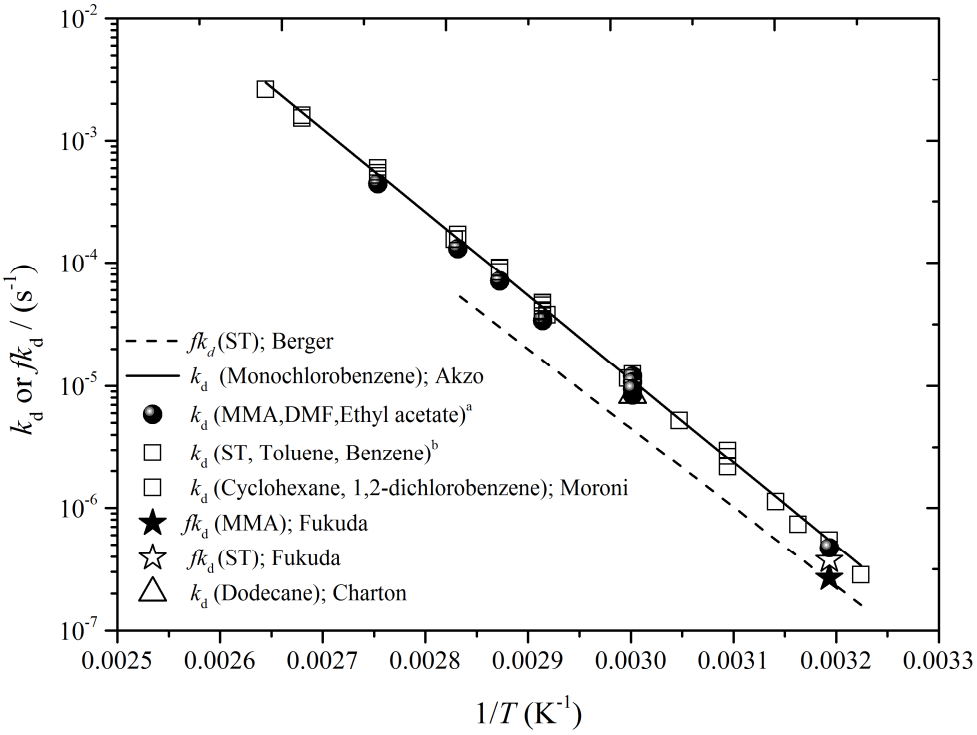

Figure 4-4. Comparison of literature results for k_d and fk_d for AIBN from references as indicated, where superscript a refers to results obtained by Moroni, Szafko, Bawn in MMA, DMF and Ethyl acetate respectively. Superscript b refers to results obtained by Moad and Breitenbach in ST, Bywater and Van Hook in Toluene and Kristina, Bawn and Van Hook in Benzene.[7, 11, 12, 14, 16-23]

Referring to Figure 4-4, it is important to note that fk_d values are plotted only for Berger [11] and another two points.[12] The equation used for the Berger data is

$$fk_d(\text{AIBN}) = 1.017 \times 10^{14} \exp\left(\frac{-123.5\ \text{kJ mol}^{-1}}{RT}\right)$$

Figure 4-4 clearly illustrates that the k_d fit provided by AkzoNobel is consistent with other studies, even with ST as solvent, as also used by Berger. As a consequence, the AkzoNobel value for k_d is employed entirely in this work, which corresponds to the expression:

$$k_d(\text{AIBN}) = 2.89 \times 10^{15} \text{s}^{-1} \exp\left(\frac{-130{,}23 \text{ kJ mol}^{-1}}{RT}\right) \qquad (4)$$

In the absence of more specific information about initiator decomposition rate of AIBN, it was assumed that there is no effect of the type of monomer on the k_d as this assumption might be fulfilled for the present work since low conversion and dilute solution polymerization were carried out. Hence, Eq. 4 will be used both for AIBN in both MMA and ST, notwithstanding what is written above about possible variation from monomer to monomer.

4.3.3. Initiator efficiency of AIBN, *f*

The question left is the effect of temperature on *f*. Despite the importance of having an accurate knowledge of initiator efficiency for investigation into polymerization kinetics, only a few studies have actually investigated it. Without such information, it is difficult to have a meaningful kinetic analysis or modelling implementation. In fact, some factors have been found to have an influence on *f,* such as viscosity, conversion and temperature. It is also important to mention that constant *f* values are often used because measurement of *f* under different conditions is not always available in the literature. In the present study, it is reasonable to assume that *f* is viscosity and conversion independent, as polymerization was restricted to low viscosity solutions and to low conversion (up to approximately 20%). The temperature effect has, in particular, been considered. The temperature effect on the efficiency of the AIBN initiator was obtained from literature,[6] where the following expression was deduced (data shown in Figure 4-5).

$$f(\mathrm{AIBN}) = 5.04 \exp\left(\frac{-5.70\ \mathrm{kJ\ mol^{-1}}}{RT}\right) \qquad (5)$$

This expression results in f = 0.80 at 100 °C, in good agreement with another study.[6, 24]

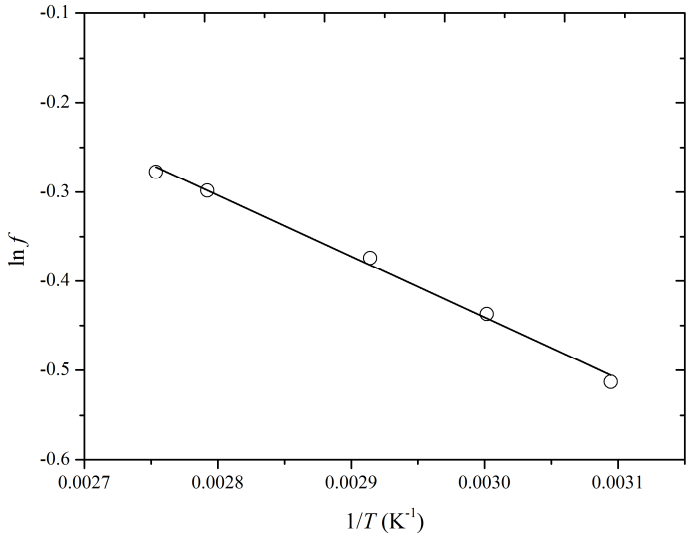

Figure 4-5. Arrhenius plot of AIBN initiator efficiency data used to obtain Eq. 5, which is deduced from reference.[6] Points: experimental data; line: best linear fit.

Although all parameter values obviously cannot be guaranteed, it should be evident that effort has been expended in gathering hopefully correct parameter values. It is interesting that $E_a(fk_d)$ = (130.2 + 5.7) kJ mol^{-1} = 135.9 kJ mol^{-1} has been deduced here, cf. the value 123.5 kJ mol^{-1} previously used, from the Berger data. This discrepancy most likely just illustrates the trickiness of measuring such E_a accurately. Indeed, it is visually evident from Fig. 4-4 that the Berger fk_d values are in reasonable quantitative agreement with other literature data, and that the difference in E_a, while it looks numerically significant, in fact is very hard to see when data are plotted.

How does all this affect the value of $E_a(\langle k_t \rangle)$? The activation energy of termination, $E_a(\langle k_t \rangle)$, is a function of $E_a(fk_d)$. The effect can be simply explained by looking into Eq. 6,[25] which shows that the value of fk_d influences the obtained $\langle k_t \rangle$ value. The thing to remember is that

$E_a(<k_t>)$ is relatively small, meaning that there has to be cancellation of large activation energies in Eq. 6. So although a change of $E_a(fk_d)$ from 123.5 to 135.9 kJ mol^{-1} might not look like a lot in percentage terms, in fact when used in Eq. 6 it turns out to have a large influence on the $E_a(<k_t>)$ obtained from experimental rates.

$$\text{Rate} = \frac{-\text{d}\ln(1-x)}{\text{d}t} = k_\text{p}\left(\frac{fk_\text{d}c_\text{I}}{\langle k_\text{t}\rangle}\right)^{0.5} \Rightarrow k_\text{t} = fk_\text{d}c_\text{I}\left(\frac{k_\text{p}}{\text{Rate}}\right)^2 \qquad (6)$$

4.3.4. Re-analysis of previous data

By employing the revised values of $E_a(k_d)$ and $E_a(f)$ in the analysis of the previous experimental polymerization data of MMA and ST, one obtains a remarkable change in $E_a(<k_t>)$ into values that are astoundingly consistent with what Eq. 3 predicts for a weak chain-length dependence of termination. Figure 4-6 illustrates the effect of using the recommended $E_a(f)$ and $E_a(k_d)$ of both the MMA and ST polymerization discussed above. By re-analysing the data using the suggested $E_a(f)$ and $E_a(k_d)$ activations, the value of $E_a(<k_t>) > E_a(k_t^{1,1})$ is obtained, as one would expect for thermal polymerization. To be precise, termination activation energies of 22.38 kJ mol^{-1} for ST and 18.33 kJ mol^{-1} for MMA are obtained, which correspond to chain-length dependence, found by Eq. 3, of e = 0.24 and 0.17 respectively. These results are quite consistent with chain-length dependent termination of the expected magnitude and with $E_a(<k_t>,\text{ST}) > E_a(<k_t>,\text{MMA})$, as found by other workers.[2]

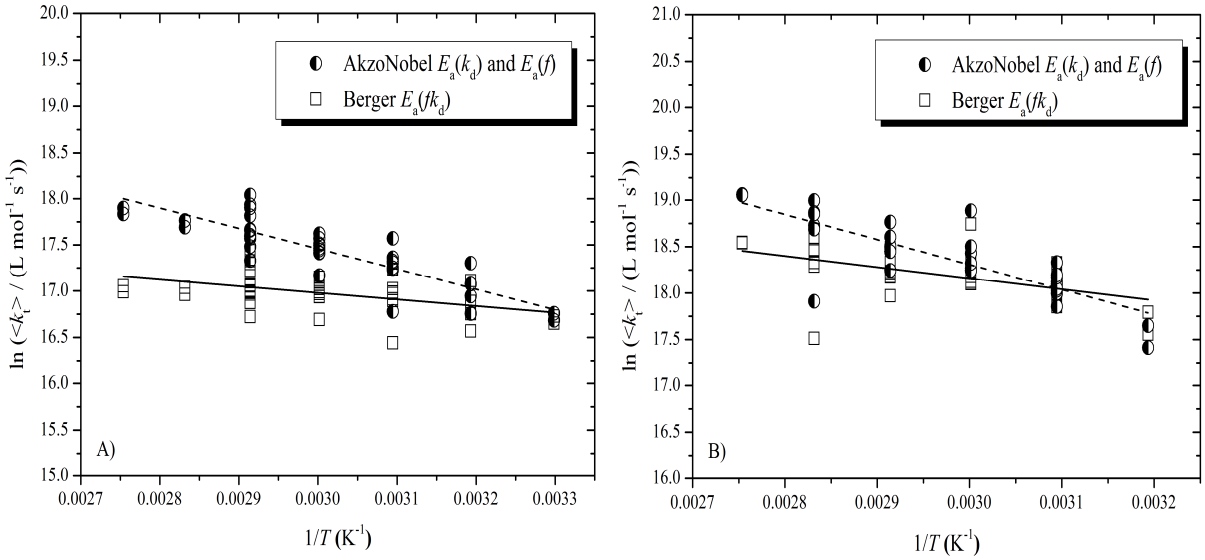

Figure 4-6. Arrhenius plots of average termination rate coefficient,$<k_t>$, versus inverse temperature for bulk polymerization of MMA (Figure A) and ST (Figure B) with different $E_a(fk_d)$ as indicated. Points: experimental values[2]; lines: best linear fit.

4.3.5. Comparison with literature values

The results of this work lie very close to the best fit of more refined literature data for MMA and ST. The agreement between refined literature values of $<k_t>$ and our results is shown in Figure 4-7 for MMA and Figure 4-8 for ST. In addition, both results from the previous one [2] and this work are presented. For both MMA and ST, it is clear that using the refined values for $E_a(f)$ and $E_a(k_d)$ results in a vast improvement and better agreement to the best fit of literature values of $<k_t>$. It is also important to note that the slight deviation of this work from the literature fit with increasing temperature is partly due to the inclusion of the initiator efficiency temperature effect, which is usually ignored or assumed to be constant.

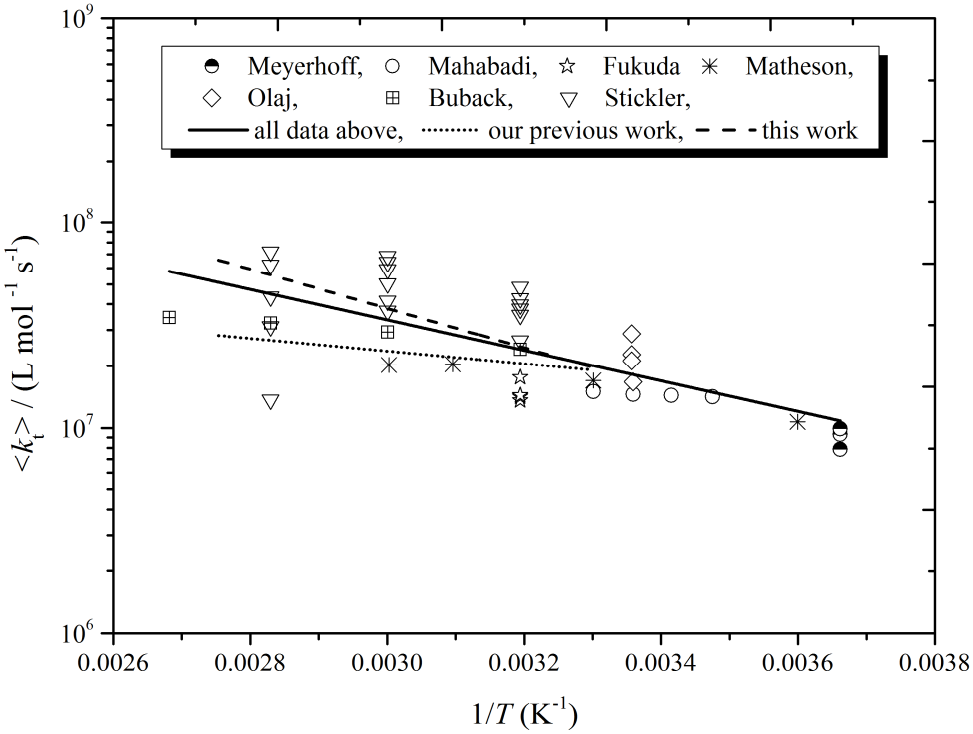

Figure 4-7. Arrhenius plot of termination rate coefficient, $<k_t>$, versus inverse temperature, T^{-1}, for bulk polymerization of methyl methacrylate. Points: values from Mahabadi and O'Driscoll,[26] Fukuda et al.,[12] Meyerhoff and Sack-Koulombris,[27] Buback and Kowollik,[28] Stikler [29] (as evaluated by Smith[30]), Olaj and Vana,[31] and Matheson et al.[32] Lines: Arrhenius fits of all literature data mentioned above, previous work[2] and this work.

These interesting results can be taken as the confirmation that the gravimetric technique can yield detailed mechanistic information when done carefully. Also, it shows the importance of employing correct kinetic parameters for data analysis. In particular, for studies of temperature variations it seems to be critical for highly accurate estimates of $E_a(f)$ and $E_a(k_d)$ to be employed: using the above-suggested values for k_d (Eq.4) and f (Eq.5) seems to provide good agreement between experimental values and what Eq. 3 predicts. This thus demonstrates the potential of using $E_a(<k_t>)$ to observe CLDT.

In the light of the above, one may wonder as to the accuracy of literature values of $<k_t>$, especially in relation to correct k_d and f values having been used to deduce them. Indeed, values in Figs. 4-6 and 4-7 may be in error due to assumed f and k_d being in error, especially

where AIBN was used. However it may be hoped that such errors would largely cancel out in fitting many different data sets, as has been done. In a sense this is like a metanalysis.

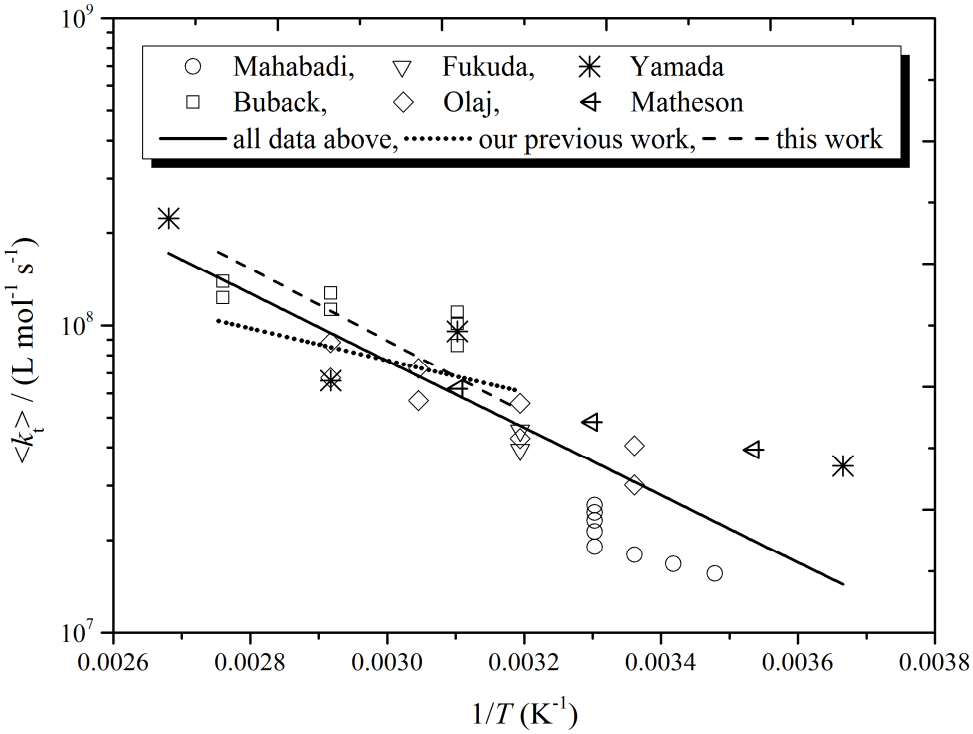

Figure 4-8. Arrhenius plot of termination rate coefficient, $<k_t>$, versus inverse temperature, T^{-1}, for bulk polymerization of styrene. Points: values from Mahabadi and O'Driscoll,[26] Fukuda et al.,[12] Yamada et al.,[33] Buback and Kuchta,[34] Olaj and Vana,[35] and Matheson et al.[36] Lines: Arrhenius fits as indicated.

4.4. Variation of $E_a(<k_t>)$ with chain length

Using correct kinetic parameter values is not the only factor that can affect the reliability of the value of $E_a(<k_t>)$. One should also be aware that $<k_t>$ depends not just on temperature but also on the degree of polymerization, *DP*.[37] A temperature increase is usually accompanied by a change in the radical chain-length distribution (CLD). Increasing temperature will lead to an increase in fk_d, which will make the living radical distribution weighted towards smaller chain lengths. If termination is chain-length dependent then the variation of $<k_t>$ should be influenced by any variation of the radical CLD caused by temperature, which can result in a different $E_a(<k_t>)$.

Nowadays, it is well established that termination occurs well with the so-called composite model, where two distinguished regimes are observed.

$$k_{\mathrm{t}}^{i,i} = k_{\mathrm{t}}^{1,1} i^{-e_S}, \qquad i \leq i_c \qquad (7)$$

$$k_{\mathrm{t}}^{i,i} = k_{\mathrm{t}}^{1,1} (i_c)^{-e_S + e_L} i^{-e_L} = k_{\mathrm{t}}^{0} i^{-e_L}, \qquad i > i_c \qquad (7a)$$

This model has been found to describe the chain-length dependent termination kinetics of many monomers,[37] including MMA and ST.[37] For long chains, MMA has been found to have $e_L \approx 0.16 - 0.20$, supported by a wealth of data.[31, 37-41] For small chains it has been found that $e_S \approx 0.5 - 0.6$, in accord with measurements [4, 38, 42] and with theoretical expectations.[43]

In view of this, the $E_a(\langle k_t \rangle)$ has to be assessed for a definite chain-length regime. To address this issue, information about chain lengths is essential. This information, of course, can be obtained experimentally using size exclusion chromatography (SEC). It can also be estimated using the Mayo equation (Eq. 8).

$$\frac{1}{DP_{\mathrm{n}}} = \frac{(1+\lambda)(f k_{\mathrm{d}} c_{\mathrm{I}} \langle k_{\mathrm{t}} \rangle)^{0.5}}{k_{\mathrm{p}} c_{\mathrm{M}}} + C_{tr,X} \qquad (8)$$

However, estimation of DP_n using the Mayo equation requires determination of $\langle k_t \rangle$ for the same polymerization alongside an accurate value of other kinetic parameters. The termination rate constant is system dependent, and thus has to be determined experimentally for the system under investigation.

Therefore, relating $E_a(\langle k_t \rangle)$ to each regime becomes crucial because of different chain-length-dependent termination that is correlated with chain length. To be precise, termination behaviour will be dictated by the long-chain equation when $DP_n > i_c$ and by the small-chain equation when $DP_n < i_c$.

4.4.1. $E_a(<k_t>)$ for large polymer chains

The preceding results for $E_a(<k_t>)$ in bulk MMA and ST were estimated for $DP_n > i_c$, where the CLDT is relatively small; thus the contribution of chain-length dependence on termination rate caused by temperature within that regime is weak. Results for large polymer chains, $DP_n > i_c$, where $i_c = 100$ for MMA and $i_c = 50$ for ST, yielded $E_a(<k_t>)$ values of 18.3 kJ mol^{-1} for MMA and 22.4 kJ mol^{-1} for ST. These results are quite consistent with the segmental-diffusion control that is expected in this region. Although DP_n has not been determined for these experiments, it may easily be estimated via the Mayo equation, which yields values well in excess of $i_c = 100$ for all experiments, even allowing for uncertainties in the values of the kinetic parameters used. This leads to an obvious experimental suggestion for trying to observe the value of $E_a(<k_t>)$ for short polymer chains, where e_S is identified as being a lot larger than e_L.

4.4.2. $E_a(<k_t>)$ for short polymer chains

As yet, no known determination of the $E_a(<k_t>)$ has been carried out specifically for thermal induced polymerization for the small chain length regime, i.e. $DP_n < i_c$. In this section it is attempted to assess the $E_a(<k_t>)$ over such a small chain length regime. Before proceeding with this work, it is noted that Eq. 3 suggests a large activation energy for small polymer chains, on account of $e_S \approx 0.5 - 0.6$ for such chains. To verify this situation, further experiments were carried out under different conditions such that most polymer chains have $i < i_c$.

Alteration of the radical chain-length distribution (CLD) can be brought about in many ways. For example, the radical CLD might be weighted toward small chain length by increasing the rate of initiation, whether by increasing initiator concentration or by increasing k_d through

increasing the temperature or using an initiator with high k_d. Another way it could be done is by reducing the frequency of propagation, for example by introducing more solvent and thereby reducing the monomer concentration. It is worth pointing out that the idea of implementing chain transfer agent cannot be used here, as it will make termination shift towards the limit of transfer-control limit, in which Eq. 3 is not applicable.[43, 44]

Altering radical CLD toward small chains was performed in this work by using a low monomer concentration and relatively high initiator concentration. Because of possible variation of $<k_t>$ with c_I and c_M (see Eq. 2 above and Chapter 3), the activation energy of $<k_t>$ was determined by carrying out the experiments at constant c_I and c_M. In addition, since $E_a(k_d)$ and $E_a(f)$ are expected to vary from initiator to initiator, the $E_a(<k_t>)$ might be expected to be a function of the type of initiator. Therefore, some experiments were carried out using a different initiator, bis(3,5,5,-trimethylhexanoyl peroxide (BTMHP).

It was considered important to establish that the effect of temperature on the molar mass distribution was as expected. Therefore, a confirmation of decreasing the molar mass with increasing the temperature for the system under investigation was obtained. The temperature effect on the molar mass distribution employing constant c_I and c_M, is shown in Figure 4-9. Furthermore, bearing in mind that $DP_n \approx ½ (M_{peak}/100.12 \text{ g mol}^{-1})$, one sees that $DP_n \leq 100$ for all but the experiment at 50 °C.

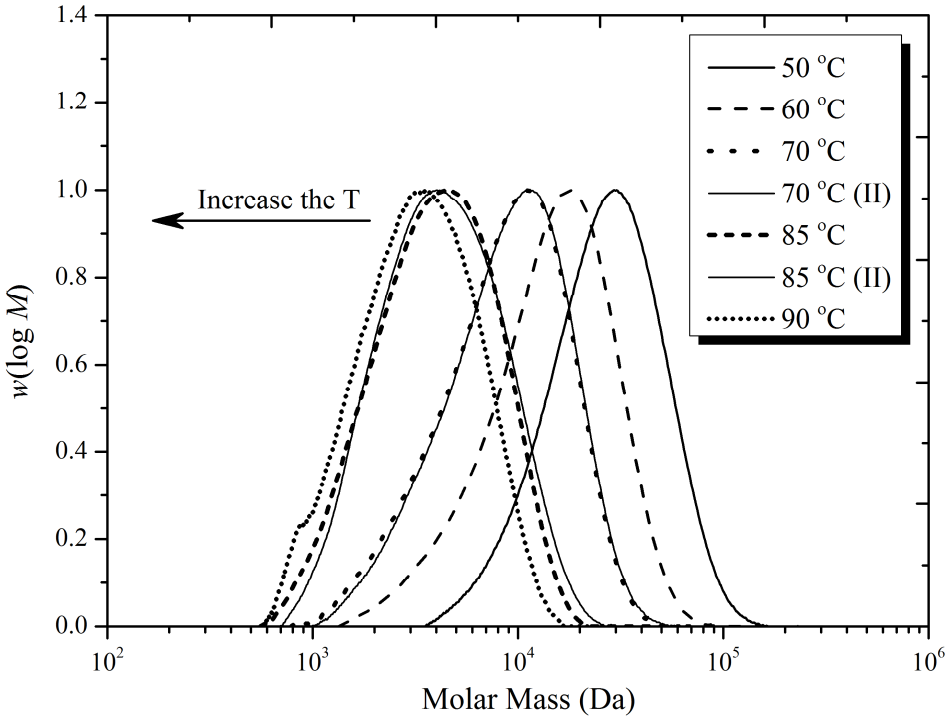

Figure 4-9. Molar mass distributions of PMMA samples obtained at different temperatures, as indicated, for polymerizations of 0.67 mol L^{-1} MMA in TFT employing 0.05 mol L^{-1} AIBN. The peak height has been normalized to 1 in each case.

Second, the effect of temperature on $\langle k_t \rangle$ is studied. Increasing the temperature results in an increase in the $\langle k_t \rangle$. Determination of $E_a(\langle k_t \rangle)$ for such small polymer chains, DP_n of order 100 or less, yields a value of 37.6 kJ mol^{-1} for MMA polymerization (Figure 4-10). This $E_a(\langle k_t \rangle)$ value corresponds to e = 0.44 via Eq. 3. Two different initiators, BTMHP and AIBN, were tested. Both initiators seem to agree with each other within experimental error. It is important to note that due to the difference of decomposition rate of BTMHP, the concentration of BTMHP in these experiments was adjusted to have rate of initiation close to that of the AIBN system, in order to ensure close chain-length polymer production. Despite the effect of chain length dependent propagation (CLDP) that is possible for short polymers, this effect has not been accounted for in our analysis. Thus, the IUPAC-recommended

propagation rate (k_p) benchmark value for long chain MMA (Eq. 9)[45] is employed. Furthermore, the BTMHP AkzoNobel value for k_d is employed (Eq. 9a). [46]

$$k_p(\mathrm{MMA}) = 2.673 \times 10^6 \mathrm{L\ mol^{-1} s^{-1}} \exp\left(\frac{-22.36\ \mathrm{kJ\ mol^{-1}}}{RT}\right) \qquad (9)$$

$$k_d(\mathrm{BTMHP}) = 2.84 \times 10^{15} \mathrm{s^{-1}} \exp\left(\frac{-128.34\ \mathrm{kJ\ mol^{-1}}}{RT}\right) \qquad (9a)$$

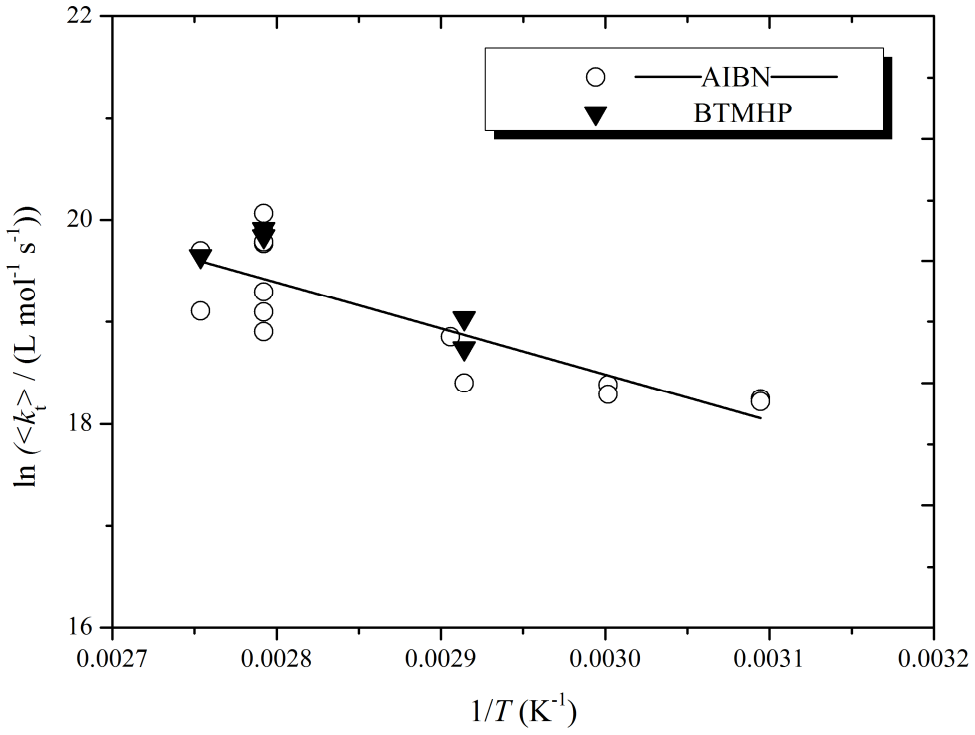

Figure 4-10. Arrhenius plot of termination rate coefficient, <k_t>, versus inverse temperature for polymerizations of 0.67 mol L^{-1} MMA in TFT employing 0.05 mol L^{-1} AIBN or 0.02 mol L^{-1} BTHMP (constant f = 0.53[47]) as indicated, where DP_n is of order or less than 100.

CLDP will result in larger k_p where DP_n is very low, i.e. at higher temperature. This means that <k_t> is underestimated here at high temperatures (see Eq. 6). Thus the real E_a(<k_t>) is in fact even higher than deduced above, i.e. CLDP only strengthens the present findings.

In spite of the large activation energy for termination, which seems admittedly unusual as it is in excess of what has been generally found in the literature, such a large value has in fact been previously reported on rare occasions.[48, 49] The value obtained in this present work is assigned specifically to a small polymer chain regime, where DP_n < 100 and where termination is recognized to be highly dependent on chain length. It is worth mentioning that the literature value of $E_a(<k_t>)$ is not usually assigned to a definite chain length regime. In addition, this value is also very consistent with what Eq. 3 predicts. That $E_a(<k_t>)$ can be this high as a result of $e \approx 0.5$ was first hinted at by calculations some two decades ago.[50]

Although this large activation energy for MMA corresponds to a chain-length dependent e = 0.44 that is slightly smaller to what is expected for MMA $e \approx 0.5 – 0.6$, it is still very close and pointing in the expected direction. Furthermore, it is also important to mention another element other than a strong CLDT, this being viscosity, which is a function of temperature. When high temperature is used, low viscosity is achieved, resulting in a higher $k_t^{1,1}$. Of course this is implicit in the calculations that have been done using Eq. 3, which assume a best-estimate for $E_a(k_t^{1,1})$, one based on measurements of diffusion coefficients of monomer or monomer analogues. The effect of viscosity is of course made manifest through diffusion coefficient variation.

If the present analysis is accepted, it would appear worthwhile to measure the $E_a(<k_t>)$ for different monomers. Therefore, in the next section, the effect of temperature on short chain radical termination for other monomers is investigated.

4.5. Variation from monomer to monomer

To be sure of the credibility of the large activation energy value obtained for short chain termination for MMA and to explore the effect of other factors such as the structure of

monomers on the $E_a(<k_t>)$, experiments were extended to include different types of monomers. Polymerization of the monomers *n*-butyl methacrylate (BMA), *n*-dodecyl methacrylate (DMA), *n*-butyl acrylate (BA) in addition to MMA and ST, all illustrated below, is investigated. Monomers were chosen to account for several aspects. First, different modes of termination were considered. ST and BA terminate by combination, whereas methacrylates are an approximately equal mixture of combination and disproportionation. Second, there is the effect of methacrylate ester-groups length. Third, the difference between methacrylates and acrylates is considered.

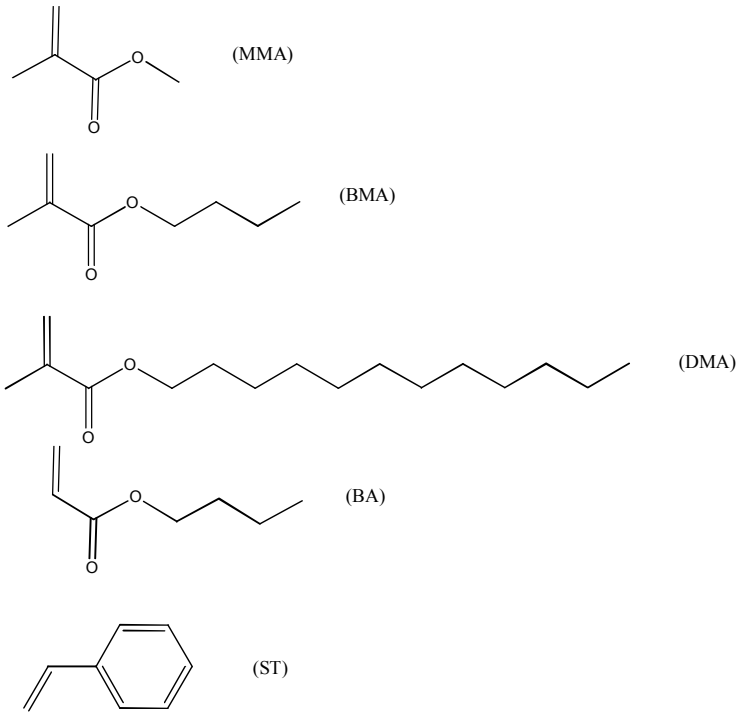

Polymerization was carried out under the same conditions as MMA and ST (see the preceding section). A low concentration of monomer, 0.67 mol L^{-1}, was used together with 0.05 mol L^{-1} AIBN. Low conversion polymerization up to no more than 20% was carried out.

Kinetics parameters

The following k_p values were used:

$$k_p(\mathrm{BMA}) = 3.802 \times 10^6 \mathrm{L\ mol^{-1}s^{-1}}\ \exp\left(\frac{-22.9\ \mathrm{kJ\ mol^{-1}}}{RT}\right) \qquad (10)$$

$$k_p(\mathrm{DMA}) = 2.512 \times 10^6 \mathrm{L\ mol^{-1}s^{-1}}\ \exp\left(\frac{-21.00\ \mathrm{kJ\ mol^{-1}}}{RT}\right) \qquad (11)$$

$$k_p(\mathrm{ST}) = 4.266 \times 10^7 \mathrm{L\ mol^{-1}s^{-1}}\ \exp\left(\frac{-32.51\ \mathrm{kJ\ mol^{-1}}}{RT}\right) \qquad (12)$$

Eqs 10-12 are IUPAC-recommended propagation rate benchmark values.[45] In the absence of more specific information about initiator efficiency and decomposition rate coefficient for AIBN, it was assumed here that there is no effect of the type of monomer on the k_d and f. Since initiation does not directly involve the monomer and in the present work the environment around the initiator is dominated by the solvent TFT, since dilute-solution conditions are used, the assumption about f and k_d might be fulfilled for the present work. The exception here might be ST, polymerization of which was carried out in ethylbenzene, EBz. Nevertheless Eq. 4 and Eq. 5, presented previously, were also used for it for k_d and f respectively.

With respect to the propagation rate coefficient of BA, the situation is more complex. The radical polymerization of acrylate type is in general complicated by the generation of mid-chain radicals (MCRs).[51, 52] MCRs are produced even at low conversions by the so-called backbiting process, where intermolecular transfer to polymer occurs via a 1,5-H shift from propagating secondary chain-end radicals (SPRs). These different radical structures exhibit very different propagation behaviour: MCRs are known to have vastly lower k_p.[51, 53]. As

the fraction of MCR increases with increasing temperature, MCR propagation must be considered during polymerization at relatively high temperature.

An attempt to resolve this is by using the effective propagation rate coefficient, k_p^{eff}, (Eq. 13) [54-56], which is defined as:

$$k_p^{eff} = \frac{k_p^{SPR}}{\frac{k_p^{bb}}{c_M k_p^{MCR}} + 1} \qquad (13)$$

where k_p^{SPR} is the propagation rate coefficient of secondary chain-end radicals, k_p^{MCR} is the propagation rate coefficient of midchain radicals, and k_p^{bb} is the backbiting process rate coefficient. BA, in particular, has been studied intensively. This allows us to take into account the effect of other propagation processes. Its individual propagation rate coefficients have been reported as [51, 52]

$$k_p^{SPR}(BA) = 2.21 \times 10^7 \text{L mol}^{-1}\text{s}^{-1} \exp\left(\frac{-17.9 \text{ kJ mol}^{-1}}{RT}\right) \qquad (14)$$

$$k_p^{bb}(BA) = 1.60 \times 10^8 \text{s}^{-1} \exp\left(\frac{-34.7 \text{ kJ mol}^{-1}}{RT}\right) \qquad (15)$$

$$k_p^{MCR}(BA) = 9.20 \times 10^5 \text{L mol}^{-1}\text{s}^{-1} \exp\left(\frac{-28.3 \text{ kJ mol}^{-1}}{RT}\right) \qquad (16)$$

Based on these equations, in this work the following expression has been deduced for the k_p^{eff} of BA for temperatures between 0 and 100 °C, using Eq. 13-16. Figure 4-11 demonstrates graphically Eqs. 13, 14, 16 and 17.

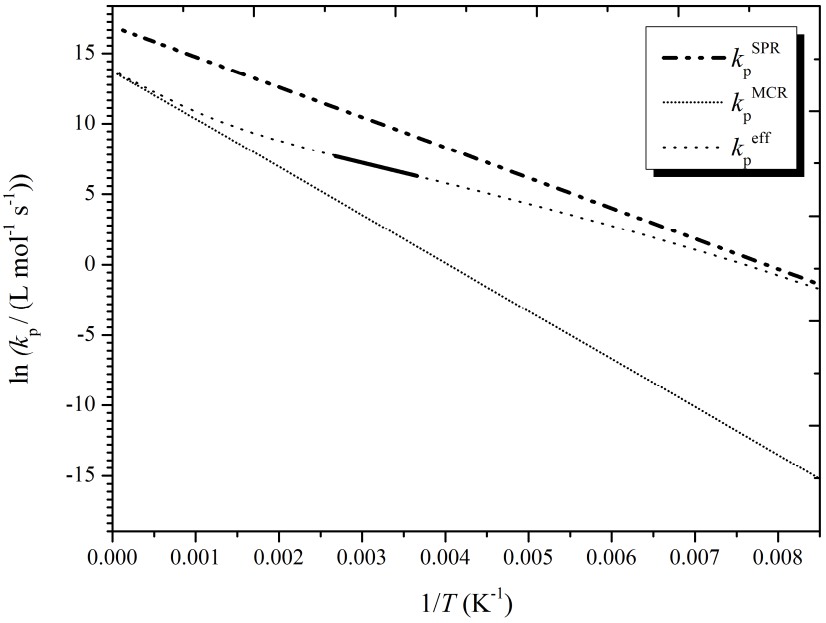

Figure 4-11. Arrhenius plot of the different propagation rate coefficients, k_p, as indicated, of *n*-butyl acrylate (BA). Eq. 17, the fit to k_p^{eff} over the temperature range 0 – 100 °C, is also shown (Solid line).

$$k_p^{eff}(\text{BA}) = 9.466 \times 10^6 \text{L mol}^{-1}\text{s}^{-1} \exp\left(\frac{-11.78 \text{ kJ mol}^{-1}}{RT}\right) \qquad (17)$$

4.5.1. Results and discussion

Typical conversion time results of polymerization of the monomers *n*-butyl methacrylate (BMA), *n*-dodecyl methacrylate (DMA), *n*-butyl acrylate (BA) in addition to MMA and ST are presented in Figure 4-12. The same trend is observed as in the literature: $k_p^2/\langle k_t \rangle$ increases as the methacrylate ester group becomes longer. This is caused by both a relatively small increase in k_p and by a larger decrease in $\langle k_t \rangle$.[57] Secondly, ST yielded a higher termination rate as compared to other monomers, which is also consistent with the literature.[2] However, BA resulted in unexpectedly higher $\langle k_t \rangle$ than DMA, which is perhaps the opposite to what one would expect. In fact, BA has the much larger propagation rate. However, the higher $\langle k_t \rangle$ value as compared to DMA can be attributed to the backbiting reactions that are known to occur for BA at high temperature. These slow its polymerization. due to the generation of mid-chain radicals (MCRs) that have a slower propagation rate than

chain-end (secondary propagating) radicals (SPRs) [52] and which also terminate faster by virtue of remaining small for longer. Both these effects contribute to the slower-than-expected rate and it can be difficult to disentangle the extent to which each is responsible. The Arrhenius plot for the investigated monomers is given in Figure 4-13, and parameters from the resulting Arrhenius fits are given in Table 4-3.

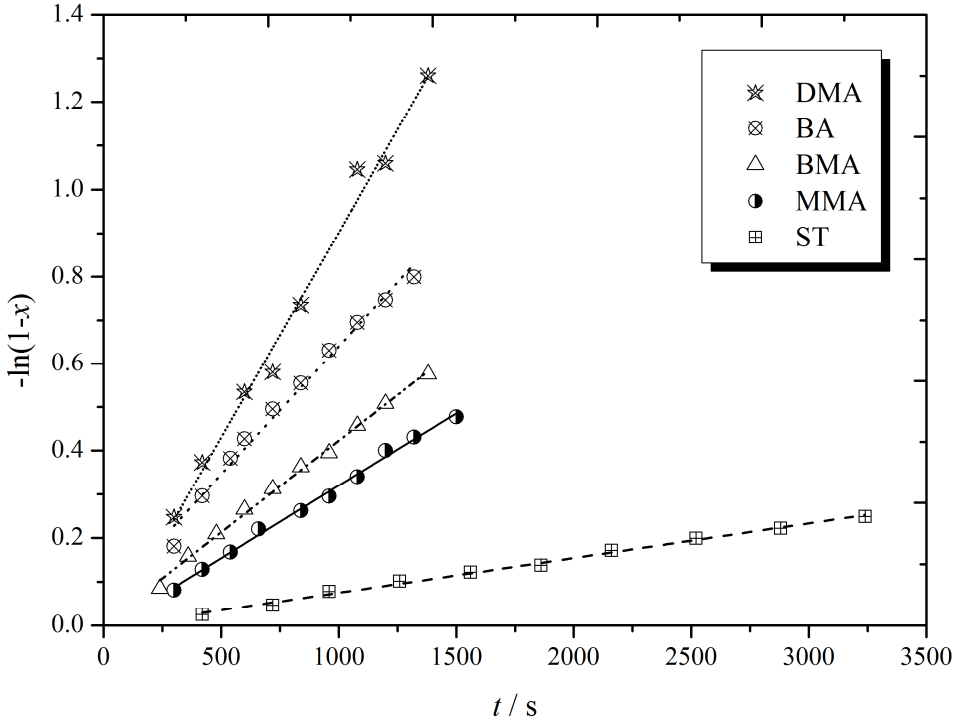

Figure 4-12. Conversion-time data from dilute solution RP of different monomers as indicated, employing 0.67 mol L^{-1} of monomer at 85 °C in TFT, except for EBz being used for ST; 0.05 mol L^{-1} AIBN was used in all cases. Points: experimental results; lines: linear best fits to each set of results.

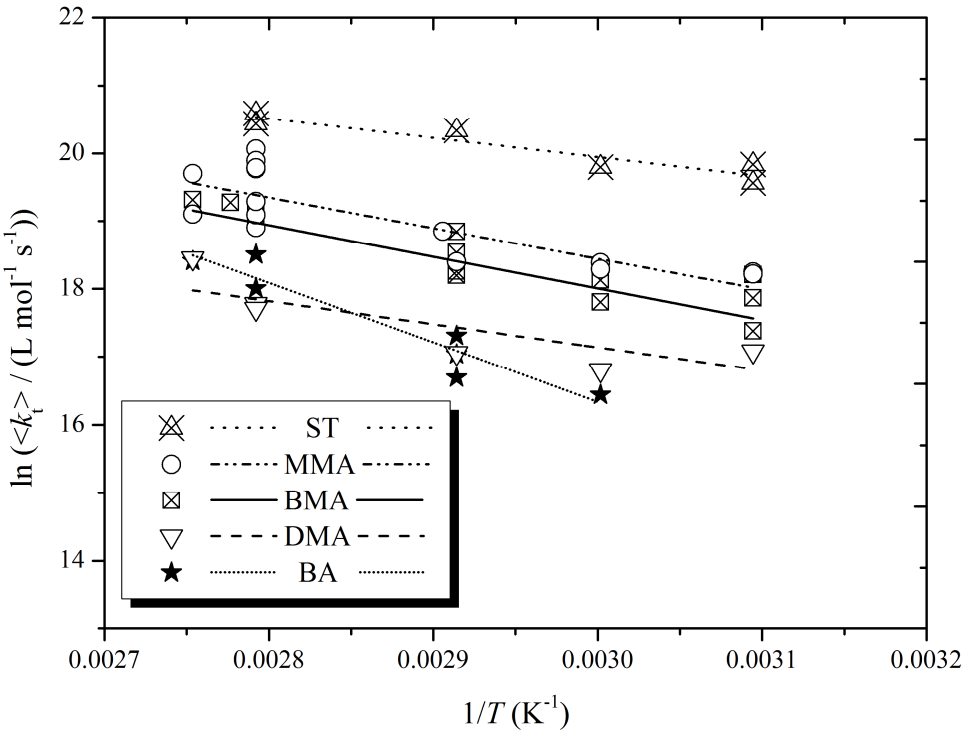

Figure 4-13. Arrhenius plot of overall termination rate coefficient, $\langle k_t \rangle$, for dilute-solution polymerization of ST, MMA, BMA, DMA and BA, as indicated, initiated by AIBN.

Table 4-3. Arrhenius parameters obtained for monomers as indicated via thermal induced polymerization in the present study.

Monomer	$E_a(\langle k_t \rangle)$/(kJ mol^{-1})	$A(\langle k_t \rangle)$/(L mol^{-1} s^{-1})	Estimated DP_n*
MMA	38 ± 12	8.3×10^{13}	< 100
BMA	39 ± 7	8.1×10^{13}	< 200
DMA	32 ± 12	2.3×10^{12}	< 200
ST	25 ± 6	2.3×10^{12}	< 50
BA	73 ± 15	3.3×10^{18}	< 300

* Obtained using Eq. 8. For convenience it has been assumed negligible dead-chain formation by transfer.

Results presented in Figure 4-13 show clearly a decrease of the $\langle k_t \rangle$ as the methacrylate ester group gets larger, $\langle k_t \rangle$(MMA)> $\langle k_t \rangle$(BMA)> $\langle k_t \rangle$(DMA), in agreement with what other studies have revealed. In addition, Figure 4-13 shows a larger value of $\langle k_t \rangle$ for ST than other methacrylates. This is also consistent with what has been reported in the literature for ST.

Referring back to the temperature effect, a large activation energy was also observed for monomers other than MMA. In fact, MMA and BMA show very similar $E_a(\langle k_t \rangle)$. DMA shows slightly smaller $E_a(\langle k_t \rangle)$ compared to MMA and BMA, though it is still close enough

and within experimental error. Therefore, these similar activation energies of termination would clearly suggest the family-type termination behaviour that is observed for methacrylate termination.

On the other hand, ST yielded a lower activation energy for termination, 24.5 kJ mol^{-1}, which is in fact quite close to what has been observed for large polymer chains, 22.38 kJ mol^{-1}(see section 4-3). However, this was not expected in terms of what has been suggested in this work in terms of the termination being chain-length dependent. In fact, for ST the situation should be the same. For large chains, ST has e_L= 0.15[35, 58, 59] and for small chains e_S = 0.53,[58, 59] in accord with short chain diffusion coefficients.[60] For such small chains a larger value, about 35 to 46 kJ mol^{-1} is predicted for $e \approx 0.5 - 0.6$ respectively.

However, ST in particular was found in another study to have weaker termination chain-length dependence with increasing temperature,[61] in accord with our present result. This unexpected activation energy of termination for ST can perhaps be ascribed to the low propagation rate that can result in the polymerization being more sensitive toward the oxygen presence that remained in the solution due to imperfect deoxygenation. Reaction with O_2 can result in a variation in the $<k_t>$ values. For instance, it might increase the $<k_t>$ value when the reaction is carried out at low temperature where the presence of O_2 in the reaction solution is expected to be higher. This, consequently, can lead to an increase in the $<k_t>$ value for the reactions carried out at low temperature and hence a reduction of the $E_a(<k_t>)$. This rationalization is supported by the observation of such a product in ESI-MS spectrum, as will be discussed and shown in Chapter 7. Nevertheless, the activation energy is still qualitatively consistent with what Eq. 3 suggests, viz. $E_a(<k_t>,\text{MMA}) > E_a(k_t,\text{ST})$ for $e > 0.2$.

The monomer BA yielded the very large $E_a(<k_t>)$ of 73 kJ mol^{-1}. This large value can be ascribed to the complexity of the termination processes due to the backbiting process.[52]

More termination processes contribute to the overall termination rate in the BA radical polymerization, making BA radical polymerization kinetics more complex. These termination processes includes SPR homo-termination, MCR homo-termination and SPR-MCR cross-termination.

In fact, there is not much literature data that supports such high activation energies for termination. A possible explanation of this trend might be as follows:

There is bulk evidence that the termination reaction is diffusion controlled at any stage of the polymerization, except under the glassy stage. The $E_a(<k_t>)$ is larger than what is expected for the diffusion processes. Although this might suggest a chemical controlled reaction, one should be careful reaching this conclusion for the following reasons. First, it is difficult to determine the effect of temperature on $<k_t>$ without altering the polymer chain length. Second, it is well established that $<k_t>$ is chain-length-dependent and temperature has an influence on the chain length, i.e. increasing the temperature leads to a decrease in the polymer chain lengths, then the influence of temperature on chain length should be considered as well. This means that the measured activation energy is in fact an accumulation of both the effect of temperature itself on the $<k_t>$ and chain length on the $<k_t>$. This would lead to the following expression:

$$E_a(<k_t>)\ \text{apparent} = E_a(k_t^{1,1}) - e \times E_a(DP_n) \qquad (18)$$

This expression follows from the well-known expression $<k_t> \approx k_t^{1,1}\ DP_n^{-e}$[43, 44, 62], which mirrors the underlying variation of $k_t^{i,i}$ with i. One can now see the influence of chain length on the apparent $E_a(<k_t>)$. Because the activation energy of DP_n is negative for thermally induced polymerization, then the activation energy for termination is always expected to be bigger than the value assigned for monomeric diffusion, which is approximately 10 kJ mol^{-1}.

In fact all the trends of Table 4-3 may be easily and convincingly explained as follows: (1) The methacrylate values cluster together because these monomers show family-type behaviour and are known to have near-identical $E_a(k_t^{1,1})$, $E_a(k_p)$ and e. (2) The ST value is smaller than these values for two reasons: (i) e_S is slightly smaller for ST than for *n*-alkyl methacrylates, which acts via Eq. 3 to make $E_a(<k_t>)$ smaller. (ii) Perhaps more importantly, $E_a(k_p)$ is larger for ST by about 10 kJ mol^{-1}, which acts via Eq. 3 to have a significant lowering effect on $E_a(<k_t>)$. (3) In the same way one may understand why $E_a(<k_t>)$ is so large for BA: (i) From SP-PLP-EPR experiments it is known that $e_S \approx 0.8$ for BA, which is considerably larger than for MMA, BMA and DMA. This raises the value of $E_a(<k_t>)$. (ii) Eq. 17 draws attention to the low value of E_a for k_p^{eff}, which will also act via Eq. 3 to raise the value of $E_a(<k_t>)$.

It should also be mention that not only does Eq. 3 explain the trends in the $E_a(<k_t>)$ values, it also is in remarkably quantitative agreement with the values, as has already been seen for MMA, and as may easily be deduced for other monomers from the discussion above.

All in all it must be said that this is remarkable science: bold predictions made by Eq. 3 are confirmed when they are looked for.

Interestingly, Eq. 18 suggests an alternative way to determine the activation energy for termination. One can estimate the apparent $E_a(<k_t>)$ if everything else in Eq. 18 is known. This is in view of the fact that the activation energy of the diffusion process is well known. Likewise the chain length dependence has been determined using other techniques. One can then obtain $E_a(<k_t>)$ simply by measuring $E_a(DP_n)$. This leaves us to the task of examining the above expression experimentally by determining the activation energy of the DP_n.

4.6. $E_a(DP)$ determination

The temperature has a different effect on the degree of polymerization (*DP*) depending on the type of initiation. *DP* decreases with increasing temperature for thermally induced polymerization, as shown in Figure 4-14. In contrast, *DP* increases with temperature for photochemical polymerization.

In the present experiments, the effect of temperature on the *DP*, where $DP = M_p/M_0$, has been determined experimentally using the SEC, where M_p is average peak molar mass and M_0 monomer molar mass. As mentioned previously M_p can be measured precisely, and using it may overcome some errors that usually are associated with M_n determination, especially for low molar mass polymers.[63, 64] However, there should be no large difference between $E_a(DP_n)$ and $E_a(DP)$. Therefore, $E_a(DP_n)$ is replaced by $E_a(DP)$. Of course, this contains an approximation of a constant polydispersity, *PD*, and might be a source of error in the results obtained from this work. However, again we think this is a good approximation, as the experiments were limited to low conversion and under very similar conditions, meaning any *PD* variation should be relatively small, hence *PD* could be assumed as constant. Furthermore, this approximation is supported by *PDI* being temperature independent for polymers produced under very similar conditions, as shown earlier (in Chapter 3, see Figure 3-8) for PMMA. More information about experimental details on SEC experiment is found in Chapter 2. Figure 4-14 shows the Arrhenius plot for the present *DP*, and the resulting Arrhenius parameters are reported in Table 4-4.

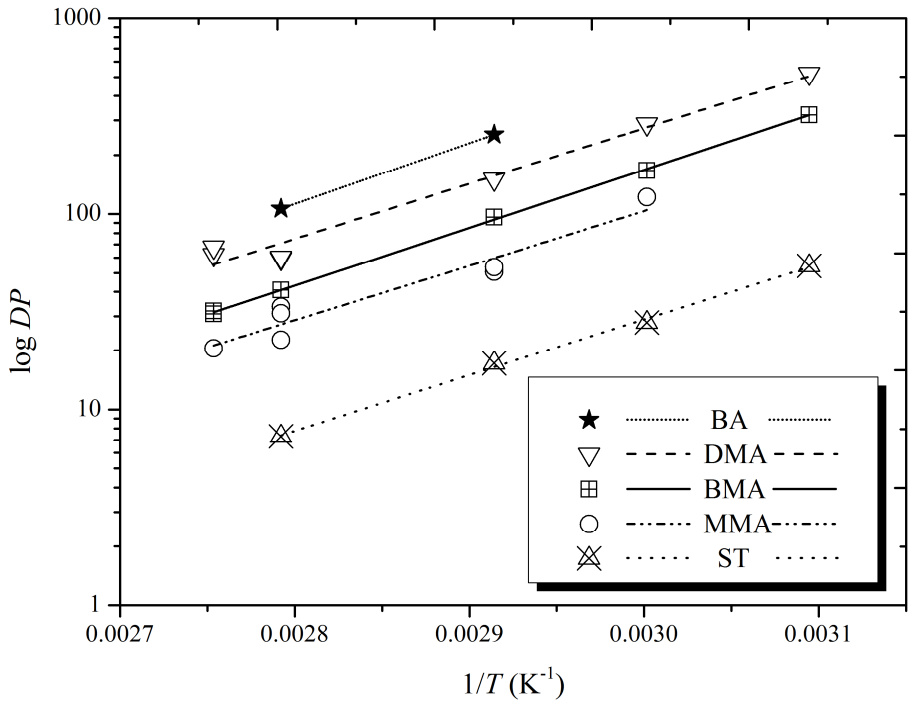

Figure 4-14. Arrhenius plot of peak degree of polymerization, *DP*, versus inverse temperature for dilute solution polymerization of different monomers as indicated.

Table 4-4. Activation energies for *DP* obtained in this study for thermally induced polymerization of the indicated monomers.

Monomer	$E_a(DP)$/(kJ mol^{-1})
MMA	–52 ± 6
BMA	–57 ± 1
DMA	–54 ± 4
ST	–55 ± 2
BA	≈ –60*

*This value is based on only two points.

This experiment gives us a direct measurement of the $E_a(DP)$. The results of these experiments show similar activation energies for all monomers. This implies a similar effect of temperature on the *DP* for all monomers. However, by applying the $E_a(DP)$ obtained into Eq. 18, one can determine the apparent $E_a(\langle k_t \rangle)$. Interestingly, the apparent $E_a(\langle k_t \rangle)$ obtained via Eq. 18 were in agreement with the large $E_a(\langle k_t \rangle)$ that were previously obtained. A value

of 42 kJ mol^{-1} is determined for MMA thermal polymerization when employing e = 0.65 [4] and $E_a(k_t^{1,1})$ = 9 kJ mol^{-1}.[4] This result evidently supports the $E_a(<k_t>)$ obtained for termination of small chains via the rate measurements. The superiority of this method is that it directly measures the $E_a(<k_t>)$, unlike the previous method where uncertainty of other factors such as employing the correct kinetic parameter values can result in doubtful results. This also can resolve any issue that might be related to the chain length dependent propagation (CLDP) effect that is probable in this short chain regime.

In contrast, it would also be of interest to determine the CLDT. By substituting $E_a(DP)$ and $E_a(<k_t>)$ found experimentally, one can calculate the chain-length dependence (e). The results are presented in Table 4-5. The results strikingly illustrate strong CLDT behaviour of small polymer chains. The chain-length dependent termination of MMA polymerization yields values of e = 0.55, in very good agreement with chain length dependence found in diffusion data of MMA oligomers, 0.56 ± 0.08 and 0.53 ± 0.12 at 25 and 40 °C respectively.[65] In addition, DMA polymerization yields a value of e = 0.41, in accord with the literature where e = 0.48 ± 0.09 is reported.[66] Though not enough points are obtained for BA, it was of interest to report the apparent results. BA chain-length dependent termination also is found to be in close agreement to what has been recently reported in the literature (e_s = 0.85 ± 0.9 and e_s = 1.04) using SP-PLP-EPR and RAFT-CLD-T methods respectively.[51, 67] This is interesting, as it shows the potential of using such simple methods to obtain information on CLDT even for a complex polymerization system such as BA.

ST polymerization resulted in $E_a(DP)$ = –55 kJ mol^{-1}; this is similar to other monomers which would suggest a similar CLDT. Determining the $E_a(<k_t>)$ using Eq. 18 results in $E_a(<k_t>)$ of 39.77 kJ mol^{-1} when employing $E_a(k_t^{1,1})$ = 10.9 kJ mol^{-1} [5] and e = 0.53.[59] This result is consistent with what is expected for small chain termination and is contrary to the unexpectedly low value (24.5 kJ mol^{-1}) found previously based on the rate measurements.

This can be used as a confirmation of probably incorrect values measured for the ST termination reaction due to the sensitivity of the reaction to O_2 as mentioned previously. It is evident from this experiment that a confirmation of a large activation energy is due to large chain-length dependent termination contribution on $\langle k_t \rangle$.

Table 4-5. Table value of *e* obtained from Eq. 18 with experimentally obtained E_a for $\langle k_t \rangle$ and *DP* together with estimated E_a for $k_t^{1,1}$.

Monomer	$E_a(\langle k_t \rangle)$/(kJ mol^{-1})	$E_a(DP)$/(kJ mol^{-1})	$E_a(k_t^{1,1})$/(kJ mol^{-1})	*e*
MMA	38	– 52	10	0.54
BMA	39	–57	10	0.51
DMA	32	–54	10	0.41
BA	73	≈ –60	10	1.05
ST	25	–55	10	0.27

4.7. Further investigation into CLDT parameters

Considering the well-known relationship $\langle k_t \rangle = G\ k_t^{1,1}\ (DP_n)^{-e}$, it was also of interest to examine this analytical expression, relating $\langle k_t \rangle$ to experimental *DP* obtained by SEC. As explained earlier, *DP* was used as it is more accurate than DP_n, which furthermore was unavailable. Therefore, an alternative is to use values of *DP*/*PD* in place of DP_n, where *PD* is one form of disparity and very often is very close to *PDI*. This leads to Eq. 19.

$$\langle k_t \rangle \approx k_t^{1,1} \left(\frac{DP}{PD}\right)^{-e} \approx k_t^{1,1} PD^e (DP)^{-e} \qquad (19)$$

This equation still would permit determination of chain-length dependency, *e* and $k_t^{1,1}$. So the slope of a plot of log($\langle k_t \rangle$) versus log(*DP*) still equals -*e*, thus giving *e*, as long as *PD* is constant from experiment to experiment. Employing *DP* should have no large effect on *e* value and rather it may make its measurement more accurate, as it overcomes some common problems associated with DP_n. Of course, this will require knowledge of *PD* in order to

determine $k_t^{1,1}$. However, because the factor PD^e is a little in excess of 1 it can be approximated to be equal to 1. To be more precise for e = 0.2 and PD =1.5 and 2, the classical limits for PDI for conventional RP at low conversion, PD^e = 1.08 and 1.15 respectively, while e = 0.65 gives 1.30 and 1.57 respectively. Hence Eq. 19 can also be used to estimate $k_t^{1,1}$ value (which also assumes $G \approx 1$). Since $G > 1$, both approximations result in overestimated values for $k_t^{1,1}$.

In reality PD is not constant and can change from experiment to experiment as a consequence of factors such as CLDT and mode of termination. In fact there is reason to think that PD dose not vary much and can be approximated as a constant. As mentioned earlier, this is supported by our experimental measurements of PDI carried out using the GPC instrument in Gottingen University (see Chapter 3, Figure 3-8). In addition, the consistent behaviour of DP throughout all the previous experimental analysis, for example $DP \sim c_M^{1.08} c_I^{-0.74}$ from Chapter 3, would be another verification of a reasonable assumption of nearly constant PD.

In truth, even if we allow for a variation of the PD value from experiment to experiment this may not have a large effect on the obtained e value and can only lead to a very minor error in e determination.

Results of $\langle k_t \rangle$ versus DP are shown in Figure 4-15 and reported in Table 4-6. The results have been found to conform to the so-called composite model for termination for small chains. Large chain-length dependencies are found for all monomers. Comparison of the different types of monomers shows that similar CLDT are obtained for MMA and BMA as expected. On the other hand, ST and DMA showed $e \approx 0.5$, which is known to hold for spherical groups. In addition, the values of $k_t^{1,1}$ obtained from the intercepts were reasonably consistent with those expected from a small molecule diffusion process. Values in the order of 10^9 L mol^{-1} s^{-1} were obtained for all monomers except for DMA, which yielded a $k_t^{1,1}$ in

order of 10^8 L mol^{-1} s^{-1}.This value can easily be rationalized: being much larger, DMA diffuses more slowly than MMA.

Furthermore, the values reported for the $k_t^{1,1}$ probably would be overestimated as mentioned earlier, where the intercept is actually equal to $k_t^{1,1}$ G $(PD)^e$ (we are approximating G $(PD)^e \approx$ 1).

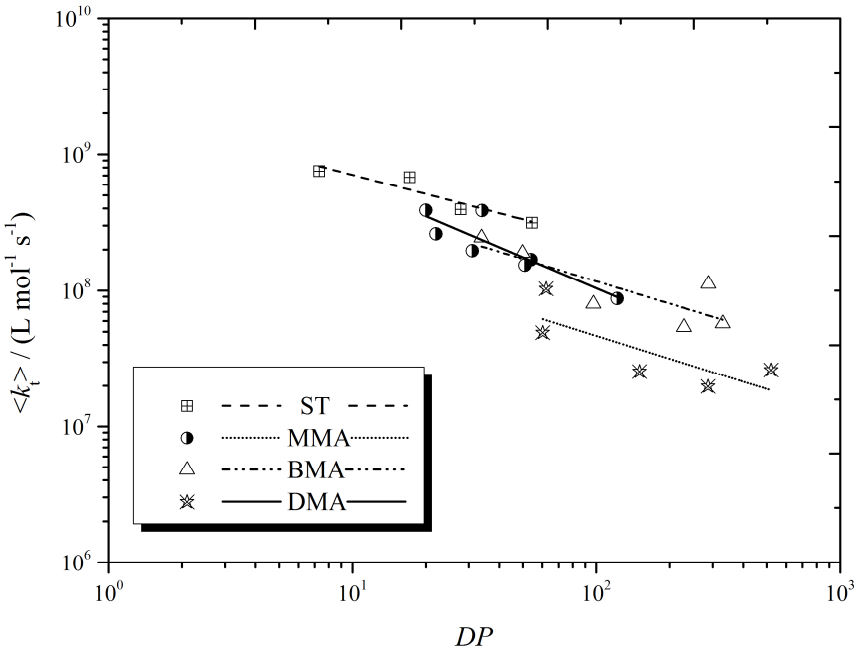

Figure 4-15. Log-log plot of experimental average rate of termination, $<k_t>$, as a function of experimental *DP* for polymerization of different monomers as indicated. Data obtained from temperature effect investigation carried out in this chapter, employed 0.67 mol L^{-1} of monomer in TFT, except for ST where the solvent was EBz. Experiments also employed 0.05 mol L^{-1} AIBN as initiator. Points: experiment results; lines: linear best fits to each set of results.

Table 4-6. The e_S and $k_t^{1,1}$ results obtained from Figure 4-15.

Monomer	$k_t^{1,1}$/(L mol^{-1} s^{-1})	e_s
MMA	3.3×10^9	0.7 ± 0.2
BMA	1.4×10^9	0.6 ± 0.2
DMA	6.1×10^8	0.5 ± 0.3
ST	2.1×10^9	0.5 ± 0.1

However, the value of the reported $k_t^{1,1}$ seems to agree with what is expected on the basis of the diffusion coefficient assigned to such monomers. For example, MMA yielded a $k_t^{1,1}$ value 3.3×10^9 L mol^{-1} s^{-1}, which appears consistent with the diffusion coefficient assigned for MMA at 25 °C, 2.25×10^{-9} m^2 s^{-1},[68] and 2.1–3.1 $\times 10^{-9}$ m^2 s^{-1}.[65] The $k_t^{1,1}$ (2.1×10^9 L mol^{-1} s^{-1}) obtained for ST is similarly consistent with the diffusion coefficient of ST, which is 1.5×10^{-9} m^2 s^{-1} [69], cf. the value obtained for toluene 2.0×10^9 m^2 s^{-1}.[60] These diffusion coefficients may be turned into $k_t^{1,1}$ values using the Smoluchowski equation. Referring to diffusion reactions, the monomer size needs to be considered as well, as larger monomers will have a slower diffusion. Indeed, this is also consistent with what this work has found for the $k_t^{1,1}$ series, viz. DMA < BMA < ST < MMA. This is analogous to what is found in the literature where $\langle k_t \rangle$ is found to increase with a decrease in the size and mass of radicals involved.[70]

4.8. Conclusion

This chapter has demonstrated the substantial effect of employing correct fk_d on $E_a(\langle k_t \rangle)$. In addition, it has also demonstrated how chain-length becomes an important factor to be specifically aware of when measuring the effect of temperature for thermally induced polymerization. By disregarding such information the result can lead to misleading apparent activation energies. A consistent value of $E_a(\langle k_t \rangle)$ to what has been found in the literature is obtained when large polymer chains ($DP > 100$) are generated for PMMA. However, a larger value of $E_a(\langle k_t \rangle)$ is obtained when small polymer chains ($DP < 100$) are generated. Although this is consistent with Eq. 3, the value is larger than what is expected for a diffusion controlled process. A contribution of the CLDT effect on $\langle k_t \rangle$ is suggested to be the cause of this large value. Evidence from experimental determination of DP was attained and consistent with such large values. Furthermore, results of large termination activation energy for short

polymers are confirmed using different types of monomers. Lastly, careful measurements of $E_a(<k_t>)$ can yield information about CLDT. This chapter has contained simply obtained but remarkable results for the variation of $<k_t>$ with temperature. Scaling of quantities that are experimentally accessible, such as $<k_t>$ with *DP*, yielded CLDT parameters in good agreement with what has been found recently in specialized PLP experiments.

4.9. References

[1] M. Buback, M. Egorov, R.G. Gilbert, V. Kaminsky, O.F. Olaj, G.T. Russell, P. Vana, G. Zifferer, Macromolecular Chemistry and Physics, 203 (2002) 2570-2582.
[2] D.R. Taylor, K.Y. Van Berkel, M.M. Alghamdi, G.T. Russell, Macromolecular Chemistry and Physics, 211 (2010) 563-579.
[3] G.B. Smith, J.P.A. Heuts, G.T. Russell, Macromolecular Symposia, 226 (2005) 133-146.
[4] J. Barth, M. Buback, Macromolecular Rapid Communications, 30 (2009) 1805-1811.
[5] S. Pickup, F.D. Blum, Macromolecules, 22 (1989) 3961-3968.
[6] M. Buback, B. Huckestein, F.D. Kuchta, G.T. Russell, E. Schmid, Macromolecular Chemistry and Physics, 195 (1994) 2117-2140.
[7] "Initiators for High Polymers", in, AKZO Nobel Chemicals, 2006.
[8] S. Beuermann, M. Buback, T.P. Davis, R.G. Gilbert, R.A. Hutchinson, O.F. Olaj, G.T. Russell, J. Schweer, A.M.v. Herk, Macromolecular Chemistry and Physics, 198 (1997) 1545-1560.
[9] M. Buback, R.G. Gilbert, R.A. Hutchinson, B. Klumperman, F.-D. Kuchta, B.G. Manders, K.F. O'Driscoll, G.T. Russell, J. Schweer, Macromolecular Chemistry and Physics, 196 (1995) 3267-3280.
[10] S. Beuermann, M. Buback, Progress in Polymer Science, 27 (2002) 191-254.
[11] K.C. Berger, Makromol. Chem., (1975) 3575.
[12] T. Fukuda, Y.D. Ma, H. Inagaki, Macromolecules, 18 (1985) 17-26.
[13] C.E.H. Bawn, D. Verdin, Transactions of the Faraday Society, 56 (1960) 815-822.
[14] C.E.H. Bawn, S.F. Mellish, Transactions of the Faraday Society, 47 (1951) 1216-1227.
[15] Z. Guan, J.R. Combes, Y.Z. Menceloglu, J.M. DeSimone, Macromolecules, 26 (1993) 2663-2669.
[16] V.A.F. Moroni, Die Makromolekulare Chemie, 105 (1967) 43-49.
[17] J.P. Van Hook, A.V. Tobolsky, Journal of the American Chemical Society, 80 (1958) 779-782.
[18] M.T. Erben, S. Bywater, Journal of the American Chemical Society, 77 (1955) 3712-3714.
[19] J.W. Breitenbach, A. Schindler, Monatshefte für Chemie, 83 (1952) 724-730.
[20] G. Moad, E. Rizzardo, D.H. Solomon, S.R. Johns, R.I. Willing, Die Makromolekulare Chemie, Rapid Communications, 5 (1984) 793-798.
[21] N. Charton, A. Feldermann, A. Theis, M.H. Stenzel, T.P. Davis, C. Barner-Kowollik, Journal of Polymer Science Part A: Polymer Chemistry, 42 (2004) 5559-5559.
[22] J. Szafko, W. Feist, Journal of Polymer Science, Part A: Polymer Chemistry, 33 (1995) 1637-1642.
[23] J. Krstina, G. Moad, R. Ian Willing, S.K. Danek, D.P. Kelly, S.L. Jones, D.H. Solomon, European Polymer Journal, 29 (1993) 379-388.
[24] V.W. Vogt, L. Dulog, Die Makromolekulare Chemie, 122 (1969) 223-236.
[25] G.T. Russell, Australian Journal of Chemistry, 55 (2002) 399-414.
[26] H.K. Mahabadi, K.F. O'Driscoll, Journal of Macromolecular Science: Part A - Chemistry, 11 (1977) 967-976.
[27] R. Sack-Kouloumbris, G. Meyerhoff, Die Makromolekulare Chemie, 190 (1989) 1133-1152.
[28] M. Buback, C. Kowollik, Macromolecules, 31 (1998) 3211-3215.
[29] M. Stickler, Die Makromolekulare Chemie, 187 (1986) 1765-1775.
[30] G.B. Smith, *Ph.D. Thesis*, The University of Canterbury in, 2007.
[31] O.F. Olaj, P. Vana, Macromolecular Rapid Communications, 19 (1998) 533-538.

[32] M.S. Matheson, E.E. Auer, E.B. Bevilacqua, E.J. Hart, Journal of the American Chemical Society, 71 (1949) 497-504.
[33] B. Yamada, M. Kageoka, T. Otsu, Polymer Bulletin, 29 (1992) 385-392.
[34] M. Buback, F.-D. Kuchta, Macromolecular Chemistry and Physics, 198 (1997) 1455-1480.
[35] O.F. Olaj, P. Vana, Macromolecular Rapid Communications, 19 (1998) 433-439.
[36] M.S. Matheson, E.E. Auer, E.B. Bevilacqua, E.J. Hart, Journal of the American Chemical Society, 73 (1951) 1700-1706.
[37] C. Barner-Kowollik, G.T. Russell, Progress in Polymer Science (Oxford), 34 (2009) 1211-1259.
[38] G. Johnston-Hall, A. Theis, M.J. Monteiro, T.P. Davis, M.H. Stenzel, C. Barner-Kowollik, Macromolecular Chemistry and Physics, 206 (2005) 2047-2053.
[39] G.B. Smith, G.T. Russell, Macromolecular Symposia, 248 (2007) 1-11.
[40] H.K. Mahabadi, Macromolecules®, 18 (1985) 1319-1324.
[41] M. Buback, M. Egorov, A. Feldermann, Macromolecules, 37 (2004) 1768-1776.
[42] J. Barth, M. Buback, G. Schmidt-Naake, I. Woecht, Polymer, 50 (2009) 5708-5712.
[43] G.B. Smith, G.T. Russell, J.P.A. Heuts, Macromolecular Theory and Simulations, 12 (2003) 299-314.
[44] O.F. Olaj, G. Zifferer, G. Gleixner, Die Makromolekulare Chemie, Rapid Communications, 6 (1985) 773-784.
[45] S. Beuermann, M. Buback, T.P. Davis, R.G. Gilbert, R.A. Hutchinson, A. Kajiwara, B. Klumperman, G.T. Russell, Macromolecular Chemistry and Physics, 201 (2000) 1355-1364.
[46] Initiators for High Polymers, in: A.N.P. Chemicals (Ed.), Akzo Nobel Polymer Chemicals, 2006.
[47] M. Buback, F. Günzler, G.T. Russell, P. Vana, Macromolecules, 42 (2009) 652-662.
[48] J. Brandrup, E.H. Immergut, E.A. Grulke, Polymer Handbook, 4th ed., Wiley, 1999.
[49] S. Beuermann, *Dissertation*, in, Göttingen, 1993.
[50] G.T. Russell, Macromolecular Theory and Simulations, 4 (1995) 549-576.
[51] J. Barth, M. Buback, P. Hesse, T. Sergeeva, Macromolecules, 43 (2010) 4023-4031.
[52] J.M. Asua, S. Beuermann, M. Buback, P. Castignolles, B. Charleux, R.G. Gilbert, R.A. Hutchinson, J.R. Leiza, A.N. Nikitin, J.P. Vairon, A.M. Van Herk, Macromolecular Chemistry and Physics, 205 (2004) 2151-2160.
[53] A.N. Nikitin, R.A. Hutchinson, M. Buback, P. Hesse, Macromolecules, 40 (2007) 8631-8641.
[54] C. Plessis, G. Arzamendi, J.R. Leiza, H.A.S. Schoonbrood, D. Charmot, J.M. Asua, Macromolecules, 33 (2000) 4-7.
[55] A.N. Nikitin, P. Castignolles, B. Charleux, J.-P. Vairon, Macromolecular Rapid Communications, 24 (2003) 778-782.
[56] A.N.F. Peck, R.A. Hutchinson, Macromolecules, 37 (2004) 5944-5951.
[57] N.A. Plate, A.G. Ponomarenko, Polymer Science U.S.S.R., 16 (1974) 3067-3081.
[58] G. Johnston-Hall, M.J. Monteiro, Macromolecules, 41 (2008) 727-736.
[59] G. Johnston-Hall, M.J. Monteiro, Journal of Polymer Science, Part A: Polymer Chemistry, 46 (2008) 3155-3173.
[60] M.C. Piton, R.G. Gilbert, B.E. Chapman, P.W. Kuchel, Macromolecules, 26 (1993) 4472-4477.
[61] O.F. Olaj, P. Vana, Journal of Polymer Science Part A: Polymer Chemistry, 38 (2000) 697-705.
[62] O.F. Olaj, G. Zifferer, G. Gleixner, Macromolecules, 20 (1987) 839-850.
[63] J.P.A. Heuts, D. Kukulj, D.J. Forster, T.P. Davis, Macromolecules, 31 (1998) 2894-2905.

[64] G. Moad, C.L. Moad, Macromolecules, 29 (1996) 7727-7733.
[65] M.C. Griffiths, J. Strauch, M.J. Monteiro, R.G. Gilbert, Macromolecules, 31 (1998) 7835-7844.
[66] M. Buback, M. Egorov, T. Junkers, E. Panchenko, Macromolecular Rapid Communications, 25 (2004) 1004-1009.
[67] T. Junkers, A. Theis, M. Buback, T.P. Davis, M.H. Stenzel, P. Vana, C. Barner-Kowollik, Macromolecules, 38 (2005) 9497-9508.
[68] R.A. Waggoner, F.D. Blum, J.M.D. MacElroy, Macromolecules, 26 (1993) 6841-6848.
[69] G.T. Russell, Macromolecular Theory and Simulations, 4 (1995) 497-517.
[70] H. Fischer, H. Paul, Accounts of Chemical Research, 20 (1987) 200-206.

Chapter 5. The Effect of Pressure on Termination Rate Coefficients at Low Conversion

In this chapter, the kinetics of the termination process are further addressed. The mechanism and kinetics of radical polymerization (RP) under high pressure are first briefly reviewed. In particular, the effect of pressure on the rate coefficient of termination for short polymers at low conversion polymerization will be probed.

5.1. Introduction

Many industrial polymerization processes are carried out under high pressure. This might be partly because of the influence of high pressure on the rate of polymerization, resulting in greater productivity. However, high pressure also has an effect on the properties of polymer product. For example, RP under high pressure might have a profound effect on polymer structure, via chain branching, and on degree of polymerization. Polymer syntheses at high pressure can provide some unique conditions not usually met under normal conditions. The production of different types of polyethylene (PE) is an excellent example. Low-density polyethylene (LDPE) production requires high pressure whereas high-density polyethylene (HDPE) production does not. Hence high pressure polymerization can be an alternative route to new polymers. For instance, radical reactivity of different monomers can be increased with pressure. Styrene and vinyl acetate will not co-polymerize appreciably at 1 bar whereas at 1 000 bar they give copolymer at a reasonable rate.[1] Another example is that MMA-acrylonitrile copolymerization is nearly ideal at 1 000 bar.[2]

Because pressure influences polymerization, application of high pressure on radical polymerization has generated much interest.[3, 4] High pressure is advantageous for

mechanistic investigations because of the diverse pressure dependence of the individual rate coefficients. For instance, chemically-controlled bimolecular reactions such as propagation are typically accelerated at high pressure, whereas diffusion controlled ones such as termination proceed at lower rates. Therefore, investigation of the pressure effect on the various steps of RP kinetics becomes important. In fact, the pressure dependence on the rate constant for initiator decomposition and for chain propagation are readily understood in terms of the activation-volume concept. However, the effect of pressure on the rate of termination, in particular, has not been extensively studied. Indeed, understanding the pressure dependence of k_t is still blurry because different types of diffusion controls operate during polymerization.

The primary intention of the present work is to study the effect of pressure on the rate of termination of radical polymerization of methyl methacrylate (MMA) in a dilute solution, such that short polymers are dominant. Additional interest originates from the different temperature dependence that has been found for $<k_t>$ as a function of chain length, as discussed in Chapter 4.

5.1. Experimental section

The high-pressure MMA radical polymerization experiments were performed in the laboratory of Professor Michael Buback at the Georg-August University in Göttingen, Germany. Polymerization was carried out in a stainless-steel optical pressure cell. The schematic diagram of the high-pressure cell is shown in Figure 5-1. This cell allows experiments to be carried out up to 3 500 bar. The cell is also equipped with optical windows that allow the use of near-infrared (NIR) radiation to monitor monomer conversion. In addition to the cell being suited for high pressure, it is also suited for thermally initiated

polymerization, as the cell can be electrically heated from the outside by a resistance wire that is mounted on a brass support.

The polymerization procedure was, in general, similar to those used previously. Polymerization was carried out in trifluorotoluene (TFT) at 85 °C using the thermal initiator 2,2'-azobisisobutyronitrile (AIBN) at different pressures. Dissolved oxygen was removed by flushing the mixture with nitrogen for about 15 minutes before the mixture was injected into the preheated high-pressure cell. The system under investigation was connected to the pressure generator, enabling a desired pressure to then be applied to the mixture. The polymerization mixture was directly fed into the high-pressure cell. As soon as the desired pressure was reached, the NIR spectrometer was immediately started and the reaction monitored for a certain time. Also, an important point to note is that the high-pressure cell is made of stainless-steel and contains some significant amounts of nickel and cobalt which may cause some catalytic activity.[5]

Monomer conversions were monitored via online NIR spectroscopy of the C-H modes at the C=C double bond around 6 170 cm^{-1}. Molar mass distributions were determined by means of regularly calibrated size-exclusion chromatography. Experimental details of the SEC have already been reported in Chapter 2.

Size exclusion chromatography of the product polymer was also carried out at Göttingen University, meaning that, in contrast to the preceding chapters, values of DP_n were obtained and therefore used.

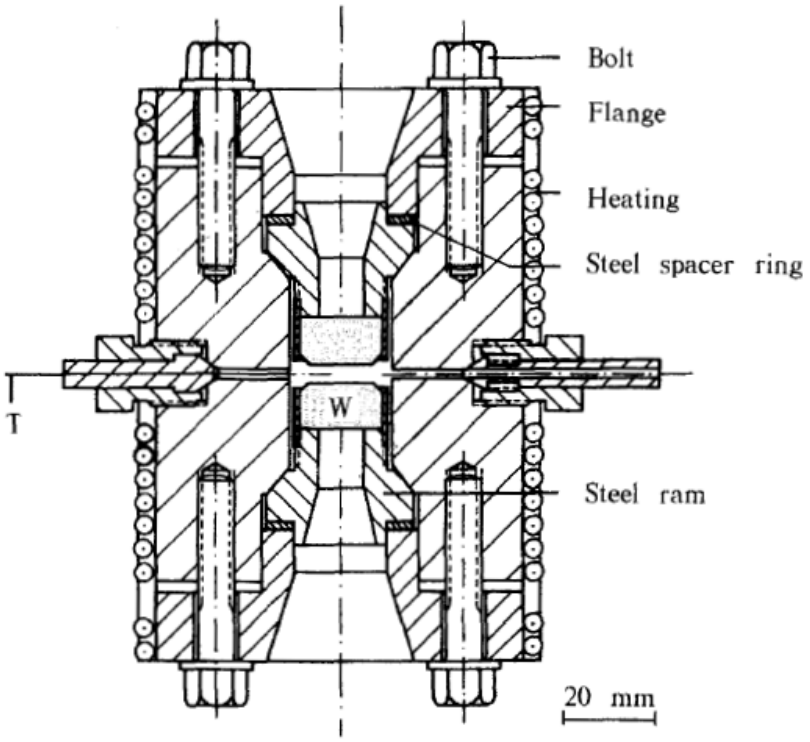

Figure 5-1. Schematic diagram of the optical high-pressure cell, where W denotes window and T sheathed thermocouple.[5]

5.2. NIR spectroscopy

Vibrational spectroscopy is useful for quantitative analysis as it covers a wide concentration range. Thus NIR enables accurate monitoring of monomer concentration during the course of polymerization. The application of NIR spectroscopy has proven to be perfectly suited for this purpose.[6] Therefore the change of the MMA concentration was measured via online Fourier-transform NIR spectroscopy. The integrated peak area of the peak of the unsaturated C-H stretching vibration around 6 170 cm^{-1}, which is well suited to quantitative measurement of MMA in radical polymerization,[5] was used for determination of monomer conversion. Figure 5-2 shows a series of NIR spectra taken during thermally induced polymerization of MMA in TFT at 85 °C and 1 000 bar.

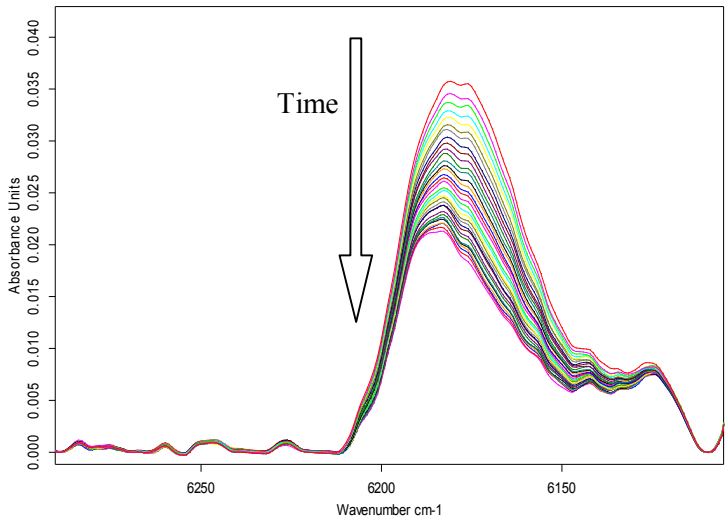

Figure 5-2. Absorbance spectra recorded during solution polymerization of MMA in TFT at 1 000 bar and 85 °C using AIBN as initiator. As shown, monomer absorption decreases with time as monomer is converted into polymer.

5.3. Data analysis

To obtain average termination rate,$\langle k_t \rangle$, Eq.1, the steady state recommended equation, is used.

$$\text{Rate} = \frac{-\text{d}\ln(1-x)}{\text{d}t} = k_\text{p}\left(\frac{f k_\text{d} c_\text{I}}{\langle k_\text{t}\rangle}\right)^{0.5} \Rightarrow \langle k_\text{t}\rangle = f k_\text{d} c_\text{I}\left(\frac{k_\text{p}}{\text{Rate}}\right)^2 \qquad (1)$$

Where: x refers to monomer conversion; k_d, k_p and $\langle k_\text{t}\rangle$ are the rate coefficients for initiator decomposition, propagation and termination respectively; and c_I and f are the initiator concentration and efficiency respectively.

It is also to be expected that the pressure will affect the rate of chain transfer to monomer, solvent and polymer. However, these were all minimised by using low monomer concentration and using TFT as a solvent, since it has no labile hydrogens. Moreover, having the polymerization performed in dilute solution permits us to ignore any conversion-related issues. Thus experiments were limited to the low-conversion region wherever possible.

Again, as mentioned earlier, the accuracy in $\langle k_t \rangle$ depends on accuracy in k_p and fk_d. Since this work was performed under high pressure, it is first of all appropriate to address the influence of pressure on the kinetic parameters k_p, f and k_d.

The effect of high pressure on the kinetics of polymerization is an important topic. Investigations of kinetics at high pressure have been carried out by several groups. The most extensive work on high-pressure polymerization has been done by the Buback group. Buback and co-workers measured the propagation rate coefficient for homopolymerization of different monomers and also investigated their termination rates under such conditions using highly developed pulsed-laser techniques.[7-10]

High pressure is known to have a large effect on the overall rate of radical polymerization. In particular, the rate of propagation of RP, k_p, increases with increasing pressure. Since propagation is a bimolecular reaction, propagation should indeed be accelerated under conditions of high pressure. An overview of k_p as a function of pressure for different monomers is summarized in Figure 5-3.[5] It is evident from Figure 5-3 that the propagation rate increases with increasing pressure. Also, no large influence of temperature is noticed, i.e. one may declare that to good approximation the activation volume of propagation is temperature independent.[10] Also, similar activation volumes are observed for monomers of the same family, as shown in Figure 5-3.

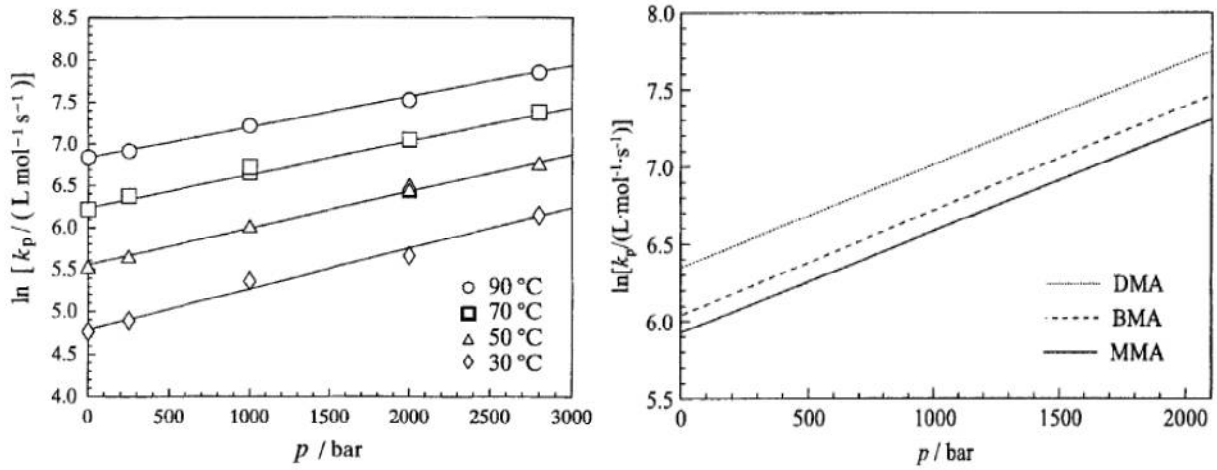

Figure 5-3. Pressure dependence of the propagation rate coefficient in the radical homopolymerization of styrene at various temperatures (left).[5] This shows that there is no major effect of temperature on activation volume. Variation of the propagation rate coefficient, k_p, with pressure, as obtained from PLP-SEC experiments on methyl methacrylate (MMA), *n*-butyl methyacrylate (BMA) and dodecyl methacrylate (DMA) at 30 °C (right). Results are presented as the best fits to the experimental data.[5] They show that activation volume is much the same for all *n*-alkyl methacrylates.

On the other hand the value of k_d has been found in the literature to be less influenced by pressure.[5, 11] This result is as expected for a unimolecular dissociation reaction, where volume expansion is expected for the initiator going to the transition state, which involves stretching of a covalent bond. Therefore, a small positive activation volume is expected for the decomposition rate. In addition, the results presented in Figure 5-4 show the effect of pressure on different type of initiators, as obtained by Buback et al.[5] Results in Figure 5-4 demonstrate the difference between primary and tertiary peroxyesters, as exemplified by *tert*-butyl peroxyacetate (TBPA) and *tert*-butyl peroxypivalate (TBPP) respectively. Primary peroxyester is found to be affected by pressure whereas tertiary is not. This clear difference is assigned to single bond scission in the primary peroxyester, which is associated with a pronounced increase in the molar volume of the transition state.[9] On the other hand, tertiary peroxyesters undergo almost concerted bond scission with the immediate production of the linear CO_2, giving rise to only a weak increase in the transition state volume. This can be

applied to AIBN, where the tertiary radical is produced with an immediate production of N_2. Therefore, regarding the k_d of AIBN, the Akzo value [12] at 1 bar was used and an assumption of constant k_d with pressure was made. Even if there is some variation with pressure, it is noted that it must be minimal, and therefore the error introduced by the approximation here can only be small at most, as variation of polymerization rate with pressure is determined by the much larger contributions from other rate coefficients.

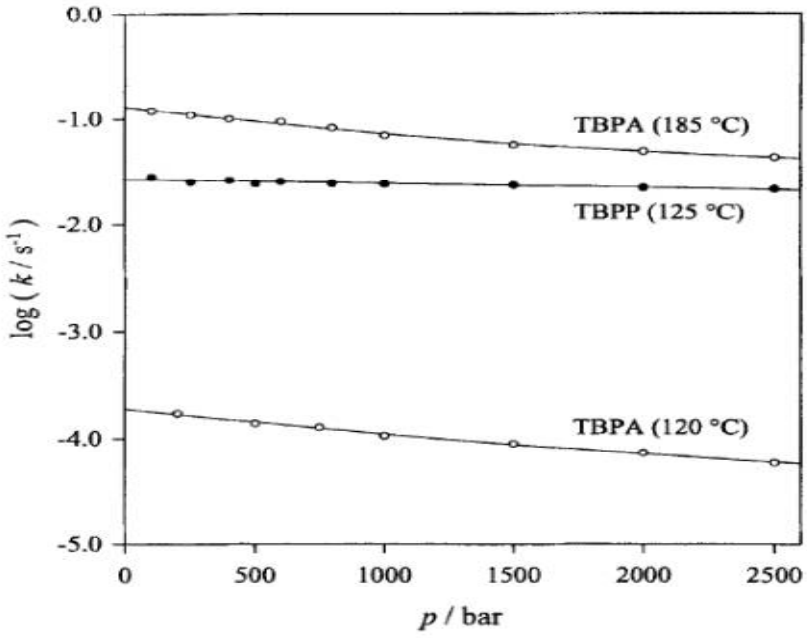

Figure 5-4. Comparison of the pressure dependence of the decomposition rate coefficient, k_d, as observed for *tert*-butyl peroxyacetate (TBPA) and for *tert*-butyl peroxypivalate (TBPP).[5]

In fact, any effect of pressure change on R_i may be largely attributed to the efficiency of initiator; hence, only the initiator efficiency was considered here to change with pressure. In fact f is found to be affected by increasing the pressure as expected: it drops with increasing pressure, because of diffusion becoming slower, meaning that newly generated radicals are less likely to escape their solvent cage before recombination can occur. The result to this effect deduced from Buback et al. work [13] is presented in Figure 5-5.

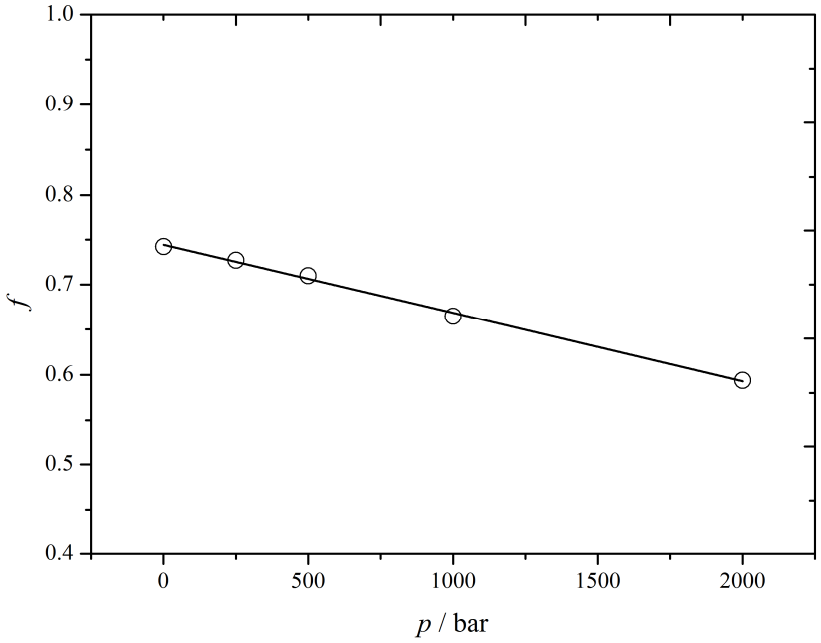

Figure 5-5. Variation of initiator efficiency *f* with pressure at 85 °C, as deduced from reference [5].

In summary, negative activation volume is found for k_p while positive activation volume is deduced for *f* from the data of Buback et al.[13] The present study has used the activation volumes in conjunction with the activation energies for MMA to obtain the following expression for k_p:

$$\ln\left[k_p\ /\mathrm{L\ mol^{-1}s^{-1}}\right] = 14.80 - \frac{2689.44}{T/\mathrm{K}} + \frac{0.201}{T/\mathrm{K}}\left(\frac{p}{\mathrm{bar}} - 1\right) \qquad (2)$$

Similarly, the activation volume and energy for AIBN efficiency, *f,* leads to the following expression:

$$\ln f = 1.62 - \frac{686.07}{T/\mathrm{K}} - \frac{0.041}{T/\mathrm{K}}\left(\frac{p}{\mathrm{bar}} - 1\right) \qquad (3)$$

A temperature-independent activation volume is assumed for both k_p and *f*.

Considering now the termination process, the quantitative effect of pressure on termination rate coefficient is calculated in the usual way, viz. using Eq. 4:

$$\left(\frac{d\ln\langle k_t\rangle}{dp}\right)_T = -\frac{\Delta V^*}{RT} \qquad (4)$$

Here ΔV^* is the activation volume and p the pressure. Thus from the slope of $\ln\langle k_t\rangle$ vs. p at constant T, the activation volume is determined.

5.4. Results and Discussion

Since different chain-length dependencies are identified for the termination process for free radical polymerization (see Chapter 4), it appeared worthwhile to study the effect of chain length on the activation volume. This was done by measuring $\langle k_t\rangle$ as a function of pressure under dilute-solution conditions, where short chains are generated and strong CLDT is expected, as discussed in Chapter 4. Such data is interesting from a mechanistic point of view because it can be seen how such short chain radicals influence the activation volume. In the present study, the effect of pressure on $\langle k_t\rangle$ is determined for thermal polymerization of a dilute solution of MMA in TFT employing AIBN as initiator, where short chains up to about $DP_n \approx 100$ were generated. Results are presented in Table 4-1 for MMA solution polymerization.

Table 5-1. Results from low-conversion, solutions polymerization of MMA, employing 0.67 mol L^{-1} of monomer in TFT, 0.05 mol L^{-1} AIBN at 85 °C and pressure as indicated. The experimentally determined quantity $\frac{-\mathrm{dln}(1-x)}{\mathrm{d}t}$, has been used to calculate average termination rate coefficient $\langle k_t \rangle$, according to Eq. 1.

Pressure/ (bar)	$\frac{-\mathrm{dln}(1-x)}{\mathrm{d}t}$ / (s^{-1})	$\langle k_t \rangle$/(L mol^{-1} s^{-1})	DP_n	PDI
1	3.00×10^{-04}	2.61×10^{8}	31	1.55
1	3.46×10^{-04}	1.96×10^{8}	-	-
1	2.03×10^{-04}	5.70×10^{8}	27	1.44
1	2.47×10^{-04}	3.85×10^{8}	36	1.53
1	2.45×10^{-04}	3.91×10^{8}	-	-
1	2.05×10^{-04}	5.58×10^{8}	-	-
500	3.98×10^{-04}	2.50×10^{8}	36	1.63
1000	6.37×10^{-04}	1.58×10^{8}	47	1.68
1000	4.93×10^{-04}	2.66×10^{8}	46	1.76
1500	9.29×10^{-04}	1.25×10^{8}	69	1.82
2000	1.49×10^{-03}	7.99×10^{7}	97	1.85
2000	8.72×10^{-04}	2.34×10^{8}	84	1.91

5.4.1. Effect of pressure on rate of polymerization and molar mass

High pressure has an appreciable effect on the overall polymerization rate and on polymer molar mass. To be specific, it results in an acceleration of the overall rate of polymerization, R_p, and an increase in DP_n for thermally initiated polymerization. To be precise, pressure induced an increase in R_p by a factor of about 7 when going from ambient pressure to 2 000 bar. As was expected, increasing the pressure also led to an increase in molar mass, as illustrated in Figure 5-6. This is consistent with a number of studies that have shown an increase of the molar mass of polymers and rate of polymerization when the polymerization is carried out under high pressure.[14] Also, the experiments show a faster increase of R_p than DP_n with pressure. Figure 5-7 shows DP_n as a function of pressure, where short chains are clearly evident.

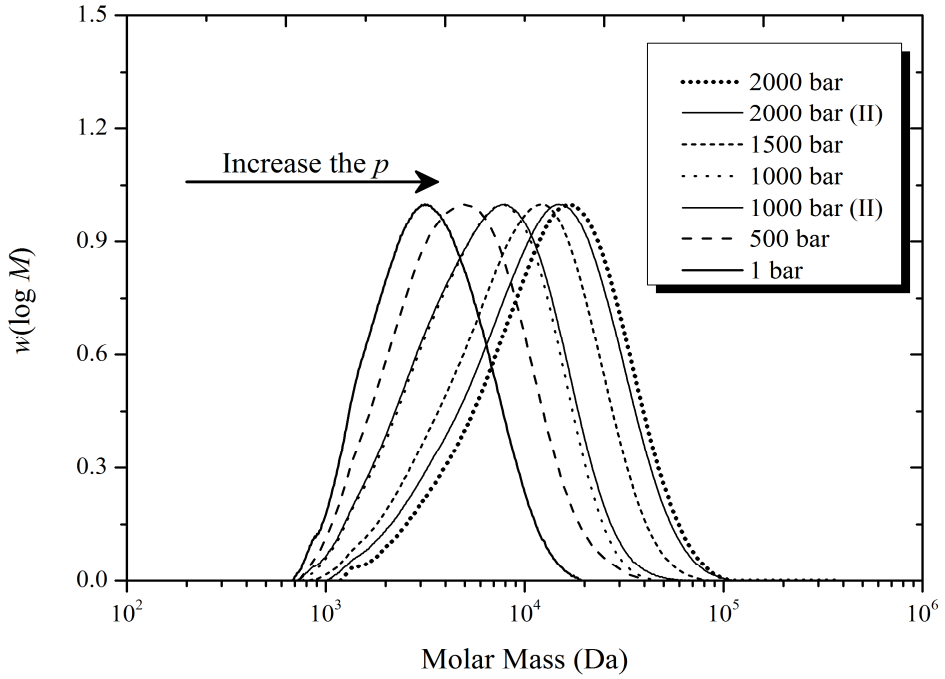

Figure 5-6. Normalized molar mass distributions of PMMA samples obtained at different pressures, as indicated, for solution polymerization of 0.67 mol L^{-1} MMA in TFT at 85 °C and employing 0.05 mol L^{-1} AIBN.

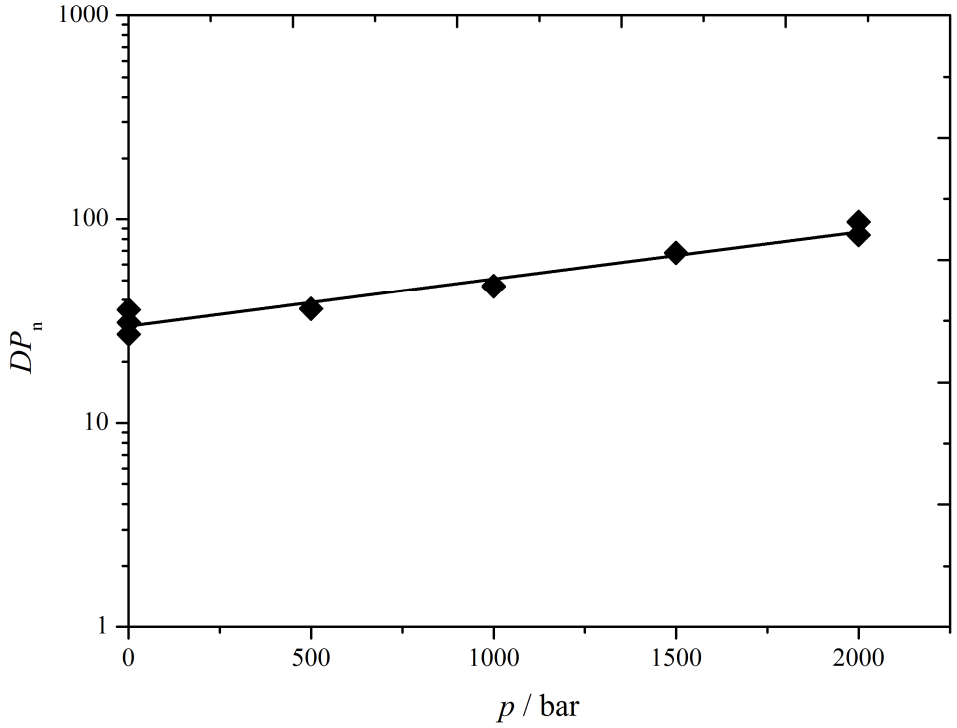

Figure 5-7. DP_n as a function of pressure for the polymerizations of Figure 5-6.

5.4.2. Effect of pressure on $\langle k_t \rangle$

This study shows a deceleration in the rate of radical termination as pressure is applied (Figure 5-8). Chain termination represents a bimolecular process of termination of two radicals. Pressure should accelerate the rate of a chemically-controlled bimolecular reaction. On the contrary, pressure is found to decrease the termination rate coefficient, i.e. termination is found to have a positive activation volume, in agreement with the literature.[15-17] Table 5-2 shows the results obtained and comparison with literature values. This retardation can be explained by termination being diffusion controlled, as diffusion coefficients are known to decrease, and viscosity increase, as pressure increases.[18, 19] This may be taken as confirmation of diffusion control for short chains. This is the first time such experiments have been done for very short chains.

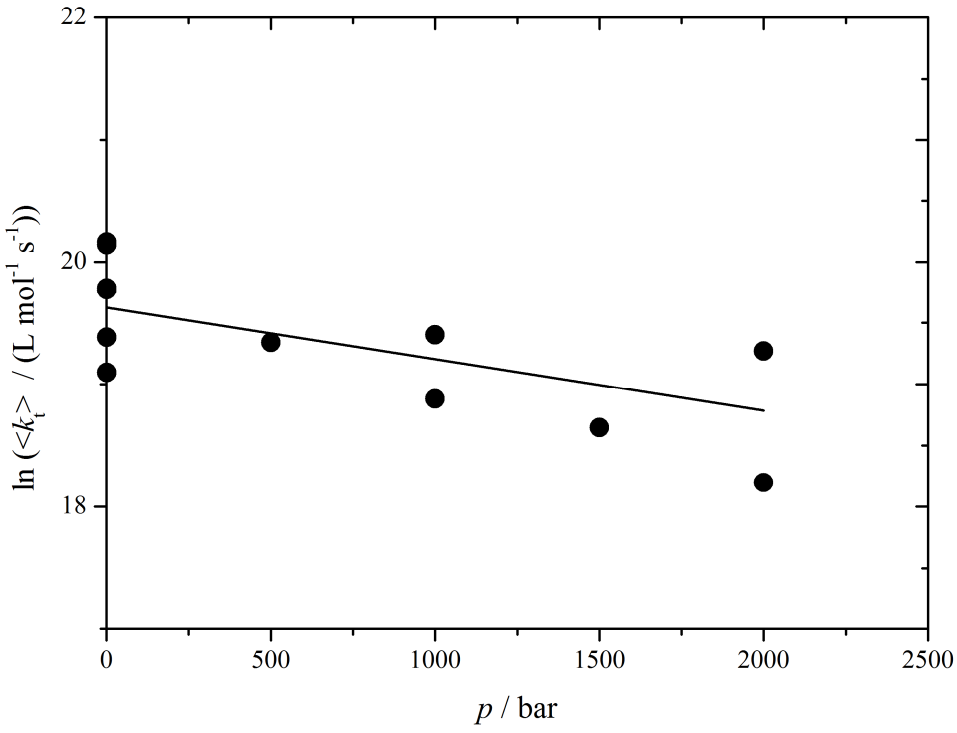

Figure 5-8. Pressure dependence of average rate coefficient of termination, $\langle k_t \rangle$, for dilute-solution polymerization of methyl methacrylate (MMA) in trifluorotoluene (TFT) employing 2,2-azobisisobutyronitrile (AIBN) as initiator at 85 °C.

Table 5-2. Activation volumes, $\Delta V^{\ddagger}$, in cm^3 mol^{-1} of MMA polymerization; this work: in TFT initiated by AIBN at 85 °C; literature: in bulk MMA.

Rate parameter	$\Delta V^{\ddagger}$ (this work)	$\Delta V^{\ddagger}$ (literature)
$<k_t>$	16 ± 6	15 ± 5 [16, 20]
k_p	–	–16.7 [16]
f	–	3.4 [13]
DP_n	–16 ± 2	–
R_p	–23 ± 3	≈ –20 ± 5 [14]

An activation volume of +16 ± 6 cm^3 mol^{-1} is obtained for MMA polymerization in TFT at 85 °C. This value is assigned for short chains, where motion of small non-entangled radicals is believed to control the termination. It is consistent with the activation volume measured for large chain polymers of PMMA.[16, 20] This suggests a chain-length independent result for activation volume.

Hence, the termination process is affected by viscosity. Thus its activation volume should be close to the corresponding activation volume that characterizes the pressure dependence on the inverse of the monomer viscosity.[21] This then may be compared with the values of the activation volume of the inverse viscosity of MMA. The activation volume of the inverse viscosity of MMA is 14.0 cm^3 mol^{-1},[22] as reported by Ogo et al. This value is close to the activation volume obtained in this work for short chain termination, within experimental uncertainty. Styrene also has a termination activation volume, 14 cm^3 mol^{-1}[22] and 15.1 ± 3.6 cm^3 mol^{-1}[21] are two measurements, that is close to that of its inverse viscosity, 14.6 cm^3 mol^{-1} at 30°C.[22] The close agreement of termination rate and of inverse monomer viscosity under pressure indicates the dominant influence of viscosity on diffusion control of $<k_t>$.

In addition to knowing the activation volume, this should shed light on the mechanism. A value of approximately similar size may provide further evidence of the central role played

by the rate determining step. The termination reaction for large-chain radicals of MMA is determined by a segmental diffusion process, i.e., the rate controlling step consists of the diffusion of radical sites of two entangled macroradicals approaching each other to undergo chemical reaction.[23, 24] Having similar activation volumes would provide an indication of similar termination behaviour under high pressure. Though the data is not conclusive, taking notice of the complicated character of $<k_t>$, it seems that there is every reason to believe that viscosity must be the major factor behind the decrease of $<k_t>$ with pressure. In view of the fact that different diffusion processes of both large and short chain termination is acknowledged, one may conclude a similar termination rate-determining step. These similar positive activation volumes of both short and large chains to MMA fluidity might suggest translational diffusion controlled process under high pressure, i.e. as pressure increases, the rate determining step for both short and large chain radicals become similar. This can be ascribed to the high pressure effect that leads to an increase in the viscosity and thus hindering translational diffusion rather than segmental diffusion, making translational motion the rate determining step for both large and short macroradical termination. In addition, this would also suggest a low effect of pressure on mobility of chains required for segmental diffusion. This interpretation is supported by a similar activation volume observed for self-diffusion of other molecules such as benzene,[25, 26] where translational diffusion is the main control, and where the correlation between $<k_t>$ and self-diffusion might be a proof of the translational diffusion control of termination.[27]

Further, in discussing the similarity between termination activation volumes of both large and short chains, the notion of additional coil-size effect being relevant to $<k_t>$, as argued by Cameron [28] and O`Driscoll [15], seems to be less important. That is, the idea appears unlikely that $<k_t>$ varies as a result of decreasing coil dimensions of macroradical through high pressure, as caused by the pressure itself or by changing the thermodynamic properties

of the solution under high pressure conditions.[29] As argued by Cameron,[28] coils could become so tightly coiled that the termination reaction could be severely hindered. As a result, $\langle k_t \rangle$ should decrease as pressure is applied. Bearing in mind the coil effect postulate, one would expect less effect of pressure on uncoiled polymers. However, this was not observed. The result of our present study showed very similar influence of pressure of small (uncoiled) chains to what has been found in the literature for long (coiled) chains. Consequently, this would back up translational diffusion being the rate-determining step at high pressure, and thus being affected by the change in bulk viscosity rather than monomer viscosity. Furthermore, this result would suggest similar solvent interaction of TFT and MMA on the termination process.

5.4.3. Pressure effect on *PDI*

With respect to MMD broadness, polymers with relatively narrow polydispersity index (*PDI*) were formed at ambient pressure: *PDI* of ~1.5 was observed. This value is contrary to what is predicted based on ideal conventional RP polymerization, where the lower bond comes out at about *PDI* = 1.94 using λ = 0.65 when employing Eq. 5, which holds for e = 0 (no CLDT).[30] Allowing for chain-length dependent termination cannot explain this low *PDI* value, as CLDT lead to a larger *PDI*.

$$PDI = \frac{1}{2}(1+\lambda)(3-\lambda) \qquad (5)$$

In spite of this discrepancy, a similarly low *PDI* value (1.44 – 1.55) has been reported for similar MMA polymerization in acetone with AIBN as initiator.[31]. Also, these findings may be related to the mode of termination being responsible for the observed different *PDI*. One explanation of narrow *PDI* values of 1.5 at ambient pressure in the present study would be that termination must be proceeding primarily by combination. However, this would not be completely true for MMA. Alternatively, this low *PDI* might be related to the low

monomer concentration, as *PDI* has been observed to be influenced by monomer concentration. Namely, the *PDI* of isothermal polymerization of MMA is reported to decrease with dilution.[32] Of course lower monomer concentration means short chains, and if chains are short enough, then chain-length-dependent propagation comes into play, it being known to lower *PDI*. Basically, this is because faster propagation at low chain lengths acts to compress an MMD.

Application of high pressure results in wider chain-length distribution, i.e. the resulting *PDI*s are appreciably elevated. This is clearly evident by inspecting Figure 5-9. Although one would expect *PDI*s to be lower as a result of the combined effect of the increase of the propagation rate and decrease in termination rate and initiator efficiency, *PDI*s were found to increase with pressure, as can be seen from Figure 5-9.

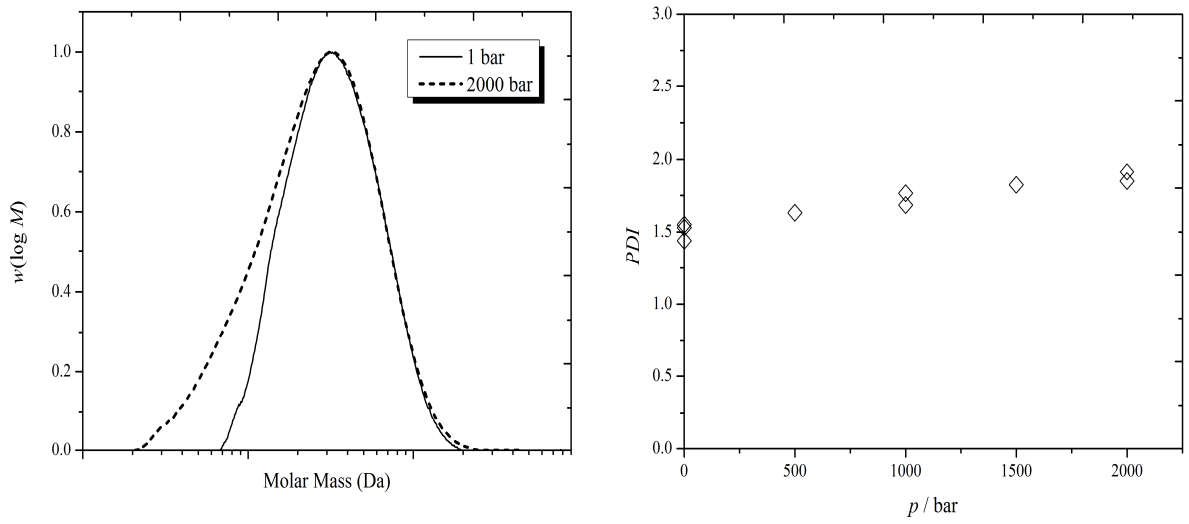

Figure 5-9. Molecular mass distribution comparisons of PMMA resulting from conventional thermally induced polymerization of MMA in TFT employing AIBN at 85 °C and different pressure as indicated. Left: overlaying two distributions for assessment, where peak height has been normalized to 1; right: *PDI* values as a function of pressure.

This increase in the *PDI* with pressure was difficult to explain in terms of known effects of pressure on the normal component processes. However, several explanations may be given. This increase in *PDI* seems to be connected to the observation of obtaining faster change in

R_p than DP_n. This would prove a genuine increase in *PDI* with pressure. This would be explained like that of any change in monomer throughout polymerization should be reflected in a polymer's length and distribution. Therefore, adding up the effect of pressure on both DP_n and *PDI* should result in a value close enough to the activation volume of the overall rate of polymerization. Interestingly, addition of activation volumes of DP_n (-16 ± 2 cm^3 mol^{-1}) and *PDI* (-3.3 ± 0.3 cm^3 mol^{-1}) yields a value of -19.3 ± 2.1 cm^3 mol^{-1}, which is in agreement (within experimental uncertainty) with the activation volume of -23 ± 3 cm^3 mol^{-1} obtained for R_p.

The increase in the *PDI* might be related to a possible chain transfer under high pressure that could be the cause of increasing *PDI* with pressure; this might be supported by the fact of observing a faster change in R_p than DP_n.

Another possible explanation for increased *PDI* is that the increase in *PDI* with pressure could be connected to the CLDP effect. As pressure increases, the chain length of the polymer increases, which then reduces the effect of CLDP and results in a wider distribution. This is thought to be the most likely explanation, perhaps with there also being a contribution from transfer.

A further possible explanation includes the scenario of different modes of termination being responsible for the different *PDI* observed. However, little information is available for the mode of termination. This moves us to the next topic of this work, where the mode of termination is investigated.

5.5. Conclusion

In conclusion, pressure has appreciable influence on $<k_t>$. In spite of different activation energies assigned for radical termination of MMA polymerization for different chain length regimes, the activation volume of termination is found to be chain-length independent. Moreover, on the basis of the data on the influence of pressure on the rate and average degree of polymerization, the same rate determining step may be suggested for both large and short polymer chains under high pressure conditions. Last but not least, clear proportional dependence of *PDI* on pressure is observed under such polymerization conditions. However, the rationalization of this dependence of *PDI* on pressure is still not clear.

References

[1] F.R. Mayo, F.M. Lewis, C. Walling, Discussions of the Faraday Society, 2 (1947) 285-295.
[2] N. Zutty, R. Burkhart, 'Polymer Synthesis at High Pressures, in: Polymerization and polycondensation processes: a collection of papers based on the Symposium on Polymerization and Polycondensation Processes, ACS Publications, 1962, pp. 52.
[3] C. Walling, Journal of Polymer Science, 48 (1960) 335-341.
[4] Y. Ogo, Journal of Macromolecular Science—Reviews in Macromolecular Chemistry and Physics, 24 (1984) 1-48.
[5] S. Beuermann, M. Buback, High Pressure Research, 15 (1997) 333-367.
[6] M. Buback, (1994) Absorption Spectroscopy in Fluid Phases, in E. Kiran and J. Levelt-Sengers (eds.) *Supercritical fluids-fundamentals for application*, Kluwer Academic Publishers, Dordrecht; Boston, London, PP 499-526.
[7] M. Buback, A. Kuelpmann, C. Kurz, Macromolecular Chemistry and Physics, 203 (2002) 1065-1070.
[8] M. Buback, Macromolecular Symposia, 182 (2002) 103-118.
[9] S. Beuermann, M. Buback, 4.35 - Radical Polymerization at High Pressure, in: M. Editors-in-Chief: Krzysztof, M. Martin (Eds.) Polymer Science: A Comprehensive Reference, Elsevier, Amsterdam, 2012, pp. 875-901.
[10] S. Beuermann, M. Buback, G.T. Russell, Macromolecular Rapid Communications, 15 (1994) 351-355.
[11] J.C. Martin, in "Solvation and Association, Chap.20 in Free radicals, Vol. 2, Kochi, J. K., Wiley New York, 1973.
[12] "Initiators for High Polymers", in, AKZO Nobel Chemicals, 2006.
[13] M. Buback, B. Huckestein, F.D. Kuchta, G.T. Russell, E. Schmid, Macromolecular Chemistry and Physics, 195 (1994) 2117-2140.
[14] G.G. Odian, Principles of polymerization, in, Wiley, Hoboken, N.J., 2004.
[15] K.F. O'Driscoll, Die Makromolekulare Chemie, 178 (1977) 899-903.
[16] S. Beuermann, M. Buback, Progress in Polymer Science, 27 (2002) 191-254.
[17] M. Buback, C. Kowollik, Macromolecules, 31 (1998) 3211-3215.
[18] P.W. Bridgman, Proceedings of the National Academy of Sciences of the United States of America, 11 (1925) 603-606.
[19] R.L. Cook, H.E. King, D.G. Peiffer, Macromolecules, 25 (1992) 2928-2934.
[20] K. Matyjaszewski, T.P. Davis, Handbook of radical polymerization Wiley-Interscience, 2002.
[21] M. Buback, F.-D. Kuchta, Macromolecular Chemistry and Physics, 198 (1997) 1455-1480.
[22] Y. Ogo, T. Kyotani, Die Makromolekulare Chemie, 179 (1978) 2407-2417.
[23] O.F. Olaj, P. Vana, A. Kornherr, G. Zifferer, Macromolecular Chemistry and Physics, 200 (1999) 2031-2039.
[24] J. Barth, M. Buback, P. Hesse, T. Sergeeva, Macromolecules, 42 (2009) 481-488.
[25] M.A. McCool, A.F. Collings, L.A. Woolf, Journal of the Chemical Society, Faraday Transactions 1: Physical Chemistry in Condensed Phases, 68 (1972) 1489-1497.
[26] D.W. McCall, D.C. Douglass, E.W. Anderson, The Journal of Chemical Physics, 31 (1959) 1555-1557.
[27] G.T. Russell, Macromolecular Theory and Simulations, 4 (1995) 497-517.
[28] G.G. Cameron, J. Cameron, Polymer, 14 (1973) 107-110.
[29] K.F. O'Driscoll, Die Makromolekulare Chemie, 180 (1979) 2053-2056.

[30] M. Buback, G.T. Russell, Kinetics of Polymerizations, in: Encyclopedia of Radicals in Chemistry, Biology and Materials, John Wiley & Sons, Ltd, 2012.
[31] K. Liu, E. Kiran, Industrial and Engineering Chemistry Research, 47 (2008) 5039-5047.
[32] T. Malavasic, U. Osredkar, I. Anzur, I. Vizovisek, Journal of macromolecular science. Chemistry, A25 (1988) 55-64.

Chapter 6. Investigation into the Mass Spectrometric Method for Determination of Mode of Termination in Radical Polymerization

In this chapter an investigation into the mass spectrometric method for determination of the fraction of termination by disproportionation, λ, or, in other words, mode of termination, in radical polymerization of methyl methacrylate (MMA), is carried out.

6.1. Mass spectrometry, MS

Radical polymerization has attracted significant attention over the past few decades. It has been investigated via a variety of experimental techniques. In recent times, one of the most important of these is mass spectrometry (MS). Since its establishment in 1933 by Thompson and Aston, MS has been considered one of the most important tools in chemistry. This technique can provide measurement of molar mass with sensitivity and resolution, together with structural information. Although for many decades its application was limited to small molecules, its capability has now been extended to involve macromolecules such as synthetic polymers; to be precise this has been the case since the discovery of the soft ionisation method. Thus the use of MS in polymer research has exploded since 1988, the year in which major breakthroughs in matrix-assisted laser desorption/ionization (MALDI) and electrospray ionization (ESI) techniques were announced. These techniques essentially removed barriers preventing MS from being effectively used on macromolecules due to problems of excessive fragmentation. A series of reviews that have highlighted the strength of MS for studying radical polymerization (RP) can be found in ref. [1, 2].

Today with the advent of ESI and MALDI, the analysis of polymers by MS has become much easier than early techniques such as field desorption (FD)[3] and fast bombardment (FAB).[4] MALDI-MS is an important technique by which a large variety of polymers are still being characterized today, including PS and PMMA.[5-7] However, the difficulty in carrying out MALDI-MS arises in the more complicated sample preparation, the appropriate choice of solvent [8] and the matrix composition,[9, 10] all of which are crucial for successful analysis. Low resolution is another limiting factor in use of MALDI, not to mention that instrument cost is significantly greater. Nevertheless, MALDI has the advantage of being able to measure relatively high molecular masses. [2] Similarly, ESI-MS has been used to characterize a variety of polymers including PMMA.[11, 12] In spite of the ESI-MS mass range limitation, it provides better resolution than MALDI. Thus, it has been extensively used in mechanistic studies.[13-18] In particular, it has been extensively employed for the study of initiation processes, for example rapid decarboxylation.[14]

Although MS use for polymer analysis remains limited, its importance has started to be realized. Recently, MS has become increasingly important for probing mechanistic features of polymerization processes such as mode of termination,[19] initiation efficiency [20] and chain-length dependence of propagation.[21] For more information on the highlighted utilities of MS to study conventional RP mechanisms, readers are referred to a recently published book chapter.[22]

6.2. Overview of mode of termination

Termination in radical polymerization (RP) occurs via the reactions of combination and disproportionation, as depicted in Scheme 1 for methyl methacrylate (MMA).

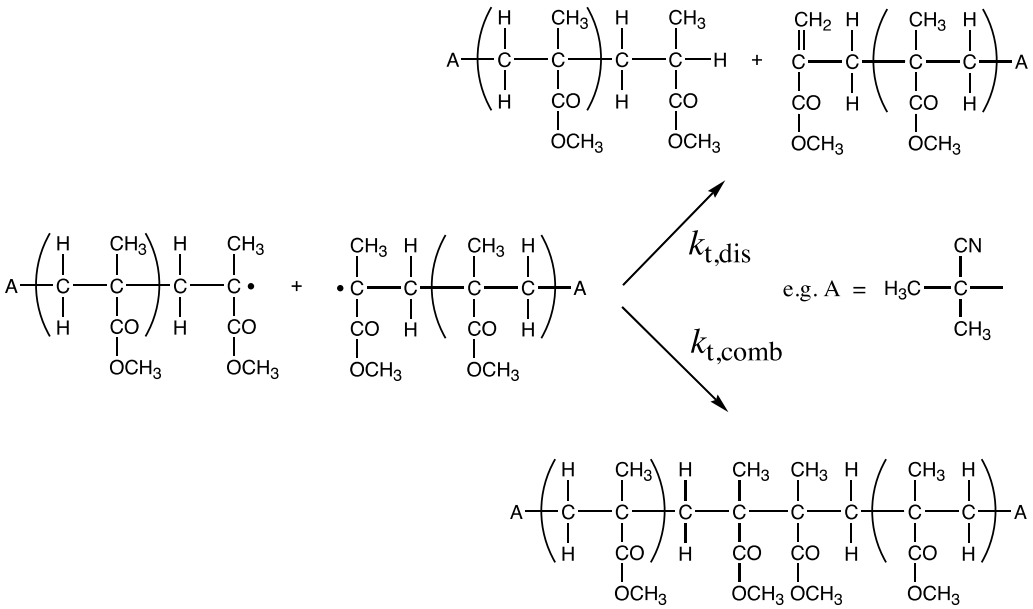

Scheme 1. The competing termination reactions of disproportionation, rate coefficient $k_{t,dis}$, and combination, rate coefficient $k_{t,comb}$, in radical polymerization of methyl methacrylate. Where AIBN is used as initiator, the end-group A is as indicated

There are several reasons why one would expect the kinetics of these two processes to be very well understood. One is that the existence of this situation, that is, the occurrence of the two reaction pathways, has been known for so long, essentially since day one of the mechanistic understanding of RP. Another reason is that it is a fundamental aspect of RP, in that termination is a quintessential part of the process. A third reason is that it is important in several ways. Although the mode of termination has no apparent influence on the rate of radical polymerization, it has an obvious influence on molar mass distribution (MMD). Most obviously, combination results in dead polymer molecules of double the number-average size of those from disproportionation, as is immediately evident from there being only half the number of product molecules (see Scheme 1).

Since material properties are intimately linked to polymer size, it is therefore of importance to know the balance between combination and disproportionation that occurs in a system.

Above and beyond this, Scheme 1 also makes clear that these two reactions generate different end-group functionalities: in the former case both end-groups will be initiator residues (assuming the occurrence of transfer to a negligible extent), while in the latter only one end-group will be of this nature. Again, this can be important in terms of material properties, especially if the polymers are small in size, and furthermore it can be vital if polymer modification reactions are to be carried out, whether through exploitation of the functionality contained in the initiator residue or that of the carbon-carbon double bond generated by disproportionation. Additionally, combination is like head-to-head addition in that it places bulky substituent groups adjacent to each other (see Scheme 1). The resulting steric strain may conceivably promote polymer degradation to some degree. Finally, the mode of termination is also present in many rate-parameter expressions.

Bearing all this in mind, it is a great surprise to find that there is enormous scatter and barely any agreement in literature compilations [23, 24] of measurements of the extent of disproportionation versus combination in RP systems, insofar as such determinations even exist (see Figure 6-1).

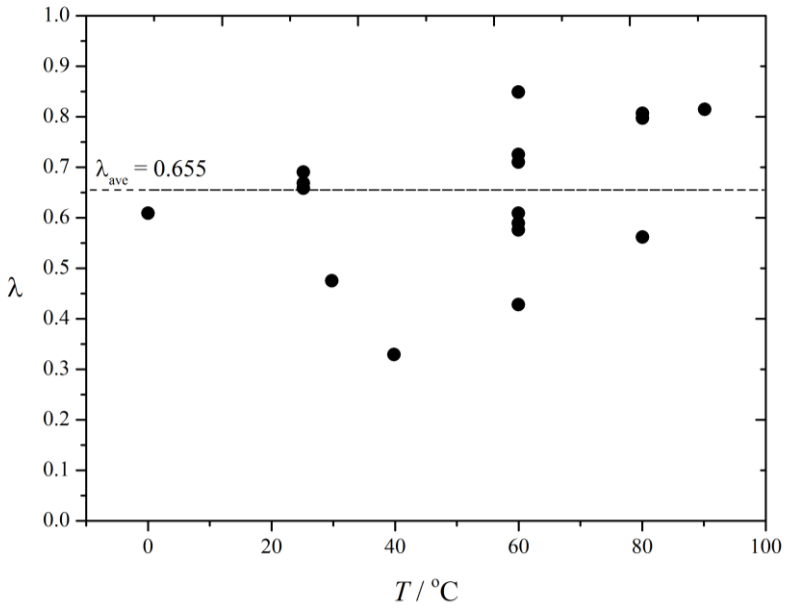

Figure 6-1. Literature measurements of λ for MMA as a function of temperature using several experimental approaches.[24]

Commonly, two quantitative indexes are used for mode of termination, being interrelated as indicated:

$$\lambda = \frac{k_{t,dis}}{k_t} = \frac{k_{t,dis}}{k_{t,dis} + k_{t,comb}} = \frac{\delta}{\delta + 1} \tag{1a}$$

$$\delta = \frac{k_{t,dis}}{k_{t,comb}} = \frac{\lambda}{1 - \lambda} \tag{1b}$$

Here $k_{t,dis}$ is the rate coefficient for disproportionation, $k_{t,comb}$ that for combination (see Scheme 1) and $k_t = k_{t,dis} + k_{t,comb}$ is the overall rate coefficient for termination. In recent work on this topic,[19] and as can be seen from Figure 6-1, it was illustrated that there is essentially no consistency in the literature values for λ as a function of temperature for MMA, which is the most studied system in this regard.

Why is this the case? In fact, though quantitative comparison of the signals from chain ends must make it possible to give λ, identification and quantification of chain ends are not always possible. For example, it is difficult for spectroscopic techniques to be used especially with polymers, as chain ends contribute only small signals relative to the rest of the polymer chain. Though this has been overcome to some extent by isotopic labelling of initiator end groups as NMR sensitive molecules, the mode of termination has been difficult to measure accurately, as manifested by the spread in the data reported in Figure 6-1. One might say that while measurement of λ was qualitatively sound in principle, in quantitative practice there was not confidence. Moreover, even with the advent of MALDI, knowledge about λ was not achievable. MALDI has been applied primarily only to confirm chain end groups for polymers as a qualitative guide to the mechanism. Furthermore, the works of Olaj and Schnöll-Bitai [25] and of Sarnecki and Schweer [26] have challenged whether MALDF-TOF can be used quantitatively to obtain end group information.

Despite the experimental approaches that have been taken to determine λ in radical polymerization,[27-32] there was a great deal of motivation to develop a new method for determining this much neglected parameter. This was built on the pioneering work of Zammit et al.,[33, 34] who were early recognizers of the potential of large-molecule mass spectrometry (MS) [35, 36] to shed light on previously tricky matters regarding the elucidation of mechanisms of RP.[37, 38] They took stock of the fact that, in contrast to size exclusion chromatography, MS yields clearly distinguishable signals for polymer molecules of identical degree of polymerization, *i*, but with different end-groups. For example, and of particular relevance, a polymer molecule of size *i* formed by combination has a different molar mass, *M*, to one formed by disproportionation, because the former molecule has two termini from initiation, the latter only one. By comparing the sizes of these two distinguishable MS signals, the sizes of course reflecting the number of such species present, the value of λ (or, alternatively, δ) should be deducible. The beauty of this approach is that MS provides a direct visualization of the molecules from the two different termination pathways, and thus it avoids having to make assumptions in this regard, which is essentially the problem that has plagued historical methods for determination of λ.

It turns out that the data analysis necessary to obtain λ from MS is more complicated than was realized by Zammit et al.[34] This is because of the fundamentally different nature of the chain length distributions from each mechanism of termination: disproportionation yields what is essentially an exponential distribution, but combination generates a distribution essentially of the form $i \exp(-ki)$, where *k* is a constant. Thus there must be a dependence on *i* of the ratio from the two different signals of chain length *i*, a pivotal realization that was overlooked by Zammit et al. in the excitement of their discovery. If $F_{dis}(i)$ is the fraction of chains of degree of polymerization *i* formed by disproportionation (i.e. containing one end-group from initiator) relative to the total number of chains from both disproportionation and

combination, then one may show from classical kinetics, without invoking the long-chain assumption, that [19]

$$F_{\mathrm{dis}}(i) = \frac{1}{1 + \frac{1}{2}(i - 1)C(\frac{1}{l} - 1)} = \frac{1}{1 + \frac{1}{2}(i - 1)C(\frac{1}{d})} \tag{2}$$

Of course $F_{\mathrm{dis}}(i)$ may be determined from quantitative analysis of MS spectra, although even this matter turns out to be more involved than at first suspected, in that, strictly speaking, one must sum the areas (obtained by numerical integration) of all peaks that are part of the isotopic distribution of M for a particular molecule. Happily, $F_{\mathrm{dis}}(i)$ may also be shown to be accurately obtained from the heights of the first peak of each relevant cluster.[19]

Of perhaps more surprise is the appearance in Eq. 2 of

$$C = \frac{2k_{\mathrm{t}}c_{\mathrm{R}}}{k_{\mathrm{p}}c_{\mathrm{M}}} = \frac{\left(2k_{\mathrm{t}}R_{\mathrm{init}}\right)^{0.5}}{k_{\mathrm{p}}c_{\mathrm{M}}} = \frac{\left(4fk_{\mathrm{d}}c_{\mathrm{I}}k_{\mathrm{t}}\right)^{0.5}}{k_{\mathrm{p}}c_{\mathrm{M}}} \tag{3}$$

where c_{R} is the overall concentration of polymerizing radicals, c_{M} is the monomer concentration, k_{p} is the propagation rate coefficient and R_{init} is the rate of initiation. For thermolabile initiators, as used in this work, $R_{\mathrm{init}} = 2fk_{\mathrm{d}}c_{\mathrm{I}}$, where f is initiator efficiency, k_{d} is initiator decomposition rate coefficient and c_{I} is initiator concentration, as incorporated into Eq. 3 above. In physical terms, C is the reciprocal of the better-known quantity of kinetic chain length. It can be seen that, as well as depending on i, there is also a dependence of $F_{\mathrm{dis}}(i)$ on c_{I}. In hindsight both of these predictions were evident in the results of Zammit et al.[34]

An important realization from Eqs. 2 and 3 is that the mass spectrometric method for determination of λ requires prior knowledge of the rate parameters fk_{d}, k_{p} and k_{t}. Accurate values of the first two of these are available from the literature for many systems by now, but

the third, k_t, is problematic in that it is so system-dependent. [39] Thus there is really no choice but to make a simultaneous measurement of k_t in generating polymer for the MS determination of λ. Unfortunately this was not recognized by Zammit et al.[34]

Taking cognizance all of the above, Buback et al. successfully employed the MS method to determine λ for solution polymerization of MMA at 85 °C.[19] Perhaps not surprisingly, the value of $\lambda = 0.63 \pm 0.10$ obtained is very close to the average of all literature values (see Figure 6-1), suggesting a random nature to error across the various different historical methods. While this is pleasing, the fact is that the method was employed using only one initiator, namely bis(3,5,5,-trimethylhexanoyl peroxide) (BTMHP), as shown in Scheme 2, in one solvent, benzene. Therefore it remains for the method to be tested more stringently, in order to determine its robustness – this will be done in the present chapter.

Specifically, still working with the system MMA at 85 °C, it is of interest to see how the MS method performs with different initiators and with different solvents. In the initial work,[19] it was shown that λ is independent of variation of c_I by a factor of 2, as one would expect; here we extend this to factor-of-10 variation of c_I. We also carry out a variation of MS instrumentation, having only used electrospray ionization (ESI) MS before; here we also vary the means of ionization and of detection. All these 'consistency checks' of the method are important in establishing its general fitness for use.

6.3. Mass analysis

Most MS results were obtained via electrospray ionization (ESI), using the positive ion mode within the m/z range 800–4 000 Da, together with a regularly calibrated time-of-flight (TOF) detector. Other instrument details include: capillary temperature 200 °C, N_2 flow 4 L min^{-1} and capillary voltage 4 500 V. The polymer samples were dissolved in a 1/2 v/v

CH_2Cl_2/MeOH mixture at a concentration of about 300 μg mL^{-1}. 10 μL of 0.1 mol L^{-1} sodium acetate was also added to the sample mixture. The samples were then introduced into the electrospray interface by injection via a syringe pump at 240–300 μL hr^{-1}.

At times other MS instrumentation was used, as follows. The spectra from ion-trap detection were obtained in the positive mode within the *m/z* range 150–2 000 Da and at spray voltage 4 500 V with capillary temperature 200 °C. Nitrogen was used as sheath gas and He as the bath gas. Polymer-sample solvent, concentration and injection were as with TOF detection. Matrix-assisted laser desorption/ionization (MALDI)-MS spectra were obtained in the positive mode within the *m/z* range 500–10 000 Da. The instrument was operated in the linear mode. The ions were accelerated under a potential of 20 kV. The spectra were the sum of 500 shots of nitrogen laser with a wavelength of 337 nm. The sample was prepared by mixing 20 μL of the matrix 2,4-dihydoxybenzoic acid (DHB, Aldrich) in THF at 10 mg mL^{-1} with 20 μL of poly(methyl methacrylate) in THF at 10 mg mL^{-1}. 0.4 μL of the resulting mixture was spotted on the MALDI sample plate and air-dried before being placed in the instrument.

6.4. Classical kinetics

To derive Eq. 2 one can start with the steady-state result of classical kinetics for radical concentration,

$$c_{\mathrm{R}} = \left(\frac{R_{\mathrm{init}}}{2k_{\mathrm{t}}}\right)^{0.5} \tag{4}$$

where $R_{\mathrm{init}} = 2fk_{\mathrm{d}}c_{\mathrm{I}}$ for chemically initiated polymerization. From the fundamental radical polymerization scheme, the population balance equations of dead-chain concentrations can be obtained, which are what we seek in order to understand the data yielded by ESI-MS, with the relevant results being

$$\frac{\mathrm{d}c_{\mathrm{dis}}(i)}{\mathrm{d}t} = 2\ k_{\mathrm{t,dis}} c_{\mathrm{R}_i} c_{\mathrm{R}} = 2\lambda k_{\mathrm{t}} c_{\mathrm{R}_0} \alpha^i c_{\mathrm{R}} = \lambda R_{\mathrm{init}} \mathrm{C} \alpha^i \qquad (5)$$

$$\frac{\mathrm{d}c_{\mathrm{comb}}(i)}{\mathrm{dt}} = \sum_{j=1}^{i-1} k_{\mathrm{t,comb}} c_{\mathrm{R}_j} c_{\mathrm{R}_{i-j}} = (i-1)(1-\lambda) k_{\mathrm{t}} \alpha^i \left(c_{R_0}\right)^2$$

$$= \frac{1}{2}(i-1)(1-\lambda) R_{\mathrm{init}} \mathrm{C}^2 \alpha^i \qquad (6)$$

where *C*, the reciprocal of kinetic chain length, is

$$C = \frac{2k_{\mathrm{t}} c_{\mathrm{R}}}{k_{\mathrm{p}} c_{\mathrm{M}}} = \frac{(2k_{\mathrm{t}} R_{\mathrm{i}})^{0.5}}{k_{\mathrm{p}} c_{\mathrm{M}}} \qquad (7)$$

In the above equations the following expression for $c_{\mathrm{R}i}$ has been used:

$$c_{\mathrm{R}_i} = c_{\mathrm{R}_{i-1}} \alpha\ =\ c_{R_0} \alpha^i \qquad (8)$$

where α is the probability of propagation

$$\alpha = \frac{1}{1 + \frac{2k_{\mathrm{t}} c_{\mathrm{R}}}{k_{\mathrm{p}} c_{\mathrm{M}}}} \qquad (9)$$

and c_{R_0} is the concentration of primary radicals:

$$c_{\mathrm{R}_0} = \frac{R_{\mathrm{init}}}{k_{\mathrm{p}} c_{\mathrm{M}}} \qquad (10)$$

In steady state one has that d$c_{\mathrm{dis}}(i)$/dt and d$c_{\mathrm{comb}}(i)$/dt are constant, and thus the value of $c_{\mathrm{dis}}(i)$ and $c_{\mathrm{comb}}(i)$ at any given time are related to Eq. 5 and 6, respectively, by the same proportionality constant. Similarly, for any given volume of polymer solution, $n_{\mathrm{dis}}(i)$ and $n_{\mathrm{comb}}(i)$, the number of chains from disproportion and combination, respectively, are related to $c_{\mathrm{dis}}(i)$ and $c_{\mathrm{comb}}(i)$ by the same constant of proportionality. Therefore, one can use Eq. 5 and

6 to express ratios of $n_{dis}(i)$ and $n_{comb}(i)$ (Eq. 11), which is the ratio that can be obtained from ESI-MS signal intensities:

$$\frac{\frac{1}{2}n_{\mathrm{dis}}(i)}{n_{\mathrm{comb}}(i)} = \frac{1}{(i-1)\mathrm{C}\left(\frac{1}{\lambda}-1\right)} = \frac{\delta}{(i-1)\mathrm{C}} \qquad (11)$$

It is preferred to use the fraction of chain of length *i* formed by disproportionation, $F_{dis}(i)$, which is

$$F_{\mathrm{dis}}(i) = \frac{n_{\mathrm{dis}}(i)}{n_{\mathrm{dis}}(i) + n_{\mathrm{comb}}(i)} \qquad (12)$$

From Eqs. 5, 6 and 12 one obtains that

$$F_{\mathrm{dis}}(i) = \frac{1}{1+\frac{1}{2}(i-1)\mathrm{C}(\frac{1}{\lambda}-1)} = \frac{1}{1+\frac{1}{2}(i-1)\mathrm{C}(\frac{1}{\delta})} \qquad (2)$$

where $F_{dis}(i)$ accurately can be obtained from the heights of the first peak of each relevant cluster of MS data,[19], i.e., $F_{dis}(i)$ can be obtained from

$$F_{\mathrm{dis}}(i) = \frac{2h_{\mathrm{dis}}(i)}{2h_{\mathrm{dis}}(i) + h_{\mathrm{comb}}(i)} \qquad (13)$$

where *h* denotes the height of the first peak in a cluster.

6.5. Results and Discussion

6.5.1. k_t Determination

Typical results for fractional conversion, *x*, obtained gravimetrically, as a function of time, *t*, are presented in Figure 6-2. Such data were analyzed in the recommended way,[40] using:

$$\frac{-\mathrm{d}[\ln(1-x)]}{\mathrm{d}t} = k_\mathrm{p}\left(\frac{fk_\mathrm{d}c_\mathrm{I}}{k_\mathrm{t}}\right)^{0.5} \tag{14}$$

From the slope of a plot of the nature of Figure 6-2, knowledge of k_p, f and k_d is required in order to obtain k_t, average termination rate coefficient (denoted also as $<k_\mathrm{t}>$). The following best-quality literature values were utilized: k_p = 1 465 L mol^{-1} s^{-1} for MMA at 85 °C,[41] and

$$k_\mathrm{d}(\mathrm{AIBN}) = 2.89\times10^{15}\exp\left(\frac{-130.23\,\mathrm{kJ\,mol^{-1}}}{RT}\right),\ f = 0.80 \tag{15a}$$

$$k_\mathrm{d}(\mathrm{BTMHP}) = 2.84\times10^{15}\exp\left(\frac{-128.34\,\mathrm{kJ\,mol^{-1}}}{RT}\right),\ f = 0.53 \tag{15b}$$

$$k_\mathrm{d}(\mathrm{TMPPP}) = 3.51\times10^{13}\exp\left(\frac{-112.16\,\mathrm{kJ\,mol^{-1}}}{RT}\right),\ f = 0.50 \tag{15c}$$

$$k_\mathrm{d}(\mathrm{DDP}) = 3.64\times10^{15}\exp\left(\frac{-130.48\,\mathrm{kJ\,mol^{-1}}}{RT}\right),\ f = 0.58 \tag{15d}$$

The above Arrhenius expressions are from AkzoNobel product data [42] while the f values are taken from: AIBN,[43] BTMHP,[19] TMPPP [44] and DDP.[45] While the given value for k_p was determined in bulk, all the solvents in this work are very similar in size and (as will be seen) viscosity to MMA; therefore, the bulk value should hold extremely well in such solution conditions.[46]

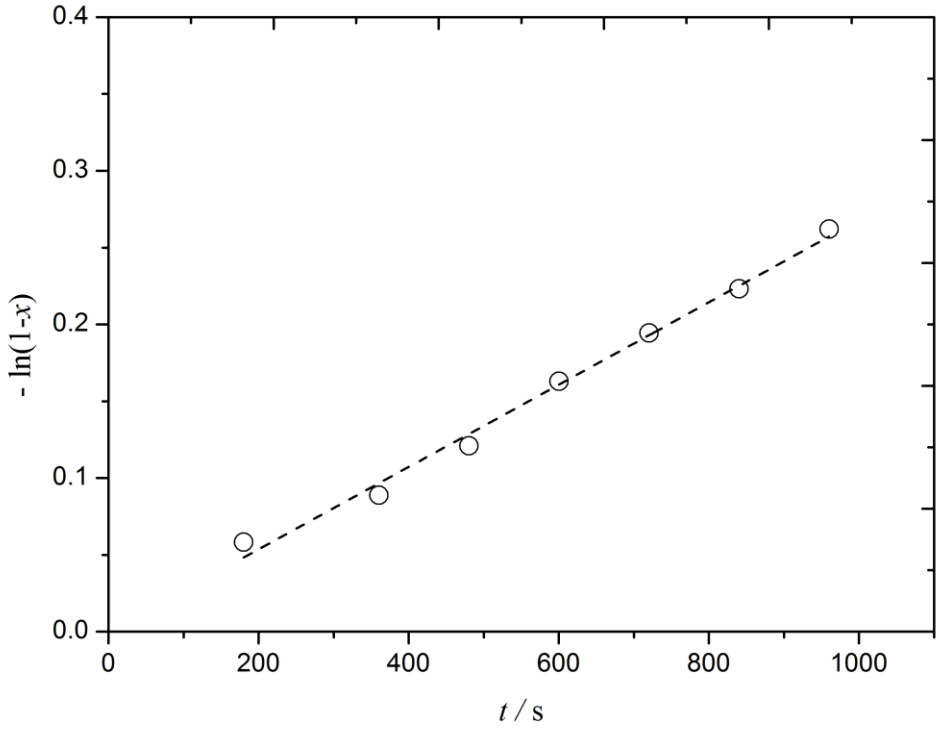

Figure 6-2. Results from radical polymerization of methyl methacrylate in TFT at 85 °C with c_{AIBN} = 0.055 mol L^{-1} and c_{MMA} = 0.67 mol L^{-1}, where x is fractional conversion and t is time. Points: experimental results; line: best fit for determination of k_t (see text).

Table 6-1. Average termination rate coefficient, k_t, in L mol^{-1} s^{-1} for polymerization of methyl methacrylate at 85 °C with bis(3,5,5-trimethylhexanoyl)peroxide (BTMHP), 2,2'-azobisisobutyronitrile (AIBN), 1,1,2,2-tetramethylpropyl peroxypivalate (TMPPP) and di-*n*-decanoyl peroxide (DDP) as initiator, concentration as indicated, in benzene, methyl isobutyrate (MIB) and trifluorotoluene (TFT) as solvent, where c_{MMA} = 0.67 mol L^{-1} in all cases. Pure solvent viscosity, η, at 20 °C is also given.

	η	**BTMHP**	**AIBN**	**TMPPP**	**DDP**
	(cp)	0.016 mol L^{-1}	0.055 mol L^{-1}	0.020 mol L^{-1}	0.038 mol L^{-1}
Benzene	0.65	1.41×10^8 [a]	3.20×10^8		
		3.46×10^8	3.20×10^8		
MIB	0.58	3.43×10^8	4.33×10^8		
			4.30×10^8 [b]		
TFT	0.57	4.14×10^8	3.85×10^8	5.60×10^8	3.66×10^8
		4.44×10^8		3.34×10^8 [c]	

[a] Value from previous work;[19] [b] c_I = 0.0055 mol L^{-1}; [c] c_I = 0.008 mol L^{-1}.

Table 6-1 presents all values of k_t obtained as part of this work. The values are high because of the high temperature and the high rates of initiation. The small variation in k_t values is likely due to error of nature either random or systematic [40] (e.g. values of rate coefficients used in data analysis) than it is to any mechanistic cause. There should be no dependence of k_t on initiating end-group per se, as it would have at most an extremely small impact on chain diffusion. Since we chose c_I values so as to give approximately equal R_{init} for the different initiators, any variation in k_t on this account due to chain-length-dependent termination should be very small.[47] Similarly, it is evident from the literature values [48] given in Table 6-1 that (solvent) viscosity, η, is much the same from system to system, so there should not be significant variation of k_t in this regard. In fact, it is noticeable that the solvent with the highest η, benzene, does indeed seem to give marginally lower k_t values, which is as one would expect.[47]

6.5.2. λ Determination

Representative MS results are shown in Figure 6-3. The chemical origin of the peaks in this spectrum will be discussed in due course. For now it is sufficient to note that there is a clear distinction of the species generated by disproportionation and combination.

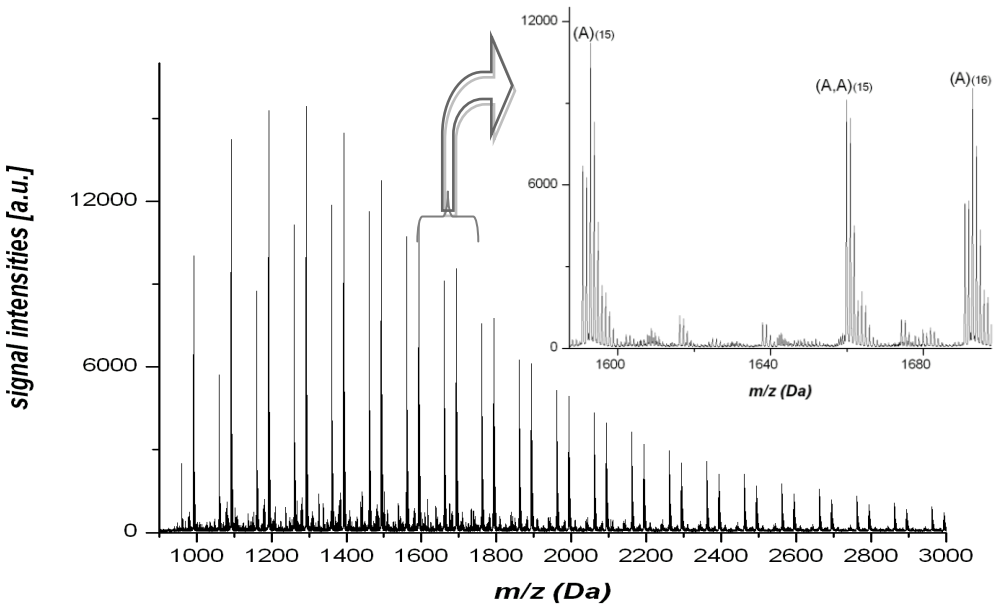

Figure 6-3. ESI-MS spectrum of poly(methyl methacrylate) obtained from radical polymerization in MIB at 85 °C with c_{AIBN} = 0.055 mol L^{-1}. The close-up shows a portion of the MS spectrum that is typical for one repeat unit, with A and A,A denoting signals from disproportionation- and combination-generated species, respectively, the degree of polymerization being as indicated, and A being the primary radical from AIBN (see Scheme 1).

Thus the $F_{dis}(i)$, the number fraction of chains of degree of polymerization i arising from disproportionation, could be determined from quantitative analysis of the peaks, as detailed in the prior work.[19] Eq. 2 was then fitted to these results, with λ being the only fitting variable, because of C being known from k_t determination. Typical fitting results are presented in Figure 6-4. It is evident that Eq. 2 describes the data adequately and that λ is obtained to high precision by historical standards.

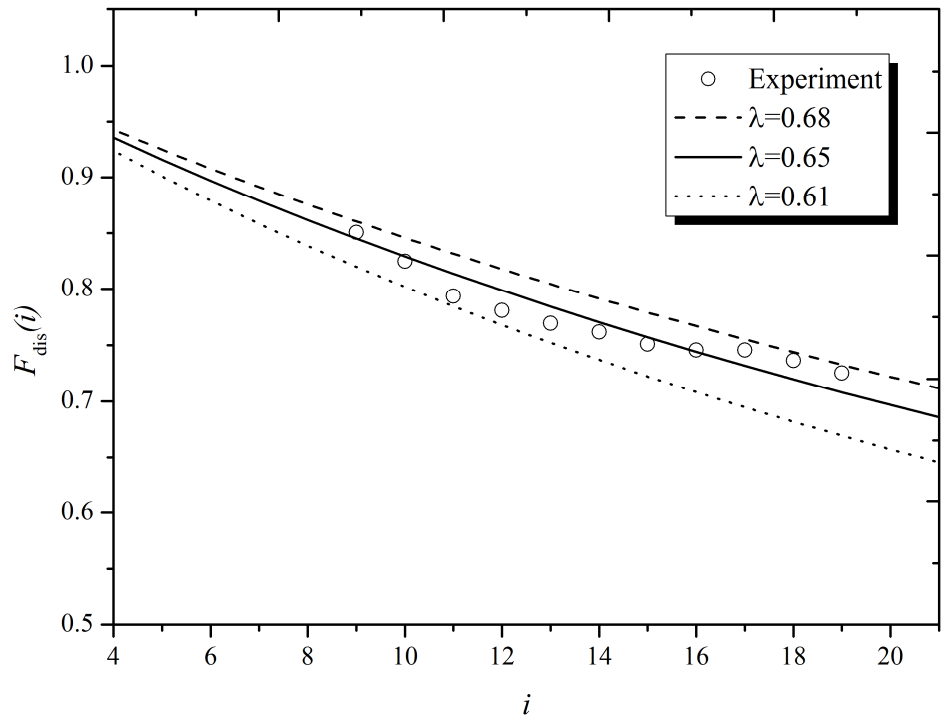

Figure 6-4. Number fraction of chains arising from disproportionation, $F_{dis}(i)$, as a function of chain length i, for PMMA from radical polymerization at 85 °C in TFT with c_{BTMHP} = 0.016 mol L^{-1} and c_{MMA} = 0.67 mol L^{-1}. Points: experimental values obtained from ESI-MS results; curves: evaluations of Eq. 2 with λ as indicated.

It is noteworthy and to bear in mind that there are still some experimental difficulties that need to be considered in the measurement of termination mode. Again, beside the precise determination of k_t, additional chain stopping processes have to be considered when interpreting chain-end data, such as chain transfer and primary radical termination. They complicate the MS spectra analysis and could increase the uncertainty in existing termination mode measurements. Zammit et al. [31] have shown that, for instance, at high initiator concentration there is a significant contribution from primary radical termination as a chain stopping mechanism. Thus if termination occurred by combination with primary radicals this could lead to an overestimation of combination. Transfer also could occur by hydrogen abstraction or addition; consequently, it will lead to an identical species to an oligomer

produced by termination via disproportionation. Thirdly, optimum MS conditions have to be found. Finally, ionization ability of the chains is of importance: preferably the mass bias over polymer chain length should be small, although the method of comparing only signals of identical degree of polymerization should minimize this as a source of error.

In the previous work,[19] a number of consistency checks were designed to guard against our MS method yielding artefactual results for λ as a result of mass- and/or end-group related bias in the MS ionization process. These checks were once again carried out for selected data sets, and no evidence of systematic error was discernible. This is as expected, because a neat aspect of the MS method is that it quantitatively compares data of the same *i* only, thereby meaning that any systematic biases in ionization tendency should (largely) cancel out.[19, 34] Table 6-2 gives all values of λ obtained in the present work. They are as found previously,[19] and will now be discussed.

Table 6-2. As for Table 6-1, but giving fraction of termination by disproportionation, λ.

	η	**BTMHP**	**AIBN**	**TMPPP**	**DDP**
	(cp)	0.016 mol L^{-1}	0.055 mol L^{-1}	0.020 mol L^{-1}	0.038 mol L^{-1}
Benzene	0.65	0.63 ± 0.10 [a)]	0.58 ± 0.10		
		0.66 ± 0.10	0.61 ± 0.10		
MIB	0.58	0.63 ± 0.10	0.59 ± 0.10		
			0.53 ± 0.10 [b)]		
TFT	0.57	0.65 ± 0.10	0.63 ± 0.10	0.59 ± 0.10	0.70 ± 0.15
		0.68 ± 0.10		0.53 ± 0.15 [c)]	

[a)] Value from previous work;[19] [b)] c_I = 0.0055 mol L^{-1}; [c)] c_I = 0.008 mol L^{-1}.

6.5.3. Effect of initiator

Scheme 2 shows the primary-radical-generating reactions for the four initiators used in this work. In each case only one type of primary radical is yielded, leading to the expectation of

MS spectra consisting of only two series of peaks, viz. a series from each of the products shown in Scheme 1, there being only one type of A end-group. It is already evident from Figure 6-3 that this expectation is met with AIBN. In the previous work [19] this was verified for BTMHP. Echoing earlier studies,[49, 50] Figure 6-5 confirms this for TMPPP and DDP also. The simplicity of these spectra obviously recommends the use of such an initiator, i.e. one producing just a single type of primary radical, for studies aimed at determining λ.

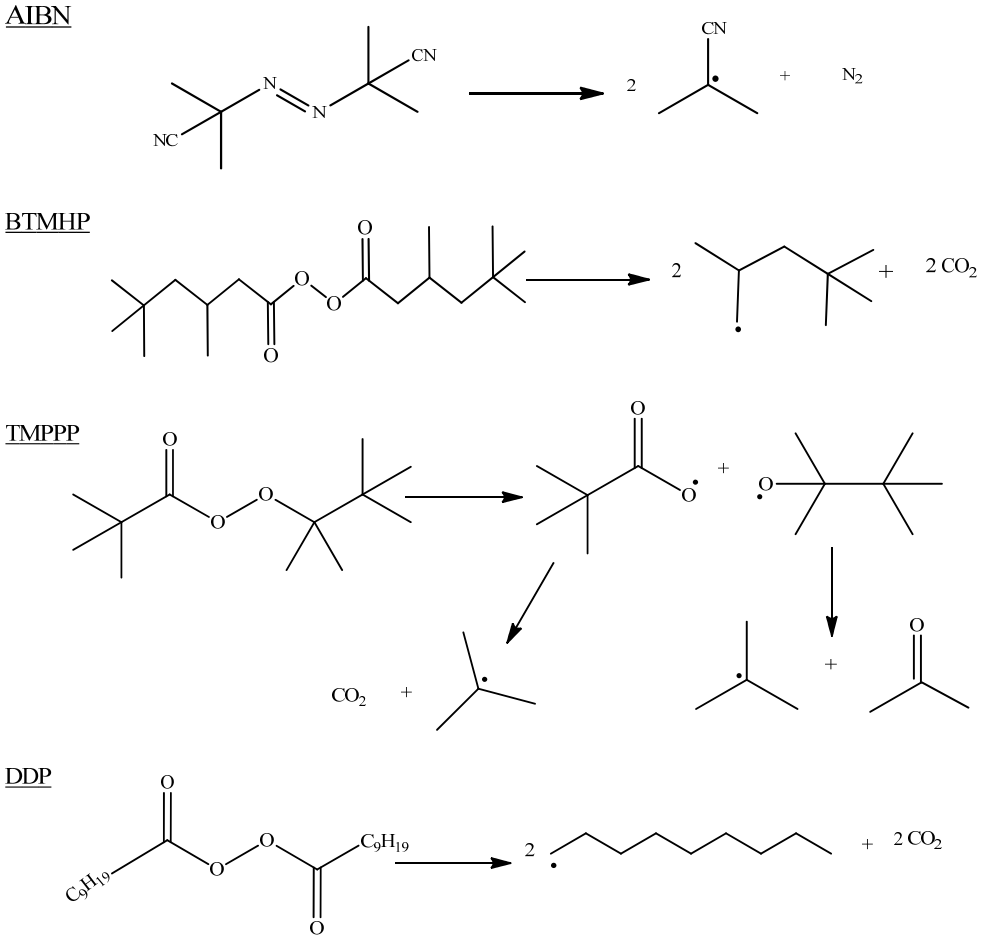

Scheme 2. Primary-radical-generating reactions for the four initiators used in this work: 2,2'-azobisisobutyronitrile (AIBN), bis(3,5,5-trimethylhexanoyl)peroxide (BTMHP), 1,1,2,2-tetramethylpropyl peroxypivalate (TMPPP) and di-*n*-decanoyl peroxide (DDP), as indicated.

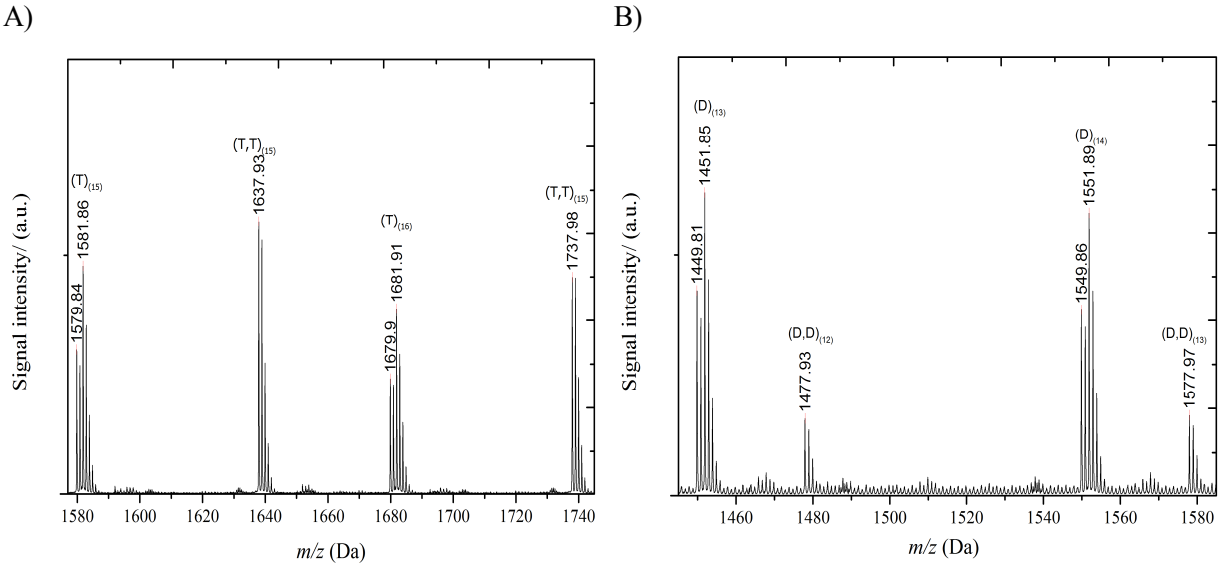

Figure 6-5. A) Portion of the ESI-MS spectrum of poly(methyl methacrylate) obtained from radical polymerization in TFT at 85 °C with c_{TMPPP} = 0.020 mol L^{-1}, where T and T,T denote signals from disproportionation- and combination-generated species respectively, the degree of polymerization being as indicated, and T being the primary radical from TMPPP (see Scheme 2). B) Portion of the ESI-MS spectrum of poly(methyl methacrylate) obtained from radical polymerization in TFT at 85 °C with c_{DDP} = 0.038 mol L^{-1}, where D and D,D denote signals from disproportionation- and combination-generated species respectively, the degree of polymerization being as indicated, and D being the primary radical from DDP (see Scheme 2).

A conclusion one may draw from Scheme 1 is that the value of λ should be independent of initiator type. This is because radical functionality is remote from the end-group A, which therefore should exert no influence on whether termination takes place via combination or disproportionation. Table 6-2 makes clear that this expectation was borne out in this work: all values of λ are the same within experimental error, even though 4 initiators of quite different chemical nature – one azo (AIBN), two diacyl peroxides (BTMHP and DDP) and one alkyl peroxypivalate (TMPPP) – were employed. This constitutes a very stern consistency check of the MS method for λ determination, and therefore strongly recommends it as a means for measuring this parameter value.

6.5.4. The importance of correct parameter values

It was just expounded that λ should be independent of initiator. In first carrying out the present work, we used the following Arrhenius expression for AIBN rather than that of Eq.15a:

$$fk_{\mathrm{d}}(\mathrm{AIBN}) = 1.017\times10^{14}\exp\left(\frac{-123.5\,\mathrm{kJ\,mol^{-1}}}{RT}\right) \tag{16}$$

Our reason for using Eq. 16 [51, 52] was that it stems from direct measurements of fk_{d},[53] as opposed to separate measurements of each of f and k_{d}, most likely under different conditions.

Employing Eq. 16, we found that MS data for determination of λ were well described, as shown in Figure 6-6. Confoundingly, however, the obtained λ value – see Figure 6-6 – is quite different from the values of Table 6-2 and our previous work.[19]

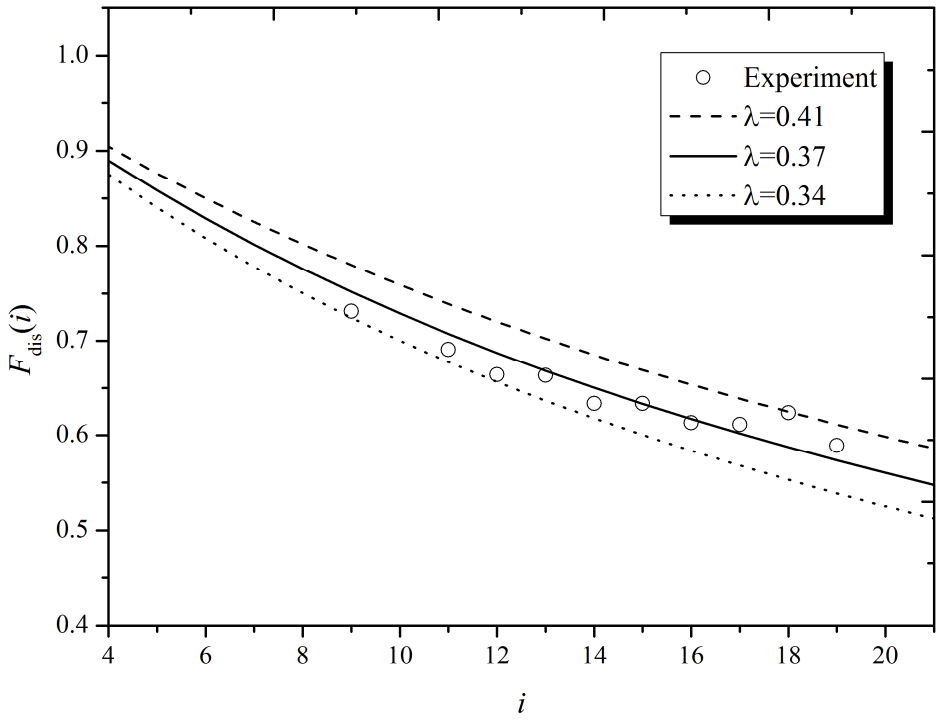

Figure 6-6. Number fraction of chains arising from disproportionation, $F_{\mathrm{dis}}(i)$, as a function of chain length i, for PMMA arising from radical polymerization at 85 °C in benzene with c_{AIBN} = 0.055 mol L^{-1} and c_{MMA} = 0.67 mol L^{-1}. Points: experimental values obtained from ESI-MS results; curves: evaluations of Eq. 2 with λ as indicated. Note that all analyses here were with Eq. 16 rather than Eq. 15a.

This finding, for which there is no plausible explanation, was resistant to all manner of changes – solvent, initiator concentration, MS instrumentation – as long as AIBN was employed. Furthermore, we could reproduce the previous value of λ, obtained using BTMHP, in the present work when we changed to this initiator.

Eventually we wondered whether Eq. 16 might be the problem. These values of fk_d were determined for AIBN in bulk styrene. Since both f and k_d are known to depend on solvent,[54, 55] we decided to switch to using Eq. 15a, since these values were determined for "a dilute solution of the initiator in monochlorobenzene",[42] conditions more akin to those of the present work. Furthermore, it was felt that the AkzoNobel determinations, since they are recommended for high-volume commercial use of initiators, are more likely to be accurate over an extended temperature range.

It is evident from Table 6-2 that use of Eq. 15a results in λ values for AIBN that are fully consistent with those for all other systems. This was further explored by treating fk_d as a variable in data analysis, viz. k_t and then λ determination. The results are shown in Figure 6-7. It is evident that the value of λ that is obtained is quite sensitive to the value of fk_d. This finding was unexpected and emphasizes that the method is quite dependent on employment of accurate parameter values. Indeed, it seems remarkable that even though so many different parameter values are involved in this work – viz. f and k_d for 4 different initiators, and k_t for each individual system – a highly uniform set of λ values (see Table 6-2) is still obtained.

A) B)

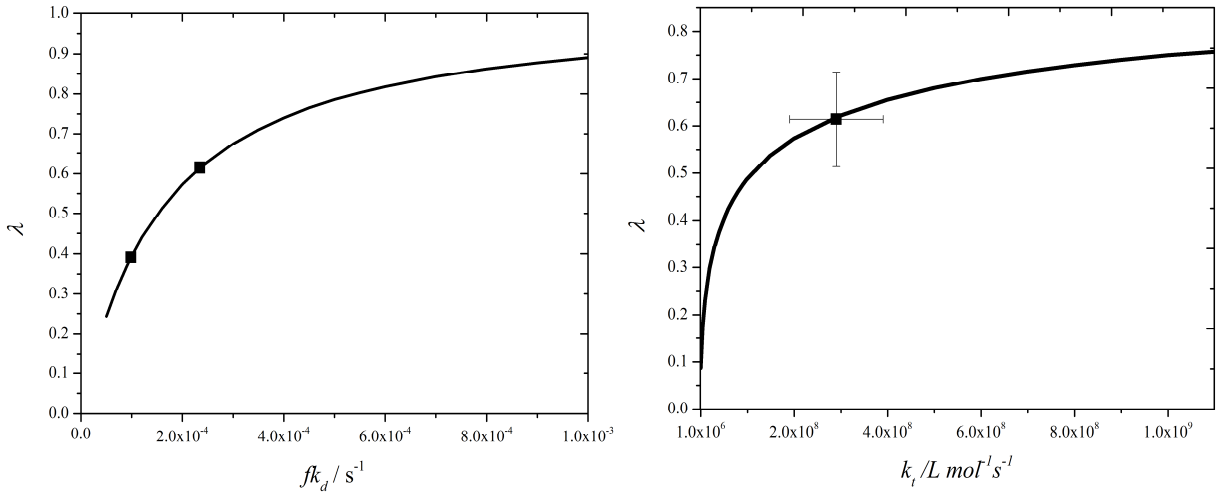

Figure 6-7. A) Influence on λ of the assumed value of fk_d for the data of Figure 6-6, i.e., PMMA arising from radical polymerization at 85 °C in benzene with c_{AIBN} = 0.055 mol L^{-1} and c_{MMA} = 0.67 mol L^{-1}. The upper and lower points are the values obtained using Eqs. (15a) and (16) respectively (see text). B) Influence on λ of the assumed value of k_t for the same data using Eq. (15a) for k_d and f = 0.8; the point represents the experimental k_t.

In view of all this, the exercise portrayed in Figure 6-7A was repeated but with k_t varied; results are presented in Figure 6-7B. Again it was found that the λ obtained from $F_{dis}(i)$ is sensitive to the value of k_t, indeed the resulting graph has the same shape as Figure 6-7A, because these variables are present as a factor fk_dk_t in Eq. 3. To give a feeling for quantitative effect, decreasing k_t from 3×10^8 L mol^{-1} s^{-1} to 1×10^8 L mol^{-1} s^{-1} resulted in λ decreasing to about 0.5, while doubling it to 6×10^8 L mol^{-1} s^{-1} raised λ to about 0.7. This reinforces the desirability of having at hand an accurate value of k_t that is precise for the system under investigation, as opposed to assuming a value from another system.

Notwithstanding the above, the following is noted. All the k_t values of Table 6-1 are in the just-quoted range of $(1 - 6) \times 10^8$ L mol^{-1} s^{-1}. In fact all, apart from two, fall within $(3.2 - 4.5) \times 10^8$ L mol^{-1} s^{-1}. Thus the sole value below this range, 1.41×10^8 L mol^{-1} s^{-1}, which in fact is from the previous work, [19] may be an outlier. Nevertheless it has just been seen that

even this value only results in a 20% uncertainty in λ, namely from 0.6 down to 0.5. This illustrates that serious error in λ only arises where the uncertainty in fk_d or k_t approaches an order of magnitude.

6.5.5. Effect of initiator concentration

An idea that regularly resurfaces in RP kinetics is that so-called primary-radical termination may be important, i.e. that a significant fraction of the overall termination rate involves a primary radical, e.g. cyanoisopropyl in the case of AIBN and nonyl for DDP (see Scheme 2). Such species will not be distinguishable in MS terms from those of regular termination, because both types of interaction still result in polymer with either one or two initiator-derived end-groups. Nevertheless this effect is relevant in the present context in that termination between a primary radical and a monomer-centred radical cannot be expected to have the same λ value as termination between two monomer-centred radicals (as shown in Scheme 1), because the environment around the radical site may be quite different for each type of radical, most relevantly in regard to steric hindrance. If primary-radical termination is significant, one may therefore observe a different value of λ.

To probe this idea, experiments were carried out in which c_I was varied. Specifically, c_{AIBN} was decreased by a factor of 10 and c_{TMPPP} by a factor of 2.5. If primary radical termination is significant at the higher c_I, then a different overall (or effective) value of λ should be observed at lower c_I, because the relative concentration of primary radicals will be lower. It is evident from the results of Table 6-2 that no such effect is observed within experimental error.

Again, this is an important validation of the MS method for determination of λ, because primary radical termination is an effect that potentially undermines it, in that the point of the method is to obtain λ for macroradicals, as opposed to a value that includes also a (differing) component from primary radicals. We could not discern any evidence of such an undesired effect taking place. Note that this is not to say that no primary-radical termination occurs. Rather, it is just to say that such as does occur does not have a tangible influence on the value of λ obtained, which therefore must be that for macroradicals.

6.5.6. Effect of solvent

Studying the termination of small-molecule radicals, Fischer showed that solvent viscosity affects the disproportionation-to-combination ratio of tertiary radicals.[56] Specifically, as viscosity increases, the fraction of disproportionation products increases. The explanation for this effect is that the occurrence of combination is reliant on the coincidence upon collision of the principal (parallel) axes of the two radicals, so that a C-C bond may form, whereas disproportionation is not so reliant on there being a particular orientation of the two radicals. As viscosity increases, the ability of two radicals to reorient upon collision in order to find an alignment conducive to combination is hindered, and thus the occurrence of disproportionation is promoted. Given that MMA generates tertiary radicals (see Scheme 1), one would expect this effect to be present in such polymerizing systems, i.e. λ should increase as a solution becomes more viscous. However Fischer's results show that it requires appreciable changes in η for such an effect to be observed.[56]

While in the future it would be interesting to test for the presence of such an effect, in the present work we chose conditions such that it would be absent. Specifically, we employed solvents of very similar viscosity, ones very close to that of the pure monomer, which is 0.57

cp at 20 °C.[57] This assures that the perturbing influence of monomer on overall solvent viscosity is absolutely minimal, meaning that the viscosity of these dilute solutions of monomer was essentially that of pure solvent.

Referring to Table 6-2, it is evident that for 2 different initiators, λ was found to be the same for all three solvents of this work, exactly as one would expect on the basis of Fischer's findings.[56] This establishes that there is no effect of solvent per se on λ. Furthermore, it constitutes yet another pleasing demonstration of the rigor of the MS method.

Furthermore, again the attraction of using methyl isobutyrate (MIB) as solvent is that it is the saturated analogue of the monomer, MMA. Hence it should result in solution properties nearly identical to those of neat monomer; this is why we employed it as solvent. On the other hand, MIB contains a H that is bonded to a tertiary C, and thus this H is relatively labile in terms of chain transfer. Referring to Table 6-2, it is evident that the use of MIB had no effect on the obtained value of λ, even though (in hindsight) it is known that chain transfer to solvent was occurring. This is heartening, as the occurrence of such a reaction may be regarded as potentially undermining the MS method for λ determination. Evidently it does not, or at least it does not when it occurs at the levels of our experiments. Nevertheless one would advise to use a solvent that is not susceptible to chain transfer, for example TFT (or benzene, notwithstanding that it comes with other difficulties). This would result in dead chains of so-called 'naked' or 'pure' polymer, i.e., PMMA with MMA groups at each end (one of which arises from MIB, of course).

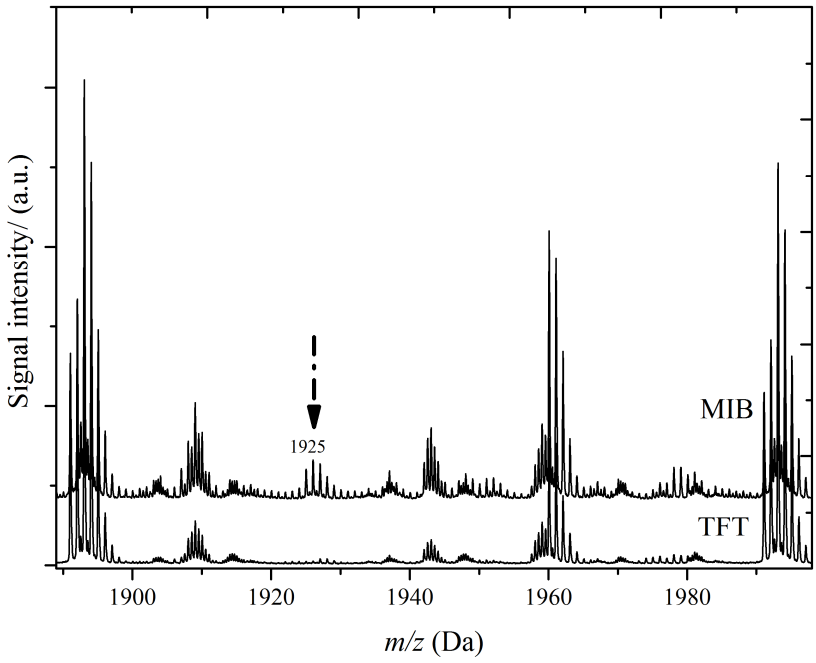

Figure 6-8. Portions of the ESI-MS spectra of poly (methyl methacrylate) obtained from radical polymerization in methyl isobutyrate (MIB; upper spectrum) and trifluorotoluene (TFT; lower). The arrow indicates pure polymer of chain length 19 (together with Na from the ESI process). This species is not observed with TFT and results from chain transfer to MIB.

One of the beauties of MS is that takes such speculations beyond the realm of cheap talk and actually enables them to be scrutinized.[38] Referring to Figure 6-8, one sees that the use of MIB as solvent results in the appearance of a new set of signals at exactly the molar mass of pure polymer: although relatively small in intensity, these signals are undeniably present, whereas when TFT (Figure 6-8) or benzene are used, there are no such signals, (presumably) because these molecules do not contain a labile H. This constitutes direct evidence for the occurrence of chain transfer to MIB. As far as we are aware, this is the first direct demonstration of the occurrence of such a chain-transfer-to-solvent reaction. Despite being the subject of much hypothesizing, it is remarkable how little is known with certainty about chain-transfer-to-small-molecule reactions.[58] Determination of the transfer constant to MIB

is discussed earlier in Chapter 3. Although the abundance of naked polymer is relatively small in our systems (see Figure 6-8), it should be remembered that we used conditions designed to make small polymer molecules. Where polymer of more normal length is generated, chain transfer to MIB would occur to a greater extent.

6.5.7. Accuracy of mass spectrometry

Figure 6-9 presents a comparison of experimental and theoretical MS results. Shown is the peak cluster for a species from combination and disproportionation. The simulation is the output from the program *mMass* (version 3.1.0).[59] Input for this program is the chemical formula of a polymer product, from which *m*/*z* values and isotopic patterns are generated.

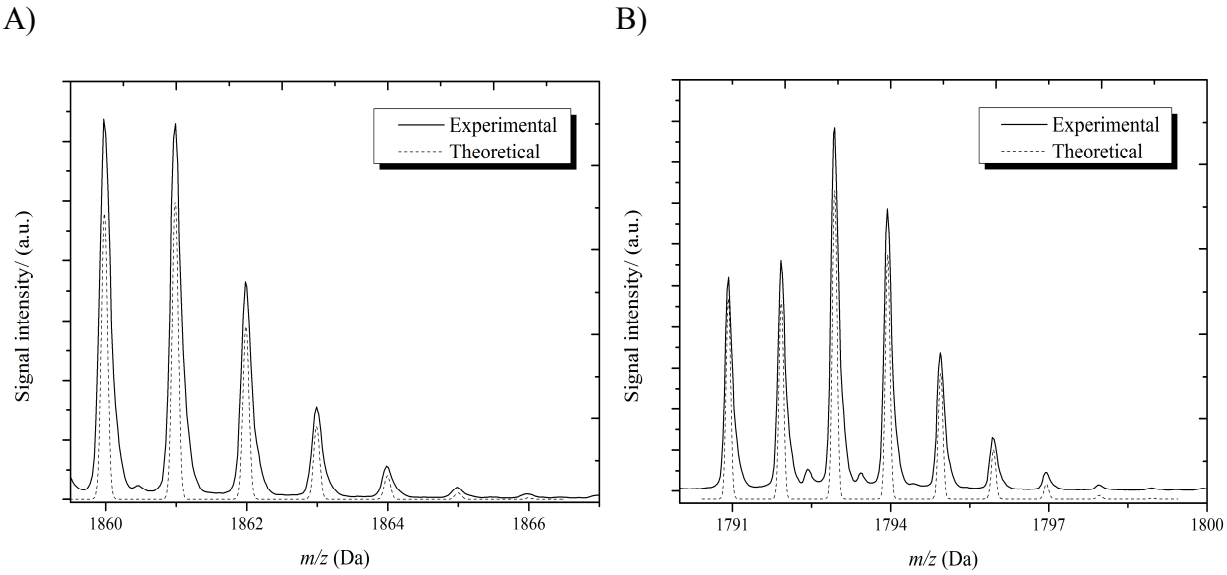

Figure 6-9. Close-up of the ESI-MS spectrum of poly(methyl methacrylate) obtained from radical polymerization in TFT at 85 °C with c_{AIBN} = 0.055 mol L^{-1}. Shown in (A) is the cluster from combination product of chain length 17. Shown in (B) is the cluster from disproportionation product of chain length 17. Unbroken line (upper spectrum): experiment; broken line (lower spectrum): simulation.

The comparison between theory and simulation in Figure 6-9 is excellent. Findings of identical quality were obtained for signals arising from both combination (Figure 6-9A) and disproportionation (Figure 6-9B). Firstly this shows the phenomenal accuracy with which MS

can determine molar mass. For example, the first peak of the cluster presented in Figure 6-9A is experimentally observed at 1859.97 Da while the theoretical value is 1859.98 Da. This gives complete confidence in the identification of species corresponding to observed signals. Secondly, the figure shows how well the relative signal intensities of the isotope distribution of a species are observed experimentally. This imparts confidence in the quantitative use of signal intensities for λ determination.

6.5.8. Choice of detector

Figure 6-10 shows MS results from using ion-trap rather than time-of-flight detection. Comparing Figure 6-10 with any of our results from using TOF detection (e.g. Figures 6-3, 5 and 8), it is evident that resolution is poorer with ion-trap detection. This recommends using TOF detection where possible.

In fact without controversy one may generalize this recommendation: data evaluation will improve the higher the resolving power of the detector. For example, an Orbitrap will likely outperform a TOF detector, and in turn an FTICR (Fourier transform ion cyclotron resonance) will be superior to an Orbitrap.[36] Furthermore, TOF in reflectron mode will give better results than in linear mode.

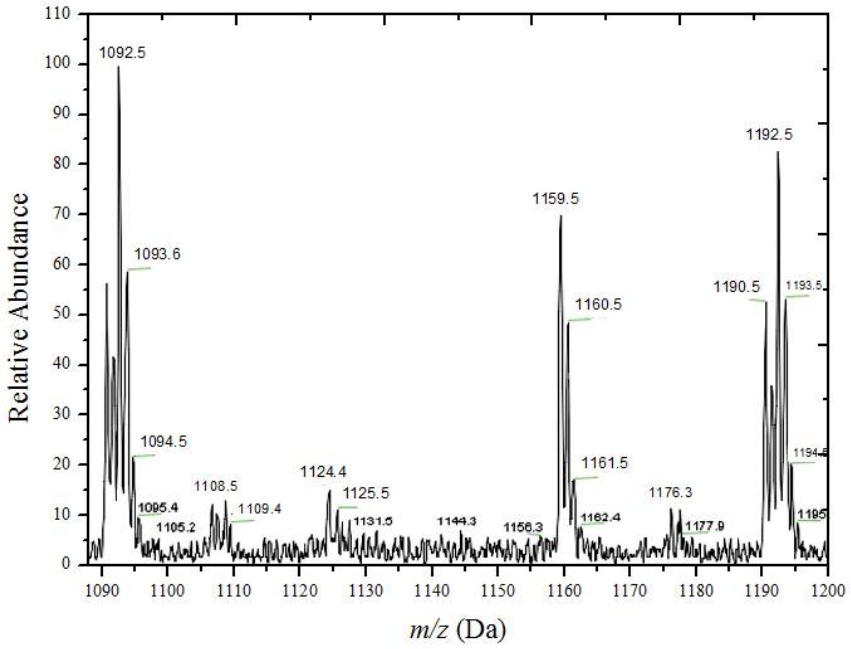

Figure 6-10. Portion of the ESI-MS spectrum of poly(methyl methacrylate) obtained from radical polymerization in MIB at 85 °C with c_{AIBN} = 0.055 mol L^{-1}, as obtained using an ion-trap detector.

6.5.9. Choice of ionization method

All results to this point were obtained using ESI. It was decided also to try MALDI. A resulting spectrum is presented in Figure 6-11. It is immediately evident that compared with preceding spectra of this work the peaks of Figure 6-11 are far broader; in fact, they are so broad that all the signals of a cluster are merged into the one combined signal. Admittedly this is not due to the ionization method per se, but rather is a consequence of an old TOF detector, which emphasizes that instrument age can also be a significant factor in data quality. However, the reality is that MALDI is a far less friendly technique to use than ESI: signal-to-noise is inferior, reproducibility is often a problem, and above all it is largely a matter of trial-and-error to find a matrix type and ratio that work for each particular polymer.

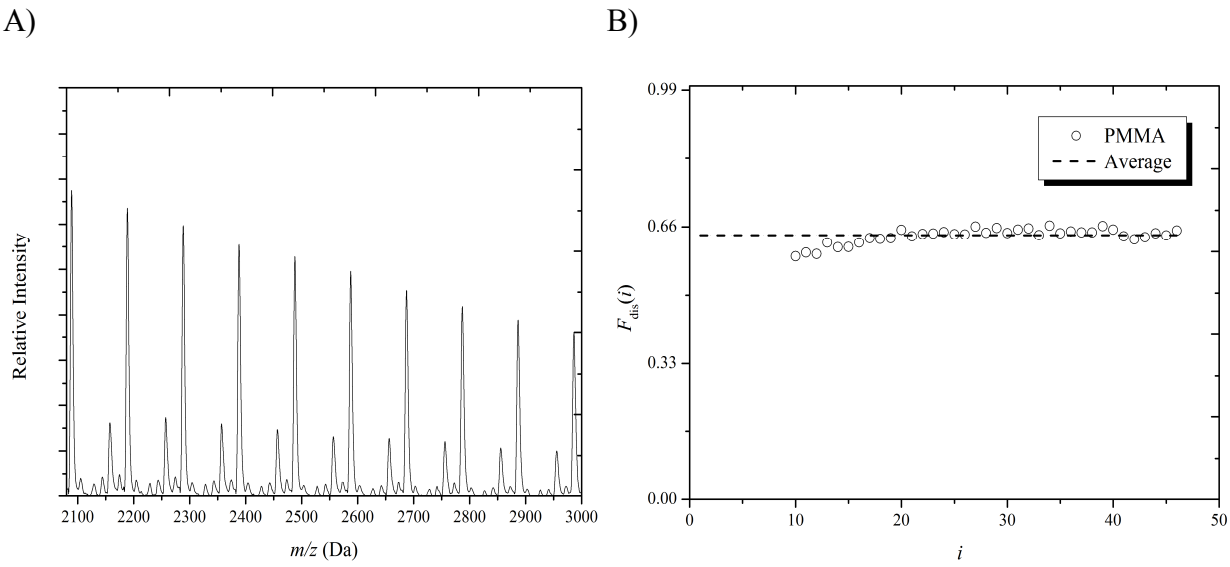

Figure 6-11. A) MALDI-TOF-MS spectrum of poly(methyl methacrylate) obtained from radical polymerization in TFT at 85 °C with c_{AIBN} = 0.05 mol L^{-1}. B) Number fraction of chains arising from disproportionation, $F_{dis}(i)$, as a function of chain length i, from the MALDI-TOF-MS results of A). Points: experimental values; line: average of all the points.

Furthermore, Figure 6-11 shows that the quantitative output for λ determination from our MALDI results is inadequate. Presented are the $F_{dis}(i)$ values resulting from the spectrum of Figure 6-11A. In principle it could be an advantage that for each chemical species there is just one broad signal, because then one only needs to determine the area of this one peak to obtain the relative abundance of a species, as opposed to when all the isotopologues are resolved, as with the ESI output of this work. In addition to this, MALDI has the well-known advantage of giving results to much higher values of M, as indeed is evident from Figures 6-11. Thus it offers a larger set of $F_{dis}(i)$ values with which to work. However, when Figure 6-11 is compared with Figures 6-3 and 6-6, it is evident that the MALDI results do not give $F_{dis}(i)$ values that decline with increasing i, as theory says must be the case (see data fits of Figures 6-4 and 6-6). Instead, Figure 6-11B displays $F_{dis}(i)$ that are essentially constant. Admittedly the resulting average value is quantitatively accurate (again, compare with Figures 6-4 and 6-6) and is very close in value to λ for this system. However one should

remember that $F_{dis}(i) \neq \lambda$, and that Eq. 2 cannot qualitatively fit the data of Figure 6-11, as already explained.

For all these reasons we recommend the employment of ESI rather than MALDI as ionization method when using the MS method for λ determination. Interestingly, two other recent comparisons[60, 61] of MALDI and ESI results for analysis of polymers from RP reached the same conclusion.

6.5.10. Chain-length dependence of termination, CLDT

In addition to the requirement of accurate k_p, fk_d and k_t for accurate λ determination, as has been seen in this work, the issue of chain-length dependent termination (CLDT) is also of importance. [47] Although demonstrably practical, how rigorous is it to use a chain-length-averaged k_t, as has been done here, for a quantity that is indisputably chain-length dependent, especially at small chain lengths, as are analyzed with the MS method?[47, 52, 62-64] Therefore, this effect also was of importance to consider. To include this effect, one still uses

$$F_{\mathrm{dis}}(i) = \frac{n_{\mathrm{dis}}(i)}{n_{\mathrm{dis}}(i) + n_{\mathrm{comb}}(i)} \qquad (12)$$

but in this equation one now employs

$$n_{\mathrm{dis}}(i) = F_n C\, i^{-0.5e} \mathrm{e}^{-C` i^P} \qquad (17a)$$

$$n_{\mathrm{comb}}(i) = (1 - F_n) A^2 P\, i^{1-e} \mathrm{e}^{-A i^P} \qquad (17b)$$

where C, $C`$, P and A are as follows

$$C = \frac{\left(2R_{\mathrm{init}} k_t^{1,1}\right)^{0.5}}{k_p c_M} = \frac{\left(4 f k_d c_I k_t^{1,1}\right)^{0.5}}{k_p c_M}, \qquad C` = \frac{C}{P}, \qquad P = 1 - \frac{e}{2}, \qquad A = \frac{4C`}{4-e} \qquad (18)$$

Here $k_t^{1,1}$ and e have their using meaning as CLDT parameters, namely $k_t^{i,i} = k_t^{1,1}\, i^{-e}$, while F_n is the number fraction of chains formed by disproportionation. Eqs. 12, 17 and 18 were used to fit the experimental F_{dis} data obtained from ESI-MS, using appropriate parameter values for MMA initiated polymerization in TFT at 85 °C employing either AIBN or BTMHP as stated in the Figures captions. The resulting F_n then gives λ via Eq. 19.

$$\lambda = \frac{F_n}{2 - F_n} \qquad (19)$$

Firstly, the effect of the CLDT parameters $k_t^{1,1}$ and e on $F_{dis}(i)$ is demonstrated in Figures 6-12 and 6-13. Two opposite and important trends are evident: (1) For i greater than approximately 7, $F_{dis}(i)$ increases with increasing e, and (2) $F_{dis}(i)$ decreases with increasing $k_t^{1,1}$. These are in addition to the usual trend of $F_{dis}(i)$ decreasing with i.

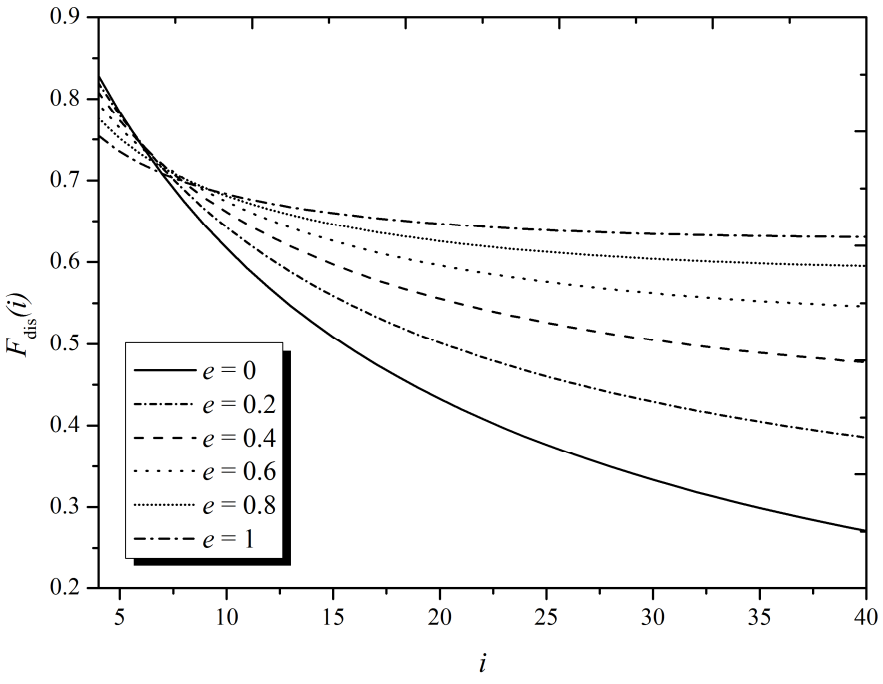

Figure 6-12. Effect of the chain length dependency, e, on the variation of F_{dis} (i) with chain length, i, as calculated using Eqs. 12 and 17-19. Parameters values appropriate for AIBN-initiated polymerization of MMA in TFT at 85 °C were used, viz. k_p = 1 465 L mol^{-1} s^{-1} , f = 0.80, k_d=2.93 × 10^{-4} s^{-1}, c_{MMA} = 0.67 mol L^{-1}, c_{AIBN} = 0.055 mol L^{-1}, $k_t^{1,1}$ = 1.0 × 10^9 L mol^{-1} s^{-1} and λ = 0.63.

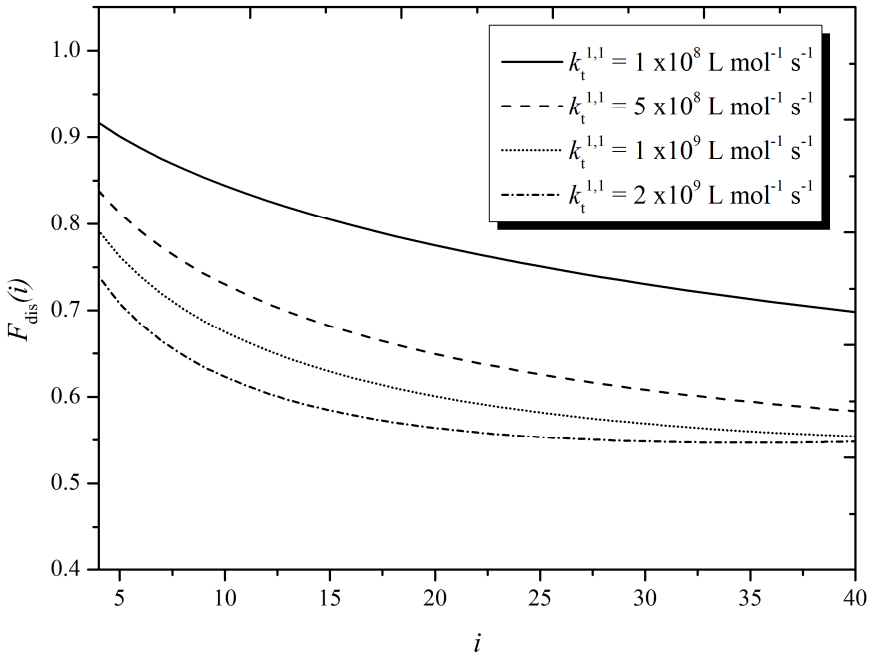

Figure 6-13. Effect of $k_t^{1,1}$ on the variation of $F_{dis}(i)$ with chain length, i, as calculated using Eqs. 12 and 17-19. Parameters values are, appropriate for AIBN initiated polymerization of MMA in TFT at 85 °C, k_p = 1465 L mol^{-1} s^{-1}, f = 0.80, k_d=2.93×10^{-4} s^{-1}, c_{MMA} = 0.67 mol L^{-1}, c_{AIBN} = 0.055 mol L^{-1}, e = 0.63 and λ = 0.63.

One needs to be aware in appraising Figures 6-12 and 6-13 that k_t is different from curve to curve. Nevertheless it is clear, especially from Figure 6-12, that CLDT does affect the way in which $F_{dis}(i)$ varies with i, and thus that there should be potential for extracting e in particular from experimental data.

With CLDT there are now 3 parameters in fitting data, viz. $k_t^{1,1}$, e and λ. However recent knowledge of MMA polymerization may be brought to bear in fitting data. As it is a fact that small-chain e is well established for MMA, this value (from SP-PLP-EPR studies) was assumed and allows us to change only $k_t^{1.1}$and λ to fit the data. In addition, it is important to note that $k_t^{1.1}$ were fitted so as to give the same experimental average termination coefficient, k_t, using the expression in Chapter 3. Thus λ was the only variable in fitting $F_{dis}(i)$ data.

Even though CLDT was found to have no great effect on the calculation of λ, as has been acknowledged by Buback et al.,[19] this statement is only true for relatively low chain

lengths (see Figure 6-14 and 6-15). As compared to Buback et al.'s investigation, the use of TOF, rather than an ion trap detector, enables us to carry out the analysis up to larger chain lengths of 4 000 Da. This gives us a better range to investigate the CLDT effect.

A set of results for $F_{dis}(i)$ over a large range of i showed a superior fit of the experimental results to the CLDT equation. Furthermore, the fitted parameters were entirely consistent with results from independent CLDT measurements. The CLIT equation was only valid for a low range of i, as shown in Figure 6-14 for AIBN initiation and 6-15 for BTMHP initiation, and if it was applied at a higher i this would give a different value for λ, whereas the CLDT equation is applicable over the whole mass range.

A) B)

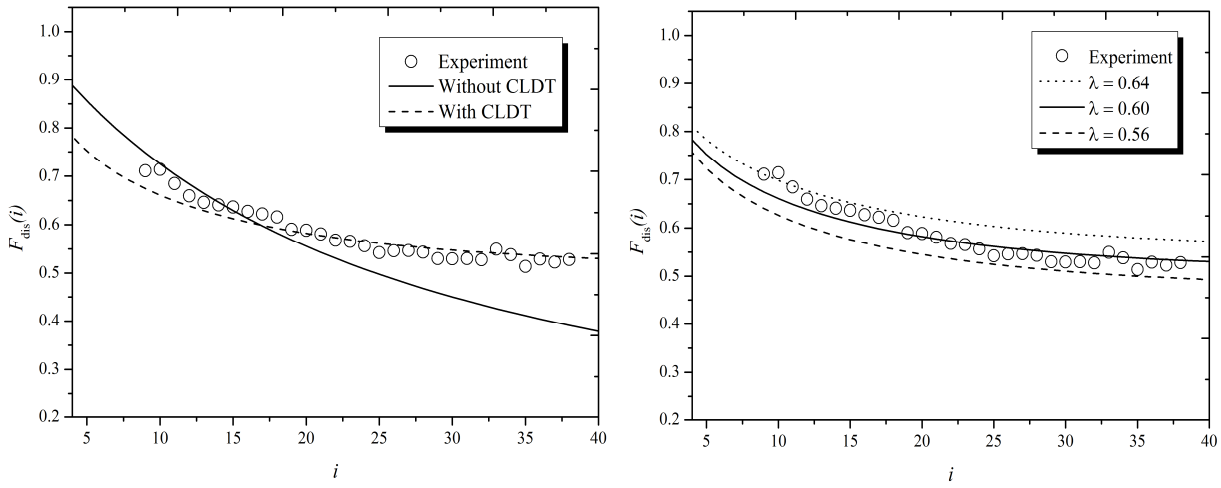

Figure 6-14. A) Number fraction of chains arising from disproportionation, $F_{dis}(i)$, as a function of chain length i, for PMMA arising from radical polymerization at 85 °C in TFT with c_{AIBN} = 0.055 mol L^{-1} and c_{MMA} = 0.67 mol L^{-1}. Points: experimental values obtained from ESI-MS results; unbroken line (without CLDT): best fit of Eq. 2 for i = 9 – 19 with λ = 0.63. Broken line (with CLDT): evaluations of Eqs. 12 and 17 – 19 with λ = 0.60, $k_t^{1,1} = 8.73 \times 10^8$ L mol^{-1} s^{-1}, e = 0.63, k_p = 1 465 L mol^{-1} s^{-1}, f = 0.80, and $k_d = 2.93 \times 10^{-4}$ s^{-1}. B) Evaluation of Eqs. 12 and 17-19 with the same rate parameters and with λ as indicated.

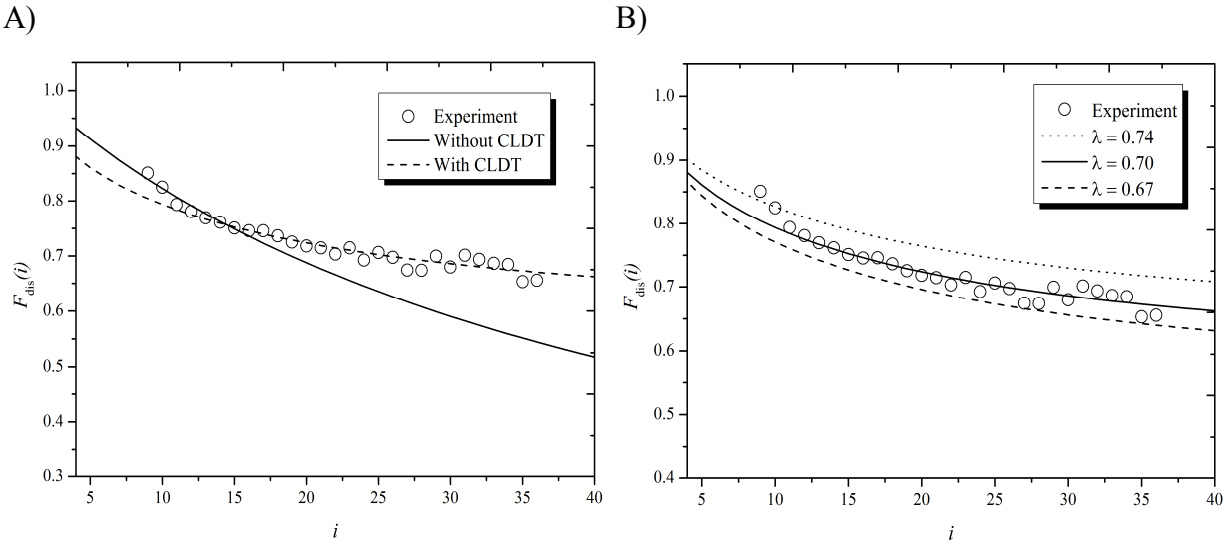

Figure 6-15. A) Number fraction of chains arising from disproportionation, $F_{dis}(i)$, as a function of chain length i, for PMMA arising from radical polymerization at 85 °C in TFT with c_{BTMHP} = 0.016 mol L^{-1} and c_{MMA} = 0.67 mol L^{-1}. Points: experimental values obtained from ESI-MS results; unbroken line (without CLDT): best fit of Eq. 2 for i = 9-19 with λ = 0.65; broken line (with CLDT): evaluations of Eqs. 12 and 17-19 with λ = 0.70, $k_t^{1,1}$ = 1.27 × 10^9 L mol^{-1} s^{-1}, e = 0.63, k_p = 1 465 L mol^{-1} s^{-1} , f = 0.53, and k_d = 5.43 × 10^{-4} s^{-1}. B) Evaluation of Eqs. 12 and 17-19 with the same rate parameters and with λ as indicated.

It is evident that CLDT equation describes the data adequately and that λ is obtained to high precision (see Figures 6-14B and 6-15B). This gives confidence in a consistent picture of radical polymerization kinetics emerging. Properly accounting for CLDT not only results in no significant change to the obtained value of λ, but additionally returns CLDT parameter values that are fully in accord with those from the recent literature.[47, 62, 63] Furthermore, the expressions for CLDT may be solved for any one unknown quantity when other parameters are known.

6.6. Conclusion

In this work, the MS method for λ determination has been subjected to a variety of consistency checks designed to establish its fitness for use. All these tests have been passed with assurance, and in no instance has the method been found wanting. Admittedly the

method is not as elementary to employ as was originally imagined:[33, 34] one must accurately know the values of k_p, fk_d and k_t, and rather than just reading off the value of δ directly from MS peak heights, one must determine $F_{dis}(i)$ (or an equivalent index) and fit Eq. 2 (or equivalent) to such data. However, these are not difficulties, but rather are just pitfalls of which to be aware. Given all this, it may be said that the method is ready for wider deployment, such as the challenges of determining the variation of λ with temperature, pressure and monomer (see the next chapter). These are all fundamental mechanistic questions in RP that might now find long overdue answers.

References

[1] G. Hart-Smith, C. Barner-Kowollik, Macromolecular Chemistry and Physics, 211 (2010) 1507-1529.
[2] C. Barner-Kowollik, T.P. Davis, M.H. Stenzel, Polymer, 45 (2004) 7791-7805.
[3] R.P. Lattimer, D.J. Harmon, K.R. Welch, Anal. Chem., 51 (1979) 1293-1296.
[4] K.L. Rinehart, L.A. Gaudioso, M.L. Moore, R.C. Pandey, J.C. Cook, M. Barber, R.D. Sedgwick, R.S. Bordoli, A.N. Tyler, B.N. Green, Journal of the American Chemical Society, 103 (1981) 6517-6520.
[5] B.S. Larsen, W.J. Simonsick Jr, C.N. McEwen, Journal of the American Society for Mass Spectrometry, 7 (1996) 287-292.
[6] S.D. Hanton, X.M. Liu, Anal. Chem., 72 (2000) 4550-4554.
[7] D.C. Schriemer, L. Li, Anal. Chem., 69 (1997) 4176-4183.
[8] T. Yalcin, Y. Dai, L. Li, Journal of the American Society for Mass Spectrometry, 9 (1998) 1303-1310.
[9] K. Linnemayr, P. Vana, G. Allmaier, Rapid Communications in Mass Spectrometry, 12 (1998) 1344-1350.
[10] R.S. Lehrle, D.S. Sarson, Polymer Degradation and Stability, 51 (1996) 197-204.
[11] D.M. Haddleton, E. Feeney, A. Buzy, C.B. Jasieczek, K.R. Jennings, Chem. Commun., (1996) 1157-1158.
[12] C.N. McEwen, W.J. Simonsick Jr, B.S. Larsen, K. Ute, K. Hatada, Journal of the American Society for Mass Spectrometry, 6 (1995) 906-911.
[13] M. Buback, H. Frauendorf, F. Günzler, P. Vana, Polymer, 48 (2007) 5590-5598.
[14] M. Buback, H. Frauendorf, F. GÃ¼nzler, P. Vana, Initiation of radical polymerization by peroxyacetates: Polymer end-group analysis by electrospray ionization mass spectrometry, in: Journal of Polymer Science, Part A: Polymer Chemistry, 2007, pp. 2453-2467.
[15] M.W.F. Nielen, Rapid Communications in Mass Spectrometry, 13 (1999) 826-827.
[16] M.C. Grady, W.J. Simonsick, R.A. Hutchinson, Macromolecular Symposia, 182 (2002) 149-168.
[17] C.B. Jasieczek, D.M. Haddleton, A.J. Shooter, A. Buzy, K.R. Jennings, R.T. Gallagher, American Chemical Society, Polymer Preprints, Division of Polymer Chemistry, 37 (1996) 845-846.
[18] P. Vana, Macromolecular Symposia, 248 (2007) 71-81.
[19] M. Buback, F. Günzler, G.T. Russell, P. Vana, Macromolecules, 42 (2009) 652-662.
[20] M. Buback, H. Frauendorf, F. GÃ¼nzler, F. Huff, P. Vana, Macromolecular Chemistry and Physics, 210 (2009) 1591-1599.
[21] R.X.E. Willemse, B.B.P. Staal, A.M. van Herk, S.C.J. Pierik, B. Klumperman, Macromolecules, 36 (2003) 9797-9803.
[22] M. Buback, G.T. Russell, P. Vana, Elucidation of Reaction Mechanisms: Conventional Radical Polymerization, in: Mass Spectrometry in Polymer Chemistry, Wiley-VCH Verlag GmbH & Co. KGaA, 2011, pp. 319-372.
[23] A. Brandrup, E.H. Immergut, E.A. Grulke, Polymer Handbook, in, Wiley-Interscience, New York, 2003, pp. 2336.
[24] G. Moad, D.H. Solomon, The Chemistry of Radical Polymerization, 2nd fully rev. ed., Elsevier, 2006.
[25] O. Olaj, I. Schnöll-Bitai, European Polymer Journal, 25 (1989) 635-641.
[26] J. Sarnecki, J. Schweer, Macromolecules, 28 (1995) 4080-4088.
[27] C.H. Bamford, R.W. Dyson, G.C. Eastmond, Polymer, 10 (1969) 885-899.
[28] G. Ayrey, A.C. Haynes, European Polymer Journal, 9 (1973) 1029-1039.
[29] M. Kinoshita, Y. Miura, Die Makromolekulare Chemie, 124 (1969) 211-221.

[30] L. Reich, S.S. Stivala, Journal of Applied Polymer Science, 17 (1973) 3709-3715.
[31] M.D. Zammit, T.P. Davis, D.M. Haddleton, K.G. Suddaby, Macromolecules, 30 (1997) 1915-1920.
[32] A.N. Nikitin, R.A. Hutchinson, Macromolecular Theory and Simulations, 16 (2007) 29-42.
[33] M.D. Zammit, T.P. Davis, D.M. Haddleton, Macromolecules, 29 (1996) 492-494.
[34] M.D. Zammit, T.P. Davis, D.M. Haddleton, K.G. Suddaby, Macromolecules, 30 (1997) 1915-1920.
[35] T. Gruendling, S. Weidner, J. Falkenhagen, C. Barner-Kowollik, Polymer Chemistry, 1 (2010) 599-617.
[36] G. Hart-Smith, C. Barner-Kowollik, Macromolecular Chemistry and Physics, 211 (2010) 1507-1529.
[37] C. Barner-Kowollik, T.P. Davis, M.H. Stenzel, Polymer, 45 (2004) 7791-7805.
[38] M. Buback, G.T. Russell, P. Vana, Elucidation of Reaction Mechanisms: Conventional Radical Polymerization, in: C. Barner-Kowollik, T. Gründling, J. Falkenhagen, S. Weidner (Eds.) Mass Spectrometry in Polymer Chemistry, Wiley-VCH Verlag & Co. KGaA, Weinheim, Germany, 2012, pp. 319-372.
[39] M. Buback, M. Egorov, R.G. Gilbert, V. Kaminsky, O.F. Olaj, G.T. Russell, P. Vana, G. Zifferer, Macromolecular Chemistry and Physics, 203 (2002) 2570-2582.
[40] C. Barner-Kowollik, M. Buback, M. Egorov, T. Fukuda, A. Goto, O.F. Olaj, G.T. Russell, P. Vana, B. Yamada, P.B. Zetterlund, Progress in Polymer Science, 30 (2005) 605-643.
[41] S. Beuermann, M. Buback, T.P. Davis, R.G. Gilbert, R.A. Hutchinson, O.F. Olaj, G.T. Russell, J. Schweer, A.M. van Herk, Macromolecular Chemistry and Physics, 198 (1997) 1545-1560.
[42] Initiators for High Polymers, in: A.N.P. Chemicals (Ed.), Akzo Nobel Polymer Chemicals, 2006.
[43] V.W. Vogt, L. Dulog, Die Makromolekulare Chemie, 122 (1969) 223-236.
[44] T. Nakamura, W.K. Busfield, I.D. Jenkins, E. Rizzardo, S.H. Thang, S. Suyama, The Journal of Organic Chemistry, 65 (1999) 16-23.
[45] A.I. Lowell, J.R. Price, Journal of Polymer Science, 43 (1960) 1-12.
[46] S. Beuermann, N. García, Macromolecules, 37 (2004) 3018-3025.
[47] C. Barner-Kowollik, G.T. Russell, Progress in Polymer Science, 34 (2009) 1211-1259.
[48] D.S. Viswanath, N.V.K. Dutt, T.K. Ghosh, D.H.L. Prasad, K.Y. Rani, Viscosity of Liquids Theory, Estimation, Experiment, and Data, Springer, Dordrecht, 2007.
[49] M. Buback, M. Egorov, T. Junkers, E. Panchenko, Macromolecular Rapid Communications, 25 (2004) 1004-1009.
[50] M. Buback, H. Frauendorf, F. Günzler, P. Vana, Polymer, 48 (2007) 5590-5598.
[51] G.T. Russell, Macromolecular Theory and Simulations, 4 (1995) 549-576.
[52] D.R. Taylor, K.Y. van Berkel, M.M. Alghamdi, G.T. Russell, Macromolecular Chemistry and Physics, 211 (2010) 563-579.
[53] K.C. Berger, Die Makromolekulare Chemie, 176 (1975) 3575-3592.
[54] M. Buback, B. Huckestein, F.-D. Kuchta, G.T. Russell, E. Schmid, Macromolecular Chemistry and Physics, 195 (1994) 2117-2140.
[55] M. Buback, C. Hinton, Z. Phys. Chem. (Munich), 199 (1997) 229-254.
[56] H. Fischer, H. Paul, Accounts of Chemical Research, 20 (1987) 200-206.
[57] M. Stickler, D. Panke, W. Wunderlich, Die Makromolekulare Chemie, 188 (1987) 2651-2664.
[58] M. Buback, G.T. Russell, Kinetics of Polymerizations, in: C. Chatgilialoglu, A. Studer (Eds.) Encyclopedia of Radicals in Chemistry, Biology and Materials, John Wiley & Sons Ltd., Chichester, U.K., 2012, pp. 1737-1784.

[59] M. Strohalm, mMass - Open Source Mass Spectrometry Tool, in, 2012.
[60] G. Hart-Smith, M. Lammens, F.E. Du Prez, M. Guilhaus, C. Barner-Kowollik, Polymer, 50 (2009) 1986-2000.
[61] C. Ladavière, P. Lacroix-Desmazes, F. Delolme, Macromolecules, 42 (2009) 70-84.
[62] J. Barth, M. Buback, Macromolecular Rapid Communications, 30 (2009) 1805-1811.
[63] J. Barth, M. Buback, Macromolecular Reaction Engineering, 4 (2010) 288-301.
[64] C. Barner-Kowollik, G.T. Russell, Progress in Polymer Science (Oxford), 34 (2009) 1211-1259.

Chapter 7. Investigation into the Dependencies of Mode of Termination on Pressure, Temperature and Monomer in Radical Polymerization

This chapter continues work on the mode of termination. Chapter 6 determined λ only for methyl methacrylate (MMA) at a single temperature and ambient pressure. It is remarkable how little is known beyond this: nothing is well known from the literature about the variation of λ with T, p and monomer. Since the foundation of the new method of ESI-MS-TOF has been laid in Chapter 6, in this part of my project it is therefore aimed to fill the aforementioned gaps. This will be done by employing ESI-MS-TOF, as in Chapter 6. Therefore one is referred back to this chapter for details about experiments and data analysis.

7.1. Overview

The mechanism of the combination reaction seems straightforward: it is usually just coupling of carbon-centred radicals to form a carbon-carbon single bond and thus a dead polymer molecule. On the other hand, the disproportionation reaction involves an intermolecular β-hydrogen transfer that leads to formation of two dead polymer molecules. Even though it usually may be predicted qualitatively what the dominant termination pathway is for a particular monomer, confirmation of this, let alone precise determination of λ, is still lacking. For example, despite general agreement that there is substantial disproportionation for MMA, there is considerable discrepancy as to the precise value of λ.

In fact, a range of factors might contribute to the termination process. For disproportionation to occur, an overlap of the unpaired electron orbital and a homolytically breaking C-H bond

is required. This requirement would make the disproportionation reaction more specific and stereoelectronic.[1] This would suggest the importance of the reorientation process for disproportionation to occur. This requirement may make it able to be influenced by other factors. The size of the radical, for example, is found to have a profound effect on the termination pathway. This is exemplified by the penultimate unit effect on the mode of termination observed for MMA radical. Dimeric MMA radicals have more disproportionation than MMA radicals.[2] This would indicate that combination is more sensitive towards steric factors than disproportionation. That said, this does not make intuitive sense, in that one would expect introducing one additional unit would promote process of combination over the more demanding reorientation disproportionation process. Furthermore, a substituent at the radical centre also has an effect. Namely, there is a marked preference for loss of hydrogen from the α-methyl substituent, and this increases with increasing substitution at the radical centre. In addition, if, as has been suggested, the disproportionation transition state is more polar, then solvent polarity might also play a role, as polar solvent stabilizes polar transition complexes. Indeed, a complete picture on what exactly determines the chemistry of combination and disproportionation has not yet emerged, a situation that cannot change until accurate values of λ appear in the literature. With the MS technique established, investigating the effects of temperature, pressure and monomer should lead to better understanding of the mechanism of the termination reaction, not to mention that quantitative knowledge of λ is also important in designing polymer syntheses and in the derivation of rate parameters at different conditions as it is also present in many rate-parameter expressions.

7.2. The effect of temperature on λ

The measurement of the fraction of termination by disproportionation, λ, as a function of temperature consisted of recording the ESI-MS-TOF spectrum of the polymers that were produced from monitored low-conversion polymerization of MMA in solution employing AIBN as initiator and TFT as solvent at different temperatures. The use of a low concentration of MMA in TFT not only allows short chains to be made for MS analysis, but also reduces any chance of complications due to chain transfer.

In spite of the fact that in both termination reactions radical destruction is involved simultaneously, the two processes can be clearly distinguished on the ESI-MS-TOF spectrum, as shown in Figure 7-1. The influence of temperature on the ratio of termination by disproportionation is evident from Figure 7-1: increasing the temperature was found to lead to an increase in the intensity of the combination signals compared with the disproportionation signals. Moreover, the figure presents a clear distinction of termination products with a good resolution, and cluster pattern identification and complications due to chain transfer are clearly absent.

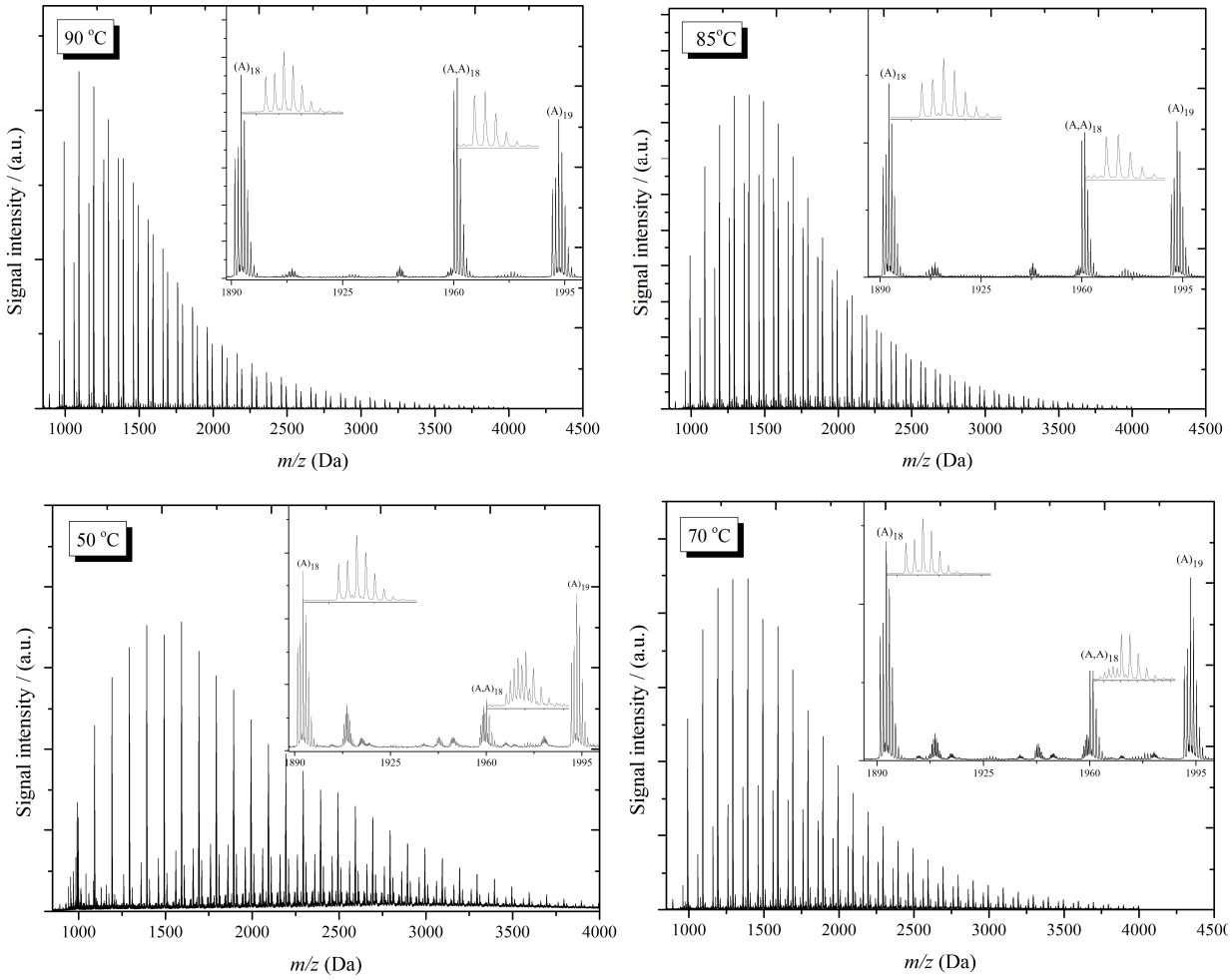

Figure 7-1. ESI-MS spectrum of poly(methyl methacrylate) obtained from radical polymerization in TFT at different temperatures, as indicated, with c_{AIBN} = 0.05 mol L^{-1} and c_{MMA} = 0.67 mol L^{-1}. In each case the close-up shows a portion of the MS spectrum that is typical for one repeat unit, with A and A,A denoting signals from disproportionation- and combination-generated species respectively, the degree of polymerization being as indicated, and A being the primary radical from AIBN.

However, it is noticeable that some small peaks become more prominent with decreasing temperature. In fact, these peaks may be assigned to doubly charged chains. It is not clear why there should be this effect, remembering that the temperature refers only to the polymerization temperature, not the temperature of MS sample preparation and analysis. In

other words, there is no reason why an 18-mer (see Figure 7-1) should ionize any differently just because it was made at a different temperature. One therefore has to suspect that this effect is related to the longer average chain lengths at lower temperature: because the fraction of longer chains is higher, and because long chains are more likely to be doubly charged than are smaller chains.

Whatever, there is no reason to think that the appearance of doubly charged species will have any effect on data analysis, because the number of charges carried by a chain is unlikely to be affected by whether it was formed by combination or disproportionation. Thus comparison of the intensities of singly-charged species should still give λ accurately at lower temperatures. It is evident that at lower temperatures there is still good resolution and thus easy distinction of the termination products in ESI-MS-TOF spectra. Figure 7-2 summarises the effect of temperature on the number fraction of chains of degree of polymerization i arising from disproportionation, $F_{dis}(i)$.

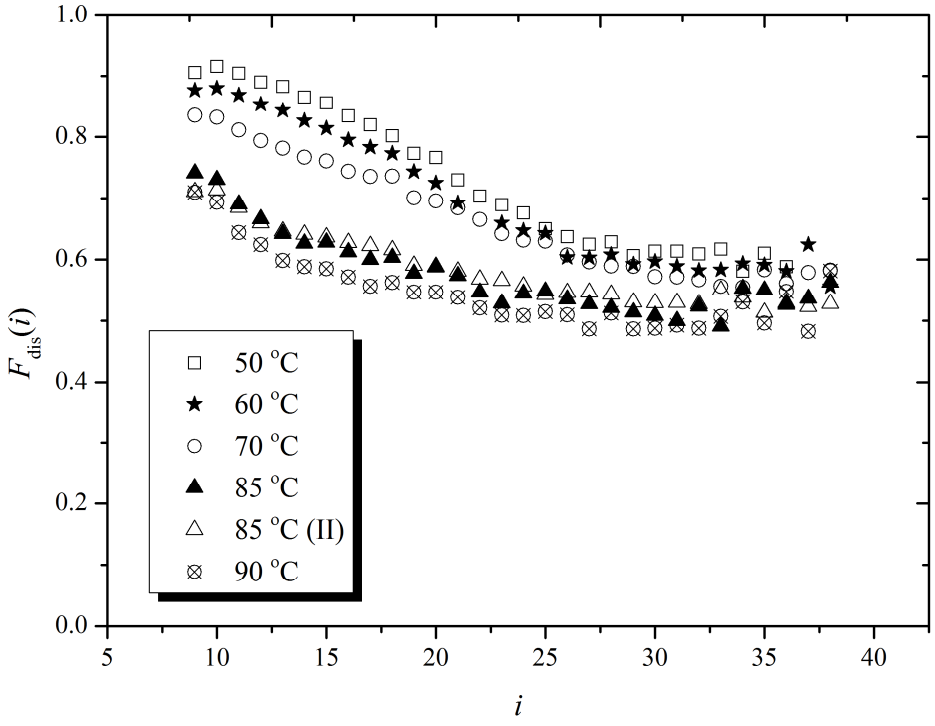

Figure 7-2. Effect of temperature on the experimental $F_{dis}(i)$, the fraction of chains formed by disproportionation, for solution polymerization of 0.67 mol L^{-1} MMA in TFT employing 0.05 mol L^{-1} AIBN as initiator at ambient pressure.

There are several points that need to be made from Figure 7-2. First, the data of the experiments seem to be of good quality, as shown by the lack of noise in all results and the good reproducibility in the results at 85 °C. Secondly, in addition to the usual decrease of $F_{dis}(i)$ with i, there is a decrease in $F_{dis}(i)$ with increasing temperature, which suggests increasing combination with increasing temperature.

In fact, this decrease is consistent with what is observed for small radicals. Model studies employing small radicals have mostly been used to investigate mode of termination, as their reaction is simplified due to reaction products being more readily detected and thus allowing for evaluation of the mode of termination, which has been found to decrease with increasing temperature, i.e., more combination occurs with increasing temperature.[1] In fact, this can be

rationalised in terms of viscosity effect, which obviously depends on temperature, and additionally the structure and rotational freedom of the radicals involved. Decreasing temperature raises the viscosity, which hinders rotation. Increasing viscosity was found to promote disproportionation over combination, as found by Fischer.[3] This would again indicate greater sensitivity of combination than disproportionation towards steric factors. In spite of the agreement between $F_{dis}(i)$ and the termination of small radicals, such studies by their very nature cannot exactly simulate the polymerization process. Thus, results from the model may not be totally applicable to polymeric radicals.

Despite the feasible explanation of $F_{dis}(i)$ reduction with temperature being related to viscosity,[3] as also discussed in Chapter 6, it is difficult to say directly that the mode of termination is affected, as $F_{dis} \neq \lambda$, because $F_{dis}(i)$ depends on other kinetic information as follows:

$$F_{dis}(i) = \frac{1}{1+\frac{1}{2}(i-1)C(\frac{1}{\lambda}-1)} = \frac{1}{1+\frac{1}{2}(i-1)C(\frac{1}{\delta})} \quad (1)$$

where

$$C = \frac{2k_t c_R}{k_p c_M} = \frac{(2k_t R_{init})^{0.5}}{k_p c_M} = \frac{(4fk_d c_I k_t)^{0.5}}{k_p c_M} \quad (2)$$

It is obvious from Eqs. 1 and 2 that prior knowledge of the rate parameters fk_d, k_p and k_t is required. Since values of f, k_d and k_p as a function of temperature are available from the literature, k_t still should be obtained experimentally, as it is known to be system dependent. The temperature dependence of the parameters k_d, k_p and f are required in order to calculate the correct k_t and then λ; they are as follows:

$$k_d(\text{AIBN}) = 2.89 \times 10^{15}\ \text{s}^{-1} \exp\left(\frac{-130.23\ \text{kJ mol}^{-1}}{RT}\right) \quad (3a)$$

$$f(\text{AIBN}) = 5.04 \exp\left(\frac{-5.70\ \text{kJ mol}^{-1}}{RT}\right) \quad (3b)$$

$$k_{\mathrm{p}}(\mathrm{MMA}) = 2.673 \times 10^{6}\mathrm{L\ mol\ s^{-1}} \exp\left(\frac{-22.36\ \mathrm{kJ\ mol^{-1}}}{RT}\right) \quad (3c)$$

Equation (3a) is taken from AkzoNobel product data [4] while equation (3b) is deduced from ref. [5] and equation (3c) is the IUPAC- recommended benchmark value.[6] For determination of k_t one is referred back to Chapter 6. Note that k_t is the average termination rate coefficient and is also referred to as $\langle k_t \rangle$. From Eq. 1 it is then possible to obtain λ, which is the only fitting variable, because C is known from k_t determination. Typical fitting results are presented in Figure 7-3. Since we demonstrated the importance of including CLDT in Chapter 6, it is meaningful to consider it too. For the equations used for λ determination with CLDT, one is referred to Chapter 6 for more information. It is evident that Eq. 1, the CLIT equation, adequately describes the low range of the data (i = 9 – 19). However, as mentioned earlier in Chapter 6, it fails to fit the MS data in entirety. In contrast, CLDT allows a better fit of the entire data. In fact, it was difficult to model $F_{\mathrm{dis}}(i)$ without knowing the approximate effect of temperature on $k_t^{1,1}$ and e. The procedure adopted was to assume a value of e, then fit $k_t^{1,1}$ using Eq. 4 and the experimental value of k_t, then fit the $F_{\mathrm{dis}}(i)$ data using these values and varying λ. If it was not possible to fit the $F_{\mathrm{dis}}(i)$ data, then this procedure was repeated using different values of e until the optimum λ was obtained.

$$k_{\mathrm{t}} = k_{\mathrm{t}}^{1,1}\left[\Gamma\left(\frac{2}{2-e}\right)\right]^{-2}\left[\frac{\left(2R_{\mathrm{i}}k_{\mathrm{t}}^{1,1}\right)^{0.5}}{k_{\mathrm{p}}c_{\mathrm{M}}}\left(\frac{2}{2-e}\right)\right]^{2e/(2-e)} \quad (4)$$

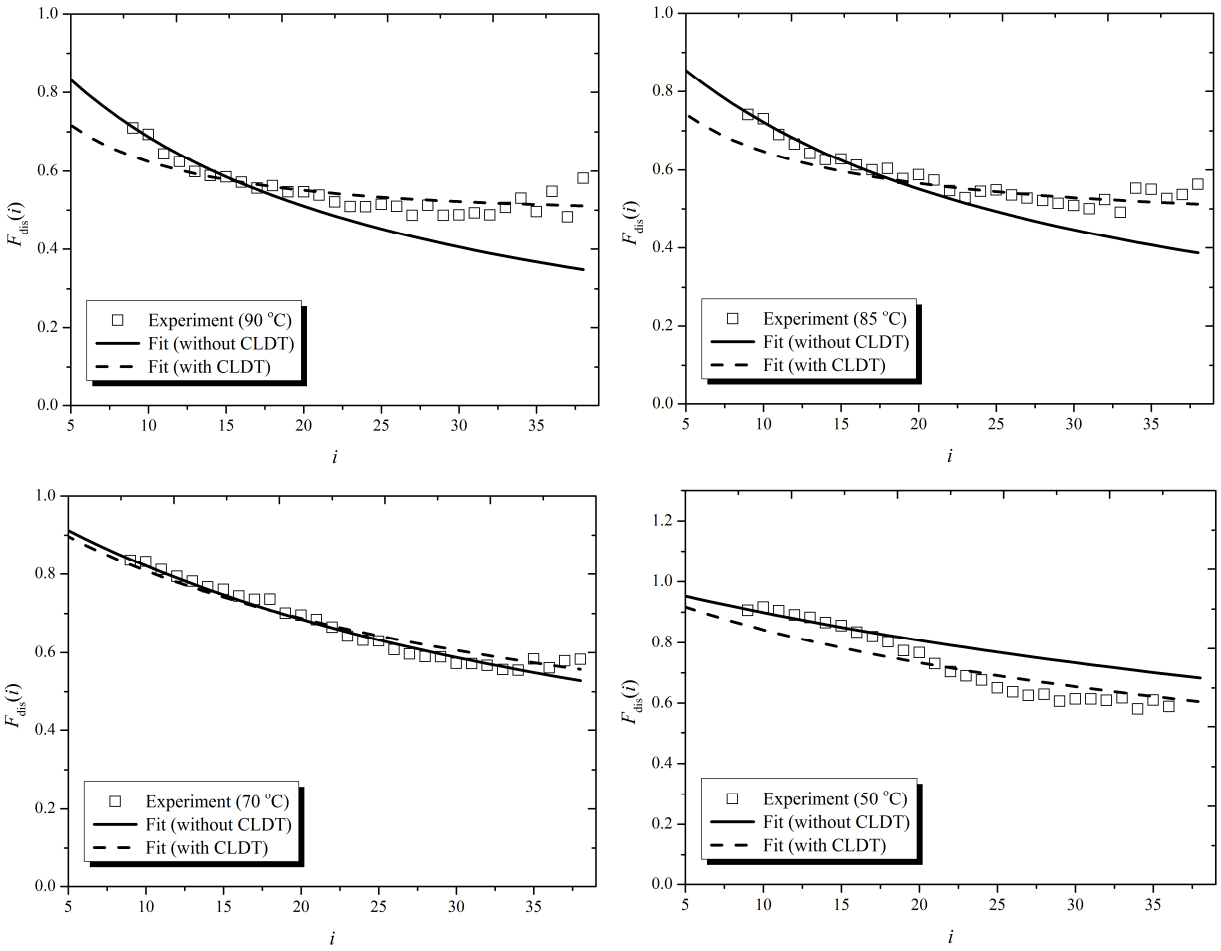

Figure 7-3. Number fraction of chains arising from disproportionation, $F_{dis}(i)$, as a function of chain length i, for PMMA arising from radical polymerization in TFT with c_{AIBN} = 0.05 mol L^{-1} and c_{MMA} = 0.67 mol L^{-1} at different temperatures as indicated. Points: experimental values obtained from ESI-MS results; curves: best fits with fit Eq. 1 (without CLDT) and with CLDT equations, with parameter values as reported in Table 7-1.

Interestingly, the CLDT parameters given in Table 7-1 result in very good fits of the data. The values of $k_t^{1,1} \approx 8\times 10^8$ L mol^{-1} s^{-1} and e = 0.63 that are assigned to small chains fit the results at 90 °C and 85 °C very well, and are consistent with CLDT. However, as the temperature was lowered the behaviour became closer to CLIT, and it was not possible to fit the data with CLDT parameters for short polymers. Instead, data was best fitted with long-chain CLDT parameters, viz. e = 0.20 and $k_t^{1,1}$ as listed in Table 7-1. This is consistent with average chain sizes being longer at lower temperatures, as is well known: although lower k_p gives rise to shorter chains, this is more than counterbalanced by the lower rate of

termination, which is primarily due to the strong effect of temperature on R_{init}, resulting in longer chains.

Table 7-1. Parameters used to fit the experimental $F_{dis}(i)$ presented in Figure 7-3 with and without CLDT accounting. Experimental k_t values are also reported.

	CLDT fitting				**λ from CLIT fitting**
θ **(°C)**	$k_t^{1,1}$ (L mol^{-1} s^{-1})	e	k_t (L mol^{-1} s^{-1})	λ	
90	8.01×10^8	0.63	3.88×10^8	0.57	0.58
90	5.23×10^8	0.63	1.98×10^8	0.59	0.56
85	9.22×10^8	0.63	3.85×10^8	0.60	0.57
85	9.52×10^8	0.63	3.91×10^8	0.61	0.63
85	7.22×10^8	0.63	2.61×10^8	0.58	0.59
85	5.93×10^8	0.63	1.96×10^8	0.56	0.50
85	1.23×10^9	0.63	5.70×10^8	0.57	0.59
71	2.56×10^8	0.20	1.54×10^8	0.43	0.40
70	2.80×10^8	0.20	1.69×10^8	0.52	0.45
70	1.72×10^8	0.20	9.81×10^7	0.53	0.46
60	1.71×10^8	0.20	8.75×10^7	0.36	0.35
60	1.87×10^8	0.20	9.64×10^7	0.43	0.29
50	1.93×10^8	0.20	8.85×10^7	0.33	0.23

Figure 7-4 shows results obtained for λ from both CLIT and CLDT fitting of the data. There are several important points to make from Table 7-1 and Figure 7-4: (1) Accounting for CLDT has no significant effect on the value obtained from λ. Thus it cannot be argued that these values are artefacts of the assumed CLDT values: the same trend and much the same values are obtained with the CLIT model. All the CLDT model does is to give superior fitting of the data and to provide affirmation of CLDT parameters obtained in other ways. (2) The obtained values of CLDT are fully in accord with those from the recent literature within experimental uncertainty.[7-9] (3) Although $F_{dis}(i)$ decreases with increasing temperature

(see above), suggesting more combination as temperature increases, in fact the fitted λ values reveal the opposite: it increases with increasing temperature, showing that in fact there is more disproportionation as temperature increases. This yet again emphasizes that $F_{dis}(i)$ should not be regarded as being tantamount to λ. In fact the value $F_{dis}(i)$ depends also on k_p, k_t and R_{init}, and it is the variation of these with temperature that give the present paradoxical result that λ increases with temperature even though $F_{dis}(i)$ decreases.

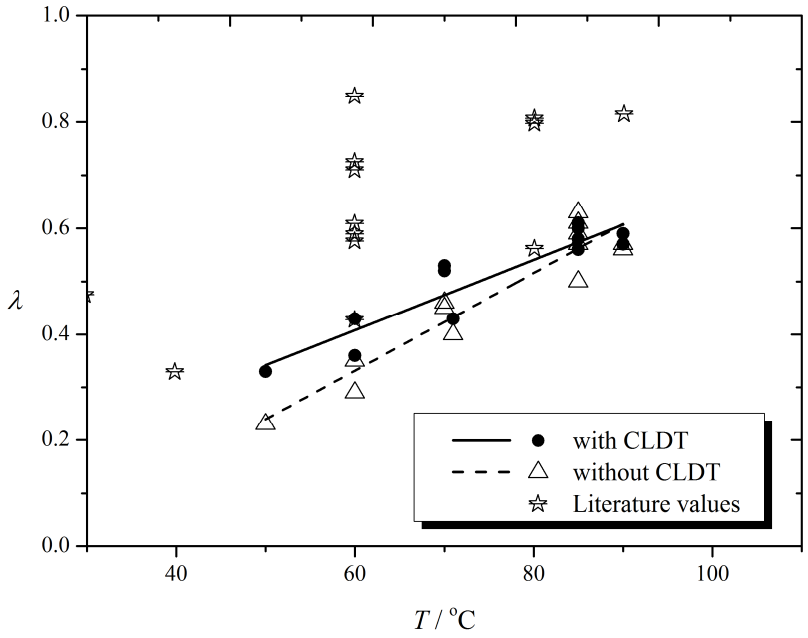

Figure 7-4. Effect of temperature on λ for free radical polymerization of MMA in TFT initiated by 0.05 mol L^{-1} AIBN and with c_{MMA} = 0.67 mol L^{-1} and analyzed by both CLDT and CLIT equations. Points: experimental values; Line: best linear fit of our results. Also the figure shows literature values obtained at similar temperature range. [1]

Figure 7-4 shows clearly that λ increases with temperature, though our resultant values appear to be within the lower limit of the presented literature values. This is in opposition to the previously mentioned small-molecule studies, which suggest increasing combination with temperature. That said, the present results make intuitive sense, in that one would expect temperature to promote the bond-breaking process of disproportionation over the barrierless process of combination. In the present work it has been found that termination occurs far

more by combination at 50 °C. This is pleasing in that it has always been hard to see how the difficult reaction of disproportionation could be occurring predominantly at such a relatively low temperature as this. After all, if disproportionation really were dominant in MMA at 50 °C, it would be hard to explain that transfer to polymer does not occur at these temperatures.

A consideration of this data leads to the reality of a positive activation energy for λ for MMA, in which the following Arrhenius expressions are obtained in temperature range between 50 – 90 °C for MMA system:

$$\lambda(\mathrm{CLIT}) = 9.94 \times 10^{2} \exp\left(-\frac{22.3 \pm 2.2\ \mathrm{kJmol^{-1}}}{RT}\right) \qquad (5a)$$

$$\lambda(\mathrm{CLDT}) = 6.59 \times 10^{1} \exp\left(-\frac{14.1 \pm 1.7\ \mathrm{kJmol^{-1}}}{RT}\right) \qquad (5b)$$

Although these results have been obtained using AIBN, they should be independent of the initiator. Eq. 5b is recommended as more accurate as fitting is of a superior quality with CLDT, which is known to be more microscopically correct.

The positive activation energies of λ gained is at variance with model studies suggesting that λ has negative small temperature dependence.[1] This has been observed, for example, for *tert*-butyl radicals in solution where the mode of termination decreases with increasing temperature.[1] This means more temperature dependence of combination reaction than disproportionation. However, the polymerization experiments are often complicated by other factors. The reason for the increase of the $E_a(k_{t,dis})$ might be due to a steric hindrance of the transition state of disproportionation reaction as the polymeric radicals become longer. Despite the contradictory behaviour to small radicals, one would think that positive $E_a(\lambda)$

should be the case since the disproportionation reaction involves breaking and reforming bonds.

As the mode of termination comes out as follows,

$$\lambda = \frac{k_{\mathrm{t,dis}}}{k_{\mathrm{t,dis}} + k_{\mathrm{t,comb}}} = \frac{1}{1 + \frac{k_{\mathrm{t,comb}}}{k_{\mathrm{t,dis}}}} \qquad (6)$$

$$\frac{k_{\mathrm{t,comb}}}{k_{\mathrm{t,dis}}} = \frac{1}{\lambda} - 1 \qquad (6a)$$

one could then get information about $E_a(k_{t,comb}/k_{t,dis})$ by plotting $\ln(\frac{1}{\lambda} - 1)$ vs. $1/T$. This is done in Figure 7-5:

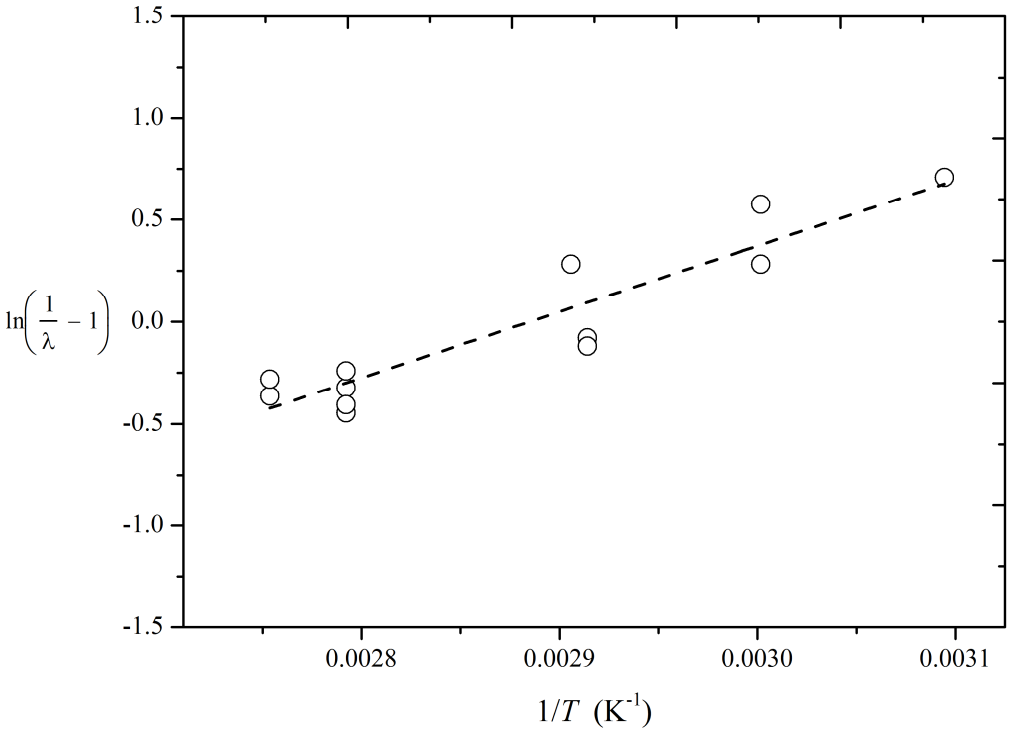

Figure 7-5. Arrhenius plot of $(\frac{1}{\lambda} - 1)$, as obtained from analysis using CLDT equations, for radical polymerization of MMA in TFT initiated by 0.05 mol L^{-1} AIBN and with c_{MMA} = 0.67 mol L^{-1}. Points: experimental values; Line: best linear fit.

As can be seen, this results in a negative activation energy; the following Arrhenius expression is obtained, indicating a larger activation energy for disproportionation than combination, as one would expect.

$$\frac{1}{\lambda} - 1 = \frac{k_{\mathrm{t,comb}}}{k_{\mathrm{t,dis}}} = 8.99 \times 10^{-5} \exp\left(\frac{26.3 \pm 3.6\ \mathrm{kJmol^{-1}}}{RT}\right) \qquad (7)$$

There are several ways one might now use to estimate $E_a(k_{t,dis})$. (1) The first is from the definition $\lambda = k_{t,dis}/k_t$, which leads to:

$$E_a(\lambda) = E_a\left(k_{\mathrm{t,dis}}\right) - E_a(k_{\mathrm{t}}) \qquad (8a)$$

$$E_a\left(k_{\mathrm{t,dis}}\right) = E_a(\lambda) + E_a(k_{\mathrm{t}}) \qquad (8b)$$

By employing the $E_a(k_t)$ value obtained in Chapter 4 for MMA, viz. 38 kJ mol^{-1}, and the current $E_a(\lambda)$ = 14 kJ mol^{-1}, from Eq. 5b, one can estimate that $E_a(k_{t,dis}) \approx 52$ kJ mol^{-1}. This is in fact quite close to what is determined for hydrogen abstraction of small radicals, where E_a = 56.52 kJ mol^{-1} is determined experimentally for hydrogen abstraction of ethyl radical from ethane.[10] This result is also in agreement with E_a for transfer to monomer in MMA polymerization,[11] a reaction that similarly involves hydrogen abstraction from the α-methyl group.

(2) From Eq. 7 one has that $E_a(k_{t,comb}/k_{t,dis}) = E_a(k_{t,comb}) - E_a(k_{t,dis}) = -26$ kJ mol^{-1}. If one makes the assumption that $E_a(k_{t,comb}) \approx 0$ on account of it being a barrierless reaction, then this leads to $E_a(k_{t,dis})$ = 26 kJ mol^{-1}, which does not seem unreasonable, even if it less than the values quoted above. On the other hand, if one takes $E_a(k_{t,dis})$ = 52 kJ mol^{-1} from above, then one obtains $E_a(k_{t,comb})$ = 26 kJ mol^{-1}, which would seem implausibly high. This calls into question the value of $E_a(k_t)$ used above. The problem here may be that this is a value based on

diffusion control and on the radical chain-length distribution, whereas what is under discussion here are chemically-controlled activation energies.

The mode of termination results may also be analyzed according to thermodynamic arguments. Two distinct transition states exist for the combination and disproportionation reactions,[12, 13] which are also supported by our experimental temperature dependence observation for λ. A consideration of different transition states leads to the idea of estimating the transition state entropy. This is performed using the well known Eyring equation (Eq. 9), which gives information about the degree of order in the transition state.

$$\ln\frac{k_\mathrm{t}}{T} = -\frac{\Delta H^*}{R}\frac{1}{T} + \ln\frac{k_\mathrm{B}}{h} + \frac{\Delta S^*}{R} \qquad (9)$$

Here k_B, h and R donate Boltzmann, Plank and gas constants, respectively, and k_t average rate coefficient of termination. Plotting data, from Chapter 4, Table 4-1, as ln k_t/T versus $1/T$ confers an intercept that is equal to Eq. 10 from which the ΔS^* can then be determined.

$$\mathrm{y(x=0)} = \ln\frac{k_\mathrm{B}}{h} + \frac{\Delta S^*}{R} \qquad (10)$$

The transition state for combination would be more likely to have an ordered structure than the that for disproportionation. Table 7-2 presents our experimental data obtained for radical polymerization of different monomers using AIBN as initiator.

Table 7-2. Transition state entropies for termination ($\Delta S^*(k_\mathrm{t})$) obtained for different monomers as indicated.

polymer	$\Delta S^*(k_\mathrm{t})$ / (J mol^{-1} K^{-1})
PMMA	12.1
PBMA	11.9
PBA	100.0
PST	–17.7
PDMA	–24.6

In discussing the results of Table 7-2, a positive value for entropy of activation indicates that the transition state is more disordered compared with reactants. A more ordered structure is observed for ST polymerization where combination is believed to be the dominant process for termination. On the other hand, similar positive values are observed for MMA and BMA polymerization, where the disproportionation process is contributing. Polymerization of BA interestingly showed the largest entropy of activation, indicating the least ordered transition state. Notwithstanding that BA termination is predominantly by combination, this value might be explained by the complication of the backbiting process in BA.[14, 15] DMA interestingly yields a negative change in activation entropy, indicating a more ordered transition state structure and implying that combination dominates. This is hard to explain given the family behaviour found here for MMA and BMA, not to mention that the size and flexibility of pendant dodecyl groups surely make it extremely difficult for combination to occur. On account of these rogue results for BA and DMA, one must question whether the present method of analysis can serve as an indication of the mode of termination. In addition, one must bear in mind that the above result is based on a termination rate determination that is known to be system dependent and can be influenced by many factors.

7.3. The effect of pressure on λ

Mode of termination investigations for MMA radical polymerization under high pressure have been attained by analysing the polymer samples that were produced by carrying out the polymerization in the high pressure cell (see Chapter 5 for experimental details). Figure 7-6 shows typical results for ESI-MS-TOF spectra obtained at different pressures. The influence of pressure on the signals is clearly evident. Increasing the pressure was found to lead, unexpectedly, to a decrease of the intensity of the combination signals compared with those

of the disproportionation signals, thereby leading to an increase of $F_{dis}(i)$, as shown in Figure 7-7. That said, the lesson should already have been learned that one should not jump to conclusions about λ on the basis of $F_{dis}(i)$ values alone.

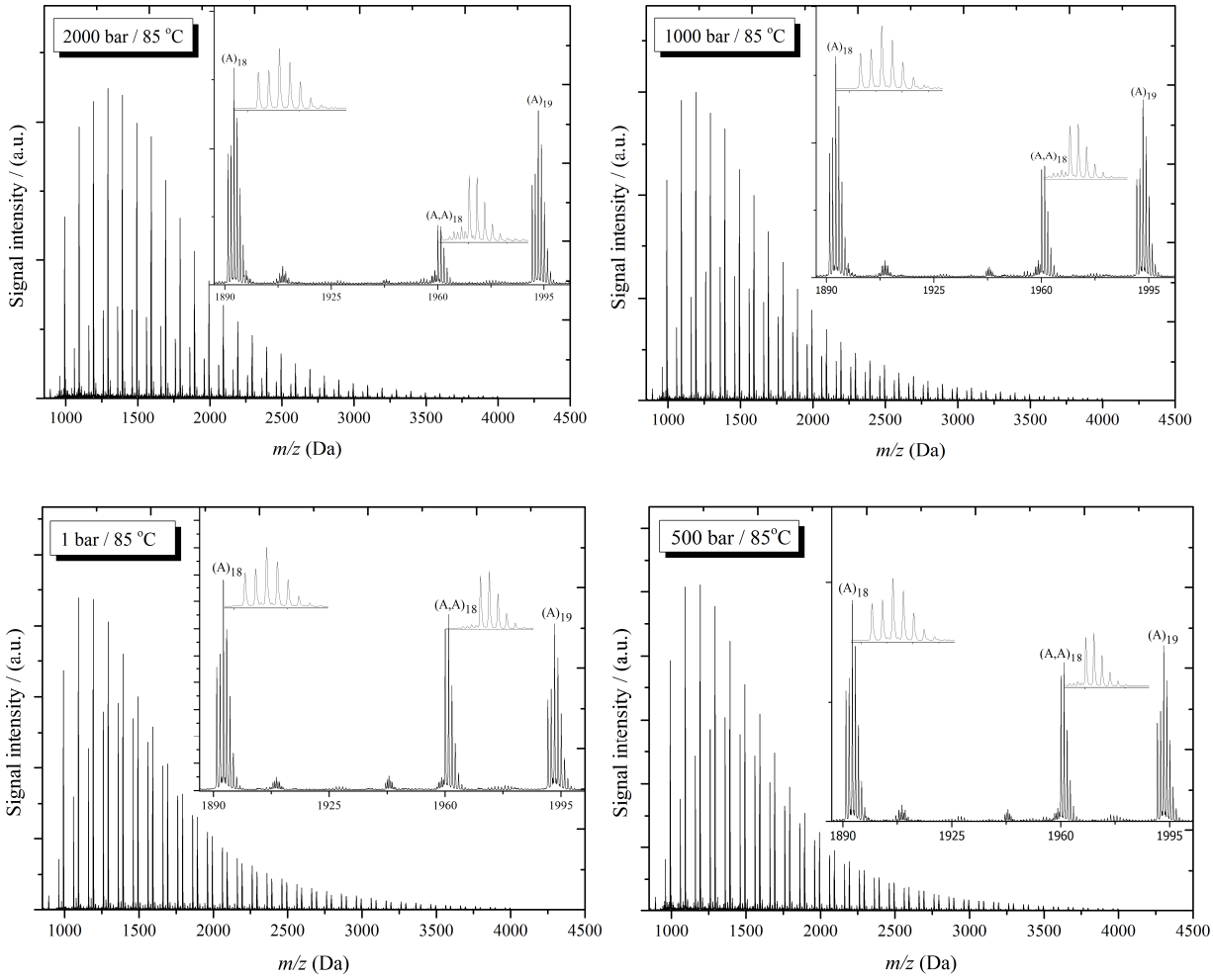

Figure 7-6. ESI-MS spectra of poly(methyl methacrylate) obtained from radical polymerization in TFT at 85 °C and at different pressures as indicated, with c_{AIBN} = 0.05 mol $L^{-1}$and with c_{MMA} = 0.67 mol L^{-1}. In each case the close-up shows a portion of the MS spectrum that is typical for one repeat unit, with A and A,A denoting signals from disproportionation- and combination-generated species respectively, the degree of polymerization being as indicated, and A being the primary radical from AIBN.

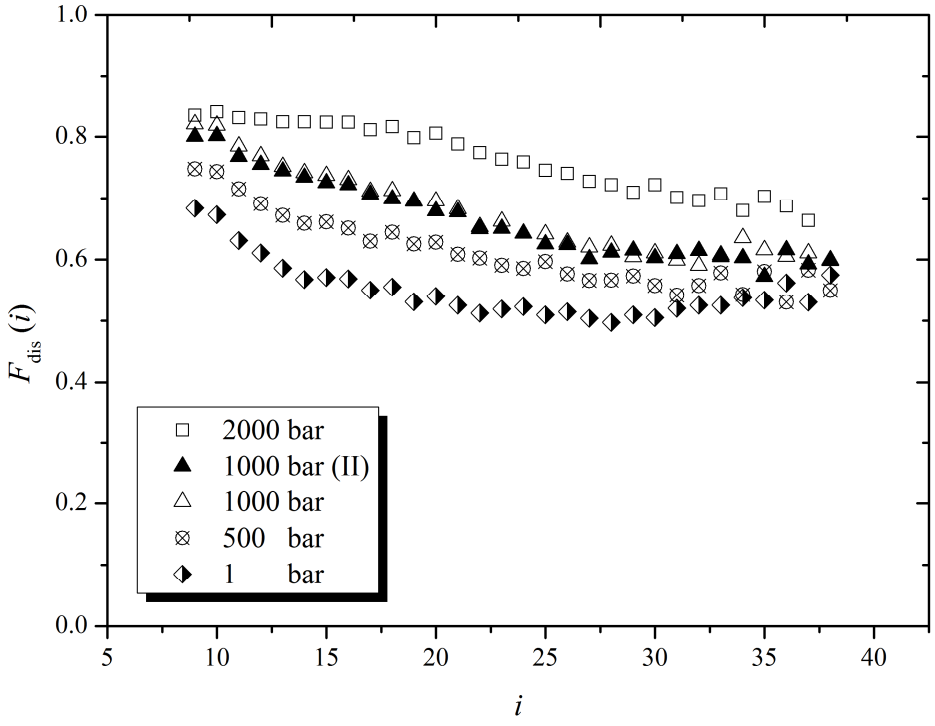

Figure 7-7. Effect of pressure on $F_{dis}(i)$, the fraction of chains formed by disproportionation, obtained from the PMMA results of Figure 7-6.

However, determination of the mode of termination requires fitting Eq. 1 to experimental $F_{dis}(i)$ data. The variation of rate parameters with pressure makes it difficult to say directly that the mode of termination changes with pressure, as these parameter values influence the analysis (see Eqs. 1 and 2). The pressure dependence of the parameters k_d, k_p and f is required in order to calculate k_t and then λ, as discussed in Chapter 5. Initiator decomposition is known from literature to be less influenced by pressure, unlike k_p, which increases with increasing pressure.[16] Initiator efficiency, f, also changes as a function of pressure: it decreases with pressure, as found by Buback et al.[5] The termination rate is still required to be determined experimentally. The present study has used the activation volumes in conjunction with the activation energies for MMA to obtain the following expression[5]

$$\ln\left[k_\mathrm{p}\ /\mathrm{L\ mol^{-1}s^{-1}}\right] = 14.80 - \frac{2689.44}{T/\mathrm{K}} + \frac{0.201}{T/\mathrm{K}}\left(\frac{p}{\mathrm{bar}} - 1\right) \qquad (11)$$

and activation volume and energy for AIBN efficiency, *f,* to obtain the following expression[5]

$$\ln f = 1.62 - \frac{686.07}{T/\mathrm{K}} - \frac{0.041}{T/\mathrm{K}}\left(\frac{p}{\mathrm{bar}} - 1\right) \qquad (12)$$

A temperature-independent activation volume is assumed for both k_p and *f*. Regarding the k_d of AIBN, the Akzo value [4] was used and an assumption of constant k_d with pressure is made, as discussed in an earlier chapter.

Typical fitting results are presented in Figure 7-8. Again, as with the temperature investigation, both CLIT and CLDT analyses are presented. The $k_\mathrm{t}^{1,1}$ values were fitted with an assumed *e* to give the experimental average termination coefficient, k_t. Similar to what was found earlier with temperature investigations, CLDT consideration allows a better fit of the entire data, though at the same time it has no large effect on the value of λ. Further, it returns CLDT parameter values that are consistent with a full overview of radical polymerization.[7-9]

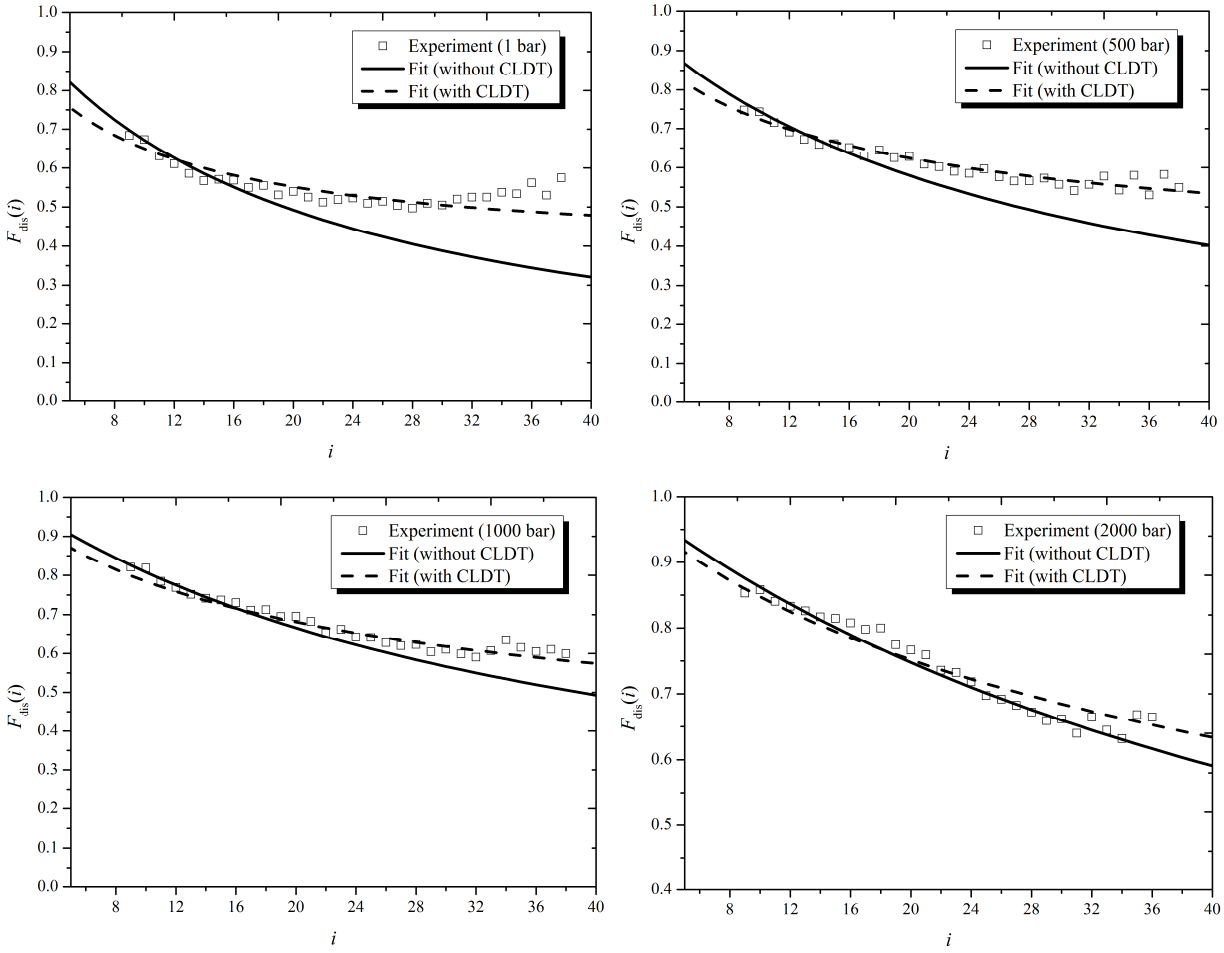

Figure 7-8. Number fraction of chains arising from disproportionation, $F_{dis}(i)$, as a function of chain length i, for PMMA from radical polymerization at 85 °C in TFT with c_{AIBN} = 0.05 mol L^{-1} and c_{MMA} = 0.67 mol L^{-1} and different pressure as indicated. Points: experimental values obtained from ESI-MS results; curves: best fits of Eq. 1 (without CLDT) and with CLDT equations, using parameter values as given in Table 7-3.

Inspection of Figure 7-8 shows similar fitting as observed with temperature. It seems that the pressure has a large effect on the shape of the curve. Large pressure makes the curve more linear and much closer to the classical (CLIT) modelling. Interestingly, the CLDT parameters, e and $k_t^{1,1}$, for small chains seems to fit the results and agree very well with what was obtained recently for CLDT parameters especially at 1 bar, 500 bar and 1000 bar. However, at higher pressure the behaviour becomes much closer to CLIT, and it was only possible to fit the data with CLDT parameters for large polymers, as reported in Table 7-3. Again, this may be explained in terms of average chain sizes being longer at higher pressure,

due both to increased k_p and smaller k_t (there is little effect of pressure on R_{init}, in great contrast to change of temperature). Thus these values provide consistent behaviour with what is known overall for radical polymerization.

Table 7-3. Parameters used to fit the experimental $F_{dis}(i)$ presented in Figure 7-8. Experimental k_t values are also reported.

pressure (bar)	**CLDT fitting**				**λ from CLIT fitting**
	$k_t^{1,1}$ (L mol^{-1} s^{-1})	e	k_t (L mol^{-1} s^{-1})	λ	
1	1.22×10^9	0.63	5.70×10^8	0.57	0.59
1	5.83×10^8	0.63	1.96×10^8	0.56	0.50
1	9.39×10^8	0.63	3.85×10^8	0.60	0.57
1	7.20×10^8	0.63	2.61×10^8	0.58	0.59
1	9.52×10^8	0.63	3.91×10^8	0.61	0.63
500	8.50×10^8	0.63	2.50×10^8	0.56	0.50
1000	1.08×10^9	0.63	2.66×10^8	0.58	0.43
1000	7.50×10^8	0.63	1.58×10^8	0.56	0.52
1500	2.25×10^8	0.20	1.25×10^8	0.45	0.43
2000	4.21×10^8	0.20	2.34×10^8	0.53	0.46
2000	1.61×10^8	0.20	7.99×10^7	0.38	0.32

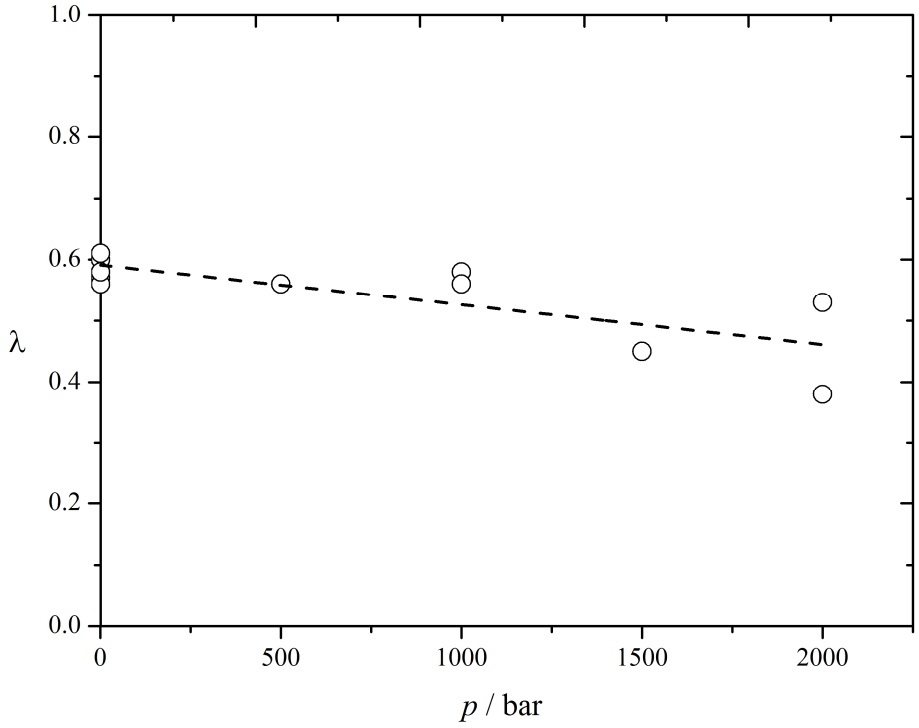

Figure 7-9. Effect of pressure on λ for free radical polymerization of MMA in TFT at 85 °C as a function of pressure employing c_{AIBN} = 0.05 mol L^{-1} as initiator and c_{MMA} = 0.67 mol L^{-1}, obtained accounting for CLDT.

Figure 7-9 shows the overall pressure effect on λ. As can be observed from Figure 7-9, λ slightly decreases with increasing pressure, in contrast to the impression created from the $F_{dis}(i)$ values, so again one sees the importance of proper kinetic modelling. This variation a positive activation volume, $\Delta V^{*}(\lambda)$ = 4.1 ± 1.2 cm^3 mol^{-1} and accounting for CLDT, determined using

$$\left(\frac{\mathrm{d}\ln\lambda}{\mathrm{d}p}\right)_T = -\frac{\Delta V^*}{RT} \qquad (13)$$

For the same reason as with temperature, $\ln\left(\frac{1}{\lambda}-1\right)$ vs. p has been plotted in Figure 7-10. This gives $\Delta V^{*}\left(\left(\frac{1}{\lambda}-1\right)\right) = \Delta V^{*}(k_{t,comb}/k_{t,dis})$ = –7.9 ± 1.1 cm^3 mol^{-1}, which indicates a larger activation volume for disproportionation than for combination.

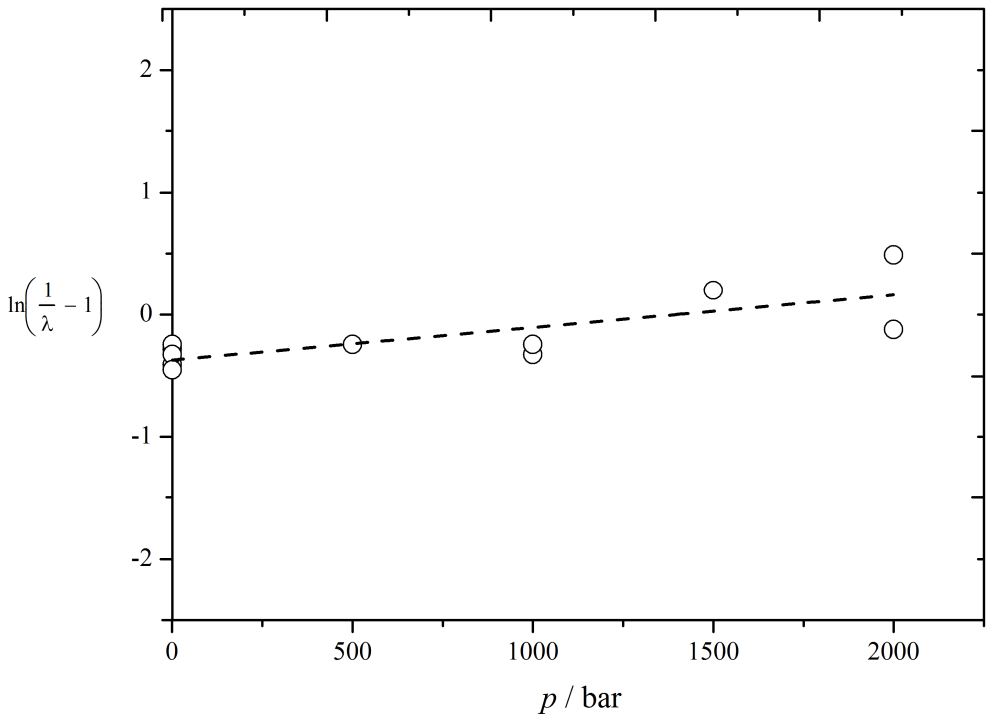

Figure 7-10. Effect of pressure on $\ln(\frac{1}{\lambda}-1)$ for radical polymerization of MMA in TFT at 85 °C as employing c_{AIBN} = 0.05 mol L^{-1} as initiator and c_{MMA} = 0.67 mol L^{-1}, obtained accounting for CLDT.

In addition, as before one can estimate the activation volume for the disproportionation process using

$$\Delta V^*(\lambda) = \Delta V^*\left(k_{\mathrm{t,dis}}\right) - \Delta V^*(k_{\mathrm{t}}) \qquad (14)$$

$$\Delta V^*\left(k_{\mathrm{t,dis}}\right) = \Delta V^*(\lambda) + \Delta V^*(k_{\mathrm{t}}) \qquad (14a)$$

This results in $\Delta V^*(k_{\mathrm{t,dis}})$ = 20.1 cm^3 mol^{-1} for termination by disproportionation employing $\Delta V^*(k_{\mathrm{t}})$ = 16 cm^3 mol^{-1}, the result that was obtained in Chapter 5 and $\Delta V^*(\lambda)$ = 4.1 cm^3 mol^{-1} from above. Since $\Delta V^*(k_{\mathrm{t,comb}}/k_{\mathrm{t,dis}}) = \Delta V^*(k_{\mathrm{t,comb}}) - \Delta V^*(k_{\mathrm{t,dis}})$ = –7.9 cm^3 mol^{-1}, one would obtain from the result here that $\Delta V^*(k_{\mathrm{t,comb}})$ = 12.3 cm^3 mol^{-1}. This makes no sense, as clearly the volume of the forming combination product must be less than the combined volumes of

the reactants, meaning that $\Delta V^*(k_{t,comb}) < 0$, as is invariably the case for a bimolecular reaction. Indeed, it similarly makes no sense that $\Delta V^*(k_{t,dis}) > 0$. Once again one is forced to wonder whether the calculations done here are valid, as they mix diffusion-controlled valued with chemically-controlled ones. Intuitively one could imagine that $\Delta V^*(k_{t,dis})$ is very small in value, due to the breaking C-H bond in the rate-determining step of disproportionation giving an increase in volume that might counteract the reduction from compression upon reaction encounter. One could perhaps nail an estimate of this value by employing as an estimate of $\Delta V^*(k_{t,comb})$ from a literature value of ΔV^* for combination of small-molecule radicals, for example *tert*-butyl or even ispropyl or methyl or ethyl.

Application of high pressure results in appreciably elevated *PDI* (results shown in Chapter 5). Increasing *PDI* with pressure could indicate that disproportionation becomes more prevalent as pressure mounts, which is in contrast to the finding here of more combination. Despite this discrepancy, similarly low *PDI* value (1.44 -1.55) has been reported for similar MMA polymerization in acetone with AIBN as initiator.[17] Assuming this is the case, low *PDI* might be rationalized by chain-length dependent propagation (CLDP), as this effect is observed with low monomer concentration; namely, *PDI*s were observed to decrease with dilution for polymerization of MMA. [18].

7.4. Effect of monomer on λ

As the chemical structure of a monomer is an important factor in the termination process, an investigation of the effect of monomer structure on λ was carried out.

7.4.1. Butyl methacrylate (BMA)

Figure 7-11 shows the ESI-MS-TOF spectrum for poly(butyl methacrylate) (PBMA) from a BMA polymerization. Distinguishable termination products are clearly evident. Typical λ fitting results are presented in Figure 7-12.

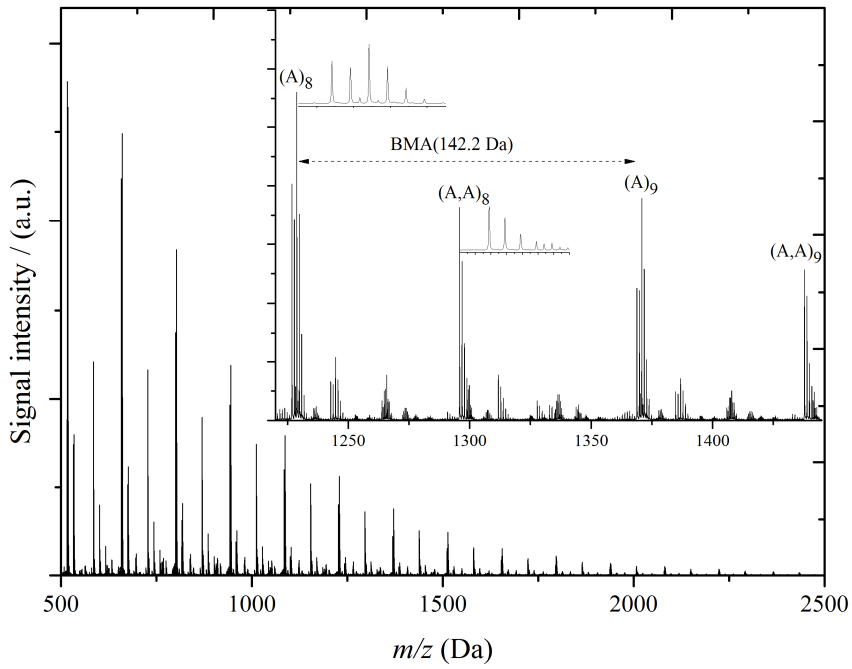

Figure 7-11. ESI-MS spectrum of poly(butyl methacrylate) obtained from radical polymerization in TFT at 85 °C with c_{AIBN} = 0.05 mol $L^{-1}$and c_{BMA} = 0.67 mol L^{-1}. The close-up shows a portion of the spectrum that is typical for two repeat units, with A and A,A denoting signals from disproportionation- and combination-generated species respectively, the degree of polymerization being as indicated, and A being the primary radical from AIBN.

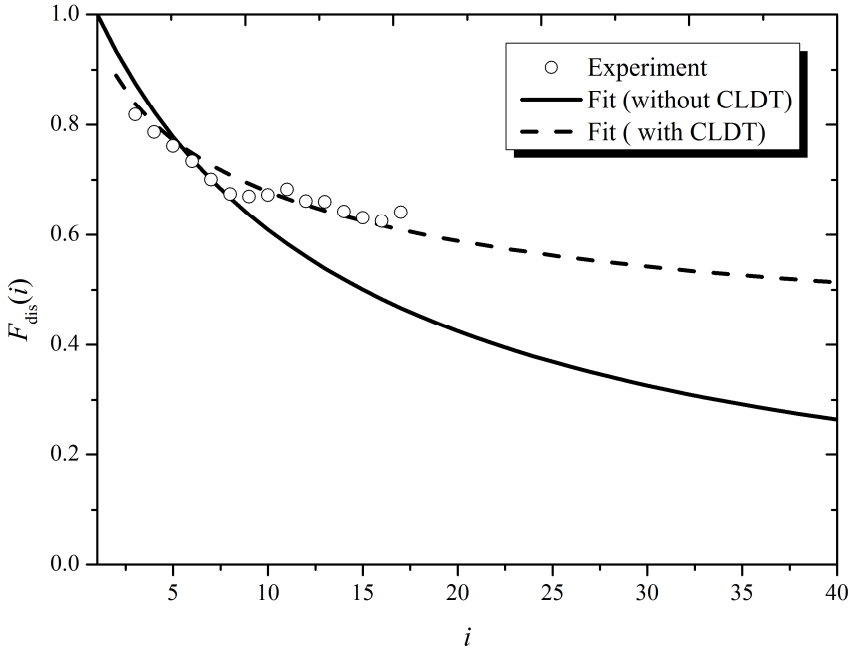

Figure 7-12. Number fraction of chains arising from disproportionation, $F_{dis}(i)$, as a function of chain length i, for PBMA arising from radical polymerization at 85 °C in TFT with c_{AIBN} = 0.05 mol L^{-1} and c_{BMA} = 0.67 mol L^{-1}. Points: experimental values obtained from ESI-MS results; curves: evaluations of Eq. 1 (without CLDT) using λ = 0.52 and with CLDT equations using λ = 0.54, e = 0.63 and $k_t^{1,1}$ = 6.5 × 10^8 L mol^{-1} s^{-1}.

Similar behaviour to MMA polymerization is clearly recognizable, i.e., Eq. 1 does describe the low-i data adequately, while including CLDT results in description of the entire range. That said, the range of i is not as extensive as with MMA. This is because of the larger molar mass of BMA than MMA that results in lower range of i.

Similar λ determination as with MMA is employed. Rate parameters employed in the analysis are the same as previously for f and k_d (Eqs. 3a and 3b), while the following Arrhenius expression for k_p, which is IUPAC-recommended, is used.[19]

$$k_p(\text{BMA}) = 3.802 \times 10^6 \text{ L mol s}^{-1} \exp\left(\frac{-22.9 \text{ kJ mol}^{-1}}{RT}\right) \qquad (17)$$

Analysis of the $F_{dis}(i)$ data with Eq. 1 (CLIT) yields λ = 0.52, which is close to but a little bit lower than the value obtained for MMA at the same temperature, although the two may be said to agree within experimental error. Also, CLDT equations with e = 0.63 and $k_t^{1,1}$ = 6.5 ×

10^8 L mol^{-1} s^{-1} fit the data very well with $\lambda = 0.54$. This e is taken from the literature while $k_t^{1,1}$ was chosen to reproduce the experimental k_t. That this $k_t^{1,1}$ is lower than that obtained for MMA at identical polymerization conditions is qualitatively consistent with the effect of monomer size on diffusion, i.e. a larger monomer will have slower diffusion.

Discussing further the MMA and BMA results, a comparison of the $F_{dis}(i)$ data shows slightly higher $F_{dis}(i)$ with BMA, as presented in Figure 7-13.

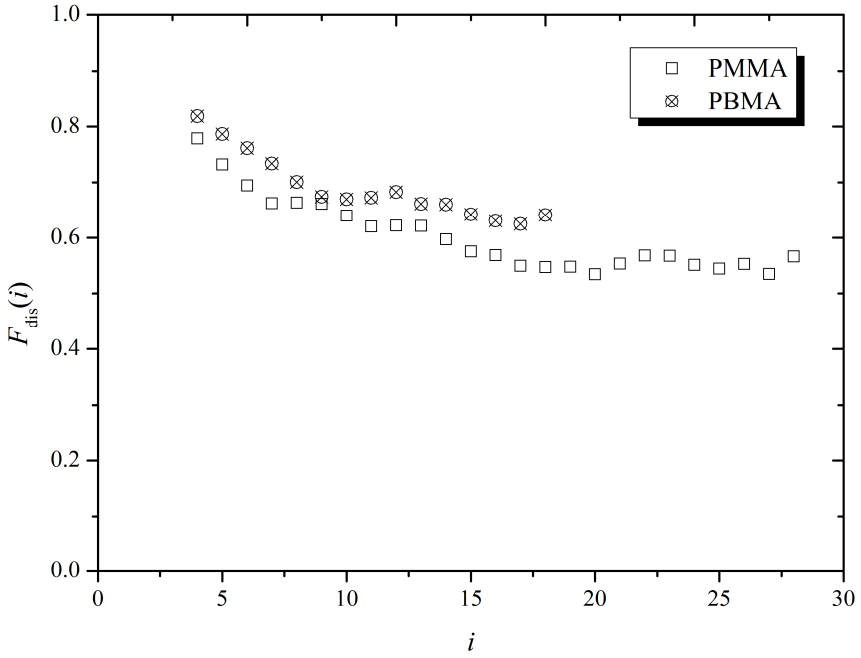

Figure 7-13. Comparison of PMMA and PBMA $F_{dis}(i)$ prepared at 85 °C employing c_{AIBN} = 0.05 mol L^{-1} and similar c_M = 0.67 mol L^{-1} in TFT.

This is in complete agreement with discussion for termination of small radicals and with the effect of viscosity. Namely, BMA has a higher viscosity than MMA, which then may affect combination process and lead to more disproportionation, which means higher $F_{dis}(i)$. In other words, this also might be related to the length of the ester alkyl group that is found to result in an increase in the disproportionation.[2, 20] That said, the true effect is told by the λ values, which if anything go in the opposite direction.

The above would point to the radical activity consideration that might have an effect on the termination pathway, in particular disproportionation, i.e. a tendency toward disproportionation for highly reactive radicals. A similar result obtained for λ for MMA and BMA would indicate no large effect. This is consistent with the low disproportionation products of polymerization of highly reactive radicals such as those in vinyl acetate and ethylene polymerization.[21]

Despite the reality that the MALDI technique is less friendly, it was also used. The MALDI spectrum for PBMA is presented in Figure 7-14

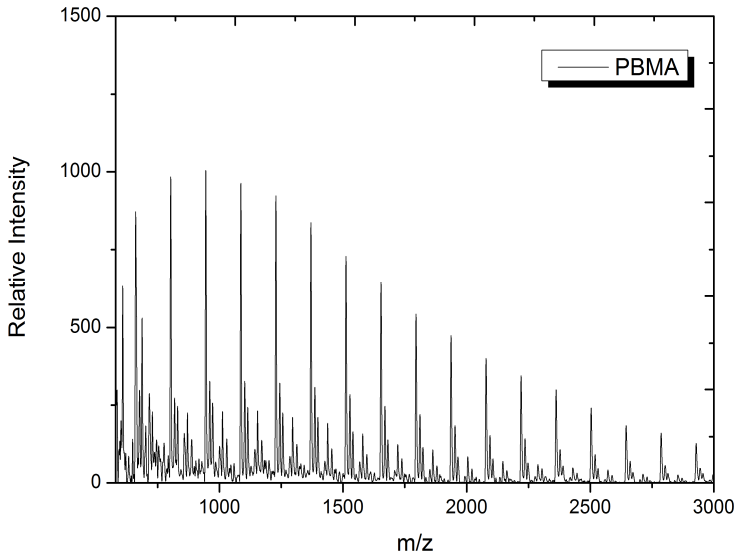

Figure 7-14. MALDI-TOF-MS spectrum of poly(butyl methacrylate) obtained from radical polymerization in TFT at 85 °C with c_{AIBN} = 0.05 mol L^{-1} and c_{BMA} = 0.67 mol L^{-1}.

Presented in Figure 7-15 are the $F_{dis}(i)$ values resulting from the spectrum of Figure 7-14. Figure 7-15 shows that the quantitative output for λ determination from our MALDI results is again inadequate. It is evident that the MALDI results do not give $F_{dis}(i)$ values that decline with increasing i, as theory says must be the case. Instead, Figure 7-15 displays $F_{dis}(i)$ that are essentially constant with average $F_{dis}(i)$ = 0.64 and 0.75 for PMMA and PBMA respectively.

However one should remember that $F_{dis}(i) \neq \lambda$, and that Eq. 1 cannot qualitatively fit the data of Figure 7-15, as already explained.

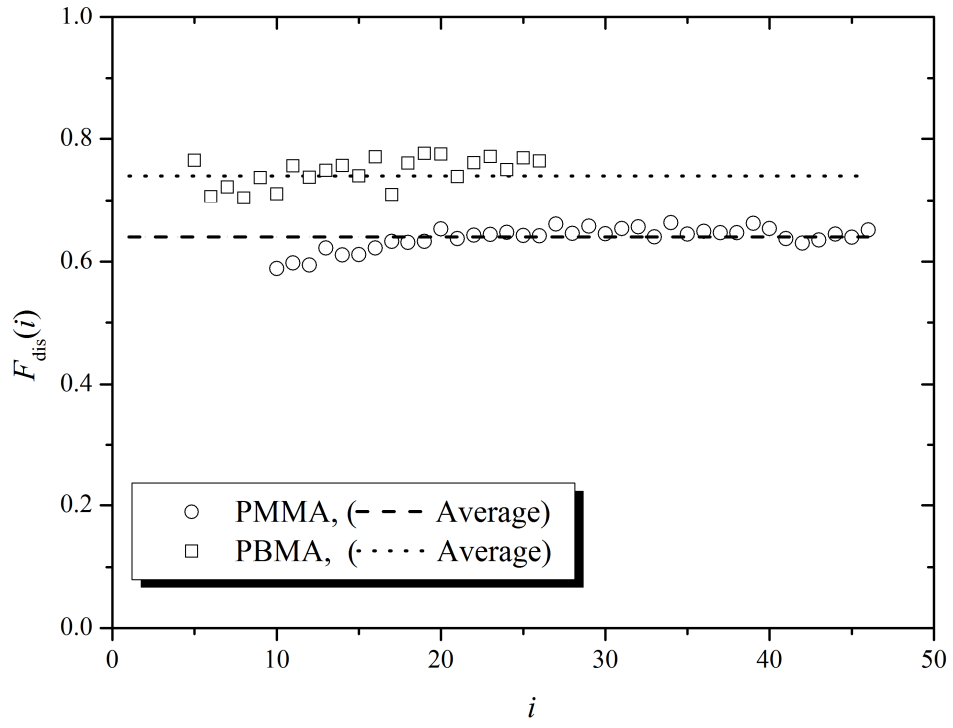

Figure 7-15. Number fraction of chains arising from disproportionation, $F_{dis}(i)$, as a function of chain length i, from MALDI-TOF-MS analysis of polymer from BMA and MMA polymerizations in TFT at 85 °C with c_{AIBN} = 0.05 mol L^{-1} and c_M = 0.67 mol L^{-1}. Points: experimental values; line: average of all the points, 0.64 and 0.74 for PMMA and PBMA respectively.

7.4.1.1. Temperature effect

Figure 7-16 clearly shows self-consistent results and identical behaviour of $F_{dis}(i)$ for PBMA to that observed for PMMA with temperature. Increasing the temperature results in decreasing $F_{dis}(i)$.

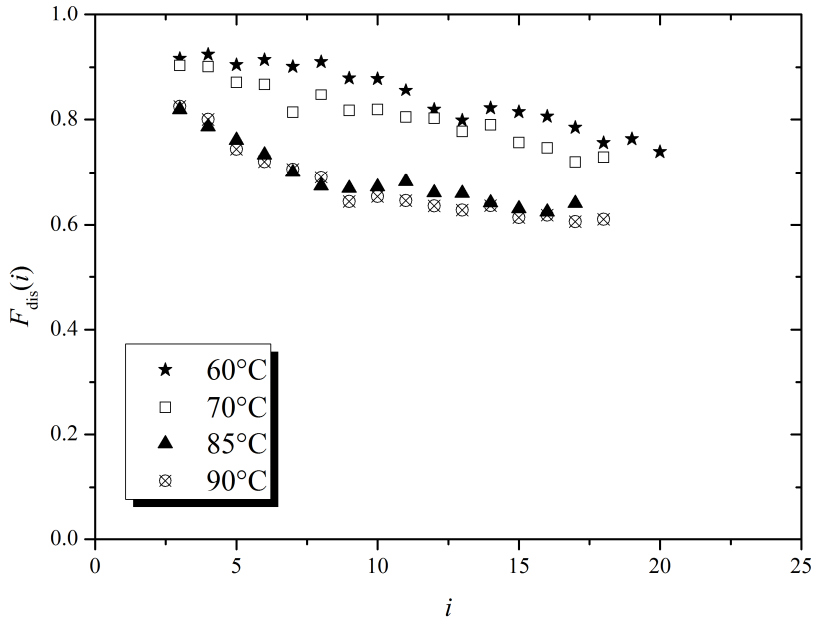

Figure 7-16. Effect of temperature on $F_{dis}(i)$, the fraction of chains formed by disproportionation, for solution polymerization of 0.67 mol L^{-1} BMA in TFT employing 0.05 mol L^{-1} AIBN as initiator at ambient pressure.

Determination of the value of λ from fitting with and without CLDT is shown in Figure 7-17. Exacatly as with MMA, and presumably for the same reason, results become better fitted by CLIT as the temperature decreases. Again, accounting for CLDT results in no large change in λ and shows consistency with the overall view of radical polymerization.

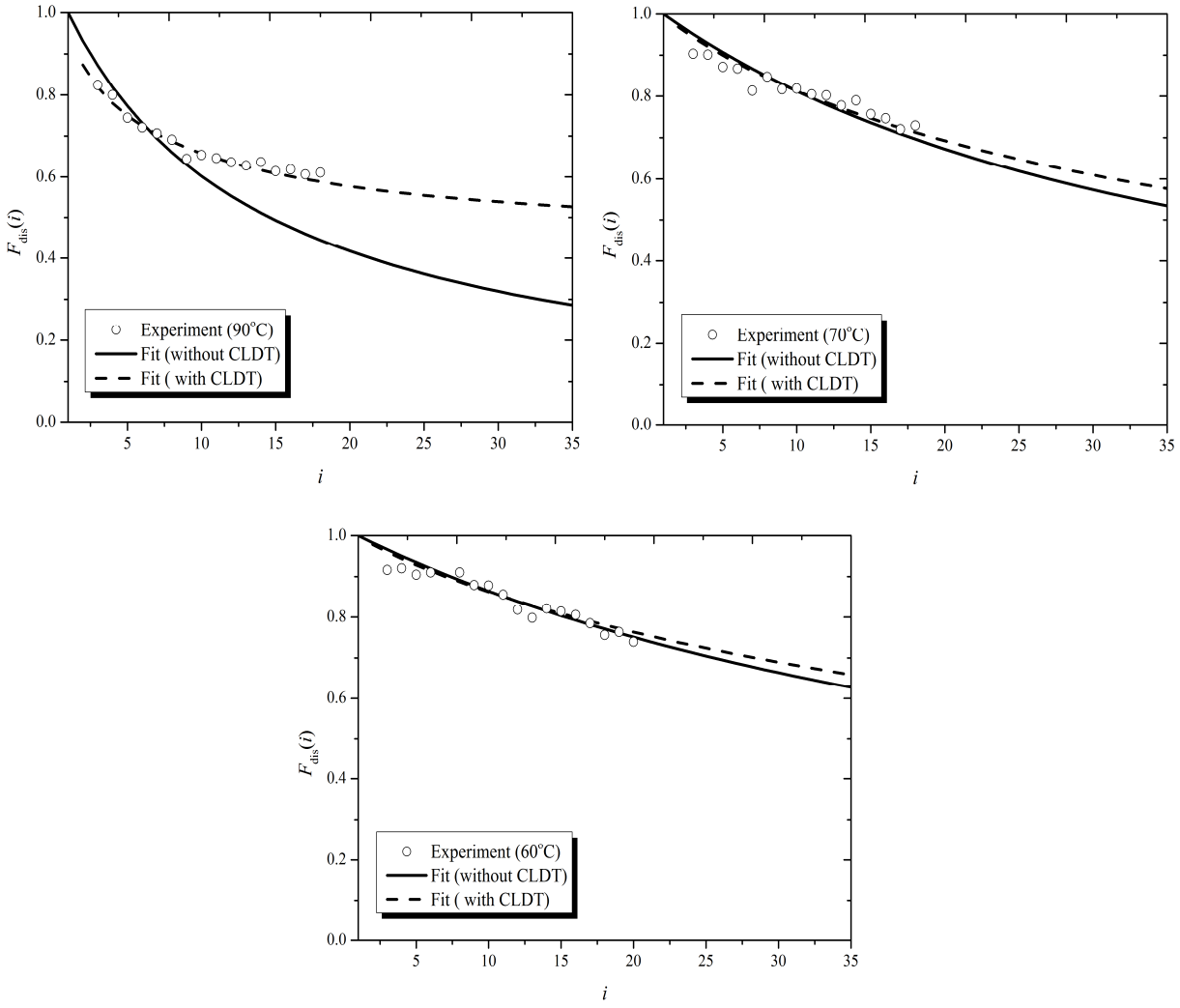

Figure 7-17. Number fraction of chains arising from disproportionation, $F_{dis}(i)$, as a function of chain length i, for PBMA arising from radical polymerization in TFT with c_{AIBN} = 0.05 mol L^{-1} and c_{BMA} = 0.67 mol L^{-1} at different temperatures as indicated. Points: experimental values obtained from ESI-MS results; curves: best fits of Eq. 1 (without CLDT) and with CLDT equations, resulting in parameter values as reported in Table 7-4.

Table 7-4. Parameters used to fit experimental $F_{dis}(i)$ with and without CLDT. The experimental k_t values are also reported.

θ (°C)	CLDT fitting				λ from CLIT fitting
	$k_t^{1,1}$ (L mol^{-1} s^{-1})	e	k_t (L mol^{-1} s^{-1})	λ	
90	6.75×10^8	0.63	2.45×10^8	0.56	0.55
85	6.44×10^8	0.63	1.89×10^8	0.54	0.52
70	1.48×10^8	0.20	8.01×10^7	0.40	0.33
60	1.14×10^8	0.20	5.39×10^7	0.34	0.27
50	1.34×10^8	0.20	5.74×10^7	0.21	0.17

For obvious reasons the results from CLDT fitting are recommended and used as the most accurate λ values. Analogous results to MMA mode of termination are obtained: the mode of termination decreases with decreasing temperature (see Figure 7-18) and is much the same in value. This is as expected, because there is no obvious reason why the length of a pendant alkyl group should affect either λ or its variation with temperature. The BMA data results in a positive activation energy for λ that is slightly high but may seem consistent with that for MMA, within experimental uncertainty, and Arrhenius expressions as follow:

$$\lambda(\mathrm{BMA, AIBN}) = 1.13 \times 10^{3} \exp\left(-\frac{22.8 \pm 4.1\ \mathrm{kJmol^{-1}}}{RT}\right) \qquad (18)$$

$$\frac{1}{\lambda} - 1 = \frac{k_{\mathrm{t,comb}}}{k_{\mathrm{t,dis}}} = 3.33 \times 10^{-6} \exp\left(\frac{37.2 \pm 3.2\ \mathrm{kJmol^{-1}}}{RT}\right) \qquad (18a)$$

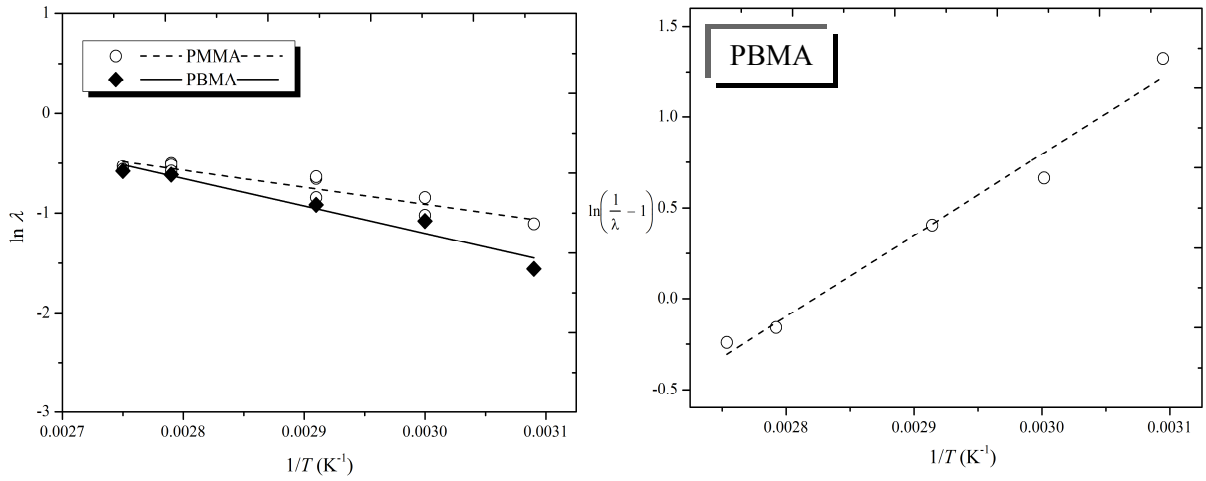

Figure 7-18. Arrhenius plots, a obtained from analysis using CLDT equations, for radical polymerization of momomers as indicated, initiated by 0.05 mol L^{-1} AIBN and with c_M = 0.67 mol L^{-1}. Points: experimental values; Lines: best linear fits.

7.4.2. Styrene (ST)

Although most methods indicate predominant combination for ST polymerization, a surprisingly wide range of values has been estimated for λ. Namely, values of 0.05 to 0.2 have been determined, although admittedly these were via indirect methods where precision was not high enough, and in which distinction between 0.05 and 0.2 was difficult.[1] In addition, and surprisingly, some studies found substantial disproportionation where λ of 0.33 and 0.40 had been estimated for ST polymerization.[22]

Usually it is said that one must do MALDI for PST analysis and with aid of silver cations for ionization. This is because of the only Ag^+ ability to ionize the PST by interacting with π-electrons of the phenyl groups. However, this seems not to be the case with small chains PST synthesised in this work. The PST small size may be the rationalization of the successful ESI-MS result obtained via Na^+ cation adducts. Our ESI-MS result for ST polymerization is shown in Figure 7-19. By inspecting Figure 7-19, one can see predominant combination products. However, an additional component in the spectrum, the signal at 1335.9, has the mass of the combination component (AA) plus 32. It is assigned to a combination of two radicals, one of which has incorporated oxygen (O_2). Such components are known to occur in the early polymerization period as a consequence of imperfect deoxygenation.[23] This might be related to slow propagation, which is the case for ST. It is interesting that no such disproportionation species, i.e. (A) plus 32, are observed, even though the (A) signals are the strongest in the spectrum. This suggests that the oligomers containing O_2 are formed from a combination involving oxygen-centered radicals that are relatively long-lived. The latter deduction explains the inhibitory role of residual oxygen at the beginning of a polymerization experiment. If it were the case that the incorporated O_2 radical quickly adds to monomer, then the absence of disproportionation product with O_2 cannot be explained unless there is no disproportionation. This may be the explanation for the +32 signals that we have observed. It

is important to note that the incorporated O_2 peaks have a molar mass very close to those of the disproportionation products, which therefore may be interpreted wrongly as being disproportionation products. Furthermore, the O_2 reaction might be another cause of the unpredicted results for ST shown in Chapter 3 from variation of R_p with c_I.

However, our results clearly show that no products of the disproportionation have been observed (see close up in Figure 7-19). This is also confirmed by the isotopic distribution that distinguishes combination from disproportionation. From these MS results one would have to say that $\lambda \approx 0$.

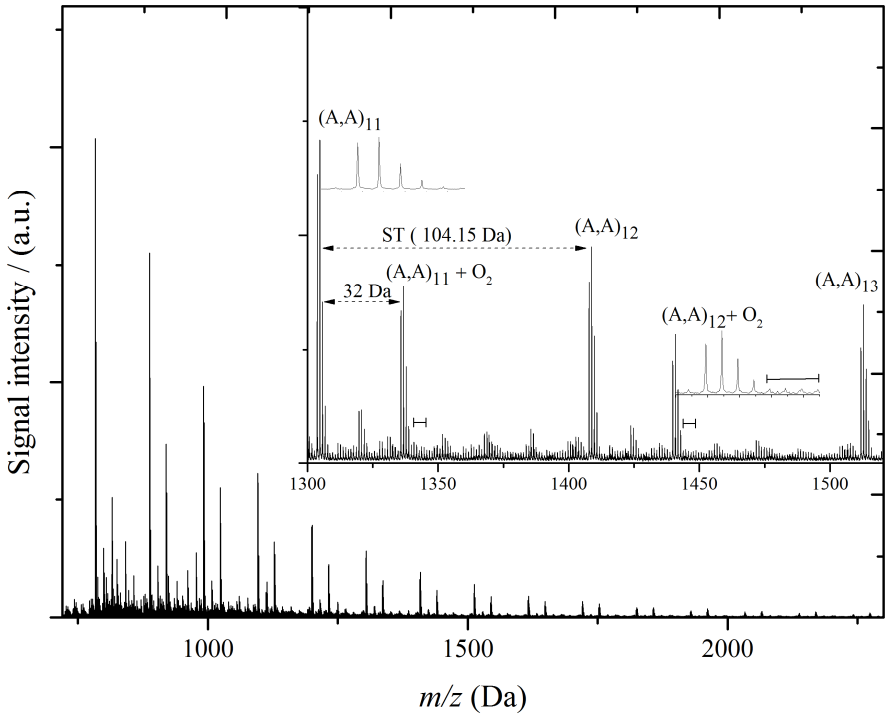

Figure 7-19. ESI-MS spectrum of polystyrene obtained from radical polymerization in EBz at 90 °C with c_{AIBN} = 0.05 mol L^{-1} and with c_{ST} = 0.67 mol L^{-1}. The close-up shows a portion of the MS spectrum that is typical for two repeat units, with A,A denoting signals from combination generated species, the degree of polymerization being as indicated, and A being the primary radical from AIBN.

7.4.3. *n*-Butyl acrylate (BA)

Acrylate termination has been estimated to be exclusively by combination.[24, 25] However, transfer reactions may lead to erroneous conclusions being drawn for these monomers. Higher temperature polymerization of acrylates involves additional mechanisms of back-biting followed by β-scission or branch formation.[26, 27] Figure 7-20 shows the ESI-MS-TOF spectrum obtained for PBA at 85 °C.

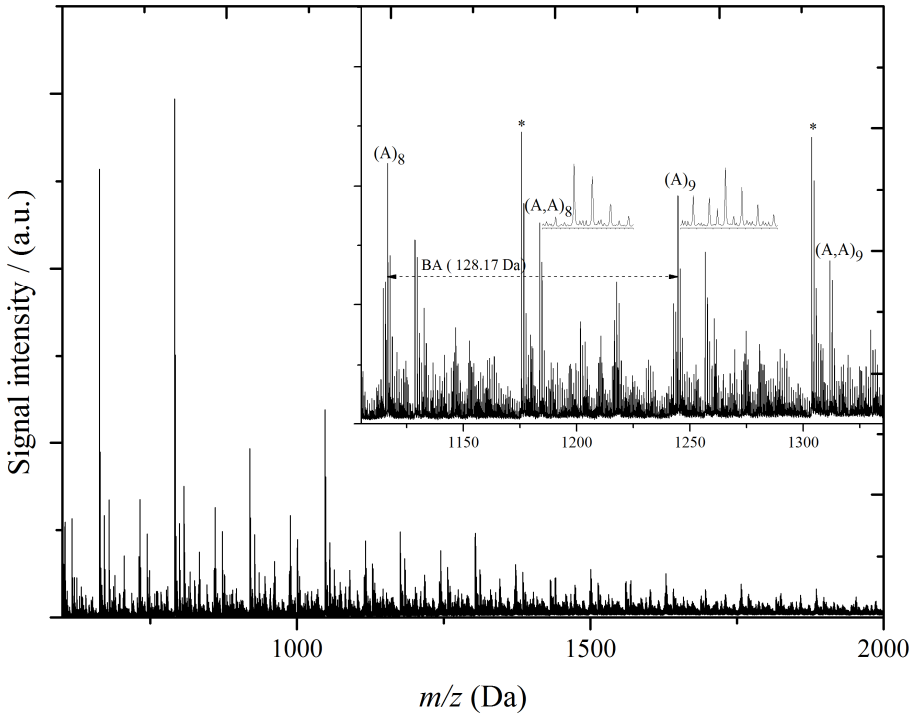

Figure 7-20. ESI-MS spectrum of poly(butyl acrylate) obtained from radical polymerization in TFT at 85 °C with c_{AIBN} = 0.05 mol L^{-1} and with c_{BA} = 0.67 mol L^{-1}. The close-up shows a portion of the MS spectrum that is typical for two repeat units, with A and A,A denoting signals from disproportionation- and combination-generated species respectively, the degree of polymerization being as indicated, and A being the primary radical from AIBN.

Not all the major peaks, and many of the minor ones, in the ESI-MS spectrum in Figure 7-20 could be identified. The presence of a plethora of peaks supports the significant contribution of chain transfer and scission of acrylates at high temperature.[28]

Note that the chain ends formed by combination and disproportionation can be readily identified; however, the presence of short-chain branches make it complicated to measure accurately the ratio between combination and disproportionation as the molar mass of the branched structure might be the same as that of a linear structure containing the same total number of BA repeat units. The overabundance of species introduced by chain transfer to polymer makes it unlikely that the MS method could be used to determine λ for acrylates at moderate to high temperatures.[29] Nevertheless it seems clear that there are disproportionation products, where such are not observable by ST. Thus it seems that $\lambda > 0$ for BA for high temperatures at least.

7.5. Conclusion

Unlike other techniques that have been commonly applied to the analysis of synthetic polymers, the ESI-MS technique involved direct observation of the products of disproportionation and combination, which is tremendously appealing in contrast to the indirect nature of other literature approaches. The dominant termination mode has been found to depend on the structure of the monomer, temperature and, to a lesser extent, on the pressure. Increasing temperature results in more disproportionation, while increasing pressure results in more combination. Properly accounting for CLDT was found to function under all conditions employed and resulted in no large change to the obtained value of λ, but at the same time it returned CLDT parameter values that are fully in accord with those from the recent literature. This gives confidence both in the reality of CLDT and the robustness of the method for determining λ: while it is best to account for CLDT in using it, no great error is introduced if one does not. Similar modes of termination were observed for MMA and BMA; however, ST shows a complete combination process and no clear disproportionation products

were observed. The BA result confirms the complicated pathways for dead-chain formation that there are in acrylate systems; these seem to prevent the use of ESI-MS-TOF for λ determination. That said, it seems qualitatively clear that there is some disproportionation in BA systems.

In summary, this chapter probably has provided the first accurate and systematic investigation into the effect of temperature, pressure and monomer on mode of termination, which is no small feat given that such a study has taken the best part of 70 years to arrive.

References

[1] G. Moad, D.H. Solomon, The Chemistry of Radical Polymerization, 2nd fully rev. ed., Elsevier, 2006.
[2] S. Bizilj, D. Kelly, A. Serelis, D. Solomon, K. White, Australian Journal of Chemistry, 38 (1985) 1657-1673.
[3] H. Fischer, H. Paul, Accounts of Chemical Research, 20 (1987) 200-206.
[4] "Initiators for High Polymers", in, AKZO Nobel Chemicals, 2006.
[5] M. Buback, B. Huckestein, F.D. Kuchta, G.T. Russell, E. Schmid, Macromolecular Chemistry and Physics, 195 (1994) 2117-2140.
[6] S. Beuermann, M. Buback, T.P. Davis, R.G. Gilbert, R.A. Hutchinson, O.F. Olaj, G.T. Russell, J. Schweer, A.M.v. Herk, Macromolecular Chemistry and Physics, 198 (1997) 1545-1560.
[7] C. Barner-Kowollik, G.T. Russell, Progress in Polymer Science, 34 (2009) 1211-1259.
[8] J. Barth, M. Buback, Macromolecular Rapid Communications, 30 (2009) 1805-1811.
[9] J. Barth, M. Buback, Macromolecular Reaction Engineering, 4 (2010) 288-301.
[10] A.A. Zavitsas, C. Chatgilialoglu, Journal of the American Chemical Society, 117 (1995) 10645-10654.
[11] M. Stickler, G. Meyerhoff, Die Makromolekulare Chemie, 179 (1978) 2729-2745.
[12] Z.B. Alfassi, Chemical kinetics of small organic radicals, CRC Press, Boca Raton, Fla., 1988, Chapter 6.
[13] M.J. Gibian, R.C. Corley, Chemical Reviews, 73 (1973) 441-464.
[14] J.M. Asua, S. Beuermann, M. Buback, P. Castignolles, B. Charleux, R.G. Gilbert, R.A. Hutchinson, J.R. Leiza, A.N. Nikitin, J.P. Vairon, A.M. Van Herk, Macromolecular Chemistry and Physics, 205 (2004) 2151-2160.
[15] A.N. Nikitin, R.A. Hutchinson, M. Buback, P. Hesse, Macromolecules, 40 (2007) 8631-8641.
[16] S. Beuermann, M. Buback, High Pressure Research, 15 (1997) 333-367.
[17] K. Liu, E. Kiran, Industrial and Engineering Chemistry Research, 47 (2008) 5039-5047.
[18] T. Malavasic, U. Osredkar, I. Anzur, I. Vizovisek, Journal of macromolecular science. Chemistry, A25 (1988) 55-64.
[19] S. Beuermann, M. Buback, T.P. Davis, R.G. Gilbert, R.A. Hutchinson, A. Kajiwara, B. Klumperman, G.T. Russell, Macromolecular Chemistry and Physics, 201 (2000) 1355-1364.
[20] K. Matyjaszewski, T.P. Davis, Handbook of radical polymerization Wiley-Interscience, 2002.
[21] C.H. Bamford, G.C. Eastmond, D. Whittle, Polymer, 10 (1969) 771-783.
[22] O.F. Olaj, H.F. Kauffmann, J.W. Breitenbach, H. Bieringer, Journal of Polymer Science: Polymer Letters Edition, 15 (1977) 229-233.
[23] M. Buback, H. Frauendorf, F. Günzler, P. Vana, Polymer, 48 (2007) 5590-5598.
[24] C.H. Bamford, R.W. Dyson, G.C. Eastmond, Polymer, 10 (1969) 885-899.
[25] G. Ayrey, M.J. Humphrey, R.C. Poller, Polymer, 18 (1977) 840-844.
[26] C. Plessis, G. Arzamendi, J.R. Leiza, H.A.S. Schoonbrood, D. Charmot, J.M. Asua, Macromolecules, 33 (2000) 4-7.
[27] J. Chiefari, J. Jeffery, R.T.A. Mayadunne, G. Moad, E. Rizzardo, S.H. Thang, Macromolecules, 32 (1999) 7700-7702.
[28] M.C. Grady, W.J. Simonsick, R.A. Hutchinson, Macromolecular Symposia, 182 (2002) 149-168.
[29] T. Junkers, C. Barner-Kowollik, Journal of Polymer Science, Part A: Polymer Chemistry, 46 (2008) 7585-7605.

Chapter 8. High-Conversion Radical Polymerization

In this chapter are presented preliminary results of the application of Raman spectroscopy to examine the radical homopolymerization of methyl methacrylate (MMA) and dodecyl methacrylate (DMA) up to the high-conversion regime. Related to this, arguments on the origin of the gel effect are discussed.

8.1. Introduction

In dealing with radical polymerization (RP), the course of the process is usually divided into three conversion regimes, namely low conversion, medium conversion and high conversion. So far in this work, polymerization was only carried out in the low-conversion regime. Carrying out the polymerisation to high conversion makes the polymerization exhibit more complex behaviour. Namely, extending the polymerization to high conversion raises two significant effects, the gel effect and the glass effect. The gel effect results in rapid increase in the rate of polymerization, while the glass effect occurs in the late stages of the polymerization, when the polymerization rate becomes very slow.

The gel effect takes place above a certain conversion, at which the rate of polymerization spectacularly increases, and polymer is produced with a large increase in size, heat production and dispersity.[1-3] This rapid increase is well known as an autoacceleration, a phenomenon that is encountered in RP of many monomers, most notably methyl methacrylate, but also for example styrene, where it has a lower degree of severity. This fascinating phenomenon is also known as the ‘Trommsdorff-Norrish effect’ or just the ‘Trommsdorff effect’, in recognition of the first scientists to report it. Figure 8-1 illustrates a typical conversion-time result for RP of MMA, showing the gel effect.

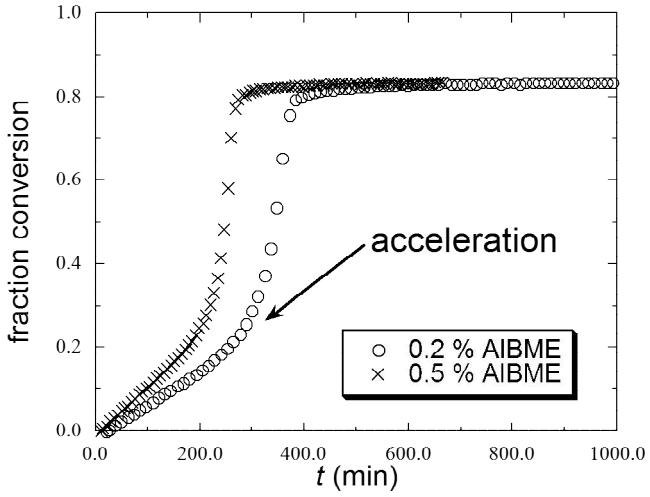

Figure 8-1. Results for bulk MMA polymerization at 50 °C with two different concentrations of azoisobutyromethylester (AIBME) as initiator.[4]

The autoacceleration behaviour leads to difficulties in controlling the polymerization reaction to completion as its exothermic nature can cause an explosion in larger reactors. Further, it also leads to difficulties in controlling the properties of the final products. Although this phenomenon can be mitigated by using a transfer agent (for reasons that are not clearly understood) or by carrying out the reaction in a solvent, these procedures are often expensive and environmentally unsafe. However, by understanding the origin of the gel effect it might be possible to control the polymerization reaction under this regime and avoid using environmentally unfriendly procedures. However, investigating this phenomenon initially requires a proper method to monitor the polymerization over the complete course of polymerization.

The initial purpose of this section was to find a proper, easy way to monitor the polymerization reaction over the complete course of polymerization. When that is satisfactorily achieved, further investigation of different factors influencing the gel effect can be then carried out. Because termination is diffusion controlled, it must be sensitive not just to conversion, but also to radical size. The latter is the phenomenon of chain-length-

dependent termination (CLDT). It is now recognized that it is responsible for many radical polymerization phenomena that otherwise defy explanation. Studying the chain length influences on the gel effect was the main goal. If the gel effect is linked to a specific physical phenomenon, it is only logical to work under different experimental circumstances where this phenomenon is reduced or eliminated. The influence on the gel effect of variation of chain length via chain transfer, temperature, initiator concentration and even RAFT agent were the main factors in mind for the present study. The idea also was to eliminate experimental difficulties in determining the rate of polymerization over the whole range of the conversion and gather enough information to provide a full experimental picture of the gel effect. Additionally, this would generate data for later modelling purposes.

8.2. Experimental section

Methyl methacrylate (MMA) high-conversion radical polymerizations were carried out in bulk employing the thermal initiator 2,2'-azobisisobutyronitrile (AIBN). MMA and AIBN were purified by standard procedures, and dissolved oxygen was removed by flushing the mixture with nitrogen for about 15 minutes. A small metal sample pan was used as the polymerization vessel. The polymerization solution was transferred quickly into the pan and covered quickly by a thin microscopic slide, which was held by surface tension, thus preventing monomer evaporation during polymerization. The pan was then transferred inside the temperature controlled stage, which was closed and placed on the Raman instrument stage. The use of a sample pan was quite satisfactory for these experiments, and it did not seem necessary to adopt any other special encapsulation procedures. Monomer conversions were monitored via online Raman spectroscopy on the double bond around 1 638 cm^{-1}, which is assigned to the monomer C=C stretching mode. By measuring the integrated peak area, conversion can then be obtained.

The Raman spectra were obtained with a Renishaw Raman System 1000 Spectrometer. The Raman spectra Linkam stage, THMS600/HSF91, was used. Temperatures were controlled by TMS94 (Linkam) temperature controller, attached to the stage and accurate to ±0.1 °C. The air-cooled Argon ion laser with a blue emission line at 488.0 nm was used as the incident light. The spectra were gathered from the optimum signal intensity during the whole polymerization; these were about 300 micron in depth under the surface of the polymerization mixture. It was found that by monitoring the surface, there was no substantial drift due to the transformation from liquid monomer to solid polymer. No internal calibration standard was required, as also reported in the literature.[5]

8.3. Raman spectroscopy

Raman spectroscopy is a well-known technique that is used to provide vibrational information about chemical bonds. It relies on a light source, usually from a laser, which interacts with molecular vibrations, thereby resulting in the energy of the laser photons being shifted up or down. Unlike FT-IR – which requires a finite thickness of the sample in order to control the absorption intensity of the molecular vibrations that might also affect the light transmission by transforming from liquid to solid state throughout the polymerization – Raman has no restriction with respect to sample size, shape or thickness.

Raman has some additional advantages, unlike other vibrational techniques: Raman spectra have no rotational broadening, and Raman bands are generally very sharp and narrow.[6] Although the phenomenon of fluorescence is considered to be a major problem in using Raman, using a different laser wavelength can eliminate such fluorescence problems. Raman provides both qualitative and quantitative information about the sample. Figure 8-2 presents typical Raman spectra from this work for bulk MMA polymerization to high conversion.

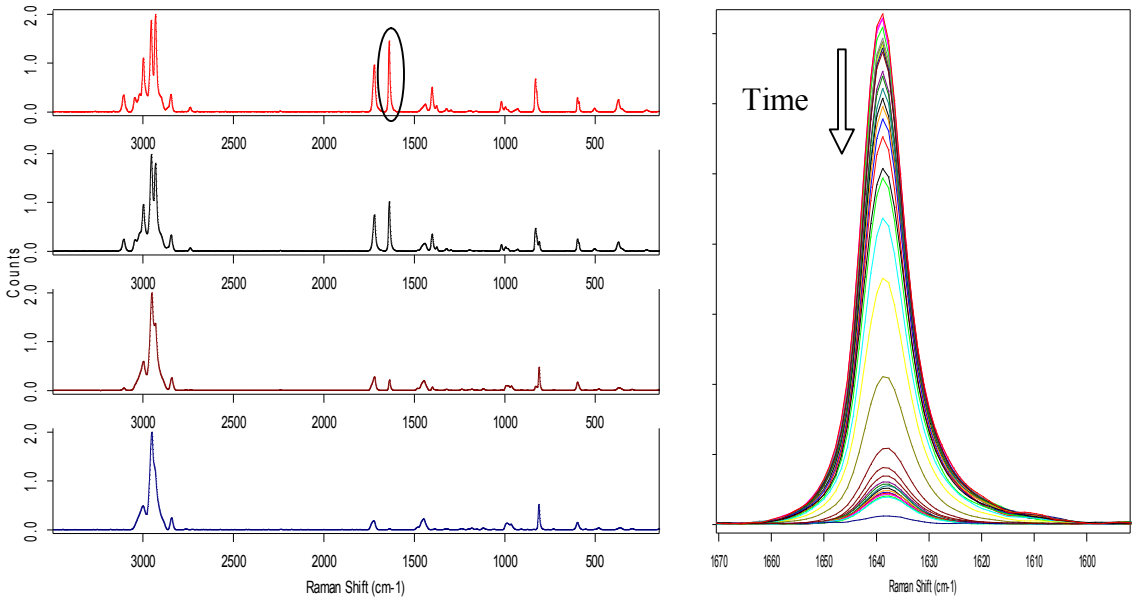

Figure 8-2. Left: full absorbance spectra recorded during radical bulk polymerization of bulk MMA at 80 °C using AIBN as initiator. Right: close-up of the 1 638 cm^{-1}peak as a function of time.

8.4. Autoacceleration overview

Essentially, the physical origins of the gel effect remain poorly understood at a fundamental level since its first observation by Norrish and Brookman in 1939.[2] To explain the effect, recall that initiation, propagation and termination are completely different chemical reactions with different responses to conditions. Termination involves the reaction between two chain ends. However, in concentrated solutions, the viscosity of the reaction mixture becomes high as polymer chains form. This high viscosity hinders the diffusion of chains, so the rate of terminations slows considerably. However, the diffusion of small monomers is hardly affected by viscosity, and besides, propagation is chemically controlled, so it proceeds as before. In addition, the initiator continues to add more free radicals to the system. On other hand, in dilute solutions, the viscosity never builds up to the point where diffusion of chains is largely slowed, so autoacceleration does not occur.

This subject has been debated for many years. Several theories have been presented that could potentially explain the gel effect. However, experimental tests to distinguish between these theories have been lacking. In spite of the many kinetic models that have been proposed to describe the gel effect, not surprisingly these models often fit experimental data equally well, due to the large number of adjustable parameters. Thus, their successful fitting does not completely prove the validity of these models, and the fact that adjustable parameters are needed of itself suggests that the autoacceleration phenomenon in RP is not perfectly understood.

Many efforts have been devoted to understanding the cause of this effect. The phenomenon is undoubtedly related to the termination process, which involves complex macromolecular dynamics;[7-10] this, in turn, is linked to the diffusion. The debate lies in the details of exactly what type of diffusion is important. Most work assumes that termination is controlled by translational diffusion at the gel-effect conversion regime.[11] Translation diffusion, in actual fact, is found to be dependent on many factors: solution viscosity, chain length, chain entanglement, polymer coil dimensions and polymer-solvent interactions are all found to influence the diffusion rate.[12] Most of these factors have been studied thoroughly but they have failed to explain the entire cause of the gel-effect phenomenon.

Increased viscosity with conversion was considered to be the cause of the gel effect by Norrish, Smith [7] and Trommsdorff et al.,[8] who concluded that higher viscosity causes an earlier gel effect. An experiment by Trommsdorff confirmed that the gel effect occurs earlier when PMMA was pre-dissolved in the reaction mixture,[8] whereas a later gel effect occurs with an increased amount of solvent.[13, 14] Conversely, other groups concluded that bulk viscosity change alone did not provide an adequate explanation for the rate determining factor in termination.[15] This theory initially presumed that the gel effect onset corresponded to the onset of diffusion controlling the termination reaction. However, now it

is well known that termination is diffusion controlled from the beginning of the polymerization.[16] In addition, later this was ascribed to the shift in different diffusion processes. It is simple to discredit viscosity alone from being the cause of the gel effect, because viscosity changes significantly from the very beginning of a bulk polymerization, but the gel effect does not commence until of order 20% conversion in the case of MMA. Most extremely, how to explain the absence of a gel effect in dodecyl acrylate (DA) polymerization, in which bulk viscosity is changing throughout.

Another theory was proposed by O'Driscoll to explain the gel effect: that it coincides with the formation of chain entanglements,[17] which can play a pivotal role in restricting chain mobility. This has been considered a potential contributing factor to diffusion-controlled termination, as entanglements should form at higher conversions. However, this has been shown not be the main reason, as found by O'Neil et al., who pointed out that entanglements begin to form at much lower conversions than the gel effect commences.[1] In fact two further studies confirmed that the gel effect can occur under conditions where the molar mass of polymer formed is too small to be considered entangled.[18, 19]

A different idea, based on free volume theory, was proposed to explain the onset of the gel effect by Balke and Hamielec.[20] Decreasing the free volume, as monomers are converted to polymer, restricts mobility and can be adequate to account quantitatively for the observed decrease in the k_t. Although this theory was effective in predicting the effect of temperature on k_t,[21] it is incomplete, for it cannot describe the lower gel effect conversion onset of MMA compared to styrene, not to mention the solvent effect on k_t.

Despite the fact that most attempts to explain the gel effect have fallen into either entanglement or free volume pictures, neither is adequate to describe the gel effect completely. A different picture to describe termination kinetics on the basis of short-long

termination has emerged.[22, 23] The idea is that termination of long chains become so hindered due to diffusion limitations caused by viscosity that they can only terminate when short chains diffuse into their vicinity. As the population of short chains is presumably small at the gel effect onset, the overall rate of termination decreases strongly. This is a process that is governed by the diffusion of the shorter, more mobile chains and by the chain length.

Because termination is diffusion controlled, it must be sensitive not just to conversion, but also to the radical size. The examples of methyl acrylate (MA) and dodecyl acrylate (DA) are interesting: k_t as a function of monomer conversion shows no change with DA but does change with MA (Figure 8-3). This behaviour is a mystery. It may illustrate that there is an influence of chemical structure on the gel effect.[24] Consequently, this may lead to the cause of the gel effect not being completely related to conversion. Further, it remains to be related properly to CLDT.

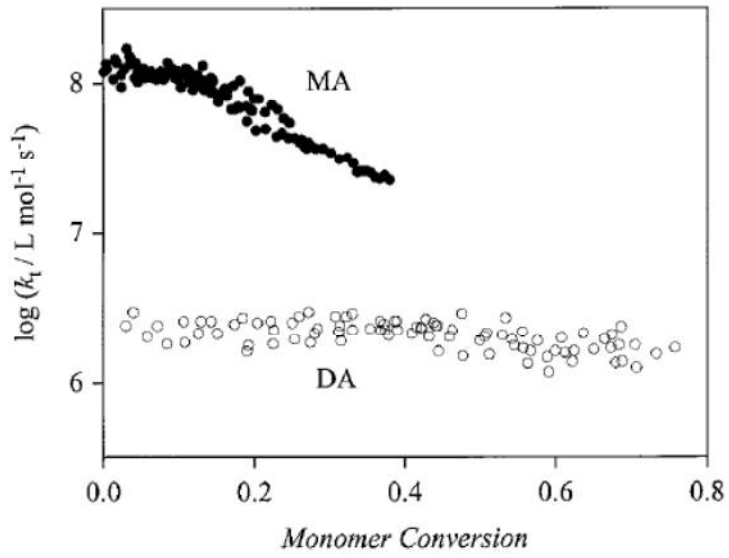

Figure 8-3. Variation of termination rate coefficients with monomer conversion, as measured by single-pulse PLP, in bulk MA and DA homopolymerizations at 40 °C and 1 000 bar.[25]

8.4.1. The effect of temperature on the onset of the gel effect

The conversion-time data for bulk MMA polymerization monitored via Raman spectroscopy at different temperatures is shown in Figure 8-4. Although conversion-time data prove adequately the ability of Raman spectroscopy to monitor the polymerization over the complete course of polymerization, the results were not as promising as those shown in Figure 8-1, for which dilatometry was used. In the present study there are fluctuations in the data, especially at the initial stage. This might affect the quality of carrying out quantitative investigations. However, clearly a qualitative picture of the gel effect can still be observed using the Raman technique. Namely, Figure 8-4 show a slow polymerization rate in the initial stage of the polymerization reaction; the rate then accelerates with an increasing extent of polymerization; and after that there is a sharp slowdown of the rate at the later stage of polymerization, the so-called glass effect. Evidently, temperature is found to have an effect on the onset of the gel effect, as shown in Figure 8-4.

It is essential to know that experimental evidence for the gel effect usually takes the form of a rise in the slope of a plot of monomer conversion versus time. Three important markers are usually assigned to the gel effect occurrence: the critical conversion at which the the gel effect starts; the onset time of the gel effect; and the severity of the gel effect. Increasing the temperature leads to the autoacceleration starting at an earlier *time*. This result is in agreement with the literature.[20, 26] On the other hand, the critical conversion seems to be slightly displaced to lower values as the temperature decreases. In addition, the severity of the gel effect appears to be reduced with lowering the temperature. Finally, the temperature also has a clear impact on final conversions, as they increase as the temperature is increased. Indeed, this is consistent with the glass transition occurring at higher weight fraction of polymer as temperature increases.

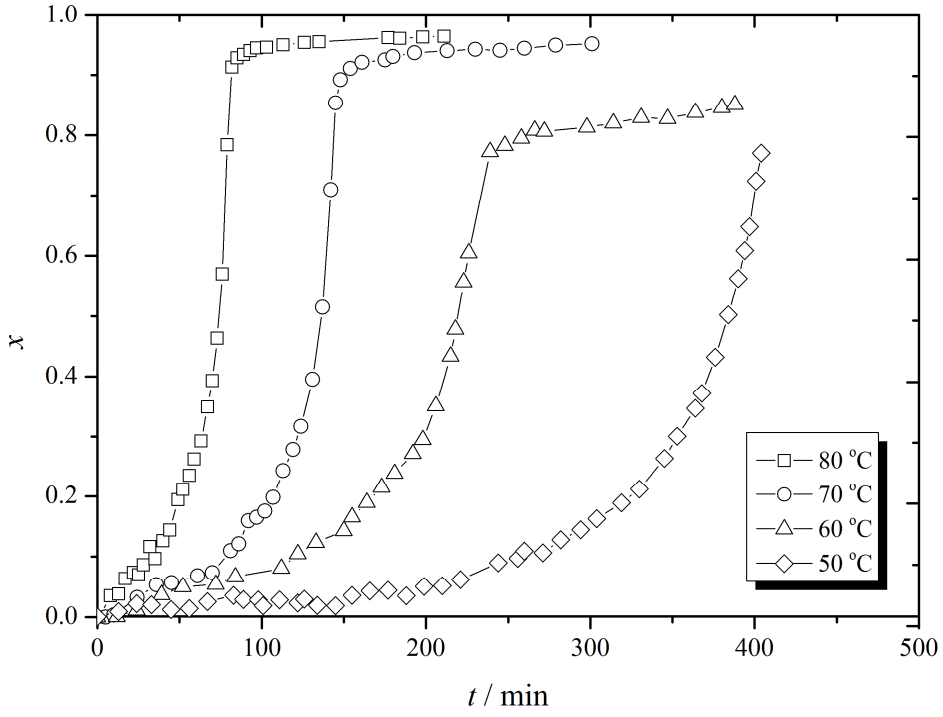

Figure 8-4. Monomer conversion, as measured by Raman spectroscopy, as a function of time for MMA bulk polymerization employing 0.5 wt.% AIBN at temperatures as indicated.

8.4.2. Initiator concentration effect on the onset of gel effect

Likewise, initiator concentration was found to have an effect on the onset of the gel effect, as shown in Figure 8-5. Namely, increasing the initiator concentration leads to an earlier onset of the gel effect. Furthermore, the critical conversion seems to be slightly displaced to lower values as initiator concentration decreases. It is noted that lower initiation concentration means longer average chain length. In addition, the severity of the gel effect seems to be slightly reduced by lowering the initiator concentration. Lastly, final conversion increased as the initiator concentration was increased, although it seems unlikely that this effect is real. For example, the data of Figure 8-1 show that a glass-effect conversion that is independent of initiator concentration, exactly as one would expect.

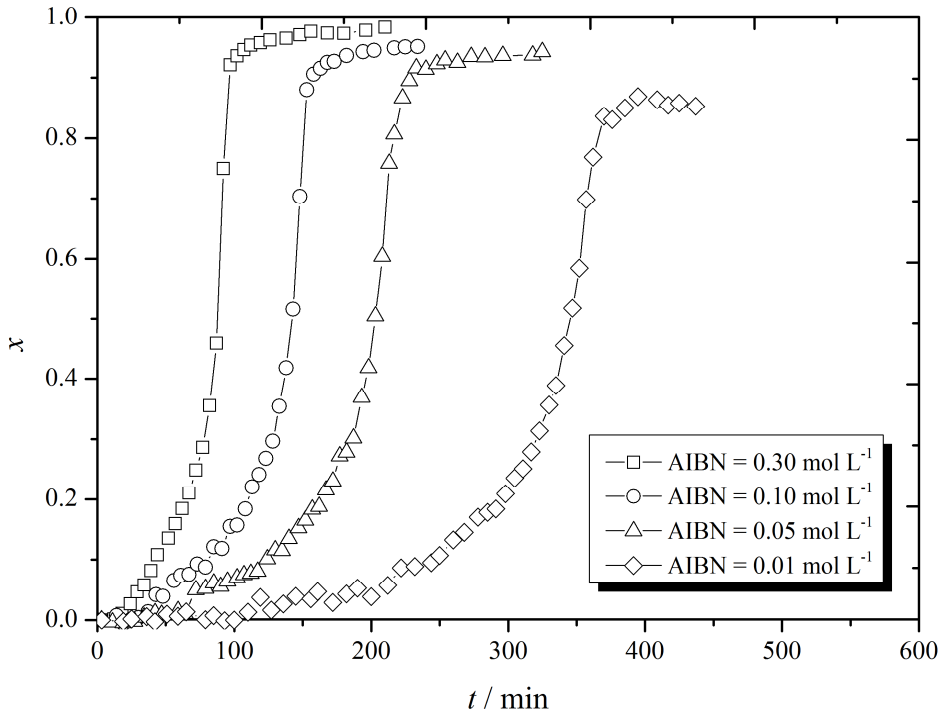

Figure 8-5. Conversion-time data for MMA bulk polymerization at 70 °C with different AIBN concentrations, as indicated.

8.4.3. DMA radical polymerization to high conversion

Figure 8-6 shows conversion-time data to high conversion for radical polymerization of *n*-dodecyl methacrylate (DMA), as deduced by Raman spectroscopy. Results show no pronounced gel effect. Interestingly, inspection of Figure 8-6 also shows a gentle transition to final conversion, unlike MMA.

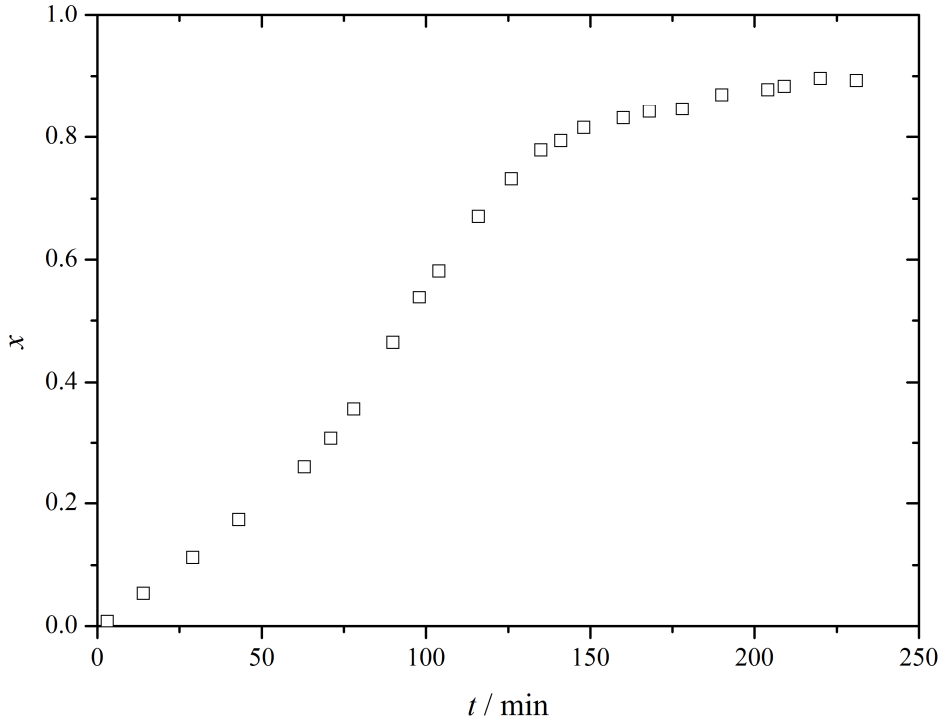

Figure 8-6. Conversion-time data for bulk DMA polymerization at 70 °C employing 0.05 mol L^{-1} AIBN.

8.5. Discussion

The common idea that the molecular weight (MW) of the polymer plays an important role in determining the gel effect onset can be discussed. In thermal polymerization, polymer MW is affected by temperature. However, there is a coupled effect of MW and temperature. Decoupling the effect of temperature and MW has been achieved by O'Neil et al. by doing experiments at constant polymer MW by varying the initiator concentration so as to counteract the effect of temperature on MW.[21] O'Neil et al. reported data for MMA and ST. The results clearly showed independence of MW on the gel effect and a trend towards a higher critical conversion at higher temperature. This is in accord with free volume theory. Despite being consistent with free volume theory, this theory alone cannot predict how

conversion varies with time, and cannot explain entirely the gel effect behaviour as discussed earlier. It is noted that independence of the gel effect on MW is consistent with short-long termination being at the heart of the gel effect, for diffusion of short chains is unaffected by average MW of a system. This notion will be returned to shortly.

On the other hand, variation of initiator concentration at constant temperature will only influence MW. Higher initiator concentration will result in low MW polymers. The results presented in Figure 8-5 illustrate effects other than temperature on the onset of the gel effect. This would suggest that MW plays a key role in the onset of the gel effect, in contrast to O'Neil conclusion. This is consistent with our temperature experiments, as temperature also results in a variation in the MW of the resultant polymer. Thus one can conclude based on our experiments that the temperature and MW have a combined influence on the onset of the gel effect.

It is possible to explain this data on the basis of short-long termination. The details of individual termination reactions become important. Considering three classes of termination reactions, those between short chains, those between a short and a long chain, and those between long chains, appear very important. As it appears likely that the reaction between two long chains would be rare, the termination between short and long would be the dominant reaction; in these the short, highly mobile chains will diffuse into the vicinity of the long chains and react with them. Thus diffusion of long chains should not be particularly important in determination of k_t (see Figure 8-7). If termination is dominated by short-long events, then short radicals in the system would be dominant at high temperature. Short radicals are only a few monomer units long. Since addition of one monomer unit onto a very short chain will affect its diffusion more than an equivalent addition into a somewhat larger chain, the diffusion of short chains may be slowed significantly for the system at a higher temperature, the gel effect will occur more severely and at higher critical conversion.

Similarly, with high initiator concentration, short chains would be dominant and would be influenced significantly by changing viscosity, leading to severe gel effect occurrence at high critical conversion.

Figure 8-7. Schematic illustration of the effect of short-long termination on bulk radical polymerization.[27]

However, the absence of a gel effect in DMA radical polymerization is still a mystery, except in that it is consistent with DA results. Figure 8-6 shows no pronounced observation of the gel effect. A possible explanation would be related to the presence of a large alkyl group. The large ester groups confound the diffusion-controlled reaction from the beginning of polymerization. These make the diffusion environment more complex. The presence of the high alkyl group also increases the free volume associated with the chain and this increases their mobility. Thus the absence of the gel effect may be ascribed to the hindrance of segmental diffusion from the beginning of the polymerization due to the interaction between ester groups with increasing ester length.[15] This suggests the important of microviscosity, which is established to correlate with system free volume.

Indeed, quantitative understanding of this phenomenon remains elusive for a variety of reasons. The cause of the onset of the gel effect has never been conclusively isolated. That the gel effect onset is caused by a single physical phenomenon seems to be far from reality; it can occur in a variety of conditions. Further, there are still problems associated with exactly defining the onset point of the gel effect. Moreover, another important factor to be considered is the effectiveness of heat transfer; this is a significant issue because it can cause inconsistent results with the gel effect.[21, 28]

Additionally, the relation between the final conversion, temperature and initiator concentration seems to be of importance. The final conversions are near complete only at a relatively high temperature or high initiator concentration, at which a low MW is expected. At a lower temperature and lower initiator concentration, the transition to glassy state occurs before polymerization is complete, i.e. the reaction shuts down when there is much less than 100% conversion. When the polymerizing mixture approaches its glassy state, not only macromolecules but also small molecules such as monomer and initiator diffuse very slowly and become diffusion controlled. Subsequently, they reach a point at which the mixture becomes a hard glass where even monomer and unreacted radicals become trapped inside. The effect of temperature on the final conversion may be explained on the basis of polymer chain length, in which a low temperature and initiator concentration may lead to the production of long enough chains to affect initiator efficiency or to have monomer and initiator trapped inside.

8.6. Conclusion

This work demonstrated the capability of using Raman spectroscopy qualitatively for monitoring polymerization of MMA and DMA in real time to high conversions. The gel

effect was clearly observed in MMA bulk polymerization. Temperature and initiator concentration were found to have an influence on the onset of the gel effect. In addition, polymerization of bulk DMA shows no clear gel effect. A quantitative understanding of this phenomenon remains mysterious. Much evidence has led to the widespread theory that the gel effect onset is related to a decrease in the rate of termination, which is linked to diffusion control and CLDT issues. However, there was insufficient data to draw firm conclusions on the cause of the gel effect. Furthermore, it is important that one should be careful when Raman quantitative investigation is carried out as there might still be some problems related to the effect of the laser on the polymerization kinetics, and defining exactly the onset point of the gel effect. Due to reaction time requirements, instrumentation availability and restricted PhD time, I could not finish what had been planned for this section of work. However, I thought it worthwhile to present the limited data that had been obtained during this investigation**.**

References

[1] G.A. O'Neil, M.B. Wisnudel, J.M. Torkelson, Macromolecules, 29 (1996) 7477-7490.
[2] R. Norrish, E. Brookman, Proceedings of the Royal Society of London. Series A. Mathematical and Physical Sciences, 171 (1939) 147-171.
[3] J. Gao, A. Penlidis, Journal of Macromolecular Science - Reviews in Macromolecular Chemistry and Physics, 36 (1996) 199-404.
[4] M. Stickler, Die Makromolekulare Chemie, 187 (1986) 1765-1775.
[5] E. Gulari, K. McKeigue, K.Y.S. Ng, Macromolecules, 17 (1984) 1822-1825.
[6] R.A. Larsen, - Raman spectroscopy of polymers, in: D.C. Clara, E.C. Charles, A.C.D.C. Jr, Charles E. Carraher, Jr. (Eds.) Applied Polymer Science: 21st Century, Pergamon, Oxford, 2000, pp. 759-785.
[7] R.G.W. Norrish, R.R. Smith, Nature, 150 (1942) 336-337.
[8] E. Trommsdorff, H. Kohle, P. Lagally, Makromol. Chem., 1 (1948) 169-198.
[9] M.S. Matheson, E.E. Auer, E.B. Bevilacqua, E.J. Hart, Journal of the American Chemical Society, 71 (1949) 497-504.
[10] G. Burnett, H. Melville, Proceedings of the Royal Society of London. Series A. Mathematical and Physical Sciences, 189 (1947) 494-507.
[11] A. Faldi, M. Tirrell, T.P. Lodge, Macromolecules, 27 (1994) 4176-4183.
[12] M. Kamachi, Influence of solvent on free radical polymerization of vinyl compounds, in: Polymerization Processes, Springer Berlin Heidelberg, 1981, pp. 55-87.
[13] V.G.V. Schulz, G. Harborth, Die Makromolekulare Chemie, 1 (1947) 106-139.
[14] M.S. Matheson, E.E. Auer, E.B. Bevilacqua, E.J. Hart, Journal of the American Chemical Society, 73 (1951) 5395-5400.
[15] N.A. Plate, A.G. Ponomarenko, Polymer Science U.S.S.R., 16 (1974) 3067-3081.
[16] S.W. Benson, A.M. North, Journal of the American Chemical Society, 81 (1959) 1339-1345.
[17] K. O'Driscoll, Pure and Applied Chemistry, 53 (1981) 617-626.
[18] E. Abuin, E.A. Lissi, Journal of Macromolecular Science: Part A - Chemistry, 11 (1977) 287-294.
[19] K. Ito, European Polymer Journal, 22 (1986) 253-256.
[20] S.T. Balke, A.E. Hamielec, Journal of Applied Polymer Science, 17 (1973) 905-949.
[21] G.A. O'Neil, M.B. Wisnudel, J.M. Torkelson, Macromolecules, 31 (1998) 4537-4545.
[22] B. Friedman, B. O'Shaughnessy, Macromolecules, 26 (1993) 5726-5739.
[23] M. Buback, B. Huckestein, G.T. Russell, Macromolecular Chemistry and Physics, 195 (1994) 539-554.
[24] F. GarcÃa, J.M. GarcÃa, F. Rubio, J.L. De La PeÃ±a, J. GuzmÃ¡n, E. Riande, Journal of Polymer Science, Part A: Polymer Chemistry, 40 (2002) 3987-4001.
[25] M. Buback, C. Kowollik, Macromolecules, 32 (1999) 1445-1452.
[26] X. Wang, E. Ruckenstein, Journal of Applied Polymer Science, 49 (1993) 2179-2188.
[27] B. O'Shaughnessy, J. Yu, Physical Review Letters, 73 (1994) 1723-1726.
[28] P.D. Armitage, S. Hill, A.F. Johnson, J. Mykytiuk, J.M.C. Turner, Polymer, 29 (1988) 2221-2228.

Chapter 9. General conclusion and future work

9.1. General conclusion

Most recent research work in RP has been directed at synthesis and characterization. Little attention has been paid to polymerization kinetics, knowledge that is critical for the optimal control of polymerization processes and product properties. The current thesis shows a detailed quantitative mechanistic study of the way the final radical polymerization products are formed utilizing the simple techniques of gravimetry and ESI-MS.

The ongoing developments in existing analytical techniques of mass spectrometry offer continuing improvements in the area of polymer mechanism investigations, specifically regarding kinetic and mechanistic pathways. The work presented in this thesis takes advantage of the accuracy and wide analysis capabilities of the ESI-MS-TOF technique. The extraction of previously inaccessible information regarding kinetic and mechanistic pathways has been realized. Besides information about the mode of termination, accounting for chain-length-dependent termination (CLDT) was found to return known values of CLDT parameters. Also, a detailed study on the robustness of this technique and the effect of different factors on the mode of termination was presented.

This PhD work has also clearly shown an important point to appreciate about the deviation from the prediction of classical kinetics and the effect of CLDT. This work has proved the capability of observing CLDT effects from such deviations, in particular with regard to the activation energy of $<k_t>$. Small chains were found to have large CLDT. The very consistent results for radical polymerization of MMA, BMA, DMA, BA and ST illustrate family behaviour for these small chains. Arrhenius parameters for the radical termination reaction of MMA, BMA, DMA, BA and ST were also determined for the temperature range 50 – 90 °C.

Very large $E_a(<k_t>)$ values were obtained, which was interpreted as another proof of the translational-diffusion control of termination for short chains. In addition, the study also presented new insights into radical chain transfer to solvent, which can play a role in shaping RP kinetics. Finally, the capability of using Raman spectroscopy for high conversion investigations was explored. Despite the potential of using Raman for such investigations, quantitative application might still be questionable.

In summary, the outstanding results of this thesis are felt to be: (1) The application of CLDT theory to better understand rate results from low-conversion polymerizations. (2) In particular, the use of CLDT principles to explain termination activation energies across a range of monomers. (3) The validation of the MS method for quantitative determination of mode of termination by carrying out an array of consistency checks. (4) Showing that MS results are consistent with CLDT theory. (5) Utilization of the MS method for the first ever reliable measurement of the variation of mode of termination with temperature, pressure and monomer.

9.2. Future work

There are several areas that are open to further study. It is clear from this thesis that an important direction for future work is expanding the experimental data on CLDT to include other monomers. The results presented in this thesis could be used in a modelling study to extract other information. The program package PREDICI may be used for such data modelling. In addition, it is now known that transfer plays a very important role in shaping RP kinetics. Therefore it is vital to have accurate values of transfer rate coefficients, k_{tr}. Measuring these by ESI-MS is underway. Further new ways of utilizing electrospray ionization mass spectrometry to study RP kinetics and mechanisms may be suggested, for

example its implementation for further CLDT investigation. At the same time the effect due to CLDP would be of great importance as it appears be related to a low *PDI* formed at low chain lengths. Finally, the systems studied in this thesis have all been at low conversion, so it would be of interest to use this theory to build on what has been learnt at low conversion in order to further investigate the still unexplained phenomenon that is the gel effect.

In summary, broad areas of future work are (1) The implementation of MS for quantitative study of RP kinetics and mechanisms, and (2) The extension of CLDT methodologies to intermediate conversions in order to reach, finally, a rigorous understanding of the gel effect.

9.3. Publications and presentations

[1] D. R. Taylor, K. Y. Van Berkel, M. M. Alghamdi, G. T. Russell, *Macromolecular Chemistry and Physics* **2010**, *211*, 563

[2] M. M. Alghamdi, G. T. Russell, *Macromolecular Chemistry and Physics* **2013**, *214*, 1384.

[3] "Mass spectrometry for the determination of the mode of termination in radical polymerization", Majed M. Alghamdi and Gregory T. Russell, 12th International Conference on Frontiers of Polymers and Advanced Materials, Auckland, New Zealand, 8 – 13 December 2013, poster presentation.

9.4. List of abbreviations

$\langle k_t \rangle$	Average termination rate coefficient
ΔV^*	Activation volume
AIBN	2,2'-azobisisobutyronitrile
BA	*n*-Butyl acrylate
BMA	*n*-Butyl methacrylate
BTMHP	Bis(3,5,5-trimethylhexanoyl)peroxide
c_I	Initiator concentration
CLD	Chain length distribution
CLDP	Chain length dependent propagation
CLDT	Chain length dependent termination
CLIT	Chain length independent termination
c_M	Monomer concentration
c_R	The overall concentration of polymerizing radicals
$C_{tr,X}$	Chain transfer constant to x
DMA	*n*-Dodecyl methacrylate
DP_n	Number-average degree of polymerization
DPP	Di-*n*-decanoyl peroxide
e	Chain length dependence of termination
E_a	Activation energy
EBz	Ethyl benzene
EPR	Electron paramagnetic resonance (spectroscopy)
ESI-MS	Electrospray-ionization mass spectrometry
f	Initiation efficiency

$F_{dis}(i)$	The fraction of chains of degree of polymerization i formed by disproportionation
GPC	Gas permeation chromatography
k_d	Initiator decomposition rate coefficient
$k_{t,comb}$	Combination rate coefficient
$k_{t,dis}$	Disproportionation rate coefficient
$k_t^{1,1}$	Rate coefficient for termination between monomeric free radicals
LCA	Long-chain approximation
MALDI	Matrix-assisted laser desorption/ionization
MIB	Methyl isobutyrate
MMA	Methyl methacrylate
MS	Mass spectrometry
MMD	Molar mass distribution
MWD	Molecular weight distribution
NIR	Near infrared
NSSP	Non steady-state polymerization
p	Pressure
PDI	Polydispersity index
PLP	Pulsed-lasers polymerization
R_i	Initiation rate
RI	Refractive index detector
R_p	Rate of polymerization
RP	Radical polymerization
SSP	Steady-state polymerization

TMPPP	1,1,2,2-tetramethylpropyl peroxypivalate
TOF	Time of flight (detection)
x	Fractional conversion of monomer into polymer